Organotin Tetrazoles And Related Compounds

Hill, Michael Stephen

Award date:
1994

Awarding institution:
University of Bath

ORGANOTIN TETRAZOLES AND RELATED COMPOUNDS

Submitted by Michael Stephen Hill

For the degree of Ph.D.

of the University of Bath

1994

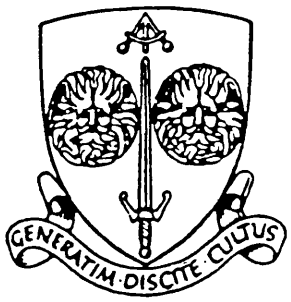

Department of Chemistry

University of Bath

Supervisor: Dr. K.C. Molloy

ProQuest LLC
789 East Eisenhower Parkway
P.O. Box 1346
Ann Arbor, MI 48106-1346

Contents

Abstract

Acknowledgements

		Page
Chapter 1	**The Chemistry and Synthetic Utility of Organotin Compounds**	
1.1	Introduction	1
1.2	Applications of Organotin Compounds	2
1.3	Synthesis of Organotin Compounds	3
1.4	Structural Variations of Organotin Compounds	6
1.4.1	Subvalent Organotin Compounds	6
1.4.2	Four-Coordinate Organotin Compounds	8
1.4.3	Five-Coordinate Organotin Compounds	10
1.4.4	Six-Coordinate Organotin Compounds	16
1.4.5	Seven-Coordinate Organotin Compounds	20
1.4.6	Self-associated Polymeric Structures	21
1.5	Spectroscopy of Organotin Compounds	29
1.5.1	Mössbauer Spectroscopy	29
1.5.2	^{119}Sn NMR Spectroscopy	35
1.5.3	Infra-red Spectroscopy of Organotins	42
1.5.4	Mass Spectra of Organotin Compounds	43
1.6	Previous Work and Aims of this Thesis	44

Chapter 2 **The Synthesis and Chemistry of Organotin-Substituted Bis-tetrazoles**

2.1 Introduction 50

2.2 Synthesis of Bis-(trialkylstannyl -tetrazoles) 54

2.3 Spectroscopy 57

2.3.1 NMR Spectroscopy 57

2.3.2 ^{119m}Sn Mössbauer Spectroscopy 62

2.3.3 Infra-red Spectroscopy 63

2.3.4 Mass Spectrometry 63

2.4 The Crystal Structure of 1,3-phenylene-bis-5,5′-(tri-butylstannyltetrazole)Bis-methanolate 65

2.5 The Crystal Structure of 1,2-phenylene-bis-5,5′-(tri-ethylstannyltetrazole) 74

2.6 The Crystal Structure of 1,2-phenylene-bis-5,5′-(tri-butylstannyltetrazole) 83

2.7 Reaction Chemistry and Attempted Macrocyclisation Reactions 93

2.7.1 Cleavage Reactions 93

2.7.2 Attempted Complexation Reactions 94

2.7.3 Attempted Macrocyclisation Reactions 97

2.8 Experimental 99

Chapter 3 **The Reaction of α,ω-dibromoalkanes and Bis-(tributyl-stannyltetrazoles) Applied to the Synthesis of Tetra-tetrazole Macrocycles**

3.1 Introduction 118

3.2 Synthesis 123

3.3 Spectroscopy of Bis-(Alkyltetrazoles) 127

3.4	The Crystal Structure of [1,5-d][5,1-h]-ditetrazolo-[1,2-f]-benzo-1,4-diazacine	131
3.5	The Crystal Structure of 1,3-phenylene-bis-5,5′-[N^2,$N^{2'}$-(2-bromoethyl)tetrazole]	137
3.6	Attempted Macrocyclisation Reactions	141
3.7	Experimental	142
Chapter 4	**The Synthesis and Structural Chemistry of Organotin-substituted Tris-tetrazoles**	
4.1	Introduction	155
4.2	Synthesis	157
4.3	Spectroscopy	160
4.3.1	NMR Spectroscopy	160
4.3.2	Mössbauer Spectroscopy	161
4.4	The Crystal Structure of Tris-[2-(5-tributylstannyl-tetrazolyl)ethyl]nitromethane	164
4.5	The Crystal Structure of 1,3,5-phenylene-tris-5-(tri-butylstannyl)tetrazole	173
4.6	Experimental	185
Chapter 5	**The Synthesis and Characterisation of some C-triorgano-metallated (metal=Sn, Si) Bis-heterocycles (Het= thiophene, pyrazole)**	
5.1	Introduction	190
5.2	Synthesis	193
5.3	Spectroscopy	197
5.3.1	NMR Spectroscopy	197
5.3.2	^{119m}Sn Mössbauer Spectroscopy	199

5.4	The Crystal Structure of methylene-bis-[1,1′-(5,5′-triphenylstannyl)pyrazole]	202
5.5	Reaction Chemistry	206
5.6	Experimental	208

Appendix I	Instrument Details	219
Appendix II	Crystallographic Analysis of **(12)**	221
Appendix III	Crystallographic Analysis of **(17)**	224
Appendix IV	Crystallographic Analysis of **(11)**	227
Appendix V	The Crystal Structure of **(20)**.$4H_2O$	230
Appendix VI	Crystallographic Analysis of **(23)**	238
Appendix VII	Crystallographic Analysis of **(31)**	240
Appendix VIII	Crystallographic Analysis of **(49)**	242
Appendix IX	Crystallographic Analysis of **(52)**	245
Appendix X	Crystallographic Analysis of **(62)**	248

References 252

Numerical Index of Compounds 268

List of abbreviations used in this work

Ala	Alanine
Bipym	2,2′,6,6′-bipyrimidine
Bu	butyl
Box	benzoxazole
Bzt	benzothiazole
CN	coordination number
DMSO	dimethyl sulphoxide
E.F.G.	electric field gradient
Het.	heterocycle
HOMO	highest occupied molecular orbital
Hz	Hertz
I.S.	Isomer shift
K	Kelvin
keV	kilo electron volt
LUMO	lowest unoccupied molecular orbital
Me	methyl
Mes	mesityl
pbp	pentagonal bipyramid
Ph	phenyl
Phe	phenylalanine
ppm	parts per million
^{i}Pr	iso-propyl
Pz	pyrazole
Q.S.	quadrupole splitting
tbp	trigonal bipyramid
THF	tetrahydrofuran
TMS	tetramethyl silane

Abstract

The preparation, characterisation and reaction chemistry of a number of organotin-substituted poly-heterocyclic compounds has been undertaken. Bis-(triorganotin-substituted heterocycles) have been identified as suitably functionalised synthons for novel macrocyclic compounds and a number of possible synthetic routes to such systems have been attempted.

Chapter two of this thesis describes a number of bis-(organotin-substituted)tetrazolyl compounds, synthesised by the established ring-building 1,3-dipolar cycloaddition of a triorganotin azide and an organic dinitrile. The structures of these compounds have been investigated by standard spectroscopic techniques and demonstrated to be polymeric in nature. 1,3-phenylene-bis-5,5′-(tributylstannyltetrazole) crystallises from methanol as a bis-solvated adduct and the crystal structure of this essentially monomeric form is described. In contrast, the crystal structures of the homologous 1,2-phenylene-bis-5,5′-(triethylstannyltetrazole) and 1,2-phenylene-bis-5,5′-(tributylstannyltetrazole) are shown to be polymeric in nature and constructed around *trans*-N_2SnR_3 trigonal bipyramidal tin sites. The differing space-filling requirements of the triethyl- and tributyltin groups result in the adoption of two- and three-dimensional supramolecular architecture respectively.

In Chapter three the reaction of 1,2-phenylene- and 1,3-phenylene-bis-5,5′-(tributylstannyltetrazole) compounds and α,ω-dibromoalkanes is examined as a proposed route to tetra-tetrazole macrocycles. The reaction of 1,2-dibromo-ethane and 1,2-phenylene-bis-5,5′-(tributylstannyltetrazole) in methanol solution results in complete elimination of the Bu_3Sn groups and the formation of a tetracyclic compound which has been characterised crystallographically.

Reaction employing the dibromoalkane as both reactant and solvent (i.e. in large excess) results in two structural isomers bromoalkyl-substituted at the N^1,$N^{2'}$ and N^2,$N^{2'}$ ring positions respectively. These are readily discriminated by both ^1H and ^{13}C NMR and their assignment is confirmed by the x-ray stuctural analysis of an example of the second of these possibilities.

Chapter four extends the theme of Chapter two to the synthesis of tris-(triorganostannyltetrazole) compounds. Two representative tributyltinsubstituted examples have been crystallographically characterised and are found to be isostructural. Both form extended sheet-like arrays based around trigonal bipyramidal tin and are dominated by large open cavities 'padded' by the tin-bonded butyl chains.

The work described in Chapter five details the synthesis of several R_3Sn- and R_3Si- C-substituted bis-thiophene and bis-pyrazole compounds. Standard spectroscopic techniques indicate monomeric stuctures with tetrahedral coordination at the metal. This is confirmed by the x-ray analysis of a representative triphenyltin-substituted bis-pyrazole.

Acknowledgements

Although there is only one name on the cover of this thesis a number of people deserve equal billing. First and foremost I would like to thank Dr. Kieran Molloy for his great help and advice during the past three years and for coming up with the fresh ideas when things weren't going quite as well as anticipated. I am also especially indebted to the skill of Dr. Mary Mahon for the considerable amount of crystallographic data contained in this thesis.

Thanks are also due to the technical staff of the University of Bath, Mr. D. Wood for the majority of the NMR data and Mr. Alan Carver for all the CHN analyses, as well as the terrific support provided by Mr. Robert Stevens, Ahmad and Mrs. Shiela Osborne. I would also like to extend my appreciation to all my colleagues around 4 West for making the last three years such a enjoyable experience especially Dr. John M^{c}Ginley, Paul Deacon and Rob Harker.

Finally I would like to thank my mum and dad for their unending support and my wife, Paula for being everything I needed her to be.

Chapter 1

The Chemistry and Synthetic Utility of Organotin Compounds

This thesis describes the preparation and chemistry of several novel poly-organostannyl heterocyclic compounds in which tin is either involved in the ring-building process or is attached via a nucleophilic substitution reaction with the appropriate heterocycle. Furthermore, bis-(organotin-substituted) heterocycles are identified as suitably functionalised precursors to tetra-heterocyclic macrocycles. By way of introduction to the work reported in this thesis, synthetic and structural aspects of organotin chemistry are reviewed.

1.1 Introduction

The group of compounds encompassed by the term organotin is one of the most structurally diverse and spectroscopically amenable in the chemical literature. Tin itself has a $5s^2 5p^2$ electronic configuration and can thus form compounds in both the +2 and +4 oxidation states. Organotin compounds, defined as containing at least one tin-carbon bond in the molecule, can be prepared in both available oxidation states. Organotin(IV) compounds however are considerably more stable and thus dominate the published literature. Numerous books and reviews on general and preparative organotin chemistry[1-9] as well as more specialised reviews[10-12] are available for reference.

Organotin(IV) compounds, R_nSnX_{4-n} are generally colourless oils or solids, thermally and aerobically stable and soluble in the usual organic solvents. Physical data for several simple examples (n = 1-4) are given in Table 1.1.

Table 1.1: Physical data of organotin compounds

Compound	m.p.(°C)	b.p.(°C/mmHg)
Me_4Sn	-	77/760
Bu_4Sn	-	145/10
Ph_4Sn	225	-
Me_3SnCl	37-38	-
Bu_3SnBr	-	120-122/2
Ph_3SnCl	105	-
Me_2SnBr_2	75-77	-
Ph_2SnCl_2	41-42	-
$MeSnBr_3$	55	-
$BuSnCl_3$	-	93/10

1.2 Applications of Organotin Compounds

Although a few organotin compounds are highly toxic, most are of moderate, low or very low toxicity. In the series R_nSnX_{4-n}, the highest biological activity occurs at n = 3. Diorganotin derivatives, R_2SnX_2, are less toxic than triorganotins, but R_4Sn compounds show enhanced toxicity due to *in vivo* transformation into R_3SnX. Mono-organotins have very small activity. The group X has little effect in this respect but the nature of the organic group, R, is very important. Maximum mammalian toxicity occurs with R = Me or Et with a marked decrease for larger groups such as butyl, phenyl or octyl.

These trends are reflected in the applications and employment of organotin compounds in industry. Whereas tetra- and tri-methyltin derivatives have found only limited usage, for example in the chemical vapour deposition of

SnO_2 thin films, certain di- and mono-octyltin compounds are completely non-toxic and suitable for food-contact applications.

On a somewhat smaller scale, tetravalent tin compounds are being increasingly exploited as versatile reagents in organic synthesis. Several books and reviews dealing specifically with this subject have now been published[4,13,14] and two recent examples of the employment of organotin compounds as chemoselective reducing agents and C-C coupling reagents are illustrated in Equations 1.1 and 1.2.

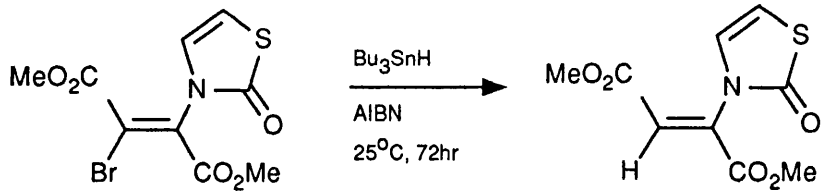

(Equation 1.1)[15]

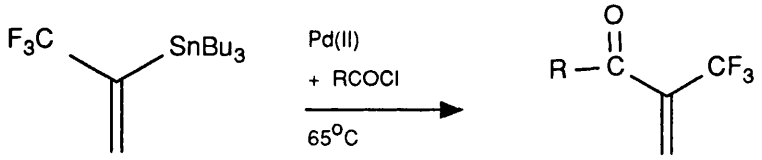

(Equation 1.2)[16]

1.3 Synthesis of Organotin Compounds

On an industrial scale, the cheap and readily available tin(IV) chloride is used to produce large quantities of symmetrical organotins. Grignard reagents are most commonly employed for the formation of tin-carbon bonds (Equation 1.3), although Wurtz-type coupling (Equation 1.4) and reaction with aluminium alkyls (Equation 1.5) have also been employed.

$$SnCl_4 + 4RMgCl \longrightarrow R_4Sn + 4MgCl_2 \qquad \text{(Equation 1.3)}$$

$$SnCl_4 + 8Na + RCl \longrightarrow R_4Sn + 8NaCl \qquad \text{(Equation 1.4)}$$

$$3SnCl_4 + 4R_3Al + 4R'_2O \longrightarrow 3R_4Sn + 4AlCl_3.R'_2O \qquad \text{(Equation 1.5)}$$

The preparation of unsymmetrical tetraorganotins commonly requires reaction of the appropriate organotin halide with organometallic nucleophiles such as Grignard and lithium reagents. Alternatively a tin-metal compound and an alkyl halide can be employed.

Mono-, di- and tri-organotin halides are easily prepared by redistribution reactions of appropriate stoichiometries of symmetrical tetra-alkyltins and tin(IV) tetrahalides (Equations 1.6-1.8).[17]

$$3R_4Sn + SnX_4 \xrightarrow{\text{ca. 200°C}} 4R_3SnX \qquad \text{(Equation 1.6)}$$

$$R_4Sn + SnX_4 \xrightarrow{\text{ca. 200°C}} 2R_2SnX_2 \qquad \text{(Equation 1.7)}$$

$$R_4Sn + 3SnX_4 \xrightarrow{\text{ca. 200°C}} 4RSnX_3 \qquad \text{(Equation 1.8)}$$

Industrially, direct synthesis has also been applied to the production of dimethyltin dichloride (Equation 1.9).[18]

$$2MeCl + Sn \xrightarrow{\text{Catalyst}} Me_2SnCl_2 \qquad \text{(Equation 1.9)}$$

Nucleophilic substitution of organotin halides provides the starting point for the synthesis of most heteroatom substituted organotin compounds and organotin hydrides. The major reactions of organotin halides are illustrated in Scheme 1.1.[6]

Scheme 1.1: Principle Reactions of Organotin Halides

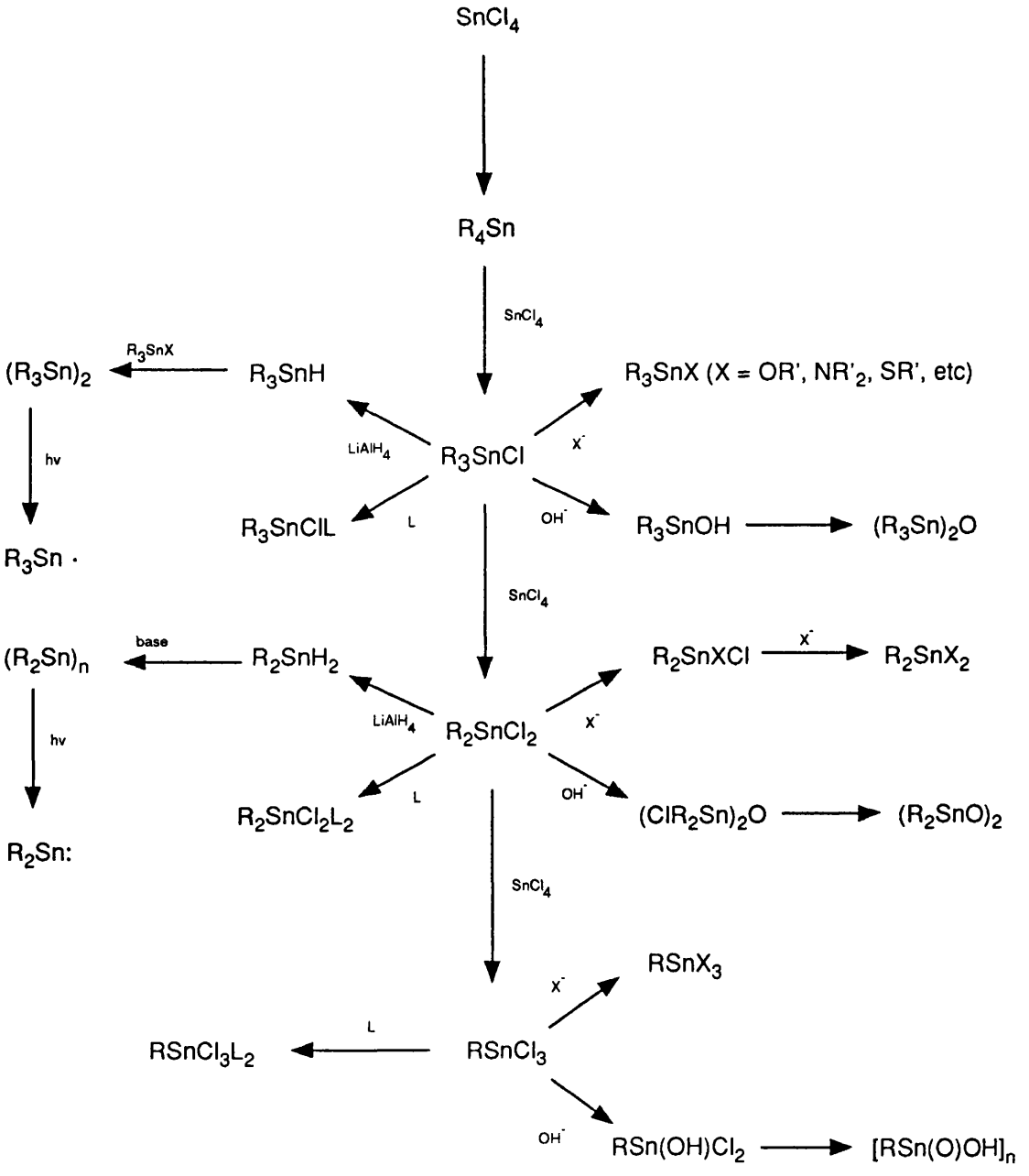

L = 2 electron donor

1.4 Structural Variations of Organotin Compounds

Until 1963 it was presumed that organotin compounds were restricted to a coordination number of four. It was then demonstrated crystallographically that the pyridine adduct of Me_3SnCl contained five-coordinate tin[19] and since then coordination numbers of two, three, four, five, six and seven have been established.

Tetravalent tin does indeed often present tetrahedral sp^3 hybridisation and this is generally the case for tetraorganotins. However if one or more organic groups is replaced by an electronegative substituent the Lewis acidity of the tin atom increases and consequently sp^3d (trigonal bipyramidal) and sp^3d^2 (octahedral) hybridisation can occur when adducted to donor ligands. A large number of such compounds have now been crystallographically confirmed and two compendia of tin crystal structures to *ca.* 1980 are available for reference.[20,21]

1.4.1 Subvalent Organotin Compounds

Several organotin species containing nominal multiple bonds to tin and coordination numbers less than four have now been structurally characterised. The rigourous division between tin(IV) and tin(II) compounds becomes somewhat blurred in such systems. The first tin analogue of an alkene (I) was initially reported by Lappert *et al.* in 1976[22] and subsequently re-evaluated in 1986.[23]

(I) (II)

R = $CH(SiMe_3)_2$

The R_2Sn molecular fragments in this molecule are bent to the extent of

41° with respect to the plane of the double bond. This was originally interpreted in terms of a double donor-acceptor linkage (II) appearing to account for both the observed geometry and the weakness of the Sn-Sn bond with respect to dissociation. Later work however reinterpreted these results in terms of the increasing stability of the *trans* folded form, relative to a planar structure, via an increase in singlet→triplet excitation energy as group 14 is descended.

More recently reported three-coordinate structures, the stannaethene (III)[24] and the stannaketenimine (IV)[25] also show this marked deviation from planarity despite shortening of the Sn-C bond length.

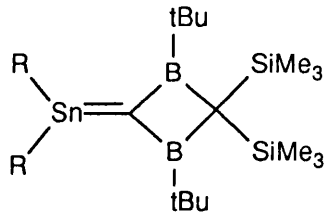

R = $CH(SiMe_3)_2$

(III)

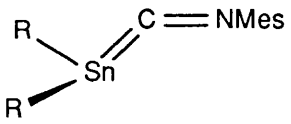

R = 2,4,6-$CF_3C_6H_2$
Mes = Mesityl

(IV)

Quantum mechanical calculations have been conducted on such 'double bonded' systems and their structures correlated with the singlet-triplet excitation energy, $\Delta E_{(s\rightarrow t)}$, of the R_2X fragment (X = C, Si, Ge, Sn).[26] When the relationship $\Sigma\Delta E_{(s\rightarrow t)} < 0.5E_{\sigma+\pi}$ ($E_{\sigma+\pi}$ = total bond energy) is fulfilled, 'classical' planar molecular structures, such as ethene, are observed. If, on the other hand, $\Sigma\Delta E_{(s\rightarrow t)} > 0.5E_{\sigma+\pi}$, 'non-classical' double bonded systems result with the molecular fragments occupying *trans* positions with respect to the plane of the double bond.

An organotin compound with a coordination number of two has recently been crystallographically characterised.[27] This was synthesised via the reaction of the stannadiyl (V) with the ketene ylide (VI) (Equation 1.10). One of the aryl

substituents, R, on the tin atom is transferred to the activated CO group of the three-coordinate intermediate ketene (VII) to produce (VIII). The tin centre in (VIII) is bonded to two sp^2 hybridised carbon atoms each of which is part of a conjugated multiple bond system. The C-Sn distance, 2.25(2)Å, is somewhat shorter than the corresponding distance in the stannadiyl (V) (2.278(5)Å), and is cited as further evidence for the multiply bonded nature of the molecule.

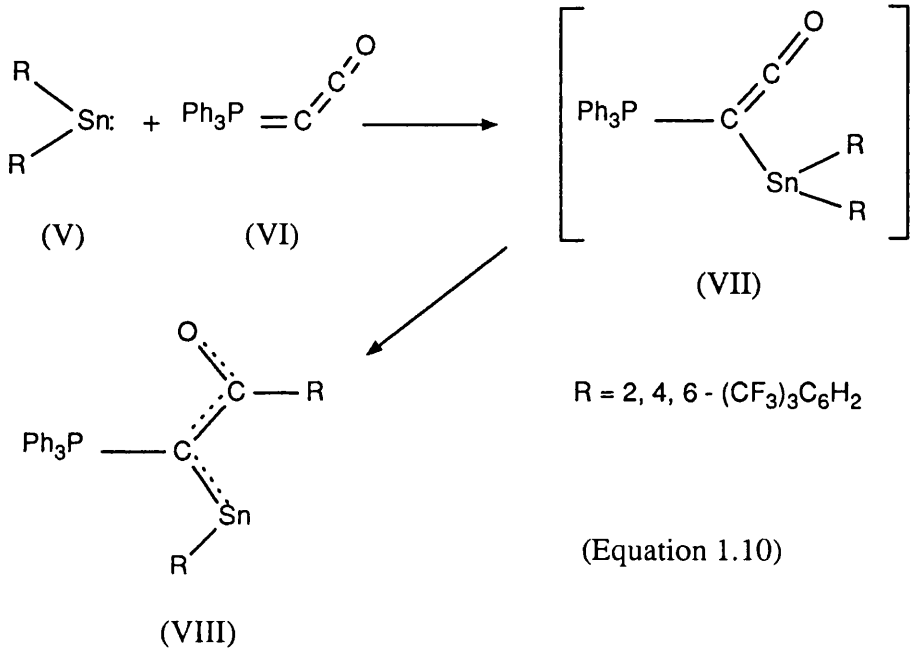

(Equation 1.10)

1.4.2 Four Coordinate Organotin Compounds

As stated earlier (Section 1.3), four coordinate tetraorganotins are invariably tetrahedral. A large number of symmetrical R_4Sn structures have been reported, including Ph_4Sn,[28] $(4\text{-Me-}C_6H_4)_4Sn$,[29] $(2\text{-thienyl})_4Sn$[30] and $(Me_2C{=}CPh)_4Sn$.[31] Equally as common are asymmetric compounds, for example of the type R_3SnR'. Structures such as Ph_3SnCH_2I,[32] Ph_3Sn(benzothiazole)[33] and, more recently, [2-(4,4-dimethyl-2-oxazolinyl)-3-thienyl]tri-*p*-tolyltin (Figure 1.1)[34] consisting of discrete slightly distorted units typify this geometry.

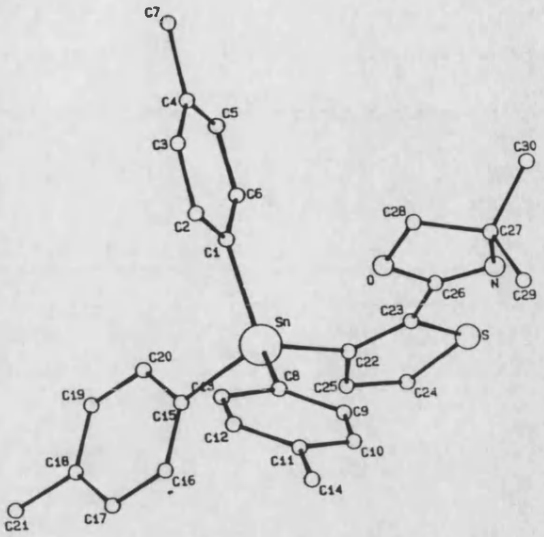

Figure 1.1: Structure of [2-(4, 4,-dimethyl-2-oxazolinyl)-3-thienyl]tri-*p*-tolyltin

As R is replaced by more electronegative groups, the Lewis acidity and hence the tendency for the coordination number to expand increases. Tetrahedral geometry can however be maintained for R_3SnX if the R groups are sterically demanding, as in $[(PhMe_2Si)_3C]Me_2SnNCS$,[35] and $[(Me_3Si)_2CH]_3SnCl$[36] or if the electronegativity of X is not too great e.g. $(2\text{-}MeOC_6H_4)_3SnI$.[37]

Examples of tetrahedral diorganotin compounds do exist where R is bulky and X is generally of low electronegativity. Bulky organic ligands tend to force the molecules into oligomeric arrangements as for example in the dimeric 2,2,4,4-tetra(2,4,6-tri-isopropylphenyl)-1-oxa-3-thia-2 ,4-distannetane (IX)[38] and the cyclic trimer $(Ph_2SnS)_3$,[39] although monomeric species have also been reported e.g. 2,2-di-t-butyl-1,3,2-dithiastannolane (X).[40]

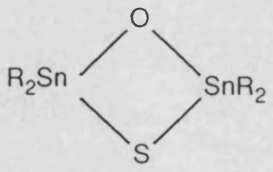

R = 2, 4, 6-$^{i}Pr_3Ph$

(IX)

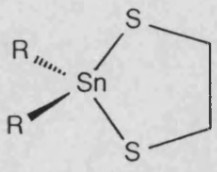

R = ^{t}Bu

(X)

Very few tetrahedral monoorganotin compounds have been reported. Methyltin sesquisulphide, $(CH_3Sn)_4S_6$, crystallises in an adamantane-like structure with each tin atom surrounded by one methyl group and three sulphur atoms in an approximately tetrahedral arrangement.[41] The structure of CH_3SnI_3 has been shown to be made up of discrete, loosely-packed monomers.[42] The average Sn-I bond length of 2.67Å is shorter than reported in similar compounds and is explained, via molecular orbital considerations, to be due to a small back donation from iodine to tin with concommitant decrease in Lewis acidity.

1.4.3 Five Coordinate Molecular Organotin Compounds

Although the limiting geometries of pentacoordinated tin compounds, trigonal bipyramidal (XI) and square pyramidal (XII), are close in energy[43,44] and readily interconvertable via the Berry mechanism[45] the latter has only been observed in two systems.

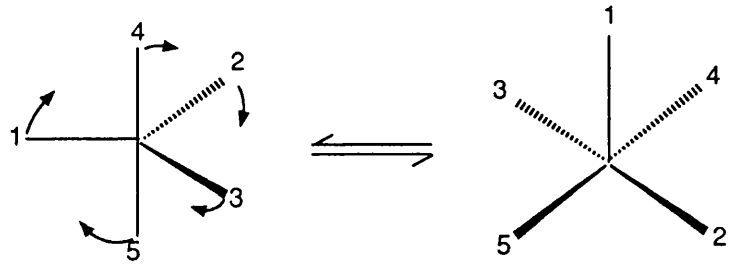

(XI) (XII)

In tribenzyl(2-pyridinethiolato-N-oxide)tin[46] the anisobidentate ligand restricts the geometry at tin resulting in a benzyl group adopting an apical position in a square pyramidal array. The basal plane, from which the tin atom is displaced by 0.64Å, is composed of the oxygen and sulphur atoms of the chelating ligand and the other two benzyl groups. A further example is provided by the anionic tin species (XIII) held in a square pyramidal array by two approximately isobidentate ethane-1, 2-dithiolate ligands.[47]

These two examples notwithstanding, five coordinate organotins are

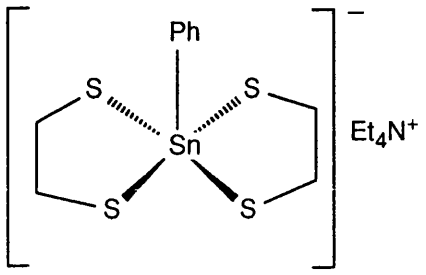

(XIII)

generally trigonal bipyramidal in shape. Due to their low Lewis acidity examples of tetraorganotins adopting this geometry are however rare. {C,N-[3-(2-pyridyl)-2-thienyl]}tri(*p*-tolyl)tin[48] (Figure 1.2) adopts a geometry intermediate between a tetrahedron and a trigonal pyramid. Two sets of C-Sn-C bond angles can be discerned, viz. 102-104°, and 113-116°, the first being those subtended at tin by the apical C(17) with each of the other *ipso*-carbons. The second axial site is provided by a weak intramolecular Sn-N bond of length 2.84Å. The C(17)-Sn-N bond angle is 166.6° and sum of the 'equatorial' angles only 343.5°.

One class of tetraorganotins, the stannatrane derivatives, $Me_2Sn(CH_2CH_2CH_2)_2NMe$ and $MeSn(CH_2CH_2CH_2)_3N$, strongly favour transannular N-Sn coordination.[49,50] The structure of the second of these has

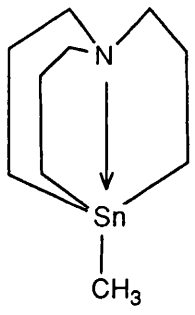

(XIV)

been confirmed revealing that the methyl group is forced into an axial site (XIV).

An interesting example of a five-coordinate triorganotin cation has recently been published.[51] In Figure 1.3 the trigonal bipyramidal tin atom is

stabilised by side-on π-coordination of an alkynylboronate moiety.

Pentacoordination has also been inferred from NMR coupling constant data for anionic species such as $SnMe_5^-$ [52] and lithium 1,1-bis(η^1-cyclopentadienyl)-halo-2,3,4,5-tetraphenylstannole.[53] No structures of this type however have been rigourously clarified and their existence may only be possible on the NMR time scale.

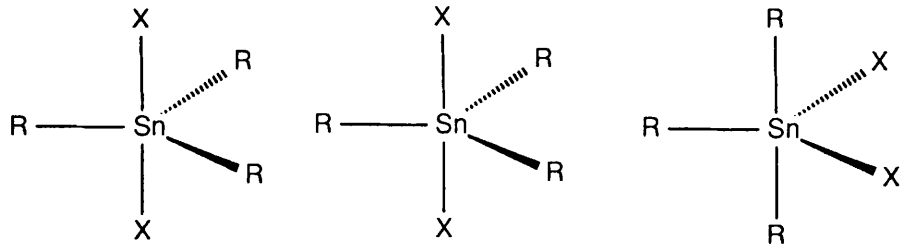

(XV) (XVI) (XVII)

For R_3SnX_2 type structures, three isomeric forms *trans*- (XV), *cis*- (XVI) and *mer*- (XVII), are possible though, as yet, no examples of the latter class have been unequivocably reported.[54]

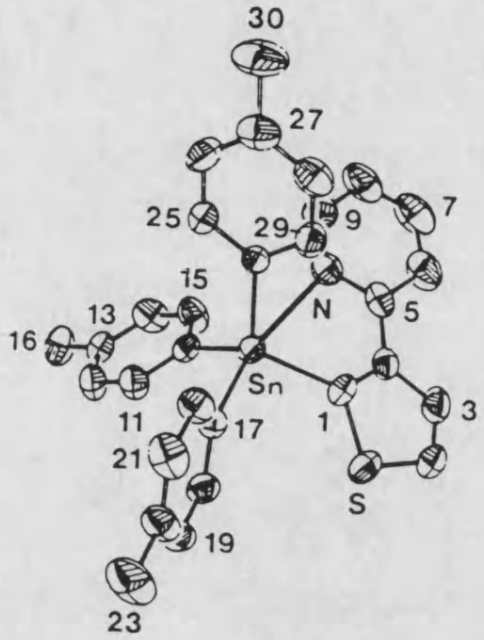

Figure 1.2: {C,N-[3-pyridyl)-2-(thienyl)]}tri(*p*-tolyl)tin

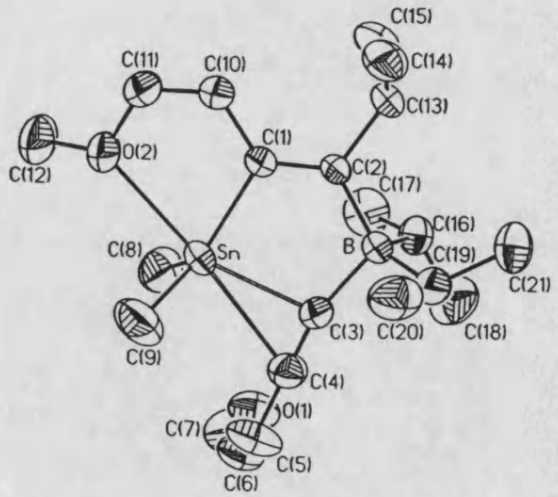

Figure 1.3: π-coordination-stabilised triorganotin cation

Of the remaining possibilities, *trans-* structures are more prevalent. These commonly occur as a result of bridging interactions giving rise to polymeric structures (see Section 1.4.6), although monomeric examples also exist. $Me_3SnCl.pyridine$,[19] $(3\text{-thienyl})_3SnBr.Ph_3PO$[55] and $Me_3SnCl.[HOC_{10}H_6CH{:}N\text{-}C_6H_4OCH_3]$[56] in which the Cl atom and the phenolic oxygen of the napthol ligand occupy the axial sites are examples. *Trans-* (bridging) and *cis-* sites have recently been reported in the same molecule.[57] In μ-oxalato-bis-(tricyclohexyltin), Figure 1.4, anisobidentate chelation of a tricyclohexyltin unit in a *cis-* fashion permits the remaining two oxygen atoms of the oxalato ligand to bind axially to two adjacent planar tricyclohexyltin groups, resulting in a linear chain structure.

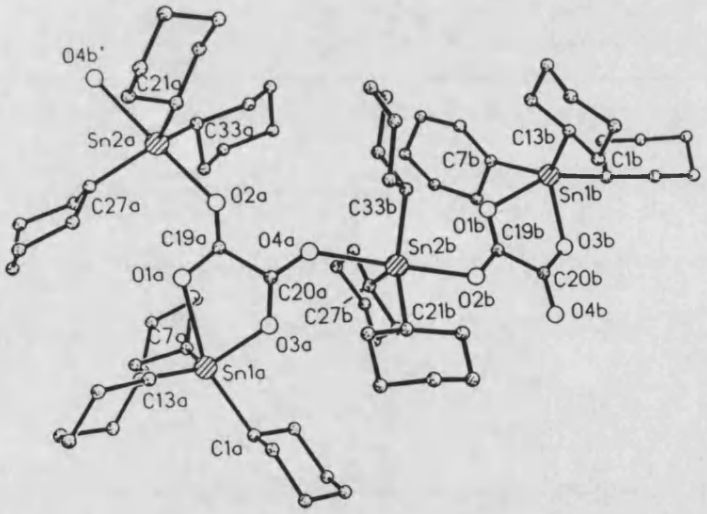

Figure 1.4: μ-Oxalato-bis-(tricyclohexyltin)

Entirely *cis-* analogues invariably arise from bidentate chelation effects. Examples include (1,3-diphenylpropanedionato)triphenyltin,[58] and recently (2-mercaptopyridine-N-oxide)triphenyltin (XVIII).[59]

Because of the tendency to increase coordination to six, examples of

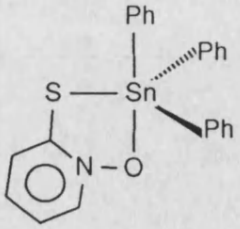

(XVIII)

five-coordinate diorganotin compounds are relatively rare. All reported R_2SnX_3 compounds are *cis-* and *mer-* with respect to the organic groups and X ligands respectively. Examples exist of both anionic, e.g. $[SnPh_2Cl_3]^-$, [60] $[(C_7H_6S_2)Ph_2SNCl]^-$, [61] and neutral forms e.g. dichloro(1-hydroxymethyl-pyrazole)dimethyltin[62] (Figure 1.5), with in all cases the organic groups occupying equatorial sites.

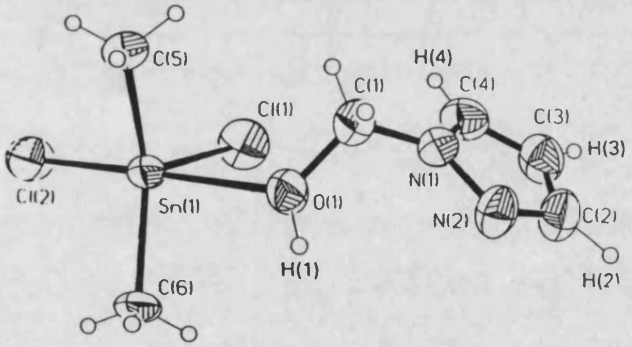

Figure 1.5: The structure of $SnMe_2Cl_2.(PzCH_2OH)$

Although examples of five coordinate $RSnX_4$ species are equally rare, anionic and neutral examples do exist. This is the case in $(Ph_4As)^+(MeSnCl_4)^-$ [63] and $Me_2N(CH_2)_3Sn(SPh)_3$,[64] in which the fifth coordination site is provided by intramolecular Sn-N coordination and the methyl group occupies an equatorial site.

1.4.4 Six Coordinate Molecular Organotin Compounds

A unique example of a hexacoordinate tetraorganotin exists. As was the case in Figure 1.2, the negligible acceptor properties of such compounds were overcome by employing 2-(3-thienyl)pyridine as an intramolecularly chelating organic ligand. The resulting bis[3-(2-pyridyl)-2-thienyl-C,N]diphenyltin (XIX)[65] presents octahedral geometry with the more electronegative pyridyl nitrogens in a *cis*- configuration,. The thienyl carbons meanwhile are in an approximately *trans*- relationship [C-Sn-C = 144.4°].

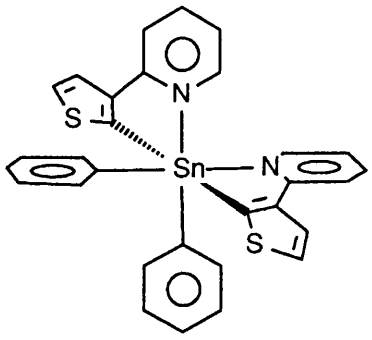

(XIX)

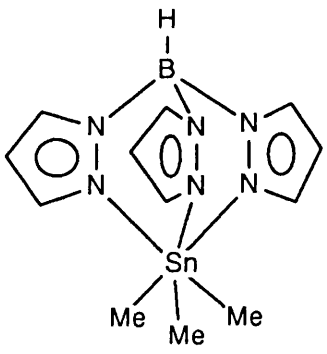

(XX)

Two examples of hexacoordinated triorganotin compounds have been crystallographically characterised, illustrating the possible isomeric forms for such systems. A *fac*-octahedral geometry is enforced by employing the uninegative, tridentate tris(pyrazolyl)borate ligand to produce $HB(pz)_3SnMe_3$,[66] (XX). *Mer*-octahedral geometry is adopted by bis[8-(methylamino)-1-napthyl]-methyltin iodide[67] (Figure 1.6), the two amine-substituted napthyl ligands providing intramolecular coordination.

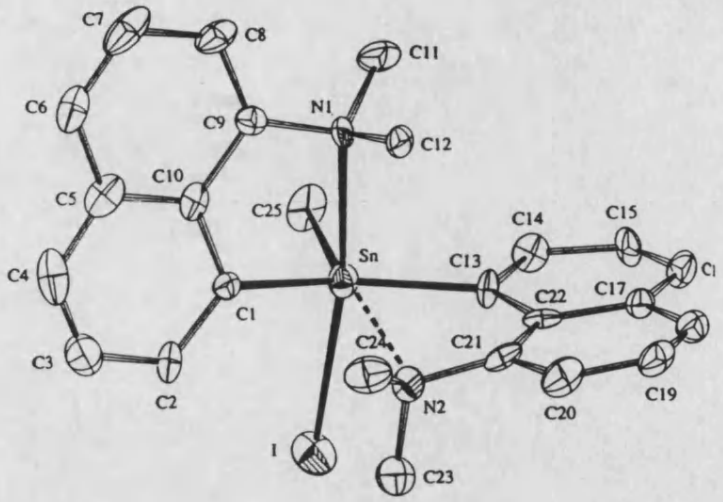

Figure 1.6: Structure of bis-[8-(methylamino)-1-napthyl]methyltin iodide

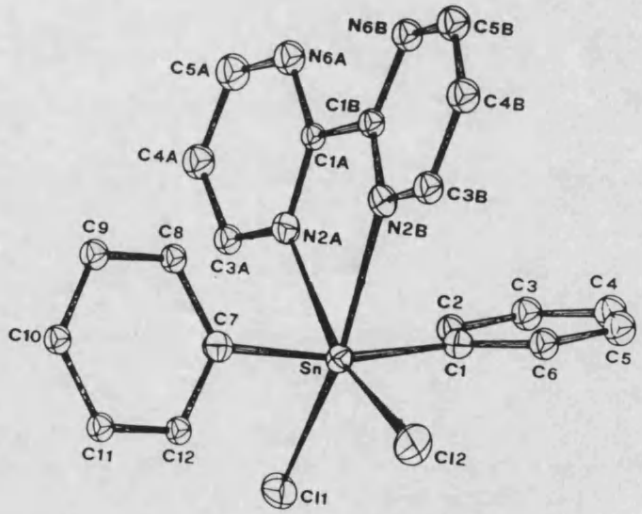

Figure 1.7: Perspective view of $[Ph_2SnCl_2.bipym]$

Six is the commonest coordination number for diorganotin compounds and, for discrete monomeric systems, both *cis*- (XXI) and *trans*- (XXII) isomeric forms are known.

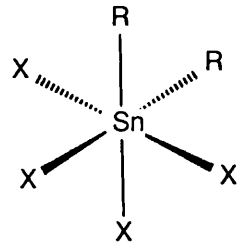

(XXI)

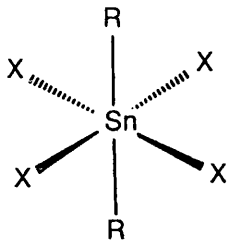

(XXII)

Trans- isomers are considerably more common and examples exist with both monodentate, e.g. $[(4\text{-}FC_6H_4)_2SnCl_2(C_2H_4SO)_2]$,[68] dibromo-bis(pyrazole)-diethyltin,[69] dichlorobis(imidazole)dimethyltin,[70] and bidentate chelating ligands e.g. [NN'-ethylenebis(salicylideneiminato)] dimethyltin[71] and Ph_2SnCl_2.bipym (Figure 1.7).[72]

Distortions from ideal octahedral geometry are common for chelated molecules. This is due to both ligand repulsions and anisobidentate interactions between the ligating unit and the tin atom. For example, the methyl groups lying above and below the S_4 plane in $Me_2Sn(S_2CNC_6H_4)_2$ subtend a C-Sn-C bond angle of 135.9°.[73] This is considerably different to the ideal *trans* angle of 180°.

Cis-octahedral geometry has also been achieved in the presence of two bidentate ligands, though the balance of factors determining the formation of such an arrangement over the *trans* possibility have not yet been fully determined. Adducts of $(4\text{-}ClC_6H_4)_2SnCl_2$ and 4,4′-Me_2bipy(2,2′) occur in both *cis*- and *trans*- forms, but isomerise to the more stable *trans* form in solution.[74]

Stable *cis*-geometry is observed in for example, $Ph_2Sn(SCSNEt_2)_2$[75] and dimethyltin bis-(8-hydroxyquinolate).[76] The structures of both these compounds are severely distorted with the ideal *cis* C-Sn-C bond angle of 90° forced open to

101.4° and 110.7° respectively.

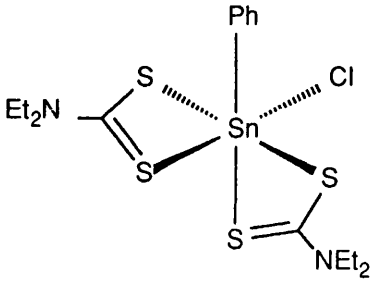

(XXIII)

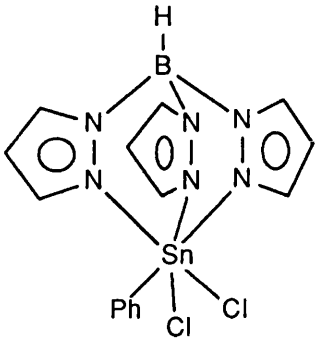

(XXIV)

Distorted octahedral geometry is also commonly observed for strongly Lewis acidic monoorganotin compounds. Examples include the OH-bridged dimer, $EtSn(OH)Cl_2.H_2O$[77], $PhClSn(SCSNEt_2)_2$ (XXIII)[78] and the *fac*-coordinated $PhCl_2Sn[HB(3\text{-}Me\text{-}Pz)_3]$ (XXIV).[79]

1.4.5 Seven Coordinate Organotin Compounds

Both di- and mono-organotins have been shown to form seven coordinate pentagonal bipyramidal (pbp) complexes. Dimethyltin di-isothiocyanate, when adducted to terpyridyl, adopts an almost ideal pbp configuration (Figure 1.8).[80] The methyl groups are in axial positions with the tin atom lying in the equatorial plane.

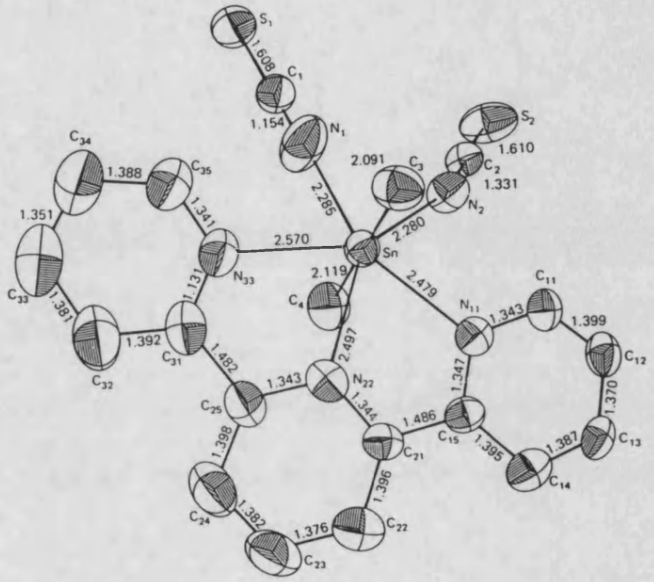

Figure 1.8: Structure of $(CH_3)_2Sn(NCS)_2(C_{15}H_{11}N_3)$

A distorted *trans*-geometry, with a C-Sn-C angle of 154.3°, is observed in $[MeOC(O)(CH_2)]_2Sn[SC(S)NMe_2]_2$.[81] Two typical examples of distorted pbp coordination in a monoorganotin system have recently been published. Tris(2-pyridinethiolato)(p-tolyl)tin[82] and n-butyl tris(2-pyrimidinethiolato-N,S)tin[83] both give rise to similar structures, with the organic ligand in an axial position above the pentagonal plane.

1.4.6 Self-Associated Polymeric Structures

The examples chosen thus far to illustrate the possible geometries adopted by organotins have all been based around discrete monomeric species. However Lewis acidic organo-substituted tin compounds, when adducted to suitably disposed ligands, will also form associated oligomeric clusters and one, two and three-dimensional polymeric networks.

Infinite one-dimensional structures of general formula R_3SnX are common. Based around a *trans*-R_3SnX_2 repeat unit, polymer propagation is provided between trigonal bipyramidal tin units by bridging X ligands. Examples include Me_3SnCl,[84] Me_3SnN_3[85] and recently $Ph_3SnN(SO_2Me)_2$ (Figure 1.9).[86]

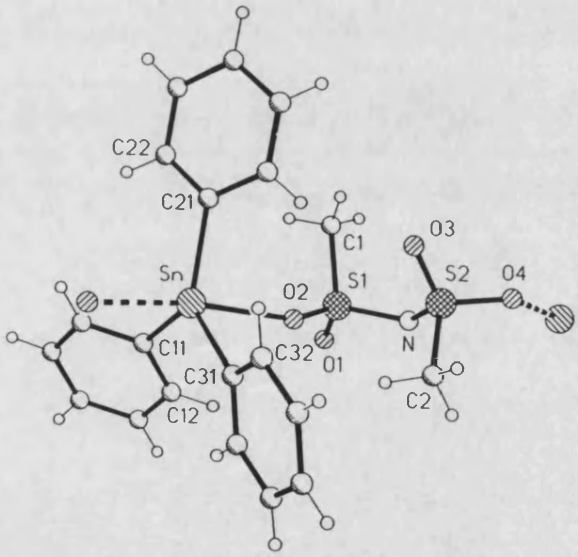

Figure 1.9: The Polymeric Structure Of $Ph_3SnN(SO_2Me)_2$

Similar one-dimensional chains, but with double atom bridges and octahedral tin, are formed by several diorganotin dihalides and pseudohalides. The structures of Me_2SnCl_2,[87] Et_2SnCl_2[88] and Et_2SnBr_2[88] are very similar with the arrangement of groups around tin now describing an irregular octhedral *trans*-R_2SnX_4 geometry with co-planar bridging halide pairs (XXV).

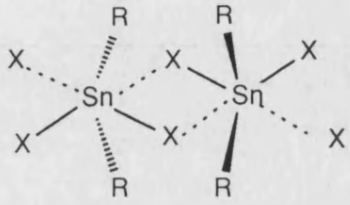

(XXV)

Diethyltin diiodide[88] and dimethyltin di-isothiocyanate[89] form a different type of structure in which the X groups bridge in a chelating fashion (XXVI).

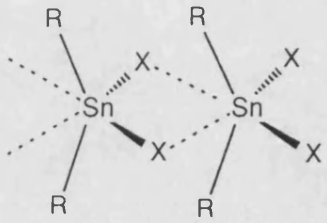

(XXVI)

Structural variations of this nature are primarily the result of varying Lewis acidities on the tin atom, though steric interactions of the organic ligands also influence the type of structure adopted. A further fine interplay of forces is observed in the crossover from discrete four or five coordinate monomeric triorganotin carboxylates, (XXVII) and (XXVIII), to five coordinated bridged polymeric systems (XXIX).

Although the mode of coordination and the manner in which polymeric systems propagate through space is largely determined by the steric demands of both the hydrocarbon and ligand residues, electronic effects also play a role in the control of structure. In this respect, the structural variations observed in twenty five triphenyltin benzoates have been discussed in terms of a qualitative molecular orbital analysis.[90]

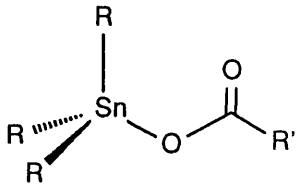

(XXVII)

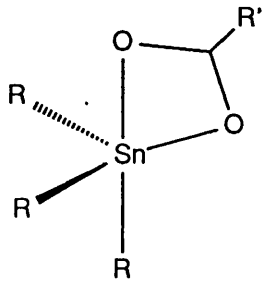

(XXVIII)

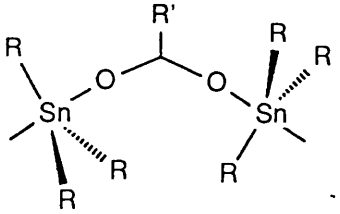

(XXIX)

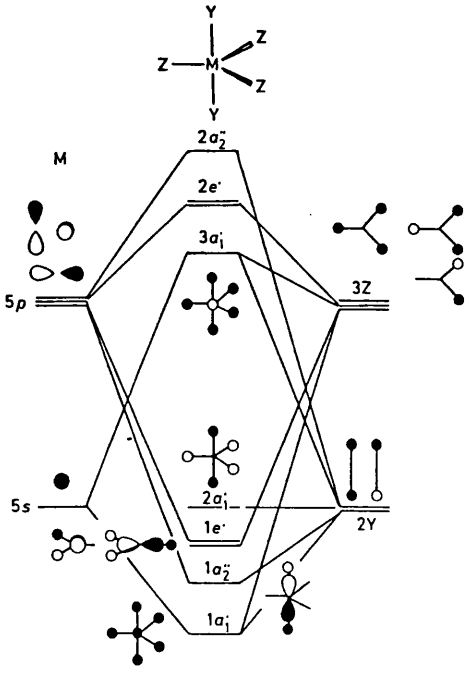

Figure 1.10: MO energy level diagram for *trans*-MZ_3Y_2

It was found that the lowest energy description of monomeric structures occurred when the ligands were of similar electronegativity to the tin-bonded carbon residues. As the relative electronegativity of the carboxylate is raised however, polymeric structures begin to dominate with intermediate systems determined by the steric requirements of the compound. For the polymeric *trans*-isomer the HOMO is a non-bonding molecular orbital (see Figure 1.10) centred on the two axial ligands. This is most stable (i.e. of lowest energy) when the electronegativity of the ligands is as high as possible.

Lattice association into two dimensions begins with the formation of cyclic oligomers. A recent crystallographic study[91] describes tri-n-butyltin-2,6-difluorobenzoate as a macrocyclic tetramer containing a sixteen-membered $Sn_4C_4O_8$ ring. A single butyl group is directed toward the inner side of the macrocyclic cavity and the compound becomes monomeric in solution. In contrast trimethyltin diphenylphophinate,[92] also shown to have a cyclotetrameric structure (Figure 1.11), retains this architecture in solution and has two methyl groups directed towards the inside of the cavity. It is not certain whether this latter structural difference is due to a feature of the macrocycle or simply to the larger size of the butyl in comparison to the methyl groups. Certainly the formation of a hexameric macrocycle is required to accommodate the more bulky phenyl groups in $[Ph_3SnO_2P(PPh)_2]_6$[93] and $[Ph_3SnO_2P(Me)(OMe)]_6$ (Figure 1.12).[94]

These represent the largest ring systems characterised thus far, and again the geometrical constraints applied by the invariant nature of the almost perfect trigonal bipyramidal triorganotin moiety should be noted.

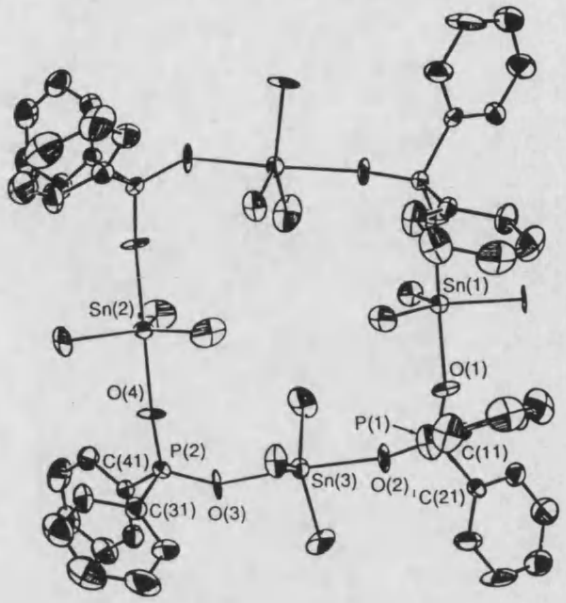

Figure 1.11: Tetrameric Structure of *cyclo*-$[Me_3SnOPPh_2]_4$

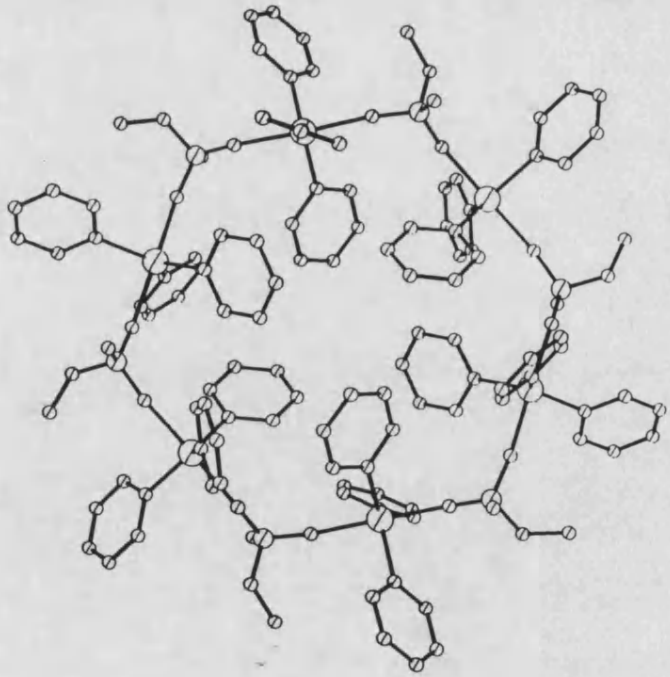

Figure 1.12: Hexameric structure of *cyclo*-$[Ph_3SnO_2P(Me)(OMe)]_6$

In the foregoing instances, the macrocyclic structures exist as discrete oligomeric species. However when intermolecular association can occur in two dimensions, ribbon and sheet structures result. For example $(Me_2Sn)_3(PO_4)_2$-$.8H_2O$ (Figure 1.13)[95] consists of infinite ribbons in which octahedral *trans*-dimethyltin, *cis*-diaquo units are *cis*-linked by PO_4 tetrahedra to give strips of eight membered rings in chair conformations.

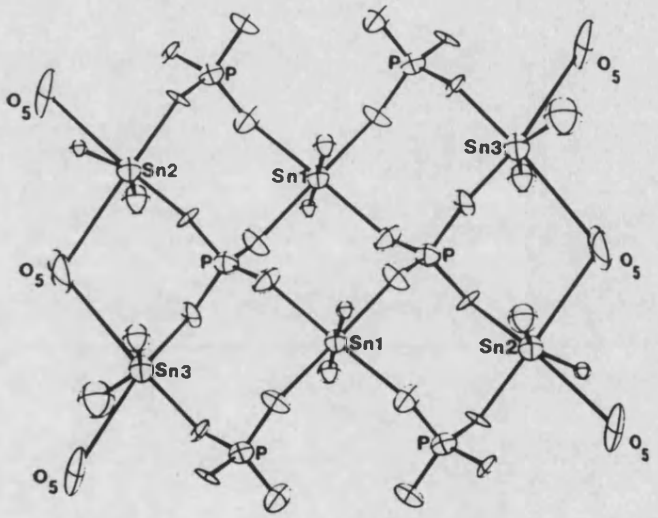

Figure 1.13: The Ribbon Structure of $(Me_2Sn)_3(PO_4)_2.8H_2O$

Examples of this type however are rare, increasing association reducing solubility and inhibiting the growth of crystals. Most available structures occur with diorganotin dihalides or pseudohalides such as $Me_2Sn(CN)_2$,[96] although more recently $(CH_3)_2Sn(O_2CH)_2$[97] has been shown to assemble in a similar fashion.

A rich cluster chemistry of organotin compounds has recently emerged based on Sn-O-Sn and Sn-S-Sn bonding formed in reactions of stannoic acids with carboxylic and phosphorus-based acids as participating ligands. Drum and

ladder structures, formed via the fusion of smaller tin-oxygen ring systems, are particularly prevalent and new structures are being published continually. Although the chemistry of these ubiquitous mono- and di- stannoxanes provides numerous examples of three-dimensional oligomers[98] [e.g. the spectacular 'football-like' $[(^{i}PrSn)_{12}O_{14}(OH)_6]^{2+}$ [99] (Figure 1.14)], genuinely three-dimensional network structures are scarce. The reactions of trimethyltin halides with polyfunctional $[M(CN)_6]^{X-}$ anions (e.g. M = Co, Fe; X = 3,4) has however provided several interesting, highly associated lattices.

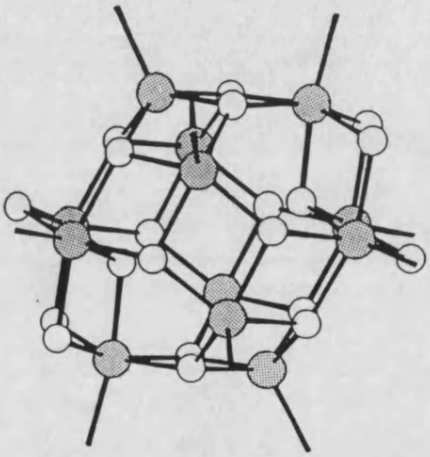

Figure 1.14: The Cage Cation, $[(^{i}PrSn)_{12}O_{14}(OH)_6]^{2+}$

The lattice of $(Me_3Sn)_3[Co(CN)_6]$ (Figure 1.15),[100] contains distorted octahedral $Co(CNSn)_6$ fragments (two thirds of the Co-C≡N-Sn sections are bent at the N atom by 157.7° or 146.2°) and trigonal bipyramidal N_2SnMe_3 units within a strictly three-dimensional network. The observation has been made that the large cavities formed through the lattice are 'padded' by the organic groups attached to tin. It is suggested that increasing the steric bulk of these groups may force all the C≡N-Sn angles to become 180°, resulting in a marked expansion and simplification of the lattice.

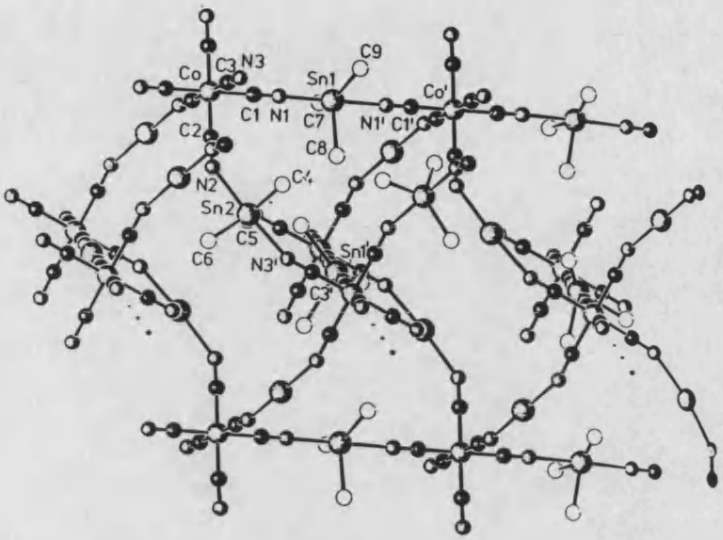

Figure 1.15: The Extended Lattice Structure of $(Me_3Sn)_3[Co(CN)_6]$

The cavities provided by lattices of this type have also been shown to provide intercalation sites for three-dimensional host-guest systems. $[(Me_3Sn)_4Fe(CN)_6.2H_2O.C_4H_8O_2]_\infty$[101] contains hydrogen bonded water and dioxane molecules between chains of octahedral $Fe(CN)_6$ and *trans*-tbp Me_3Sn units and prelimiary work has suggested that these solvent inclusions may be replaced by more complex carbohydrates.

1.5 Spectroscopy of Organotin Compounds

The vast majority of the structures taken as examples in the preceding section were extracted from single-crystal x-ray diffraction studies. However many organotin compounds do not form suitable crystals or are amorphous or liquid at room temperature. In this respect the organotin chemist is fortunate that a whole armoury of general and more specific spectroscopic techniques are available for the characterisation and structural classification of organotin compounds.

The routine techniques of ultra-violet,[2] infra-red[2,102] and mass spectrometry[4] can provide information on ligand structure as can ^{1}H and ^{13}C NMR. More direct inferences on the nature and stereochemistry of the tin centre may be extracted from ^{1}H and ^{13}C coupling constant data and the nucleus-specific techniques of ^{119m}Sn Mössbauer and ^{119}Sn NMR. These latter techniques shall be discussed in greater depth.

1.5.1 Mössbauer Spectroscopy

Mössbauer spectroscopy is perhaps more aptly described by its alternative title of nuclear gamma resonance spectroscopy, since the effect under scrutiny is the emission and resonant absorbtion of γ-rays in certain elements.

The theory and basic principles of ^{119m}Sn Mössbauer phenomena have been described comprehensively in many books[103-106] and general reviews[107-110] and only a brief summary of the physical processes and practicalities involved is presented here. The Mössbauer effect is a nuclear process observed for tin when the source, the metastable ^{119m}Sn isotope, emits a 23.875 keV γ-ray and excites a ^{119}Sn nucleus to its first excited state (Figure 1.16). γ-rays have precisely defined energies and thus the exciting radiation is strictly monochromatic. The energy of the emitted γ-rays can however be modulated employing the Doppler effect, by mounting the source on a vibrator and applying a controlled velocity. For this

reason Mössbauer parameters are expressed in units of mms^{-1}, the energy difference between pairs of nuclear energy levels (ΔE_1, ΔE_2) being necessarily small.

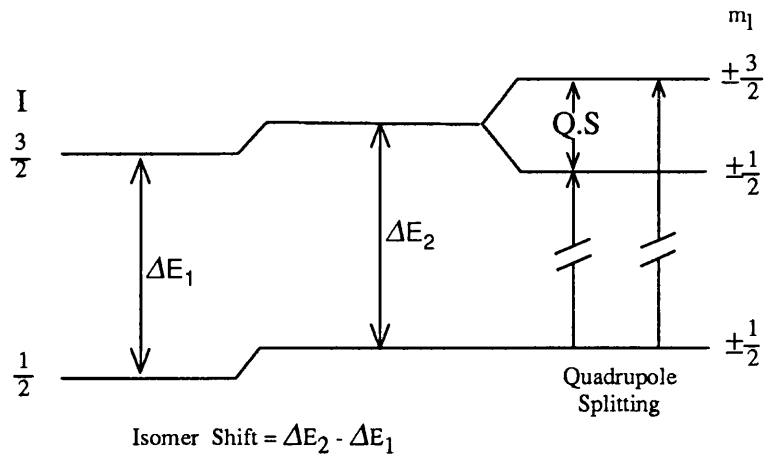

Figure 1.16: Nuclear Energy Levels, Isomer Shift and Quadrupole Splitting for I_{gr}=1/2, I_{ex}=3/2

The sample should preferentially be in the solid phase since the nuclei under investigation must be prevented from recoiling when they absorb gamma radiation. In practice only a small number of nuclei do not suffer recoil and it is this recoil-free fraction which gives rise to the observed spectrum. The recoil-free fraction can be increased by lowering the temperature and for this reason spectra are routinely run at liquid nitrogen temperatures. The temperature dependence of the recoil-free fraction can be exploited in variable temperature Mössbauer experiments to differentiate between associated and discrete molecular lattices, although a full discussion is out of the scope of this review.

The two most important Mössbauer parameters are the isomer shift, δ (mms^{-1}), and the quadrupole splitting, ΔEq (mms^{-1}), with δ usually quoted relative to SnO_2 or $BaSnO_3$ as zero.

The isomer shift is due to the mismatch between the ground and first excited nuclear energy levels respectively (ΔE_2 - ΔE_1 in Figure 1.16) and

therefore governs the overall position of the spectrum on the energy (velocity) scale. Differing isomer shift values correspond to differing chemical environments, primarily due to changes in the electron density of the valence 5*s* electrons which have a finite chance of existing at the nucleus. For this reason tin(II) and tin(IV) compounds fall into characteristic regions in the overall velocity range of *ca.* -1.00 to +5.00 mms^{-1}. Sn(IV) compounds appear between -0.5 and +2.7 mms^{-1}, whilst Sn(II) compounds, due to their lone pair of 5*s* electrons, have increased *s*-electron density at the nucleus and correspondingly larger values of δ (above + 2.10 mms^{-1}).

For tetrahedral sp^3 hybridised organotin(IV) compounds anything which perturbs the *s*-electron density will bring a concommitant change in the isomer shift. Table 1.2 illustrates how δ varies with the inductive effect of R for a series of R_4Sn and R_3SnCl compounds.[107,108] The value increases as the organic ligand becomes more electron donating.

Table 1.2: Variation of δ(mms^{-1}) with R group

R	δ(mms^{-1}) R_4Sn	δ(mms^{-1}) R_3SnCl
Me	1.20	1.43
Et	1.30	1.57
Pr	1.30	1.62
Bu	1.35	1.65
Ph	1.15	1.37

The isomer shift is also affected by the electron-withdrawing properties of the groups attached to tin. For a series of iso-organyl R_3SnL compounds the value of δ is reduced as the elecronegativity of L increases to reduce the electron density on tin (Table 1.3).[107,108]

Table 1.3: Effect of Halogen Electronegativity on δ

L	$\delta(mms^{-1})$ Ph_3SnL	$\delta(mms^{-1})$ Bu_3SnL
F	1.25	1.31
Cl	1.37	1.38
Br	1.40	1.50
I	1.41	1.52

For any given coordination number, changes in stereochemistry bring changes in δ. For example, in a series of octahedral diorganotins, *cis-* isomers generally have lower values of δ than their *trans* analogues. This is possibly due to a higher percentage of *s* character in the Sn-C bonds of the latter.

The second important Mössbauer parameter, the quadrupole splitting (ΔEq), arises from an asymmetry in the electron cloud around the nucleus. Tin nuclei with perfectly spherical symmetry, e.g. Bu_4Sn, have zero field gradient and give rise to a single line (Figure 1.16). However if an electric field gradient (e.f.g.) is generated at the nucleus by the placement of asymmetric extra-nuclear charges, the degeneracy of the quadrupolar first excited state (I_{ex} = 3/2) is partially lifted and a characteristic two line spectrum is obtained (Figure 1.17). ΔEq is the energy difference between the two transitions and δ is measured as the centroid of the two peaks relative to the source. The value of ΔEq can be applied more usefully than δ to the diagnosis of stereochemistry since, particularly for di- and tri-organotin compounds, it is found that definite ranges of ΔEq exist for particular ligand configurations (Table 1.4).

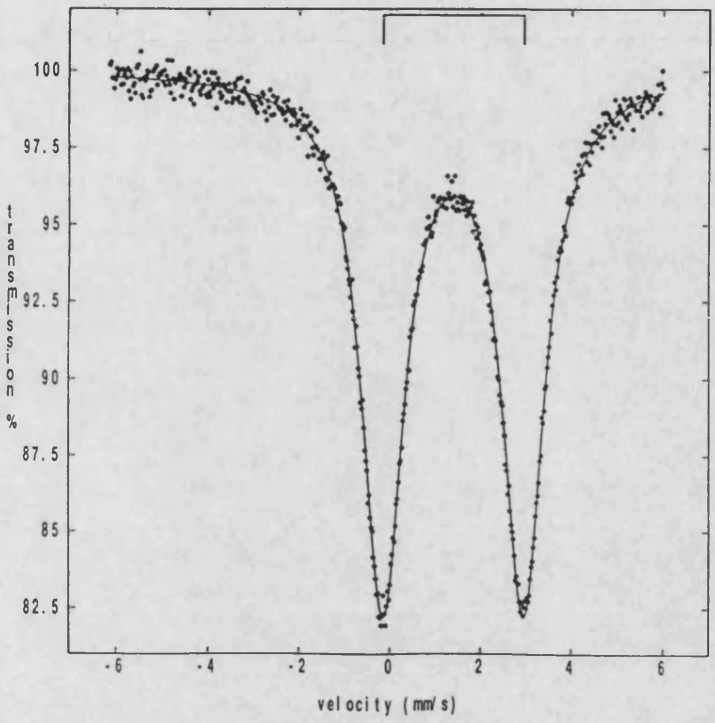

Figure 1.17: A Typical 'doublet' Mossbauer Spectrum

Table 1.4: ΔEq values for different stereochemistries

Structure	Coordination Number	Stereochemistry	ΔEq Range
R_3SnX R_2SnX_2	4	tetrahedral	1.00-2.40
R_3SnX_2	5	*trans*-tbp	3.00-4.00
R_3SnX_2	5	*cis*-tbp	1.70-2.40
R_2SnX_4	6	*cis*-Oh	1.70-2.20
R_2SnX_4	6	*trans*-Oh	3.50-4.20

Several attempts to calculate ΔEq values for various geometries have been made, based upon an additive model in which the electric field gradient is viewed as being constructed from contributions from each ligand.[111,112]

Regular tetrahedral di- and tri-organotin compounds generally show splittings within the range shown in Table 1.4. Observed splittings for trigonal bipyramidal *trans*-isomers are considerably larger than their *cis*-analogues with higher values within the set ranges being indicative of asymmetric ligand linkages. Values of ΔEq for octahedral R_2SnX_4 compounds are remarkably insensitive to the nature of X and vary preditably between ~2.00 mms^{-1} and ~4.00 mms^{-1} as the C-Sn-C bond angle moves from ~90° to 180°. Good estimates of ΔEq for diorganotin compounds can be calculated from Formula 1.1,[107]

$$|\Delta Eq| = -4[R][1 - (3/4)\sin^2\alpha]^{\frac{1}{2}} \qquad \text{(Formula 1.1)}$$

where α is the C-Sn-C bond angle and [R] is the partial quadrupole splitting for the organic group. Although agreement is noted for a wide range of C-Sn-C angles (110.7°-180°),[113] a recent example reveals the potential shortcomings of such semi-empirical relationships. Crystallographic analysis of Ph_2SnCl_2.bipym[72] (Figure 1.7), reveals a *trans*-octahedral arrangement with a C-Sn-C angle of 169.3°. Although the experimental value for ΔEq of 3.43 mms^{-1} is consistent with such an arrangement of ligands, use of Formula 1.1 gives a somewhat under-estimated bond angle of 151°.

1.5.2 ^{119}Sn NMR Spectroscopy

Elemental tin contains ten stable isotopes. Of these, three have nuclear spin of I = 1/2, ^{115}Sn (abundance 0.34%), ^{117}Sn (7.57%) and ^{119}Sn (8.58%), and are thus amenable to study by nmr spectroscopy. The latter however is the nucleus of choice because of its marginally superior abundance and receptivity ($4.44 \times 10^{-3}$with respect to ^{1}H). The practical and theoretical techniques of ^{119}Sn NMR have been exhaustively covered in numerous books[4,106,114,115] and reviews[116-119] which also contain extensive tabulated chemical shift and coupling constant data.

^{119}Sn chemical shifts of organotin(IV) compounds cover a range of some 600 ppm (Figure 1.18).[6] Spectra are quoted as relative to Me_4Sn as zero with the chemical shift, $\delta(^{119}Sn)$, values becoming progressively more negative as the nucleus becomes more shielded. The position of the observed signal is determined by a number of structure and solvent-dependent factors and is thus highly indicative of the composition and structure of the compound in question.

As the electron-releasing properties of the attached R groups increase the tin atom becomes progressively more shielded and $\delta(^{119}Sn)$ moves to higher field (Table 1.5).[116]

Table 1.5: $\delta(^{119}Sn)$ (ppm.) of Alkyl and Phenyl Tin Chlorides

R	$RSnCl_3$	R_2SnCl_2	R_3SnCl
Me	+20	+141	+164
Et	+6.5	+126	+155
^{n}Bu	+6.0	+122	+141
Ph	-63	-32	-48

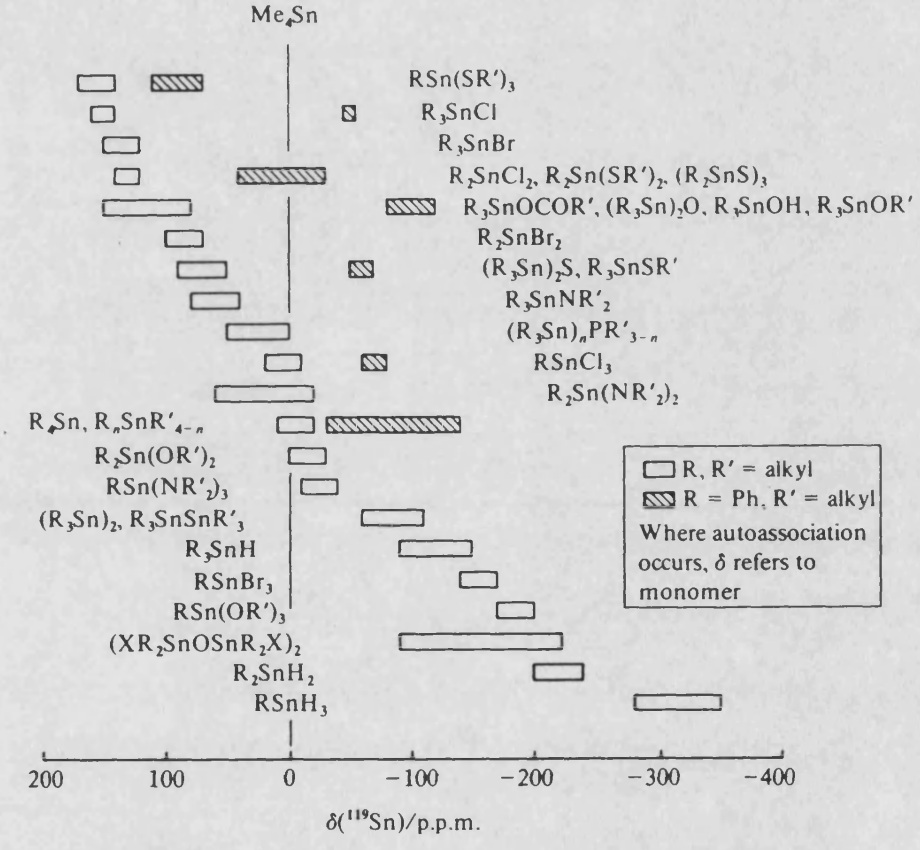

Figure 1.18: ^{119}Sn chemical shifts in non-coordinating solvent

Purely on the basis of inductive properties it would be expected that the electron withdrawing properties of phenyl groups would result in less shielding and hence more positive chemical shifts. That this is not the case is attributed to its increased polarisability and is also the case for other unsaturated substituents such as vinyl or allyl.

The electron withdrawing properties of attached ligands also affect $\delta(^{119}Sn)$, with values generally moving to lower field as, for example in a given series of R_3SnX halides, the electronegativity of X increases. For multiple substitution of electronegative groups on tin it is intuitively reasonable to expect a linear inrease in shielding for a series of $R_{4-n}Snx_n$ type compounds. Although the exact reasons are not understood the largest downfield shifts are in fact observed to occur for n = 1 or 2[120,121] (Figure 1.19). A decrease in shielding is followed by a progressive increase to give a characteristic U-shaped dependence of δ on n. Similar curves have been reported for a wide range of R and X groups.

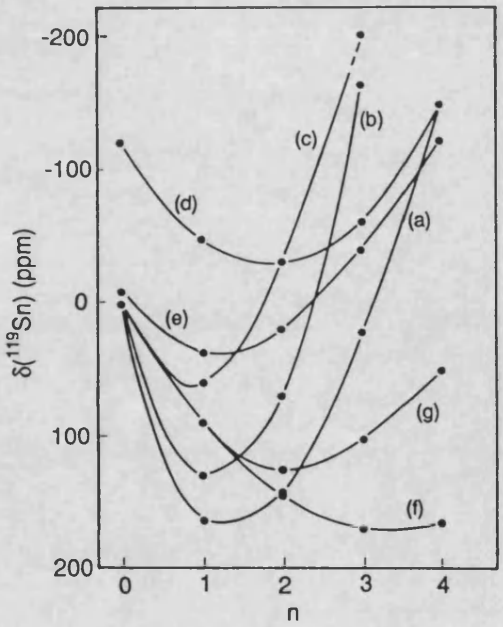

Figure 1.19: $\delta(^{119}Sn)$ vs.n for various $R_{4-n}SnX_n$ series. R,X = Me, Cl(a); Me, Br(b); Bu, O^{t}Bu(c); Ph, Cl(d); Bu, NEt_2(e); Me, SMe(f); and Me, S^{t}Bu(g).

In contrast mixed tetraorganotins of the type $RnSnR'_{4-n}$, e.g. Bu_nSnPh_{4-n},[122] do show linear dependences of shielding with progressive substitution of R′ ligands. It has been suggested that ligand polarisability may be important in this case.[119]

A further substituent effect is noted if the tin atom is incorporated into a five or six-membered ring e.g. (XXX) or (XXXI).

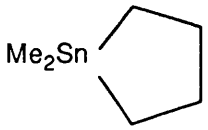

δ = +53.5

(XXX)

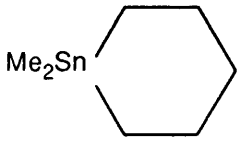

δ = -42.5

(XXXI)

Due to steric constraints the five membered ring compounds are considerably deformed from the ideal tetrahedral geometry at tin. This 'ring strain' effect causes considerable downfield shifts.[123]

Rather more dramatic chemical shift variations than the substituent effects discussed thus far are observed with changes in coordination number. Precise ranges of $\delta(^{119}Sn)$ are not encountered for particular coordination numbers as substituent variation at tin serves to mask some of the coordination effects. However for systems with similar R groups, δ moves progressively upfield in moving from four to five to six to seven coordinate geometry. This is illustrated using the unique series of thienyl-substituted tetraorganotin compounds in Table 1.6. Upfield shifts of this nature are reasoned to be due to enhanced shielding by the increased electron density on the tin atom most likely a result of increased occupancy of the extra-nuclear 5*d* orbitals of tin. This trend contrasts with the decreases noted in Mössbauer isomer shift with increases of coordination number where the dominant factor is increased usage of the 5*s* orbitals.

Table 1.6: $\delta(^{119}Sn)(CDCl_3$ solution) values for tetra-organotin compounds of varying coordination number

Compound	Coordination Number	$\delta(^{119}Sn)$	ref
$(2\text{-}C_4H_3S)_4Sn$	4	-147.0	124
$(2\text{-}C_4H_3S)_2SnPh_2$	4	-140.8	125
$LSn(p\text{-}tolyl)_3$[a]	5	-176.3	48
$LSnPh_3$[a]	5	-181.6	48
L_2SnPh_2[a]	6	-245.5	65

[a] L = [3-(2-pyridine)-2-C_4H_2S]

Solvent effects are also important in ascertaining the chemical shifts of potentially Lewis acidic organotin compounds. Polar solvents such as acetone, pyridine and dimethyl sulphoxide (DMSO) can form *in situ* adducts with resulting increase in coordination and upfield chemical shift. For example, the series of trivinyltin halides illustrated in Table 1.7[126] exhibit pronounced upfield shifts when measured in DMSO, corresponding to the formation of five-coordinate adducted species.

Table 1.7: $\delta(^{119}Sn)$ Values of Trivinyltin Halides in $CDCl_3$ and DMSO-d^6

Compound	$\delta(^{119}Sn)$(ppm) $CDCl_3$	$\delta(^{119}Sn)$(ppm) DMSO-d^6
$(CH_2{=}CH)_3SnCl$	- 52.8	-215.5
$(CH_2{=}CH)_3SnBr$	- 72.1	-210.1
$(CH_2{=}CH)_3SnI$	-132.0	-206.3

Organotin compounds with a pronounced tendency to form associated

polymeric species in the solid state will also auto-associate in solution. This phenomenon is concentration dependent and may be readily observed by variable concentration ^{119}Sn NMR studies. For example a 3M solution of trimethyltin formate in $CDCl_3$ forms five coordinate oligomeric or polymeric species with $\delta(^{119}Sn)$ = +2.5 ppm whereas in 0.05M solutions tetrahedral monomers predominate with $\delta(^{119}Sn)$ = +152 ppm.[127]

A great range of $^{n}J(^{119}Sn, X)$ (n = 1, 2, 3, 4) coupling constant data are available for a wide variety of spin I = 1/2 nuclei. Instances involving ^{1}H and ^{13}C are however most frequent and $^{1}J(^{119}Sn, ^{13}C)$ and $^{2}J(^{119}Sn, ^{1}H)$ are the most important as regards stereochemical information.

$^{1}J(^{119}Sn, ^{13}C)$ values have been observed to fall into characteristic ranges, dependent on the coordination number and geometry about tin. Examples for triphenyl,[128] tributyl[129] and tribenzyltin[130] compounds of various geometries are illustrated in Table 1.8.

Table 1.8: $^{1}J(^{119}Sn, ^{13}C)$ Values for R_3SnX Compounds

Structure	R = Ph $^{1}J(^{119}Sn, ^{13}C)$(Hz)	R = Bu $^{1}J(^{119}Sn, ^{13}C)$(Hz)	R = Bz $^{1}J(^{119}Sn, ^{13}C)$(Hz)
Monomeric R_3SnX	550 - 660	320 - 390	180 - 345
Cis - tbp	600 - 660	350 - 395	180 - 345
Trans-tbp	750 - 850	440 - 510	415 - 460

Such variations in coupling constants may reflect the amount of *s*-character in the Sn-C bond. For example, the bonding in tetrahedral R_3SnX compounds can be interpreted in terms of four sp^3 hybrid orbitals. On the other hand in *trans*-tbp structures the three Sn-C bonds are constructed fron sp^2 hybridised orbitals with the remaining 5*p* orbital participating in bonding with the

axial substituents. The value of the coupling constant, reflecting spin-spin coupling of neighbouring nuclei, depends mainly on the value of the Fermi contact term. This, and therefore the ^{n}J values, are proportional to the amount of *s*-character of the hybrid orbitals accounting for the observed differences in coupling. Similar reasoning also accounts for the higher values observed for triphenyltin (sp^2 hybrid carbon orbitals) compounds over analogous trialkyltin derivatives (sp^3 hybrid orbitals).

Correlations between angular geometry and coupling constants have also been extended to derive several semi-empirical relationships between crystallographically determined C-Sn-C bond angles and observed J values. Howard *et al.*[131] derived the following linear relationships based on seven hexacoordinate chelate complexes in $CDCl_3$ solution.

$$\theta = 2.28|^2J(^{119}Sn, ^1H)| - 46.4 \qquad \text{(Formula 1.2)}$$

$$\theta = 0.178|^1J(^{119}Sn, ^{13}C)| + 14.74 \qquad \text{(Formula 1.3)}$$

where θ = C-Sn-C bond angle. These two equations give values of θ with standard errors of $\pm 5.6^\circ$ and $\pm 12.1^\circ$ respectively.

From a more extensive study of twenty five methyl-substituted compounds, Lockhart and Manders[132] derived the quadratic relationships

$$\theta = 0.0161|^2J(^{119}Sn, ^1H)|^2 - 1.32|^2J| + 133.4 \qquad \text{(Formula 1.4)}$$

$$\theta = 0.0105|^2J(^{119}Sn, ^1H)|^2 - 1.32|^2J| + 122.4 \qquad \text{(Formula 1.5)}$$

Most of the compounds included in the study tender θ to within 4° of Formula 1.4. Curiously however the angular relationship for Me_2SnCl_2 and Me_2SnBr_2, recorded in a range of solvents, always conformed to the latter curve.

Finally a detailed study of n-butyltin compounds[133] reveals a linear

dependence of $^{1}J(^{119}Sn, ^{13}C)$ in tetra-, penta- and hexa-coordinate compounds, in $CDCl_3$ solution, on the C-Sn-C angle, θ, obtained from x-ray analyses (Formula 1.6).

$$|^{1}J(^{119}Sn, ^{13}C)|=(9.99\pm0.73)\theta-(746\pm100) \qquad \text{(Formula 1.6)}$$

1.5.3 Infra-red Spectroscopy of Organotin Compounds

Infra-red spectroscopy has two routine applications in synthetic organotin chemistry:

i) Determination of the identity of various known compounds by spectral comparison with that of an authentic sample. To this end several reviews of published i.r. data exist.[134-136]

ii) Verification of the presence of functional groups and the mode of bonding in prepared compounds.

For example, organotin esters can be successfully characterised by comparison of their spectra with those of their precursors.[137-139] The vibration associated with the COOH group of the free acid disappears indicating that the organotin moiety is bonded through the carboxyl group of the acid. Additionally the mode of coordination can be ascertained via the separation of the $\nu_{asym}(COO)$ and $\nu_{sym}(COO)$ stretches. A lowering of $\nu_{asym}(COO)$ compared with $\nu_{sym}(COO)$ of the carboxylate group and vice versa is indicative of bidentate and unidentate coordination respectively.

Depending on the symmetry of the molecule highly characteristic Sn-X stretching frequencies can be observed. Band positions are dominated by the mass effect, falling to lower frequencies as the mass of X increases. Several examples are illustrated in Table 1.9.

Table 1.9: Typical Sn-X Stretching Frequencies

Bond	Compound	ν(Sn-X)(cm^{-1})	ref.
Sn-H	Me_2SnH_2	1863	140
Sn-H	Me_3SnH	1846	140
Sn-C	Me_4Sn	526, 506	141
Sn-O-Sn	$Ph_3Sn)_2O$	777	142
Sn-N	Bu_3SnNR_2	584-603	143
Sn-S	$Me_3Sn)_2S$	367, 322	144
Sn-Cl	R_nSnCl_{4-n}	328-382	145
Sn-Br	R_nSnBr_{4-n}	222-264	145
Sn-I	R_nSnI_{4-n}	174-207	145

1.5.4 Mass Spectra of Organotin Compounds

The relative abundance of the ten stable tin isotopes makes the identification of tin-containing mass fragments relatively simple. In addition mono-, di- and tri-tin fragments are readily identifiable by the various possible combinations of isotope masses (Figure 1.20). Chambers *et al.* have summarised most of the common fragmentation patterns of organotins.[146]

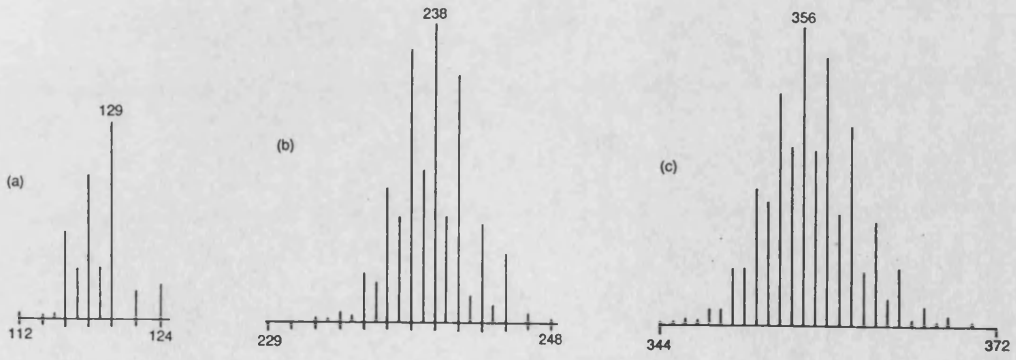

Figure 1.20: Characteristic Isotopic Distribution Patterns for Tin in (a) natural abundance, (b) Sn_2, (c) Sn_3

1.6 Previous Work and Aims of this Thesis

Work in this laboratory has previously centred upon enhancing the hydrolytic and aerobic stability of potentially biocidal triorganotin C-bonded heterocycles. This can be achieved via the inclusion of a passive alkyl chain between the two units i.e. $R_3Sn(CH_2)_nR'$ where R′ = imidazole, benzothiazole or benzoxazole.[147] In the preparation of compounds where R′ = tetrazolyl, the established ring-building 1, 3 dipolar cycloaddition of an organic nitrile and a triorganotin azide has been employed. For example the reaction of (3-cyanopropyl)triphenyltin and tributyltin azide (Scheme 1.2).

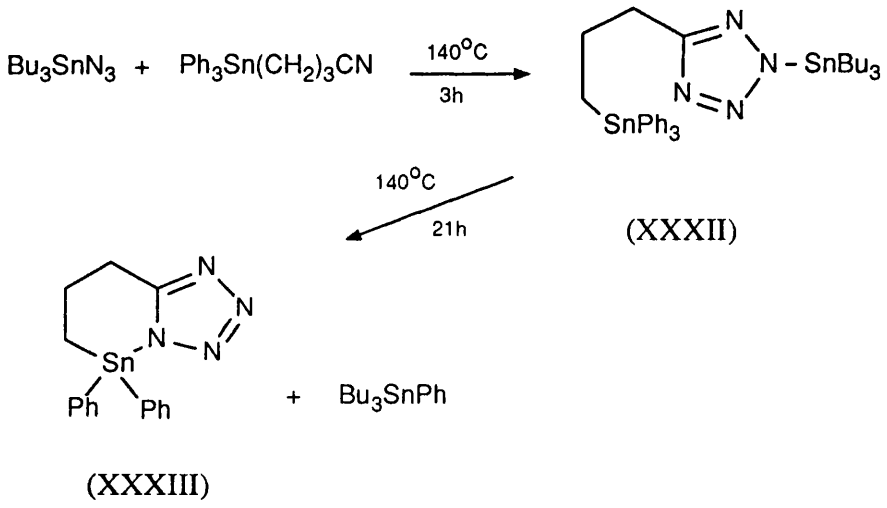

(XXXIII)

(Scheme 1.2)

Heating the neat reactants for three hours did indeed yield the desired 2-(tributylstannyl)-5-(3′triphenylstannylpropyl) tetrazole (XXXII).[148,149] Prolonged heating at the same temperature however results in a further cyclisation to (XXXIII) with elimination of Bu_3SnPh. The structure of this bicyclic compound has been confirmed crystallographically to reveal a *trans*-trigonal bipyramidal geometry about tin with tetrazole nitrogens occupying the apical sites. Of these, one arises from intramolecular chelation of the 5-propyltetrazole to yield the bicyclic structure, the other from intermolecular coordination resulting in a

one-dimensional polymeric array (see Section 1.4.6).

The formation of this compound encourages several structural and mechanistic inferences about the effect and position of the tributyltin moiety on the tetrazole ring. Variable temperature and concentration ^{119}Sn and ^{13}C NMR experiments on related tin-substituted tetrazoles have highlighted some interesting dynamic behaviour of the triorganotin unit.[148] These reveal that the tin addend is not permanently bonded to the N^2 position of the tetrazole but displays a migratory behaviour around the ring as the temperature is increased to greater than 50°C. Additionally the observation has been made that the nucleophilicty of the ring nitrogens, generally considered to be low, is substantially enhanced by the presence of the tributyltin group. Such behaviour enables a number of mechanistic possibilities for the formation of (XXXIII) to be evaluated.[148]

The research described in this thesis seeks to expand such cycloaddition chemistry to the structural characterisation of poly-tetrazole compounds synthesised from suitable tin azide and poly-nitrile starting materials. Given the polymeric nature of tin-substituted mono-tetrazoles and the increased number of potential intermolecular-linking sites, it is envisaged that such compounds will form extensive arrays with the supramolecular architecture controlled by both the spatial disposition of the initial poly-nitrile and the steric requirements of the triorganotin moiety.

Equation 1.12 illustrates the synthesis of a triorganotin-substituted bis-tetrazole. The enhanced reactivity provided by the coordinated tin makes suitably disposed compounds of this nature potential bis-heterocylic precursors to tetra-tetrazole macrocyclic compounds (Scheme 1.3).

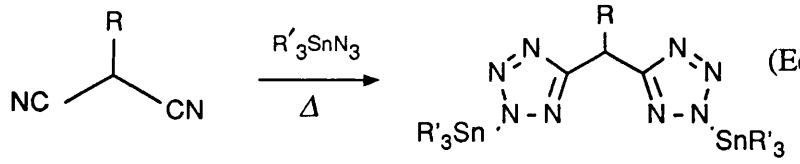

(Equation 1.12)

It may be possible to provide linkage either:

i) by direct high dilution reaction of the bis tetrazole unit with electrophiles of the form R_yAX_2 (e.g. y = 0, 1; A = S, P, B; X = Cl, Br) and elimination of trialkyltin halide or

ii) via an initial coordination complex with a templating transition or main group metal cation. Compounds with a suitable bite-size for chelation may coordinate despite the presence of the tri-organotin moiety (Scheme 1.3).

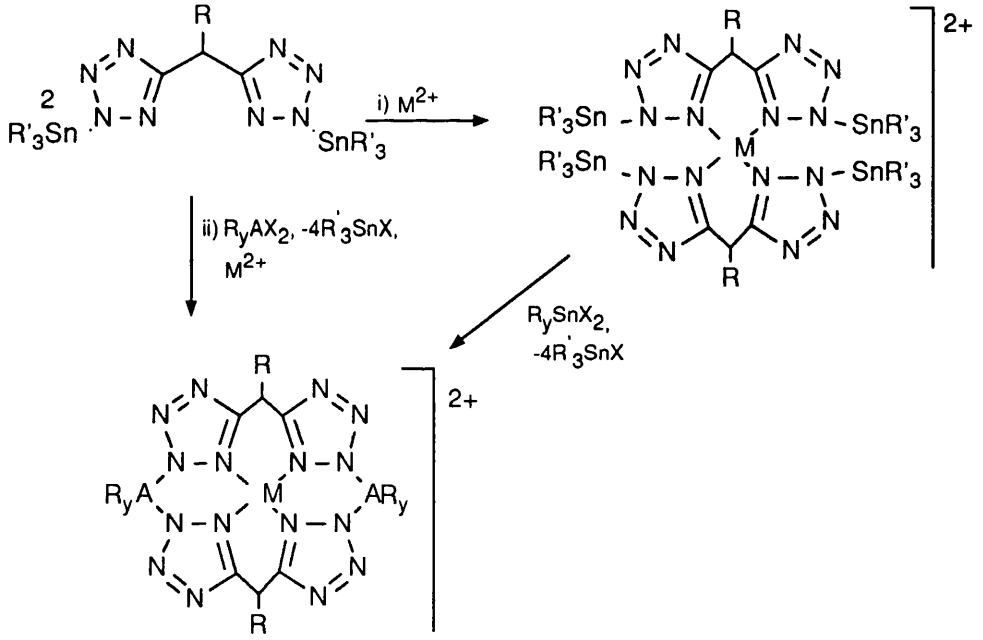

(Scheme 1.3)

In cases where linkage is provided by a single bridging atom, the completed macrocycle will bear analogous molecular architecture to the classical tetrapyrrolic porphin nucleus (XXXIV). Ring planarity in any novel macrocycles will be determined by the identity of the bridging atom or group. Thus the

synthetic approach must concentrate on producing sp^2 hybridisation at this point i.e. orthogonal p_z orbitals containing 0, 1 or 2 electrons as dictated by the 4n+2 rule for the total π-electron count.

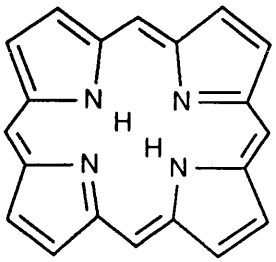

(XXXIV)

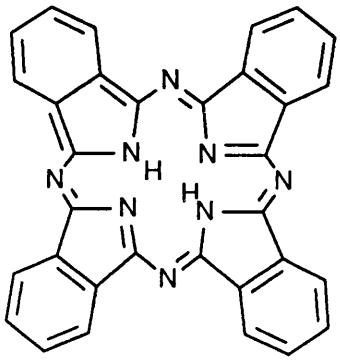

(XXXV)

The study of porphyrins and their coordination compounds now spans a variety of disciplines, owing to their importance in not only a wide range of biological processes but also their more recent application in the field of molecular electronic materials.[150] Central to this latter topic is the ability of planar conjugated macrocyclic metal complexes, containing either porphyrin or phthalocyanine (XXXV) rings, to form one-dimensional stacked arrays in the solid state.[151,152] Such arrays place the component molecules in close spatial proximity and crystallographically similar environments, providing extensive overlap of the π-electron systems and a pathway for charge carrier delocalisation.

Interlayer linkage can be enforced either by a single atom such as fluorine[153] and oxygen[154] or polydentate ligands including cyanide,[155] diisocyanobenzene,[156] tetrazole[157] and pyrazine[158] (Figure 1.21).

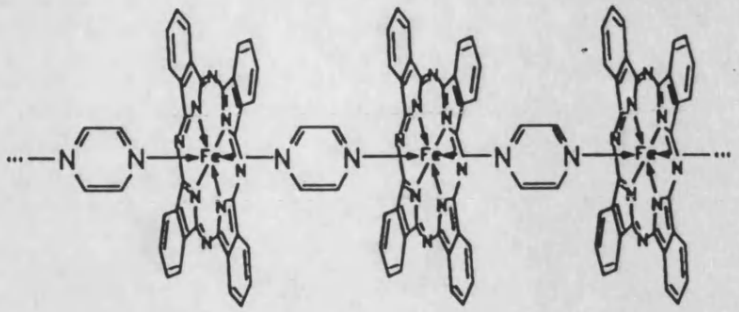

Figure 1.21: Polymeric Phthalocyanato(μ-pyrazine)iron(II)

With this in mind it is surprising that variations in the basic macrocycle skeleton have received relatively little attention. Modifications of the sort envisaged in Scheme 1.3 would undoubtedly affect the redox properties and charge distribution of the system with subsequent implications for the mode of and capacity for electrical conduction. Heteroatom bridgeheads with either vacant orbitals or lone pairs will also influence the lattice association of molecules, both in the direction of stack formation and within the lattice plane containing the macrocycle.

Although previous work directed towards the achievement of conductive stacked lattices has concentrated primarily upon tetrapyrrole macrocycles (linked conventionally through a single sp^2 hybridised carbon or nitrogen), numerous modifications on the basic architecture of (XXXIV) have been reported. Large numbers of compounds have been synthsised where pyrrole is substituted by an alternative heterocycle[159-170] and interest is currently running high in the class of compounds described generically as 'expanded' porphyrins.[171-178] The great majority of this work has been undertaken for metal complexation studies and to test the concept of aromaticity where molecules with 4n+2 π-electrons should, for

example, show observable ring-current effects.

Despite this large and expanding body of work, the replacement of the heterocycle bridging atom with alternative main group elements has been little explored. Indeed only superficially related structures such as the cyclo-tetrakis(triazoylborane) (XXXVI)[179] have been reported in the literature.

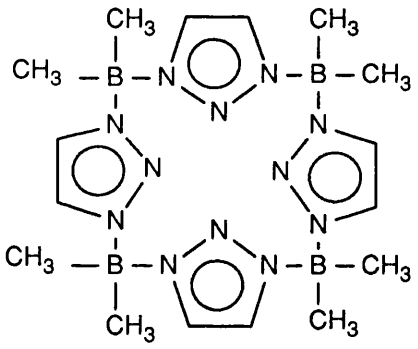

(XXXVI)

The possible diversity of such compounds is immense, with replacement of any fragment of the carbon-based pyrrole system conceivable. This thesis seeks to explore such possibilities, ostensibly through the application of triorganotin-substituted molecules in the types of reactions illustrated in Scheme 1.3. Additionally the scope of tin azide cycloaddition chemistry is expanded to produce organotin-substituted poly-tetrazoles with a view to elucidating the structural and reaction chemistry of such systems.

Chapter 2

The Synthesis and Chemistry of Organotin-Substituted Bis-tetrazoles

2.1 Introduction

Although the first tetrazole derivative was reported over a century ago, this class of higher azoles received relatively little attention until the 1960s. Increased interest was stimulated by their application in agricultural preparations and explosives and the realisation that the tetrazole subunit, with comparable acidity yet increased metabolic stability, could function as a carboxylic acid isostere. Analogues of amino acids and many other natural carboxylic acids have been synthesised and tetrazole-containing compounds have been employed as anti-allergic, anti-inflammatory and anti-convulsant agents. For example, pentamethylene tetrazole ('Metrazole') (XXXVII), is used as a stimulant for the central nervous system and to counteract the effects of barbiturate overdose. Detailed reviews of the chemistry of tetrazoles are available.[180]

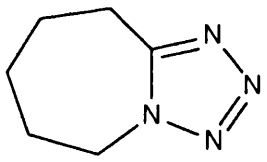

(XXXVII)

Without exception, the major syntheses of tetrazole-containing compounds involve the 1,3-dipolar cycloaddition of hydrazoic acid or azide anion to compounds containing carbon-nitrogen multiple bonds. This latter option leads, in the first instance, to metal-substituted derivatives if the azide is part of a

coordinated metal complex system (Equation 2.1). Numerous examples exist of cycloaddition reactions involving both main group[148,157,181-186] and transition metal-coordinated azides[187-192] to produce N-substituted tetrazoles, with the position and degree of substitution proving dependent on steric factors and the identity of the coordinated element. The feasability of such reactions is largely

(Equation 2.1)

determined by the symmetry and relative energies of the respective highest and lowest occupied molecular orbitals (HOMOs and LUMOs) of the reacting azide and nitrile. Frontier orbital theory provides a means of accounting for variations in the reactivity of outwardly similar systems.[193] In outline the theory proposes that concerted reaction, through a transition state in which the formation of one of the new σ-bonds is more advanced than the other, is enhanced if there is a favourable interaction between a filled π-orbital of one reactant and an empty π^*-orbital of the other. The orbitals must be of the correct phase to react [Figure 2.1(a)], the interaction must be sterically feasible, and will be stronger the closer in energy the orbitals are. The relative energies of the reactant HOMOs and LUMOs can vary, as illustrated in Figure 2.1(b).

Reactions are therefore favoured if one component is strongly 'nucleophilic' and the other strongly 'electrophilic'. More nucleophilic dipoles have higher energy HOMO values and thus the ease of reaction will be affected by electron donating ability of the attached metal. Such an effect is noted in the recent synthesis of 5-substituted tetrazoles employing trimethylsilyl azide as the participating dipole.[194] Low conversions were obtained when Me_3SiN_3 and RCN were employed as the sole reactants. However in the presence of catalytic

quantities of dibutyltin oxide (0.18 equiv.) the desired tetrazole was obtained in 86% yield. This observation was interpreted in terms of the formation and break-down of an intermediate N-[dialkyl(trimethylsiloxy)stannyl] tetrazole and a tin species that carries on in the catalytic cycle (Scheme 2.1)

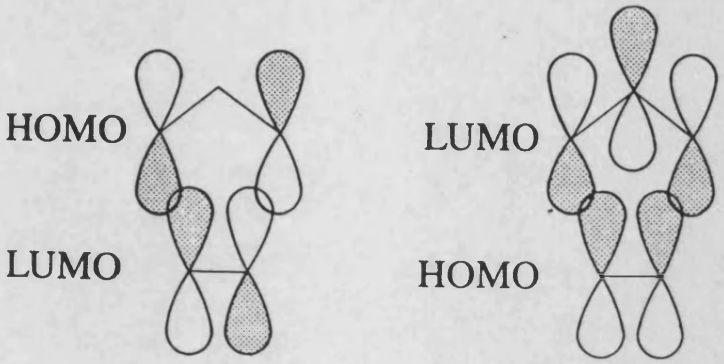

(a)

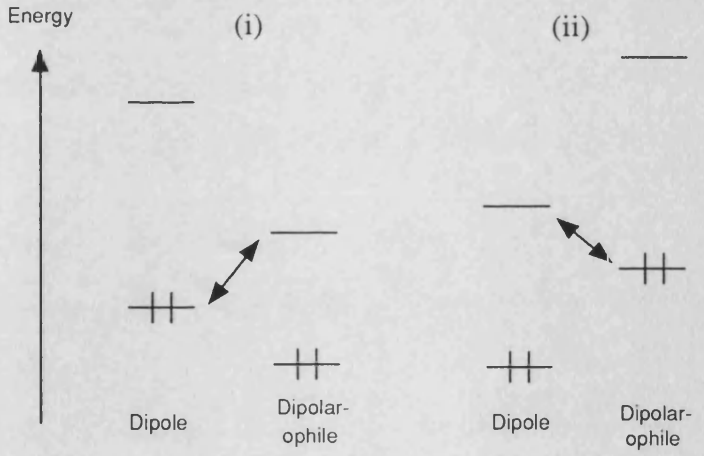

(b)

Figure 2.1: (a) Frontier Orbital Combinations in 1,3-dipolar addition. (b) Types of Interaction (i) HOMO (dipole)-LUMO (dipolarophile) dominant; (ii) LUMO (dipole)-HOMO (dipolarophile) dominant.

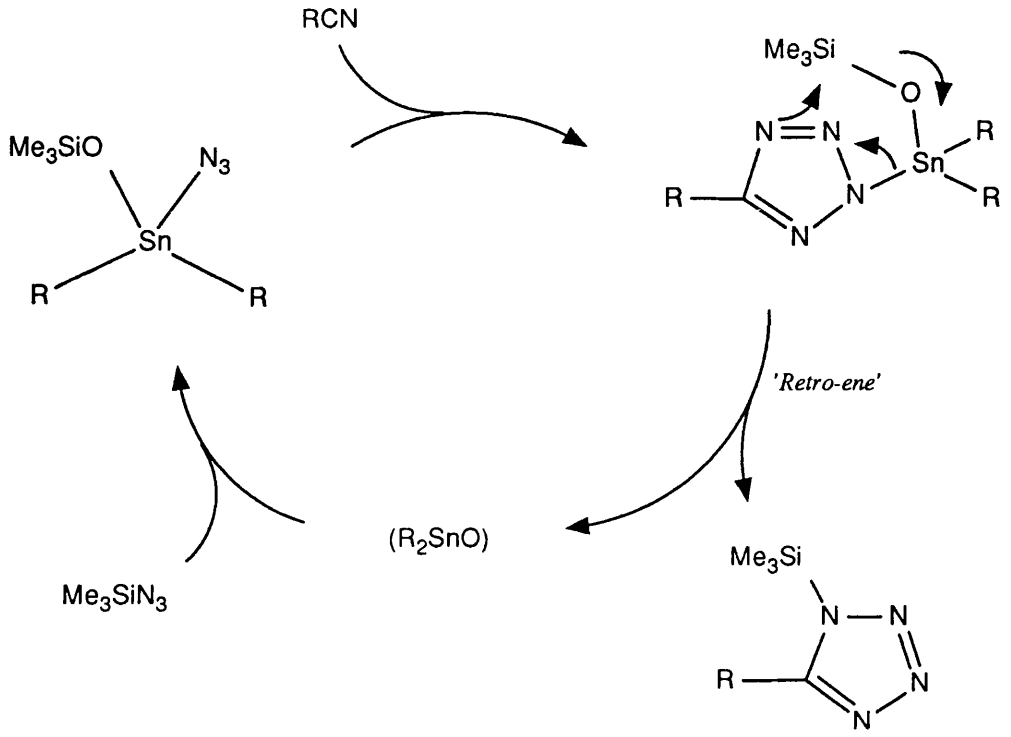

Scheme 2.1

The electron donating ability of tin renders, in some cases, the formation of triorganotin-substituted tetrazoles remarkably facile. Indeed high conversions have been observed at room temperature in the reaction of tributyltin azide and the C-N bond of phenylisothiocyanate,[195] though cycloaddition is accompanied by tin migration to the exocyclic sulphur. In this case the electron-withdrawing sulphur acts to increase the 'electrophilicity' of the dipolarophile (by a lowering of the LUMO energy) and enhances the HOMO/LUMO interaction of Figure 2.1(b)(i). Trialkyltin azides, however, are also observed to react readily with more isolated nitrile substituents and are thus versatile reagents in the general synthesis of tetrazole derivatives.

This chapter therefore describes work which seeks to extend the generality of the trialkyltin azide/nitrile reaction to bis-nitrile reactants. The previously observed polymeric nature of triorganotin-substituted tetrazole

compounds (ref. 148 and Section 1.5) is expected be considerably enhanced by the multiplicity of potential Lewis basic/acidic sites in such products and extended arrays might be anticipated. Additionally, the enhanced reactivity of organotin-substituted tetrazoles is examined in terms of potential macrocycle formation.

2.2 Synthesis of Bis-(trialkylstannyltetrazoles)

Eleven 5,5′-alkylene and phenylene bis-(trialkylstannyltetrazoles) have been synthesised (Equations 2.2 and 2.3). The preparative method parallels that of Sisido *et al.*[184] and Molloy *et al.*[148] in which the triorganotin azide is heated with a slight excess of the chosen bis-nitrile either neat or, in the case of **(18)**, in refluxing mesitylene. It was found that reaction at the elevated temperatures (*ca.* 120-150°C) adopted in the second of these reports reached completion after, in most cases, less than one hour. The extent of reaction can be easily followed by the disappearance of the IR bands due to ν(CN) at *ca.* 2250 cm^{-1} and $\nu_{asym}(N_3)$ at *ca.* 2060 cm^{-1}. The crude solid products were purified by recrystallisation from methanol, though some difficulty in this respect was encountered due to the self-associated nature and hence low solubility of some of the compounds. The tributyltin derivative **(12)** crystallises from methanol solution as a bis-solvated adduct, the crystal structure of which is presented in Section 2.4. An amorphous non-solvated product is readily produced by gentle heating under vacuum and it is this unsolvated form that the analytical and solid-state Mössbauer data of Tables 2.1 and 2.2 refer.

The trimethyl and tributyltin azides were synthesised by literature methods,[196,197] whilst the previously uncharacterised tri-isopropyltin **(4)** and triethyltin azides **(7)** were prepared by similar methods from the corresponding iodide and chloride respectively and sodium azide in an ether/water two phase system.

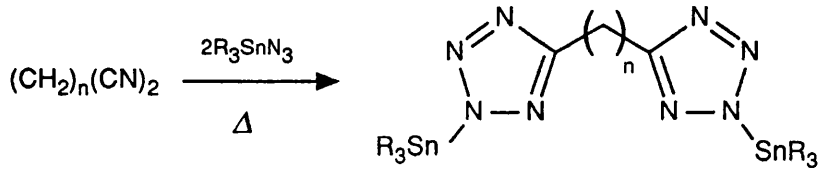

(Equation 2.2)

(8) n = 1; R = Me

(9) n = 1; R = Bu

(10) n = 2; R = Bu

(14) n = 1; R = ^{i}Pr

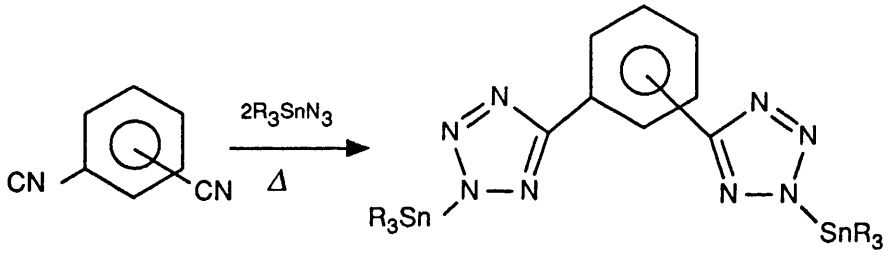

(Equation 2.3)

1,2 Phenylene Compounds

(11) R = Bu

(15) R = ^{i}Pr

(17) R = Et

1,3 Phenylene Compounds

(12) R = Bu

(18) R = Et

1,4 Phenylene Compounds

(13) R = Bu

(18) R = Et

Analytical and physical data of all the bis tetrazole compounds prepared in this study are presented in Table 2.1 while full details of synthetic and work-up procedures are included in Section 2.8.

Table 2.1: Analytical data for Triorganotin-substituted Bis-tetrazole Compounds

Compound	m.p (°C)	C(%)[a]	H(%)	N(%)
(8)	>240	23.1(22.6)	4.18(4.18)	22.9(23.4)
(9)	209-212(dec)	44.7(44.6)	7.98(7.77)	15.5(15.4)
(10)	218(dec)	44.7(45.1)	7.93(7.80)	15.2(15.1)
(11)	175(dec)	48.5(48.5)	7.48(7.45)	14.2(14.1)
(12)[b]	177-179(dec)	48.5(48.5)	7.36(7.45)	14.2(14.1)
(13)	220-222(dec)	48.4(48.5)	7.36(7.45)	13.9(14.1)
(14)	190(dec)	38.9(39.0)	6.80(6.85)	16.9(16.9)
(15)	192(dec)	46.4(44.1)	5.92(6.50)	16.5(15.8)
(16)	183(dec)	42.4(44.1)	6.51(6.50)	15.3(15.8)
(17)	230(dec)	38.3(38.5)	5.41(5.45)	17.7(17.8)
(18)	208(dec)	38.6(38.5)	5.43(5.45)	17.2(17.8)

[a] Found(calc)

[b] Refers to unsolvated form

2.3 Spectroscopy

2.3.1 NMR Spectroscopy

^{1}H, ^{13}C, and ^{119}Sn NMR data were collected for all the tin-substituted tetrazole compounds included in this study and the previously uncharacterised tri-isopropyltin and triethyltin azides **(4)** and **(7)**, apart from the succinonitrile derivative **(10)** which proved of insufficient solubility in all available solvents. NMR data on the azido compounds were collected in $CDCl_3$ while the highly coordinating DMSO-d^6 was required to break up the intrinsic polymeric nature of the remaining tetrazole compounds. ^{119}Sn NMR data of the bis-(trialkylstannyl-tetrazoles) are displayed in Table 2.2.

The ^{1}H and ^{13}C spectra of the all the tetrazole compounds under study are consistent with the proposed structures. In each case the tertiary carbon of the tetrazole ring is discernible at *ca.* 160 ppm and for the phenylene-bridged derivatives the unique signals are all apparent.

Coupling constant data are useful as a probe of local geometry around tin (see Table 1.8) and the values collected here are indicative of *trans*-trigonal bipyramidal coordination. This is further borne out by the ^{119}Sn NMR data where the collated shifts (*ca.* -40 to -80 ppm, Table 2.2) are to low frequency of for example, the four coordinated $Bu_3Sn(NMe_2)$ (δ 36 ppm).[117] Use of the necessarily highly coordinating solvent, DMSO however leaves ambiguous the nature of the actual solution species under observation. Two possibilities exist, namely a monomeric form in which adducted solvent provides the second axial substituent (XXXVIII) or short chain intermolecularly associated oligomeric species (XXXIX) possibly end-capped by adducted DMSO. This second option has previously been inferred for single tetrazole systems from both concentration dependent viscometry[198] and variable temperature and variable concentration NMR.[148] The latter study measured the ^{119}Sn NMR spectra of several simple

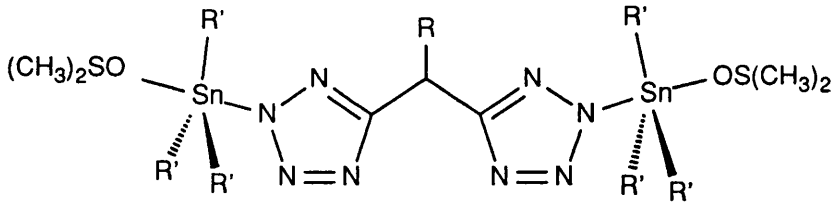

(XXXVIII)

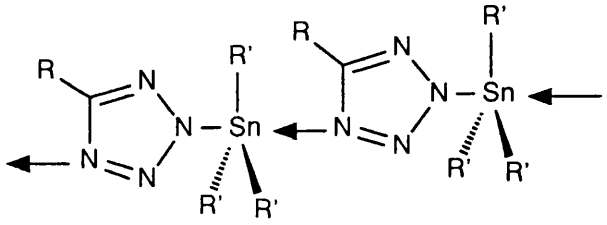

(XXXIX)

tributyltin substituted tetrazoles in non-coordinating solvent and yielded ambient temperature values of δ comparable to those of the present work [e.g. for 5-phenyl-2(tributylstannyl)tetrazole δ = -40.7 ppm]. These results were interpreted as being indicative of structures such as (XXXIX). Although it is not possible to assign such a definitive picture to the present work based purely on the data of Table 2.2, it does appear likely that a similar situation prevails given the potential for intermolecular interactions from the increased number of Lewis basic/acidic sites. A further shared characteristic of the ^{119}Sn NMR signals of **(9)**, and **(11)**-**(18)** with those of the variable temperature data of reference 148 are the observed line widths at 25°C which are broad, typically 650 Hz. at half height. Although such an effect might arise from adjacent quadrupolar ^{14}N nuclei, this is unlikely based on the previously observed temperature dependence of both the line widths and chemical shifts.[148] This revealed that at low temperatures (*ca.* -40 to 0°C) a situation prevails in which the molecules are 'frozen' into an

arrangement akin to (XXXIX), with chemical shifts consistent with five-coordination and narrow line widths (*ca.* 50 Hz.). As the temperature is raised the line widths first increase then decrease as the chemical shift moves to lower frequency, indicative of increased monomer formation. This behaviour, it has been suggested, is due to fluxional movement of the tin around the tetrazole ring. At elevated temperatures, the NMR time-scale sees a time averaged signal

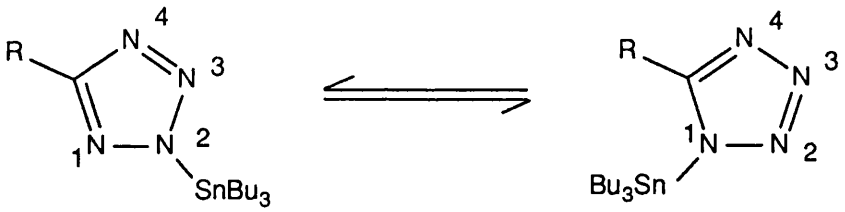

(XXXX)

as the tin accesses both N^1 and N^2 (XXXX) (a N^3, N^4 combination is identical). At room temperature however this process is not as facile leading to a detectable residence on the individual ring nitrogens and concommitant line broadening. Similar fluxional behavior has been noted previously for certain platinum tetrazoles[199] and recently via an ^{15}N NMR study of analogous cobalt systems.[200] Older quantum mechanical calculations have shown that N^1 and N^2 binding are essentially energetically equivalent.[201]

For the trimethyltin derivative (**8**) both the $^1J(^{119}Sn, ^{13}C)$ and $^2J(^{119}Sn, ^1H)$ values of 516.6 and 70.0 Hz. respectively are indicative of five coordination around tin. Use of the quadratic relationship between solution-state Me-Sn-Me bond angles and $^2J(^{119}Sn, ^{13}C)$ values formulated by Lockhart and Manders[132] (Formula 1.4) tenders an angle of 119.9°. This almost exactly the ideal value for equatorial methyl groups in a *trans*-tbp structures such as (XXXVIII) and (XXXIX).

Of the butyl derivatives (**9**) and (**11**)-(**13**), only in the case of (**9**) are the α, β and γ methylene proton resonances fully resolved. The observed multiplicities of these signals reveal that the β and γ resonances are reversed to those expected if shielding were an entirely through bond phenomenon. Such an observation has been made many times previously[116] and is attributed to the tetrahedral disposition of the methylene groups of the butyl chain and the dihedral Sn-C-C-C angle. On a time averaged picture therefore the γ protons are brought closer to the tin nucleus than the β protons. On this basis the broad multiplets at *ca.* 1.3-1.4 ppm. in the ^{1}H spectra of (**11**)-(**13**) are arbitrarily assigned to the α and γ protons. Such an effect is also reflected in the ^{13}C spectra and respective $^{2}J(^{119}Sn, ^{13}C)$ and $^{3}J(^{119}Sn, ^{13}C)$ values of *ca.* 28 and 75 Hz. respectively. The $^{1}J(^{119}Sn, ^{13}C)$ values of tributyltin compounds are a good indicator of tin coordination number. This is only discernible for (**12**) due to limitations of compound solubility and the value of 484.8 Hz. is again consistent with five coordination (ref.131 and Table 1.8). Use of the semi-empirical relationship derived by Holecek *et al.*[133] (Formula 1.6) suggests a C-Sn-C angle of 123.2°, again not inconsistent with (XXXVIII) and (XXXIX). Although no other $^{1}J(^{119}Sn,^{13}C)$ couplings were observed, the values collated for the respective $^{2}J(^{119}Sn, ^{13}C)$ and $^{3}J(^{119}Sn, ^{13}C)$ values of (**9**) and (**11**)-(**13**) are internally consistent and thus indicative of analogous solvated structures.

The observed coupling constants associated with the tri-isopropyl and triethyltin derivatives (**14**)-(**18**) are also limited due to compound solubility, although the $^{1}J(^{119}Sn, ^{13}C)$ values of 440.8 Hz. and 480.7 Hz. for (**14**) and (**17**) respectively are again within the established limits for five-coordinated trialkyltin compounds.[117]

Table 2.2: ^{119}Sn NMR[a] and Mössbauer[b] Studies of Organotin-substitued Bis-(tetrazoles)

Compound	$\delta(^{119}Sn)$[c]	(δ)	ΔEq	Γ_1	Γ_2[d]
(8)	-43.8	1.40	3.57	0.90	0.90
(9)	-52.5	1.47	3.59	0.94	0.98
(10)	-[e]	1.38	3.78	0.98	0.99
(11)	-70.5	1.43	3.73	0.89	0.89
(12)[f]	-54.0	1.41	3.65	0.87	0.88
(13)	-55.0	1.41	3.60	0.87	0.87
(14)	-84.1	1.52	3.68	0.96	0.97
(15)	-81.3	1.55	3.73	0.96	1.09
(16)	-82.2	1.53	3.64	0.91	0.91
(17)	-47.1	1.48	3.86	0.99	0.99
(18)	-49.8	1.50	3.82	0.99	1.05

[a] All spectra run as DMSO-d^6 solutions at 25°C

[b] Mössbauer data recorded at 78K and data given in mms^{-1}

[c] Values given in ppm.

[d] Refers to full width at half height of the high and low velocity components in mms^{-1}.

[e] Material not soluble

[f] Refers to unsolvated form

2.3.2 ^{119m}Sn Mossbauer Spectroscopy

The Mössbauer data of the triorganotin-substituted bis-tetrazoles are presented in Table 2.2. The isomer shift values fall within the range 1.30-1.55 mms^{-1} and the quadrupole splittings in the range 3.54-3.86 mms^{-1}, consistent with a *trans*-R_3SnN_2 trigonal bipyramidal coordination sphere about tin (Section 1.4.1). The only way this can occur is through intermolecular N-Sn interactions, of the type illustrated in (XXXIX), a tendency supported by previous structural measurements[148] and the solution state ^{119}Sn NMR data reported above. That this is even the case for the sterically hindered triisopropytin compounds indicates the strength and invariance of this interaction.

A point charge model has been used to calculate the quadrupole splitting parameters for *trans*-R_3SnN_2 systems[202] for R = alkyl and R = phenyl. These are ΔEq_{alk}= 3.25 mms^{-1} and ΔEq_{ph}= 2.80 mms^{-1}. The result for ΔEq_{alk} is of the correct order but a little low and the model is too simplistic to distinguish between different types of alkyl group. The experimental data do in fact show differences in both isomer shift and quadrupole splittings due to variation in the 5*s*-electron withdrawing properties of the various alkyl groups.

Although the figures are consistent with polymeric *trans*-tbp structures they do not allow more exact inferences on the nature of the bridging interaction to be made. The structure (XXXIX) was first postulated on the basis of viscosity measurements[198] and places tin in the least sterically hindered environment, covalently bound to N^2 and intermolecularly bridged to N^4. In contrast, the one-dimensional polymer formed by the bicyclic compound (XXXXI) employs N^1-Sn and N^4-Sn bridging interactions, although this may be a necessary constraint imposed by the three carbon linkage between the tin atom and C^5 of the tetrazole ring. The Sn-N bond lengths are almost identical indicating that the intermolecular coordination is extremely strong, a reflection of the rather sparing solubility of the bis-tetrazole compounds reported here. With this in mind it is

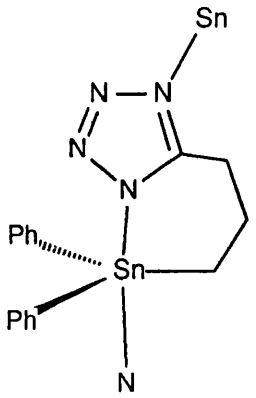

(XXXXI)

difficult to assign the solid-state tin-tetrazole linkages to any one particular mode purely on the basis of isomer shift and quadrupole splitting data. This ambiguity can only be resolved crystallographically and is addressed in Sections 2.4 and 2.5.

2.3.3 Infra-red Spectroscopy

The disappearance of υ(CN) and $\upsilon(N_3)$ at *ca.* 2250 cm^{-1} and 2060 cm^{-1} in the starting materials were utilised in following the course of all the cycloaddition reactions. The spectra of the bis-(tetrazolyl) compounds show the expected strong C-H stretches and deformations at *ca.* 2900 cm^{-1} and 1450 cm^{-1} as well as medium strength bands at *ca.* 1010 cm^{-1} and 1080 cm^{-1} ascribed to the tetrazole ring.[180] The complexity of the spectra in the 550-650 cm^{-1} region make assignment of possible Sn-N bands difficult because of coincidences with possible ν(Sn-C) stretching modes in this region.

2.3.4 Mass Specrometry

Limited mass spectral data were collected on the tributyltin-substituted compounds **(9)** and **(11)**-**(13)**, and the tri-isopropyltin substituted **(14)**-**(16)**, obtained under fast atom bombardment (FAB) conditions in nitrobenzyl alcohol

(NBA). The data are presented in Section 2.8 for even electron fragments only, the sole tin-containing fragment in the largely featureless negative ion spectra appearing at m/z = 623 and 584 for the tributyltin and tri-isopropyltin-substituted compounds respectively. This is typical of organotin compounds since even-electron species have more inherent stability and, while even electron-species are degraded to produce a neutral fragment and a further even-electron ion, odd-electron ions often lose odd-electron neutral fragments to yield a further even-electron ion.

The mass spectra of all the compounds result in numerous peaks although mono and di-tin fragments are readily identifiable due to their differing relative isotopic distribution patterns. Molecular ion peaks are found only in the cases of the triisopropyltin compounds (**14**) and (**15**), with higher mass fragments possibly being attributable to coordinated NBA. N^2-substituted tetrazoles are generally observed to give no molecular ion in contrast to N^1 derivatives, and mass fragmentation patterns have been used to distinguish between different structural isomers.[180] The most abundant species are the tri-coordinated even-electron ions $[R_3Sn]^+$, which together with $[R_2SnH]^+$ and $[RSn]^+$ carry most of the ion current. Tin hydride ions are readily produced via alkene elimination (Equation 2.4).

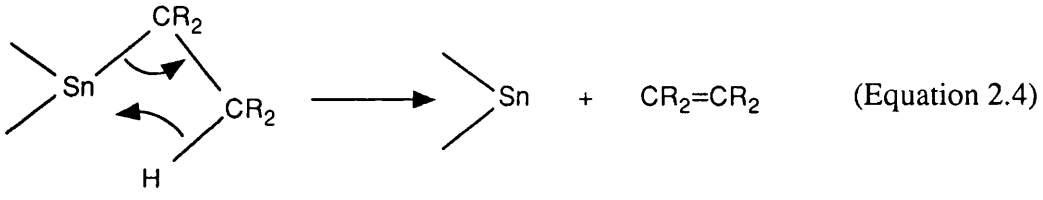

(Equation 2.4)

It is clear that only alkyl groups with a β-hydrogen, including both butyl and isopropyltin compounds, can follow this pathway.

2.4 The Crystal Structure of 1,3-phenylene-bis-5,5'-(tributylstannyltetrazole) Bis-methanolate (12).2MeOH

Suitable crystals for x-ray diffraction were grown by slow crystallisation from a methanolic solution at *ca.* -30°C. Full details of the crystallographic analysis, atomic coordinates and isotropic thermal parameters are included in Appendix II. The asymmetric unit of **(12)**, showing the geometry about tin, is illustrated in Figure 2.2. The large ellipsoids representing the equatorial butyl carbon atoms are representative of some disorder in the crystal despite data collection at low temperature, but do not affect interpretation of the gross structure. Selected bond lengths and bond angles are given in Tables 2.3 and 2.4 respectively.

Examination of Figure 2.2 reveals that **(12)** crystallises from methanol as a solvated adduct. The methanol molecules are coordinated through oxygen to provide axial substituents in what are two slightly distorted *trans*-$NOSnBu_3$ trigonal bipyramidal tin sites [N(2)-Sn(1)-O(1) = 176.6(3)°; N(6)-Sn(2)-O(2) = 177.5(3)°]. The second axial sites are provided by the N^2 nitrogens [N(2) and N(6) of Figure 2.2] of the respective tetrazole rings. This is essentially a monomeric form of what is generally recognised as a polymeric family of tin compounds and thus confirms the original assertion of Kozima *et al.*[198] that tin is covalently attached to the less sterically hindered site. This is in fact the commonest mode of coordination of C^5-substituted tetrazoles. Several monodentate tetrazolate complexes[183,186,192,203-206] have been crystallographically analysed, steric factors favouring N^2coordination particularly if the ring substituent is large or if the coordination site is crowded. For example in case of the tetrazole-substituted indium(III) porphyrin (Figure 2.3),[186] N^2 substitution is enforced because of the need to minimise steric interactions between the tetrazole C^5-substituted phenyl group and the coordinated macrocycle.

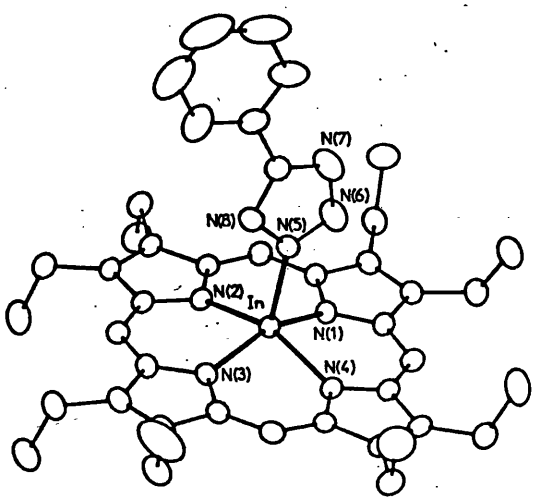

Figure 2.3: Structure of (5-Phenyltetrazolato)-(Octaethylporphinato)indium(III)

The Sn-N bonds lengths are also equivalent within the accuracy of the data [Sn(1)-N(2) = 2.281(10) Å; Sn(2)-N(6) = 2.273(11) Å] and are comparable to those in related systems (see Table 2.5). The nitrogen atoms bound to tin are part of two aromatic planar tetrazole rings. The sum of the internal C-N-N, N-C-N and N-N-N angles in both cases is 539.9°, almost exactly the 540° sum expected for an ideal, planar, five-membered ring, and the individual angles range between 103.6° and 111.5° close to that expected for a regular pentagon (108°). No tetrazole ring atom deviates from the mean plane by more than 0.001 Å in either case. The C-N and N-N bond lengths vary little around the heterocyclic rings, despite the presence of coordinated tin, indicating strong π-electron delocalisation in the tetrazole units. The mean annular C-N and N-N bond lengths of *ca.* 1.32Å are typical of metal-coordinated tetrazoles.[207] The planes of the phenyl and the two tetrazole rings subtend angles of 12.1° and 8.3 °, while the C(1)-C(2) and C(6)-C(8) bond lengths of 1.466(14) Å and 1.473(14) Å respectively are considerably shorter than the value expected for a C-C single bond (1.54Å). This effect has been noted previously in C^5-aryl substituted tetrazoles and attributed to extended conjugation of the π-systems in the two

rings.[192]

The solvated nature of **(12)** is somewhat reminiscent of the crystal structure of bis-$[(\text{cyclo-}C_6H_{11})_2NH_2]^+[(Bu_3Sn)_4(C_2O_4)_3]^{2-}.2C_2H_5OH$.[208] In that case a completely polymeric, and possibly intractible, system is prevented by the end capping of the $[(Bu_3Sn)_4(C_2O_4)_3]^{2-}$ oligomeric chain with two molecules of ethanol. The Sn-O bond lengths in the case of **(12)** [Sn(1)-O(1) = 2.398(9) Å; Sn(2)-O(2) = 2.393(9)] are shorter than that reported for the coordinated ethanol [Sn-O = 2.465(4) Å] but considerably longer than the covalent tin-oxalate linkage [Sn-O = 2.191(3) Å]. These chains are interconnected by a network of hydrogen bonds between $[(\text{cyclo-}C_6H_{11})_2NH_2]^+$ cations and ethanol molecules into a three dimensional array. Such intermolecular interactions are also a feature of the structure of **(12)** where the lattice arrangement is composed of two-dimensional sheets parallel to the *ab* plane as a result of hydrogen bonding. Typically H(1) and H(2) of the molecule as presented (the methanolic hydroxyl protons) interact with N(4) and N(8) of neighbouring molecules [N(4)-H(1) = 1.711 Å; N(8)-H(2) = 1.689 Å]. The net result of these intermolecular bonds is an array of linear polymers along the *b* axis as a result of N(8)-H(2) linkages, further cemented together along the *a* axis as a consequence of infinite linear crosslinks through N(1) and H(1). The lengths of the N(4)-H(1) and N(8)-H(2) linkages are *ca.* 0.4 Å longer than the mid-points of the N(4)-O(1) (2.677 Å) and N(8)-O(2) (2.675 Å) distances indicating that the network is weakly cemented together. The resultant sheet-like array is illustrated in Figure 2.4.

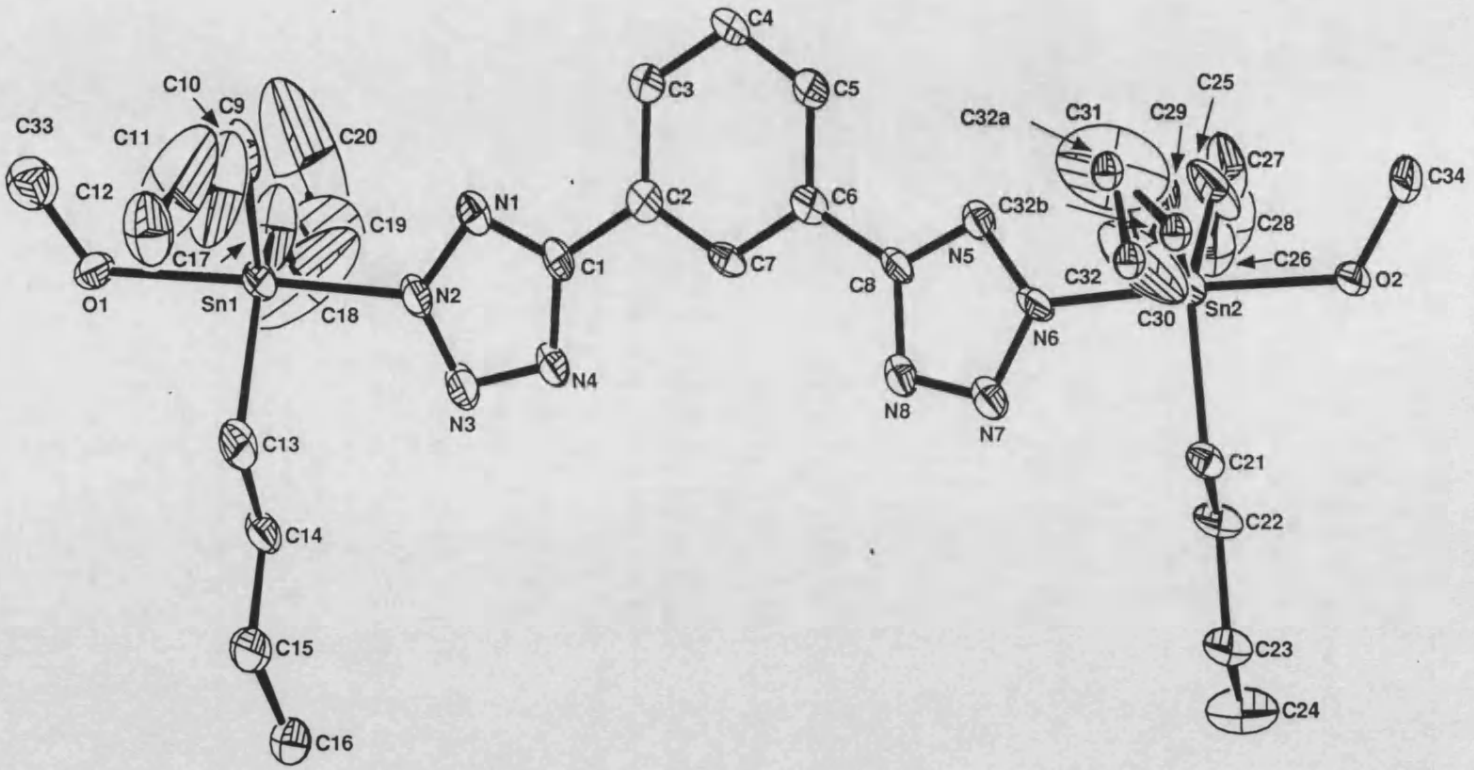

Figure 2.2: The asymmetric unit of **(12)** showing the atomic labelling scheme used in the text and tables. Hydrogen atoms omitted for clarity

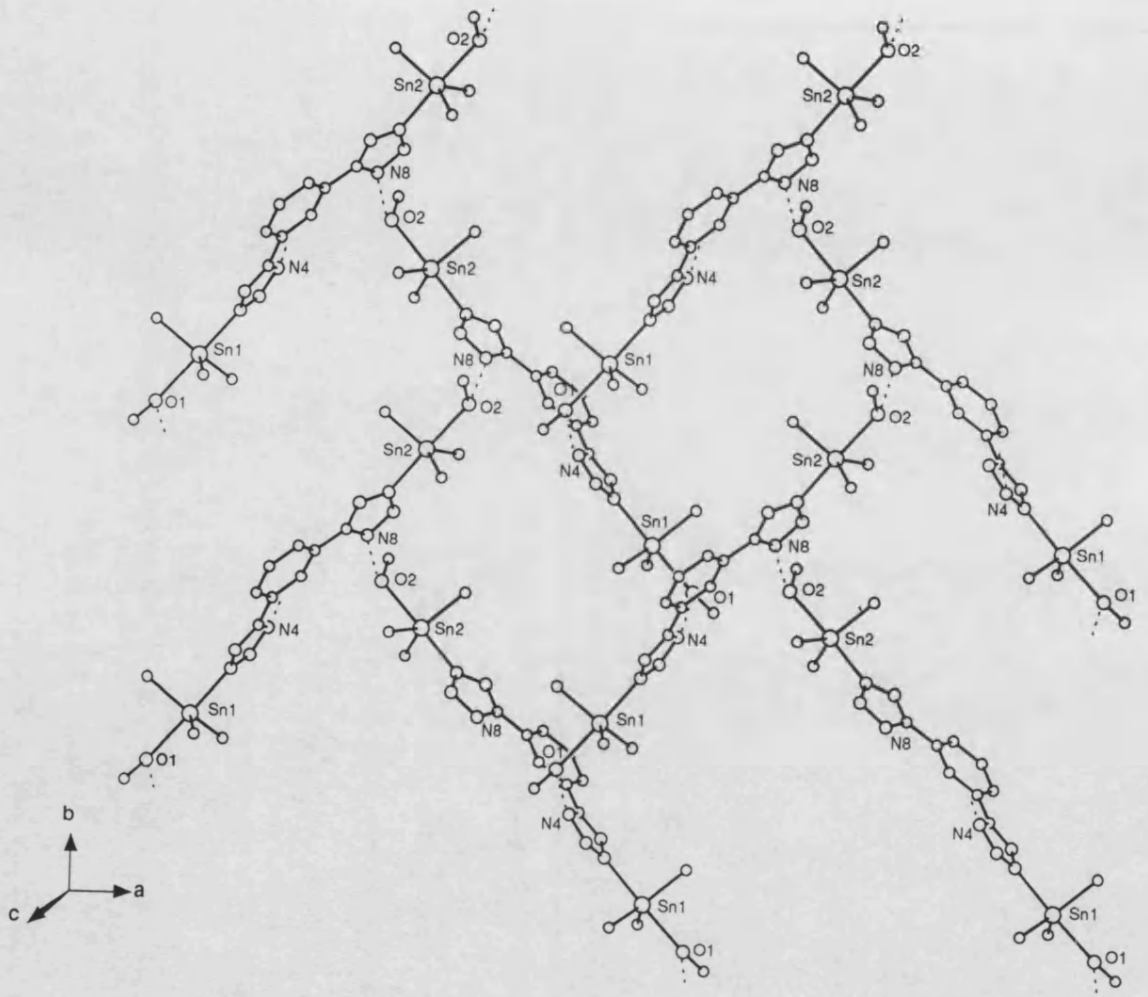

Figure 2.4: Packing diagram of (**12**) viewed perpendicular to the *ab* plane.

Table 2.3: Selected bond lengths (Å) for compound **(12)** with their estimated standard deviations in parentheses.

O(1) -Sn(1)	2.398(9)	N(2)-Sn(1)	2.281(10)
C(9)-Sn(1)	2.139(13)	C(13)-Sn(1)	2.120(12)
C(17)-Sn(1)	2.158(17)	O(2)-Sn(2)	2.393(9)
N(6)-Sn(2)	2.273(11)	C(21)-Sn(2)	2.121(10)
C(25)-Sn(2)	2.107(14)	C(29)-Sn(2)	2.120(15)
N(2)-N(1)	1.338(11)	C(1)-N(1)	1.328(12)
N(3)-N(2)	1.310(12)	N(4)-N(3)	1.339(11)
C(1)-N(4)	1.327(12)	N(6)-N(5)	1.322(11)
C(8)-N(5)	1.319(13)	N(7)-N(6)	1.329(11)
N(8)-N(7)	1.332(12)	C(8)-N(8)	1.351(12)
C(2)-C(1)	1.466(14)	C(3)-C(2)	1.401(13)
C(7)-C(2)	1.389(13)	C(4)-C(3)	1.398(13)
C(5)-C(4)	1.394(14)	C(6)-C(5)	1.386(13)
C(7)-C(6)	1.383(13)	C(8)-C(6)	1.473(14)
N(4)-O(1)	2.677	N(8)-O(2)	2.675
H(1)-N(4)	1.711	H(2)-N(8)	1.689

Table 2.4: Selected bond angles (°) for compound **(12)** with their estimated standard deviations in parentheses.

N(2)-Sn(1)-O(1)	176.6(3)	C(9)-Sn(1)-O(1)	89.3(4)
C(9)-Sn(1)-N(2)	93.8(5)	C(13)-Sn(1)-O(1)	87.9(4)
C(13)-Sn(1)-N(2)	91.6(5)	C(13)-Sn(1)-C(9)	118.1(6)
C(17)-Sn(1)-O(1)	84.0(6)	C(17)-Sn(1)-N(2)	93.6(6)
C(17)-Sn(1)-C(9)	116.1(7)	C(17)-Sn(1)-C(13)	125.0(7)
N(6)-Sn(2)-O(2)	177.5(3)	C(21)-Sn(2)-O(2)	86.6(4)
C(21)-Sn(2)-N(6)	91.3(4)	C(25)-Sn(2)-O(2)	89.7(5)
C(25)-Sn(2)-N(6)	92.6(5)	C(25)-Sn(2)-C(21)	126.5(6)
C(29)-Sn(2)-O(2)	86.3(4)	C(29)-Sn(2)-N(6)	93.4(5)
C(29)-Sn(2)-C(21)	117.0(6)	C(29)-Sn(2)-C(25)	115.9(7)
C(1)-N(1)-N(2)	103.6(9)	N(1)-N(2)-Sn(1)	125.4(8)
N(3)-N(2)-Sn(1)	122.6(8)	N(3)-N(2)-N(1)	111.5(9)
N(4)-N(3)-N(2)	107.1(9)	C(1)-N(4)-N(3)	106.2(9)
C(8)-N(5)-N(6)	104.3(9)	N(5)-N(6)-Sn(2)	124.3(7)
N(7)-N(6)-Sn(2)	124.1(8)	N(7)-N(6)-N(5)	111.6(10)
N(8)-N(7)-N(6)	107.0(9)	C(8)-N(8)-N(7)	105.6(9)
N(4)-C(1)-N(1)	111.5(10)	C(2)-C(1)-N(1)	124.7(11)

Table 2.4 continued:

C(2)-C(1)-N(4)	123.7(11)	C(3)-C(2)-C(1)	120.7(11)
C(7)-C(2)-C(1)	120.7(10)	C(7)-C(2)-C(3)	118.6(10)
C(4)-C(3)-C(2)	120.7(10)	C(5)-C(4)-C(3)	119.0(10)
C(6)-C(5)-C(4)	120.6(10)	C(7)-C(6)-C(5)	119.8(10)
C(8)-C(6)-C(5)	118.3(10)	C(8)-C(6)-C(7)	121.9(10)
C(6)-C(7)-C(2)	121.2(10)	N(8)-C(8)-N(5)	111.4(10)
C(6)-C(8)-N(5)	125.5(10)	C(6)-C(8)-N(8)	123.0(10)

Table 2.5: Comparative Sn-N bond lengths (Å) for compounds **(12)**, **(17)** and related species

Compound	CN[a]	d(Sn-N)[b]	d(Sn-N)[c]	ref.
(12)	5	2.281(10), 2.273(11)	-	[d]
(17)	5	2.354(6), 2.364(6)	2.553(7), 2.418(9)	[d]
(11)	5	2.24(5) - 2.42(5)	2.44(7) - 2.47(6)	[d]
$Ph_2Sn(CH_2)_3CN_4$	5	2.339	2.371	148
Me_3SnN_3	5	2.390	2.390	85
$Me_3SnN_3.Me_3SnOH$	5	2.442	2.612	209
Me_3SnNCN	5	2.470	2.470	210
Cy_3Sn(1,3,5 triazole)	5	2.290	2.350	211
$(CH_2=CH)_2Cl_2Sn(pyrazole)_2$	6	2.322	-	212
$Me_2Cl_2Sn(imidazole)_2$	6	2.312	-	70
$[\{Fe(CO)_2(cp)\}_2Sn(N_3)_2]$	4	2.158	-	213

[a] Coordination number

[b] Intramolecular Sn-N bond

[c] Intermolecular Sn-N bond

[d] This work

2.5 The Crystal Structure of 1,2-phenylene-bis-5,5′-(triethylstannyltetrazole) (17)

Suitable crystals for x-ray crystallography were grown by very slow evaporation of a methanolic solution. Full details of the crystallographic analysis, atomic coordinates and isotropic thermal parameters are given in Appendix III. The asymmetric unit of **(17)** is illustrated in Figure 2.5 along with the atomic numbering scheme and selected bond lengths (Å) and bond angles (°) are listed in Tables 2.6 and 2.7 respectively.

In contrast to the essentially monomeric structure of **(12)** described above, **(17)** crystallises from methanol solution as a supramolecular array dominated by polymeric two-dimensional sheets of molecules stacked along the *b* axis. Figure 2.6 illustrates the manner in which the two-dimensional framework is constructed around N(4)-Sn(1)-N(7′) (i.e. effective N^1-Sn-N^1 bonding) and N(5)-Sn(2)-N(2′) (i.e. effective N^2-Sn-N^2 bonding) intermolecular linkages. The net result of these interactions is that both tin atoms achieve *trans*-N_2SnEt_3 trigonal bipyramidal coordination spheres. It is also noteworthy that the sheet polymers are not flat, but heavily zig-zagged, as illustrated in Figure 2.7 where the lattice is viewed perpendicular to the *bc* plane. Crests and troughs of adjacent layers are defined by the 1,2 tetrazolyl-substituted phenyl groups and lie convex face to concave face. Interlamellar packing is provided by protruding ethyl groups to produce a mean perpendicular interlayer spacing between the interlaced peaks and troughs of 6.18 Å.

As shown in Figure 2.5 there are two distinct trigonal bipyramidal tin sites. The first of these, centred on Sn(1), is the more distorted of the two with an N(4)-Sn(1)-N(7′) angle of 167.8(1)° as compared to 175.0(3)° for N(5)-Sn(2)-N(2′) and sums of equatorial angles of 359.2° and 359.9° respectively. Examination of the respective *trans*-Sn-N bond lengths enables identification of the nominal covalent and coordinative linkages. For both Sn(1) and Sn(2) sites, longer and shorter Sn-N bonds are observable (see Table 2.5), in

contrast to the only previously published polymeric tin-substituted tetrazole[148] where all Sn-N bond lengths were essentially identical. It is apparent from Table 2.5 that the Sn(1)-N(7′) [2.553(7)] and Sn(2)-N(2′) [2.419(9)] bonds are to the high end of the range associated with intermolecular Sn-N bonds.

It is interesting to note that the intermolecular contacts are dictated by the crystal packing, with both N^1-Sn-$N^{1'}$ [N(4)-Sn(1)-N(7′)] interactions and the N^2-Sn-$N^{2'}$ [N(5)-Sn(2)-N(2′)] linkages originally favoured by Kozima *et al.*[198] being observed for the Sn(1) and Sn(2) sites respectively. In terms of the bidentatate action of the tetrazole rings, the individual CN_4 rings provide linkage in the least sterically hindered N^1/N^3 fashion (N^2/N^4 substitution is identical). Such an observation is consistent with the assertions of Kozima *et al.*[198] although this is the first crystallographically confirmed example of such a bonding mode in metal-substituted tetrazole derivatives. All previously reported examples have involved either N^1/N^4 substitution, as in the case of the bicyclic tin compound (XXXXI),[148] or N^2/N^3 substitution in for example the binuclear manganese anion illustrated in Figure 2.8.[214] Recently, similar two-dimensional networks have been reported for tetrazole analogues of poly-(pyrazolyl)borate in

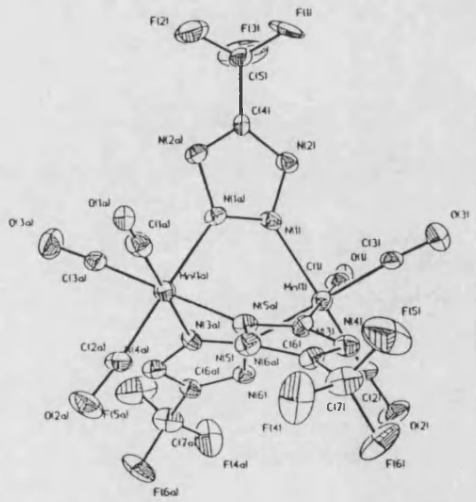

Figure 2.8: The Structure of the $[(CF_3CN_4)_3Mn_2(CO)_6]^-$ anion

coordination with cobalt, zinc and cadmium.[215] In these cases the individual tetrazoles are linked in a N^1/N^4 binding combination to boron and metal respectively. It is interesting to note that the less distorted Sn(2) site is engaged in the N^2-Sn-$N^{2'}$ bonding mode consistent with the more favoured use of the less sterically hindered tetrazole N^2 ring nitrogen atoms.

As expected the tetrazole rings are perfectly planar with sums of internal angles both equalling 540° with no atom deviating from the mean least-squares plane by greater than 0.01 Å. Neither the tetrazole C-N and N-N bond lengths vary little around the mean value of 1.34Å, again indicating strong π-delocalisation around the tetrazole ring.

Although the near co-planarity of phenyl and tetrazole rings observed in the case of **(12)** is somewhat compromised by the geometrical requirements of polymer propagation (dihedral angles of 57.5° and 48.0° between the phenyl and tetrazole rings), the observed C(1)-C(4) [1.470(8) Å] and C(3)-C(2) [1.472(8) Å] linkages are again suggestive of some form of bond-shortening hyperconjugation.

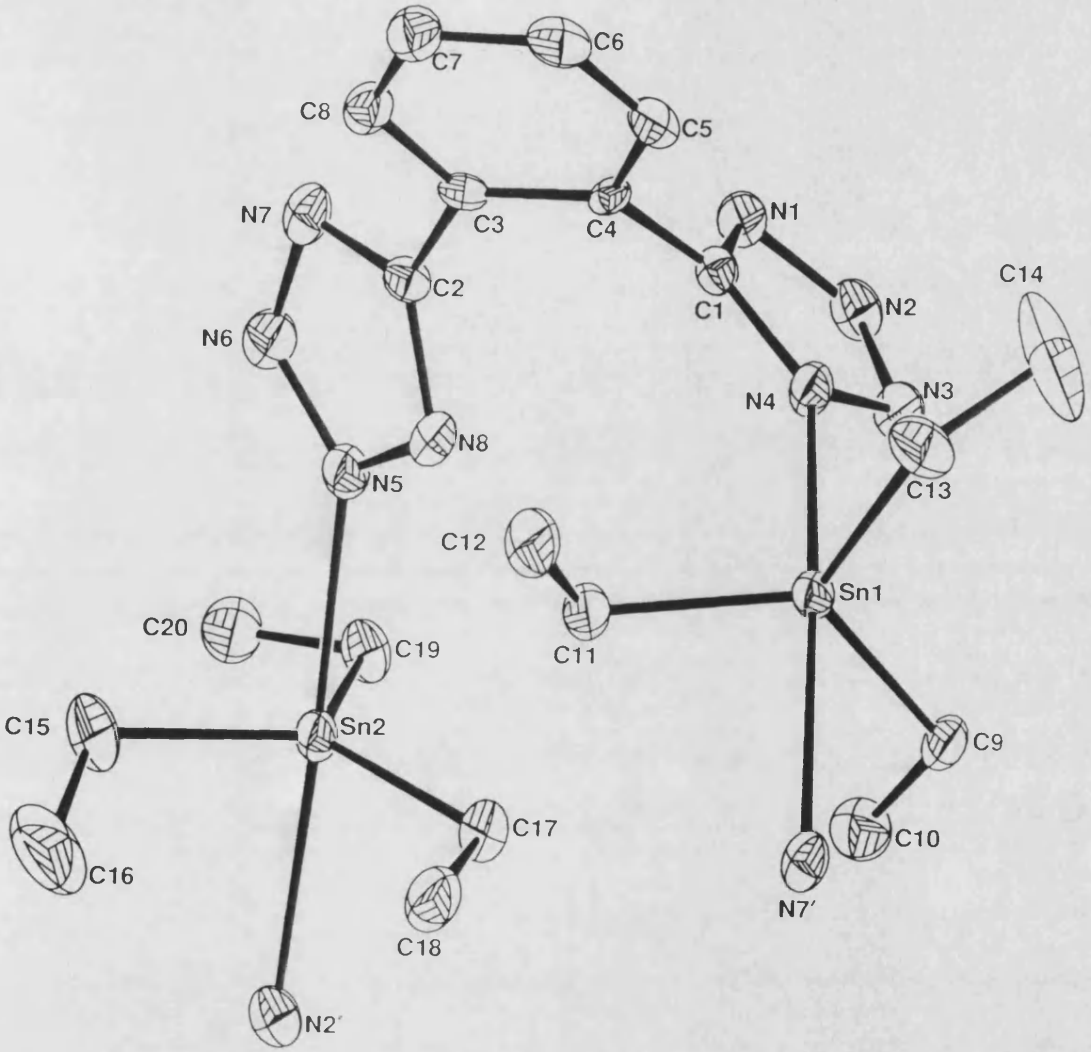

Figure 2.5: The asymmetric unit of **(17)** showing the atomic labelling scheme used in the text and tables.

Hydrogen atoms omitted for clarity.

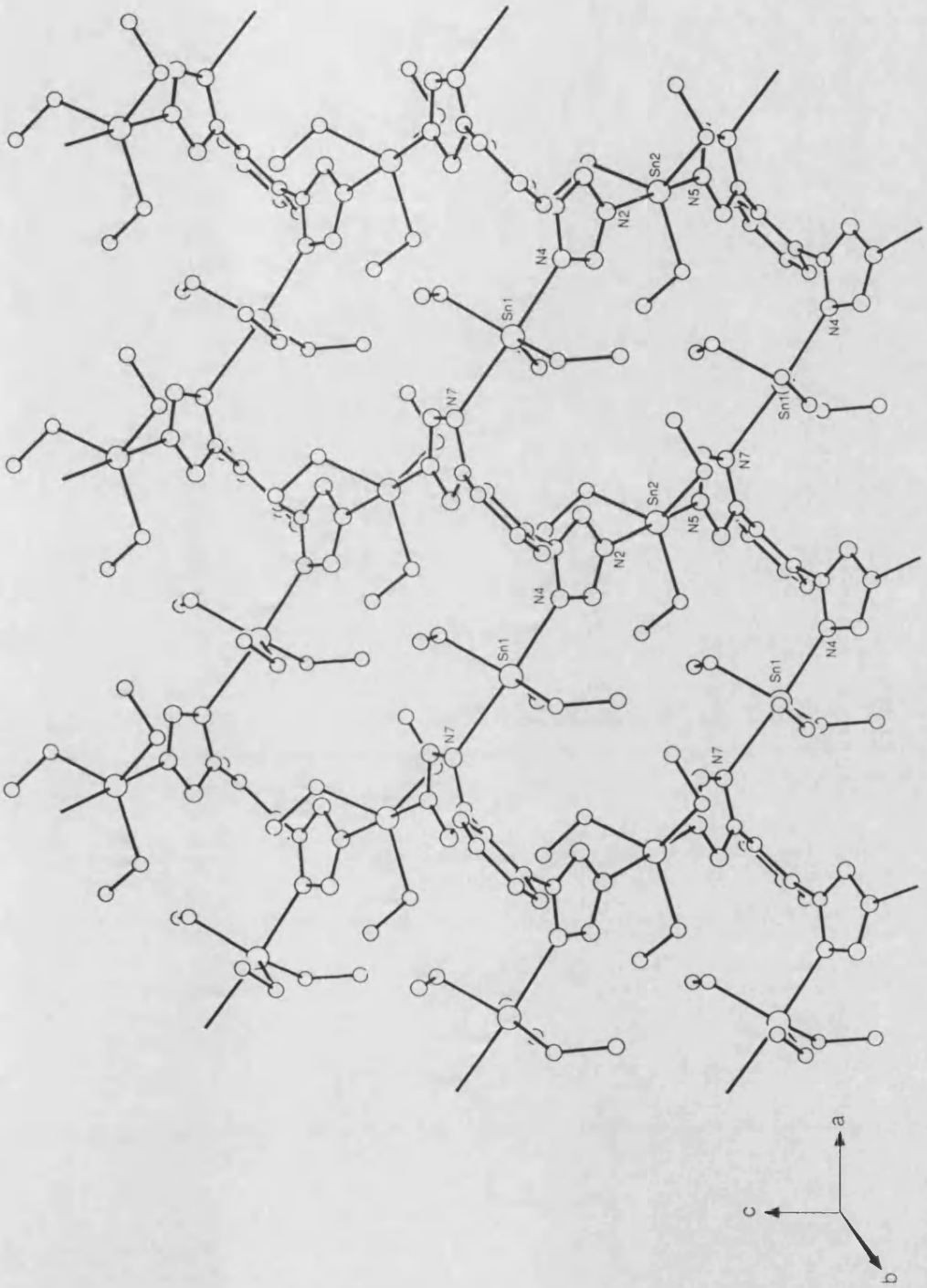

Figure 2.6: Polymeric array of (**17**), viewed along *b* axis showing construction of two-dimensional sheets

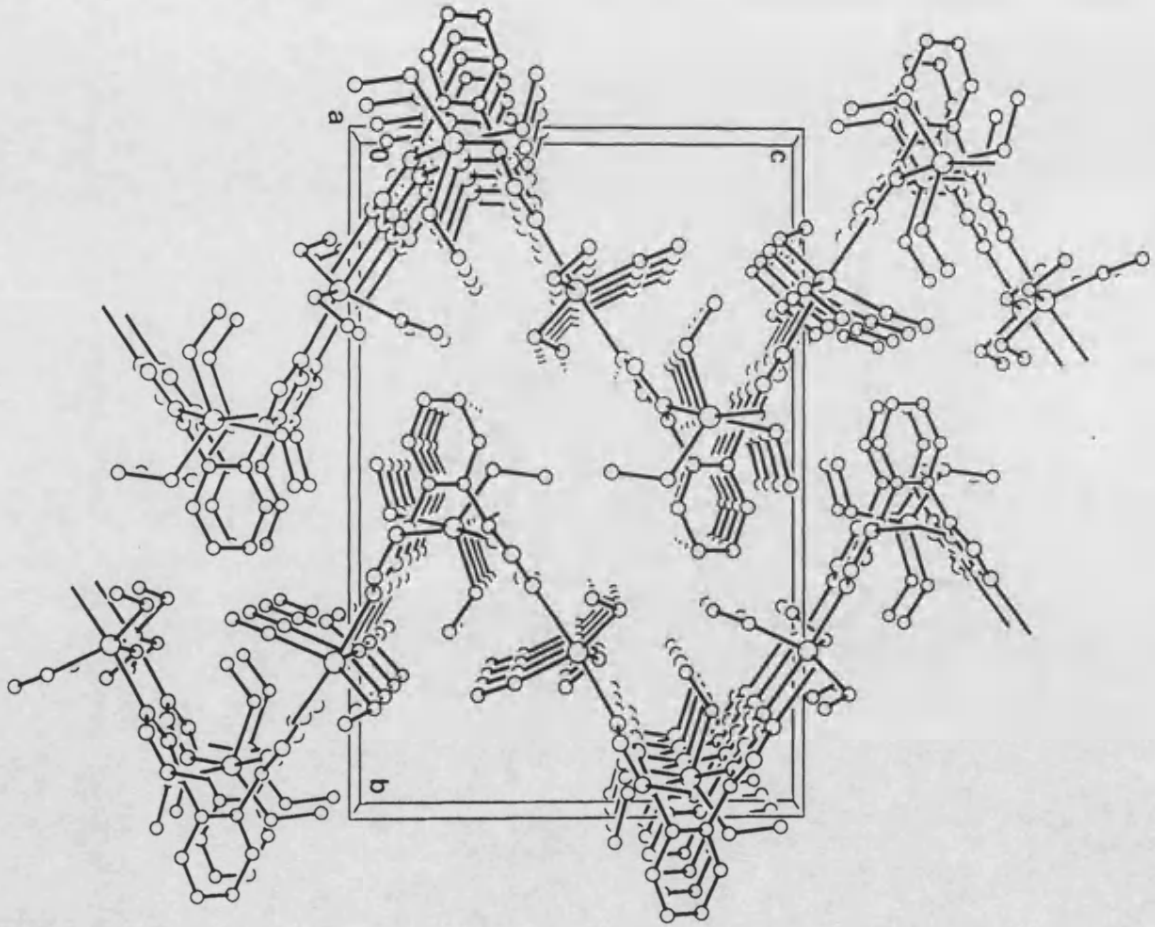

Figure2.7: View of zig-zag sheets of **(17)** viewed perpendicular to the *bc* plane

Table 2.6: Selected Bond Lengths (Å) for Compound **(17)** with their estimated standard deviations in parentheses

N(4)-Sn(1)	2.345(6)	C(9)-Sn(1)	2.126(7)
C(11)-Sn(1)	2.138(7)	C(13)-Sn(1)	2.150(7)
N(5)-Sn(2)	2.364(6)	C(15)-Sn(2)	2.134(7)
C(17)-Sn(2)	2.136(7)	C(19)-Sn(2)	2.132(7)
N(2)-N(1)	1.349(7)	C(1)-N(1)	1.330(7)
N(3)-N(2)	1.312(7)	N(4)-N(3)	1.352(7)
C(1)-N(4)	1.351(7)	N(6)-N(5)	1.321(7)
N(8)-N(5)	1.356(7)	N(7)-N(6)	1.345(7)
C(2)-N(7)	1.348(7)	C(2)-N(8)	1.336(7)
C(4)-C(1)	1.470(8)	C(3)-C(2)	1.472(8)
C(4)-C(3)	1.415(8)	C(8)-C(3)	1.388(8)
C(5)-C(4)	1.391(8)	C(6)-C(5)	1.378(9)
N(7′)-Sn(1)	2.553(7)	N(2′)-Sn(2)	2.417(9)

Table 2.7: Selected bond angles (°) for compound **(17)** with their estimated standard deviations in parentheses.

N(7)-Sn(1)-N(4)	167.8(1)	C(9)-Sn(1)-N(4)	88.9(3)
C(9)-Sn(1)-N(7)	82.7(3)	C(11)-Sn(1)-N(4)	94.2(3)
C(11)-Sn(1)-N(7)	83.6(3)	C(11)-Sn(1)-C(9)	125.2(3)
C(13)-Sn(1)-N(4)	96.0(3)	C(13)-Sn(1)-N(7)	95.6(3)
C(13)-Sn(1)-C(9)	116.8(3)	C(13)-Sn(1)-C(11)	117.2(3)
N(2')-Sn(2)-N(5)	175.0(3)	C(15)-Sn(2)-N(5)	89.0(3)
C(17)-Sn(2)-N(5)	89.5(3)	C(17)-Sn(2)-C(15)	123.2(3)
C(19)-Sn(2)-N(5)	94.2(3)	C(19)-Sn(2)-C(15)	116.9(3)
C(19)-Sn(2)-C(17)	119.8(3)	C(1)-N(1)-N(2)	103.7(5)
N(3)-N(2)-N(1)	111.8(5)	N(4)-N(3)-N(2)	107.4(5)
N(3)-N(4)-Sn(1)	116.8(4)	C(1)-N(4)-Sn(1)	134.8(3)
C(1)-N(4)-N(3)	105.6(5)	N(6)-N(5)-Sn(2)	124.2(4)
N(8)-N(5)-Sn(2)	124.5(4)	N(8)-N(5)-N(6)	111.1(5)
N(7)-N(6)-N(5)	107.9(5)	N(6)-N(7)-Sn(1)	106.7(4)
C(2)-N(7)-Sn(1)	130.2(3)	C(2)-N(7)-N(6)	105.6(5)
C(2)-N(8)-N(5)	103.6(5)	N(4)-C(1)-N(1)	111.5(5)
C(4)-C(1)-N(1)	124.4(5)	C(4)-C(1)-N(4)	123.8(5)

Table 2.7 continued:

N(8)-C(2)-N(7)	111.8(5)	C(3)-C(2)-N(7)	123.8(5)
C(3)-C(2)-N(8)	123.9(5)	C(4)-C(3)-C(2)	121.8(5)
C(8)-C(3)-C(2)	118.8(5)	C(3)-C(4)-C(1)	121.9(5)
C(5)-C(4)-C(1)	119.6(5)	C(5)-C(4)-C(3)	118.5(5)
C(6)-C(5)-C(4)	121.6(6)	C(7)-C(6)-C(5)	119.5(6)
C(8)-C(7)-C(6)	119.8(6)	C(7)-C(8)-C(3)	121.2(6)

2.6 The Crystal Structure of 1,2-phenylene-bis-5,5′-(tributylstannyltetrazole) (11)

Suitable crystals for x-ray study were grown from a methanol solution at -20°C. Full details of the crystallographic analysis, atomic coordinates and isotropic thermal parameters are given in Appendix IV. The asymmetric unit is illustrated in Figure 2.9 and selected bond lengths (Å) and bond angles (°) are presented in Tables 2.8 and 2.9 respectively.

The asymmetric unit (Figure 2.9) consists of two unique 1,2-phenylene substituted bis-tetrazole ligands and four tri-n-butyltin centres. Structural refinement was severely hampered by disorder of the n-butyl chains. The α-carbon atoms were located with a reasonable degree of certainty for Sn(1), Sn(2) and Sn(4). However the equatorial coordination region about Sn(3) was very diffuse and precluded even the location of the α-carbons in this case. Nevertheless analysis of the gross supramolecular architecture is particularly enlightening for this compound, not least because of the contrast with the arrangement discussed above for its triethyltin analogue **(17)**.

The lattice of **(11)** is in fact a three-dimensional polymeric array constructed entirely around CN_4^1-Sn-$CN_4^{3'}$ intermolecular bridging interactions. Although the large esd's associated with the relevant bond lengths and bond angles (see Tables 2.8 and 2.9) preclude any detailed discussion of the precise coordination around the tin sites, in general *trans*-trigonal bipyramidal N_2SnBu_3 coordination again prevails. Each tin is axially bound to two nitrogen atoms, one from the N^1 position of a tetrazole ring and the other from the N^3 position of another tetrazole from an alternative bis-tetrazole ligand within the asymmetric unit [Sn(1) bonds to N(2) and N(12), Sn(2) to N(5) and N(13), Sn(3) to N(4) and N(10) and Sn(4) to N(7) and N(15)]. The N-Sn-N bond angles at Sn(1) and Sn(3) [178(2)° and 179(2)° respectively] are close to ideal and interestingly both short and long tin-nitrogen distances are associated with these coordination spheres [N(2)-Sn(1) = 2.24(5)Å, N(12)-Sn(1) = 2.45(4)Å and N(4)-Sn(3) = 2.47(6)Å,

N(10)-Sn(3) = 2.32(5)Å]. In contrast, the comparatively more distorted Sn(2) and Sn(4) centres [with N-Sn-N bond angles of 175(2)° and 174(2)° respectively] have equivalent inter- and intramolecular Sn-N bond lengths [N(5)-Sn(2) = 2.46(5)Å, N(13)-Sn(2) = 2.42(5)Å and N(7)-Sn(4) = 2.40(4)Å, N(15)-Sn(4) = 2.44(7)Å]. The four unique tetrazole rings are all planar resonance hybrids with maximum estimated deviations from their respective least squares planes of 0.07Å, 0.01Å, 0.03Å and 0.05Å for the C(1), C(2), C(3) and C(4)-containing rings respectively.

The completely three-dimensional array, although somewhat difficult to visualise, is constructed as follows. Along the *b* axis propagation is achieved via N(2)-Sn(1)-N(12) and N(4)-Sn(3)-N(10) linkages. In this manner an approximately linear polymer evolves, constructed from a single tetrazole ring of each bis-tetrazole ligand linked by N^1/N^3 substitued tributyltin units. A similar arrangement prevails along the *c* axis where polymer propagation occurs via N(5)-Sn(2)-N(13) and N(7)-Sn(4)-N(15) bridging interactions and the tetrazole rings not involved in propagation along the *b* axis. The net result of both these interactions is the evolution of a two-dimensional array bearing pseudo four-fold symmetry (Figure 2.10) parallel to the *bc* plane. The resultant sheets are intermolecularly cemented along the *a* axis by N(12)-Sn(1)-N(2) and N(13)-Sn(2)-N(5) interactions, bridged alternately by the two unique phenyl-bridged bis-tetrazole ligands. This is effectively the lattice cement and is clearly visible when viewed perpendicular to the *ab* plane (Figure 2.11). Polymer propagation in this manner is made possible by the free rotation of each of the tetrazole rings about their respective C^5-phenyl ring bonds. In this respect the C(2) and C(3) tetrazole rings subtend angles of 56.6° and 125.1° with the C(5)-C(1) phenyl plane and the C(1) and C(4) tetrazoles make angles of 52.2° and 66.2° with the C(11)-C(12) phenyl plane.

Figure 2.12 illustrates the arrayed sheets stacked along the *a* axis and

reveals that large straight open channels run throughout the entire lattice. It should be understood however that the large cavities provided by this apparently open framework are in fact entirely filled by the tin-bonded butyl chains. It is also apparent that it is the increase in the relative space-filling capacity of the tributylin groups of **(11)** over the triethyltin groups of **(17)** that is the sole origin of the differing coordination mode adopted by the 1,2-phenylene-bis-tetrazole ligand and the dramatic contrast in the lattice packing adopted in both structures.

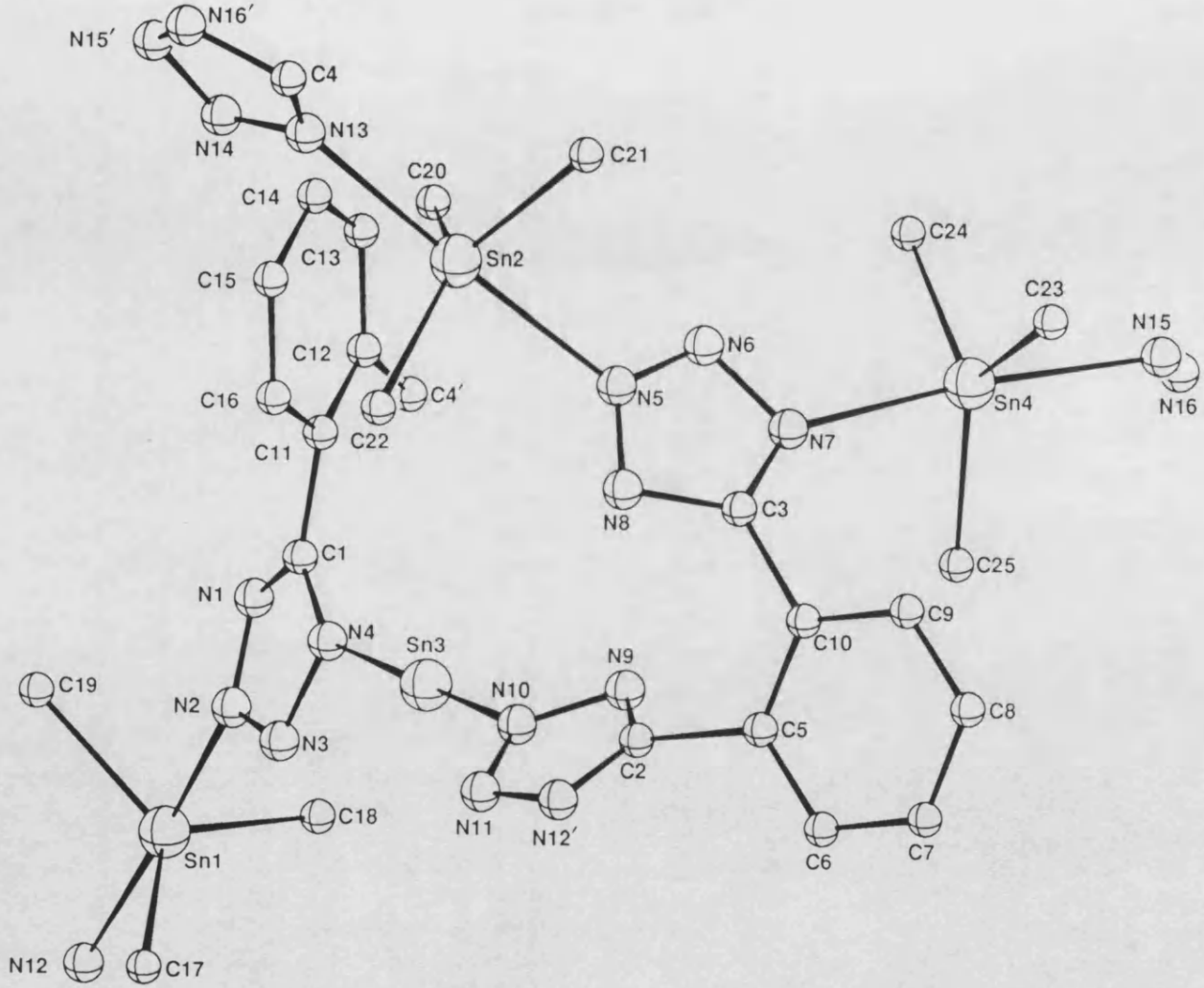

Figure 2.9: The asymmetric unit of **(11)**. Hydrogen atoms omitted for clarity.

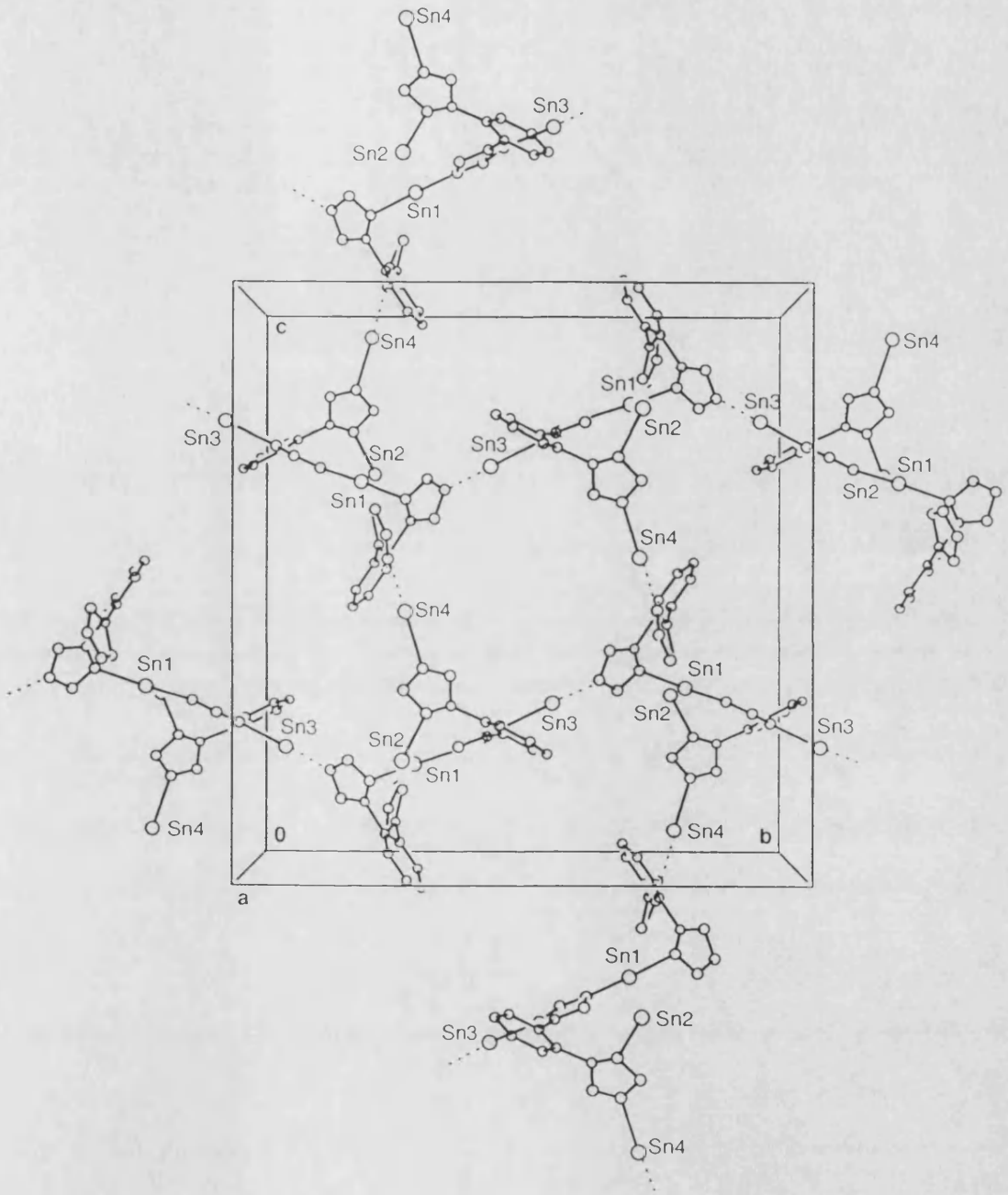

Figure 2.10: The molecular packing of (11) parallel to the *bc* plane. Butyl groups omitted for clarity.

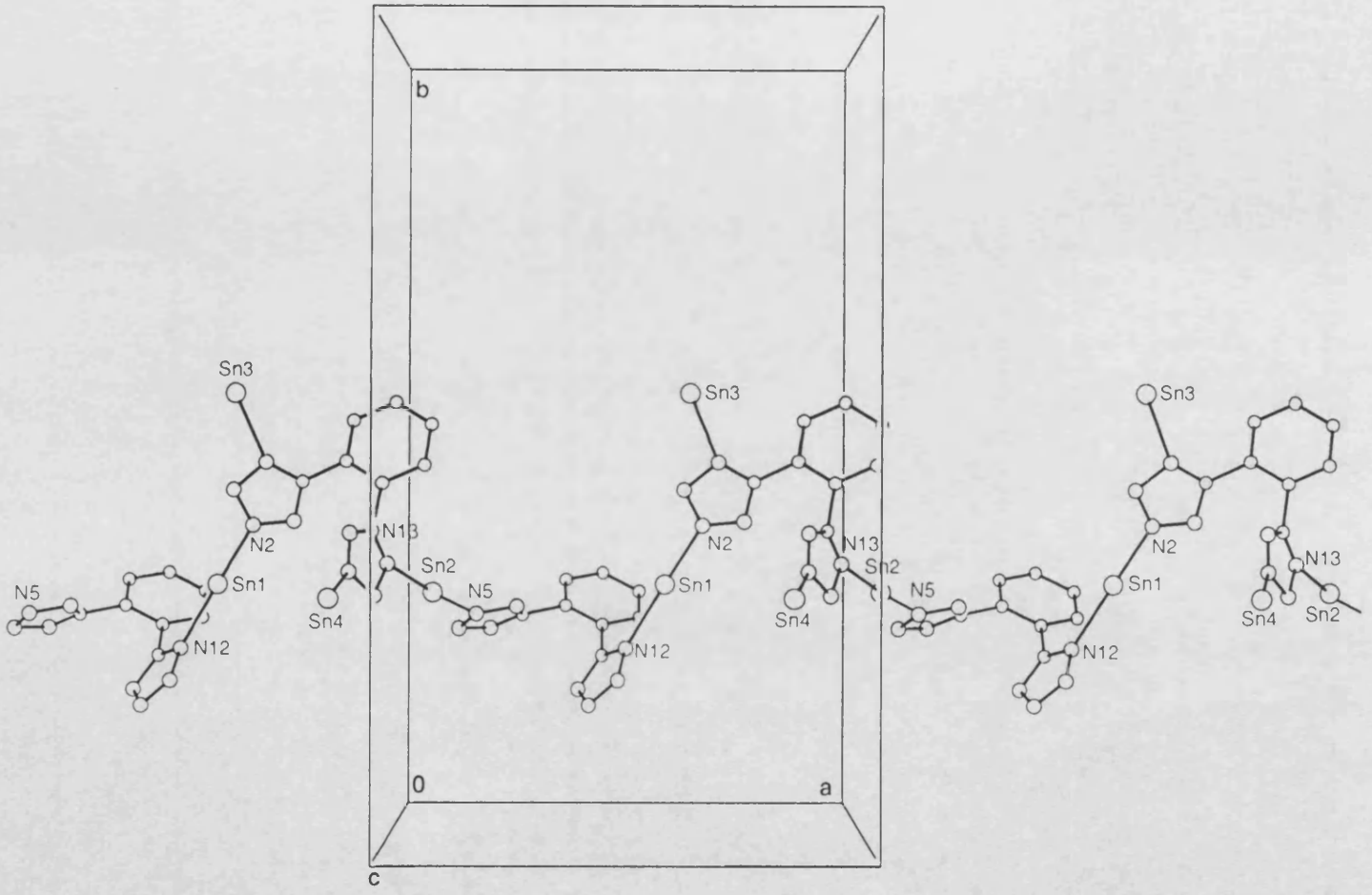

Figure 2.11: The molecular packing of **(11)** parallel to the *a* axis.

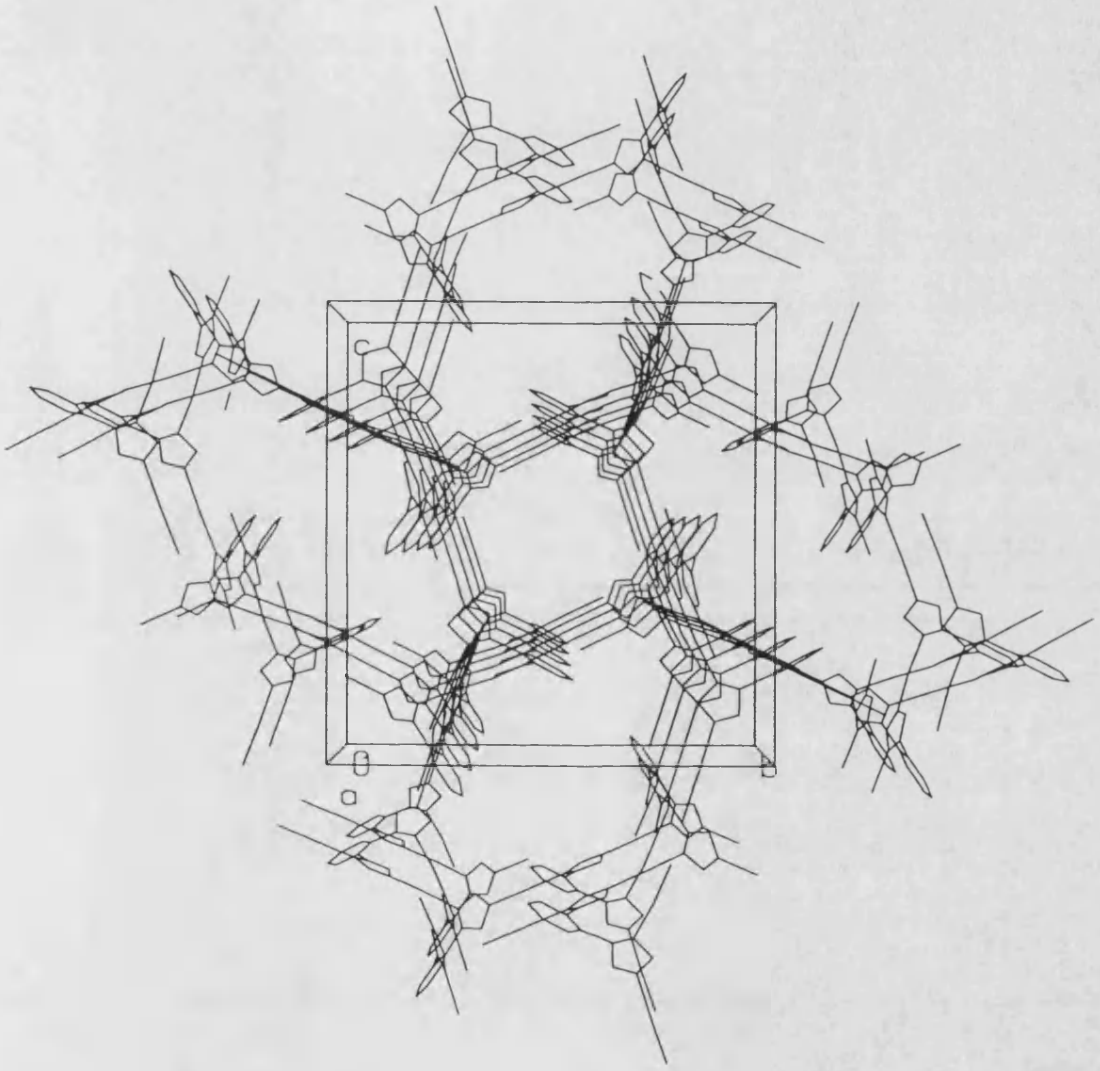

Figure 2.12: Perspective view of(**11**) along the *a* axis illustrating the microchannels extending through the lattice.

Table 2.8: Selected bond lengths (Å) for compound **(11)** with their estimated standard deviations in parentheses.

N(2)-Sn(1)	2.24(5)	N(12)-Sn(1)	2.45(4)
C(17)-Sn(1)	2.28(6)	C(18)-Sn(1)	2.18(6)
C(19)-Sn(1)	2.23(5)	N(5)-Sn(2)	2.46(5)
N(13)-Sn(2)	2.42(5)	C(20)-Sn(2)	2.43(8)
C(21)-Sn(2)	2.18(7)	C(22)-Sn(2)	2.20(6)
N(4)-Sn(3)	2.47(6)	N(10)-Sn(3)	2.32(5)
N(7)-Sn(4)	2.40(4)	N(15)-Sn(4)	2.44(7)
C(23)-Sn(4)	2.27(7)	C(24)-Sn(4)	2.22(9)
C(25)-Sn(4)	2.35(-)		

Table 2.9: Selected bond angles (°) for compound **(11)** with their estimated standard deviations in parentheses.

N(12)-Sn(1)-N(2)	178(2)	C(17)-Sn(1)-N(2)	89(2)
C(17)-Sn(1)-N(12)	91(2)	C(18)-Sn(1)-N(2)	93(2)
C(18)-Sn(1)-N(12)	89(2)	C(18)-Sn(1)-C(17)	124(2)
C(19)-Sn(1)-N(2)	81(2)	C(19)-Sn(1)-N(12)	97(2)
C(19)-Sn(1)-C(17)	121(2)	C(19)-Sn(1)-C(18)	115(2)
N(13)-Sn(2)-N(5)	175(2)	C(20)-Sn(2)-N(5)	90(2)
C(20)-Sn(2)-N(13)	94(2)	C(21)-Sn(2)-N(5)	84(2)
C(21)-Sn(2)-N(13)	91(2)	C(21)-Sn(2)-C(20)	110(3)
C(22)-Sn(2)-N(5)	90(2)	C(22)-Sn(2)-N(13)	90(2)
C(22)-Sn(2)-C(20)	130(2)	C(22)-Sn(2)-C(21)	120(3)
N(10)-Sn(3)-N(4)	179(2)	N(15)-Sn(4)-N(7)	174(2)
C(23)-Sn(4)-N(7)	94(2)	C(23)-Sn(4)-N(15)	86(2)
C(24)-Sn(4)-N(7)	96(2)	C(24)-Sn(4)-N(15)	89(3)
C(24)-Sn(4)-C(23)	109(3)	C(25)-Sn(4)-N(7)	87(3)
C(25)-Sn(4)-N(15)	90(3)	C(25)-Sn(4)-C(23)	131(3)
C(25)-Sn(4)-C(24)	120(3)	N(1)-N(2)-Sn(1)	129(4)
N(3)-N(2)-Sn(1)	124(4)	N(3)-N(4)-Sn(3)	113(4)

Table 2.9: continued.

N(6)-N(5)-Sn(2)	122(4)	N(8)-N(5)-Sn(2)	120(4)
N(6)-N(7)-Sn(4)	117(3)	N(9)-N(10)-Sn(3)	123(4)
N(11)-N(10)-Sn(3)	127(4)	N(14)-N(13)-Sn(2)	113(3)
C(4)-N(13)-Sn(2)	110(6)	N(16)-N(15)-Sn(4)	122(6)

2.7 Reaction Chemistry and Attempted Macrocyclisation Reactions

2.7.1 Cleavage Reactions

Treatment of all the bis-(triorganotin)-substituted tetrazoles with a greater than two to one excess of concentrated HCl in methanol solution results in the cleavage of the trialkyltin group. This reaction produces the free bis-(hydro)tetrazole and two molecules of trialkyltin chloride in stoichiometric yield and has been employed in the synthesis of the methylene-bridged **(19)** (Equation 2.5) and the phenylene-bridged isomers **(20)**-**(22)** (Equation 2.6).

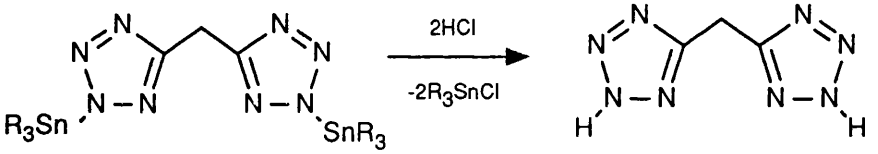

(Equation 2.5)

(19)

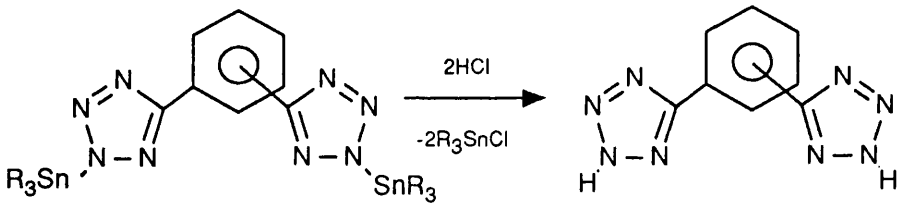

(Equation 2.6)

(20) 1,2-C_6H_4 isomer

(21) 1,3-C_6H_4 isomer

(22) 1,4-C_6H_4 isomer

Phenylene-bridged bis-(hydrotetrazoles) of this nature have been reported previously in connection with polymerisation reactions.[216] Although some difficulty was encountered in obtaining analytically pure samples from methanol solution, the recrystallised compounds forming extensive hydrogen-bonded networks with both water and protic solvents (an assertion confirmed crystallographically for **(20)**, see Section 2.6.3 and Appendix V), the compounds were fully characterised by IR and ^{1}H and ^{13}C NMR.

2.7.2 Attempted Complexation Reactions

Coordination reactions of the type envisaged in Scheme 1.3 were attempted for the tributyltin-substituted **(8)** and the tri-isopropyltin-substituted **(14)** and **(15)**. All reactions were carried out in methanol at room temperature using a two to one ratio of substituted bis-tetrazole to metal salt.

Extensive work with the tributyltin derivative has been found to result in completely insoluble polymeric products with a variety of transition metal and main group metal salts.[217] Microanalysis of the resulting amorphous powders suggested partial elimination of tin via the coordinating metal counter ion with an example of the possible type of species formed illustrated in Equation 2.6. Repetition of the illustrated reaction for X = CH_3CO_2, using the stoichiometry shown yielded a 95% yield of tributyltin acetate.[217] Representative microanalyses are presented in Table 2.10. Magnetic moments of the nickel adducts indicated that the solids were diamagnetic.

$$3CH_2(CN_4SnBu_3)_2 \xrightarrow[-4Bu_3SnX]{2NiX_2} Ni_2[(SnBu_3CN_4)_2CH_2][(CN_4)_2CH_2]_2 \qquad \text{(Equation 2.6)}$$

The ^{119m}Sn Mössbauer spectra of the resultant complexes remain unchanged from those of the starting material (see Table 2.11), indicating that the polymeric nature of the materials is in part due to intermolecular N-Sn-N linkages though, in common with previous studies,[218-221] the environment of transition metal coordination remains uncertain. In an attempt to restrict polymeric intermolecular interactions and enhance the solubility of the complexed species the sterically hindered tri-isopropyltin-substituted **(14)** and **(15)** were employed in similar reactions as part of this thesis study. This again however resulted in insoluble, polymeric materials with, from examination of the

relevant microanalyses (Table 2.10), increased elimination of the tri-isopropyltin moiety. This enhanced lability suggests that tin elimination is, at least in part, induced by relief of steric interactions around the crowded coordination centre.

Table 2.10: Elemental Analyses of Bis-(trialkylstannyltetrazole)/metal Salt Adducts[217]

Bis-tetrazole	Metal salt	C(%)[a]	H(%)[a]	N(%)[a]
(8)	$Ni(ClO_4)_2$	31.7(34.4)	5.32(5.60)	29.2(29.2)
(8)	$Ni(CH_3CO_2)_2$	32.0(34.4)	5.26(5.60)	29.2(29.2)
(8)	$NiCl_2$	32.6(34.4)	5.46(5.60)	28.2(29.2)
(8)	$Ni(BF_4)_2$	34.1(34.4)	4.16(5.60)	28.2(29.2)
(8)	$Cu(NO_3)_2$	36.3(34.1)	5.92(5.55)	24.5(28.9)
(8)	$CuCl_2$	32.8(34.1)	5.30(5.55)	28.3(28.9)
(14)	$Cu(OAc)_2$	27.6(30.0)	4.45(4.45)	28.9(31.2)
(15)	$Ni(ClO_4)_2$	35.9(39.9)	2.68(4.28)	29.5(26.6)

[a] Found(calc. for $M_2[R(CN_4SnR_3)_2][R(CN_4)_2]_2$), [**(8)**: R=$CH_2$; **(14)**, **(15)**: R=Ph]

Table 2.11: Mössbauer Data for Representative Bis-(trialkylstannyl-tetrazole)/metal salt adducts[217]

Bis-tetrazole	Metal salt	δ	ΔEq
(8)	-	1.40	3.57
(8)	$Ni(ClO_4)_2$	1.42	3.67
(8)	$Ni(CH_3CO_2)_2$	1.42	3.63
(8)	$NiCl_2$	1.42	3.69
(8)	$Ni(BF_4)_2$	1.44	3.72
(8)	$Cu(NO_3)_2$	1.43	3.76
(8)	$CuCl_2$	1.43	3.69
(14)	-	1.52	3.68
(14)	$Cu(CH_3CO_2)_2$	1.55	3.73

[a] Insufficient sample for collection of data for **(15)** + $Ni(ClO_4)_2$

2.7.3 Attempted Macrocyclisation Reactions

In attempts to synthesise macrocyclic compounds of the type illustrated in Scheme 1.3, the suitably disposed bis-(tributyltin-substituted tetrazoles) **(9)**, **(11)** and **(12)** were employed in direct reaction with a variety of electrophiles of the general form, R_xACl_2 (x = 0,1; A = S,P,B).

The reaction of **(11)** with sulphur dichloride in acetonitrile resulted in an orange solid and an oil, the latter identified as Bu_3SnCl by infra-red spectroscopy. The solid gave no ^{119m}Sn Mössbauer and proved soluble in a variety of polar solvents. Initial microanalysis data were suggestive of a mixture of products, although both ^1H and ^{13}C NMR showed no peaks other than those expected the phenyl and tetrazole signals expected for the macrocyclic product. Repeated recrystallisation from acetone/methanol eventually yielded suitable crystals for x-ray crystallography. The results of this study are reported in Appendix V and reveal a decomposition product identical to **(20)**. This is held in a heavily hydrated hydrogen-bonded network reflecting the difficulty in obtaining anhydrous forms of the bis-(hydrotetrazoles) reported in Section 2.7.1.

Reaction of the bis-(tributyltin-substituted tetrazoles) with $PhBCl_2$ and $PhPCl_2$ in THF solution also resulted in elimination of Bu_3SnCl. Similar reactions have previously been applied to the synthesis of stable monomeric nitrogen and phosphorus-containing heterocycles via the elimination of trimethylsilyl halides,[222] and precedents exist for the formation of B-N and P-N bonds from tin-substituted amines.[223,224] However the solid products isolated in this case proved polymeric, moisture sensitive and insensitive to further purification, the implication being that reaction was too facile for isolation of monomeric species.

The intractable nature of the products formed in the attempted templating reactions led to the abandonment of this strategy in potential macrocycle synthesis. Additionally direct insertion of heteroatom bridgeheads could not be

controlled for the isolation of tractable products. The viability of more stable N-C-N linkages is discussed in Chapter 3.

The crystal structures of **(17)** and **(11)** demonstrate that tin-substituted poly-tetrazole compounds can form interesting extended arrays with considerable structural variety. There is considerable current interest in self-assembled layered and three-dimensional lattices[225-227] stemming from their practical applications as catalysts and hosts in intercalation compounds, exemplified by the large body of data currently being compiled on $[Cd(CN)_2]$-based frameworks.[228,229] The invariant nature of the *trans*-N_2SnR_3 trigonal bipyramidal coordination sphere provides a geometrical constraint and thus some measure of control in the solid-state structures adopted by triorganotin-substituted poly-tetrazole compounds. The synthetic and structural chemistry of potentially more complex tin-based molecular architecture is explored in Chapter 4.

2.8 Experimental

Trimethyltin and tributyltin azides were prepared according to the methods of Thayer and West[196] and Reichle,[197] respectively. The trimethyltin derivative was recrystallised from toluene prior to use while the tributyltin compound was employed without any further purification. All nitriles and reagents were of commercial origin (e.g. Aldrich) and used without further purification.

N.B. Due to their potentially explosive nature, all preparations of and subsequent reactions with organotin azides were conducted under an inert atmosphere behind a rigid safety screen.

2.8.1 Synthesis of trichlorophenyltin (1)

Anhydrous tin(IV) chloride (49.1g, 18.8 mmol) was added, under nitrogen at room temperature, to tetraphenyltin (26.6g, 6.2 mmol). The stirred mixture was then heated to 160° for a 3 hour period, during which time it became progressively darker. Distillation of the crude product at reduced pressure yielded a single fraction, trichlorophenyltin (66g, 87%), b.p. 78°C/0.1 mmHg.

Analysis: Found(Calc. for $C_6H_5Cl_3Sn$): C 23.7(23.9); H 1.72(1.72)%

^{1}H NMR [δ(ppm), $CDCl_3$ solution]: 7.60 [m, 5H, C_6H_5].

^{13}C NMR [δ(ppm), $CDCl_3$ solution]: 130.4 [*m*-C_6H_5]; 133.2 [*p*-C_6H_5]; 134.0 [*o*-C_6H_5]; 134.5 [*i*-C_6H_5]; ^{3}J[*m*-$^{13}C_6H_5$-^{117,119}Sn] 60.1, 62.8 Hz; ^{4}J[*p*-$^{13}C_6H_5$-^{117,119}Sn] 12.7 Hz. (unresolved).

^{119}Sn NMR [δ(ppm) $CDCl_3$ solution]: -63.6.

^{119m}Sn Mössbauer (mms^{-1}): I.S.=1.12; Q.S.=1.79.

IR [(cm^{-1}), liq. film]: 3535, 3058, 1610, 1576, 1480, 1334, 1068, 991, 724, 687.

2.8.2 Alternative synthesis of (1)

Anhydrous tin(IV) chloride (138.1g, 52.8 mmol) was added, under

nitrogen at room temperature to triphenyltin chloride (101.2g, 26.3mmol). The stirred mixture was then heated to 170°C for 3 hours during which time a black oil formed. This was then distilled at reduced pressure to yield a single fraction, trichlorophenyltin (229.0g, 96%) b.p. 81°C/0.2 mmHg.

Analysis: Found(Calc. for $C_6H_5Cl_3Sn$): C 23.8(23.9); H 1.81(1.72)%

2.8.3 Synthesis of tri-isopropylphenyltin (2)

To prepare the isopropyl Grignard reagent, *i*-propyl bromide (37.3g, 30.3 mmol) in diethyl ether (50 ml) was added dropwise with stirring to magnesium turnings (8.0g, 33.5 mmol) and a crystal of iodine in dry diethyl ether (200 ml). An exothermic reaction resulted causing the ether to reflux. When this had ceased the reaction mixture was allowed to stir at room temperature for a further hour. The prepared Grignard was then filtered through a glass wool plug to remove a small amount of unreacted magnesium. To the filtrate, cooled on an ice bath, trichlorophenyltin (20.4g, 6.7 mmol) in diethyl ether (50 ml) was added dropwise. Again an exothermic reaction occurred and stirring was continued at room temperature for a further 2 hours yielding a clear yellow ethereal solution and a heavy precipitate of inorganic salts. To decompose excess Grignard reagent, dilute ammonium chloride solution was added with caution and the organic phase separated. Two resultant washings with diethyl ether were combined and dried over anhydrous sodium sulphate. *In vacuo* removal of the solvent yielded a yellow oil which was distilled at reduced pressure to give a colourless oil, triisopropylphenyltin (18.6g, 86%), b.p. 95°C/0.3 mmHg.

Analysis: Found(Calc. for $C_{15}H_{29}Sn$): C 55.5(55.4); H 8.31(8.08)%

^1H NMR [δ(ppm), $CDCl_3$ solution]: 1.35 [d,18H,$(CH_3)_2CH$]; 1.67 [m,3H,$(CH_3)CH$]; 7.44 [m,5H,C_6H_5]; $^3J[(C^1H_3)_2CH\text{-}^{117,119}Sn]$ 62.6, 65.6 Hz.

^{13}C NMR [δ(ppm), $CDCl_3$solution]: 14.7 $[(CH_3)_2CH]$; 22.2 $[(CH_3)_2CH]$; 128.0 [*o*-C_6H_5]; 137.2 [*p*-C_6H_5]; 140.9 [*i*-C_6H_5]; $^1J[(CH_3)_2{}^{13}CH\text{-}^{117,119}Sn]$ 330.6, 346.0

Hz. $^{2}J[(^{13}CH_3)_2CH\text{-}^{117,119}Sn]$ 15.4, 17.6 Hz. $^{2}J[o\text{-}^{13}C_6H_5\text{-}^{117,119}Sn]$ 25.4 Hz. (unresolved); $^{4}J[p\text{-}^{13}C_6H_5\text{-}^{117,119}Sn]$ 12.2 Hz. (unresolved).

^{119}Sn NMR [δ(ppm), $CDCl_3$ solution]: -64.2.

^{119m}Sn Mössbauer (mms^{-1}): I.S.= 1.33; Q.S.=0.0.

IR [(cm^{-1}), liq. film]: 3063, 3050, 3015, 2955, 2934, 2857, 1462, 1428, 1383, 1368, 1200, 1152, 1073, 997, 986, 870, 725, 700, 503.

2.8.4 Synthesis of tri-isopropyltin iodide (3)

To a stirred solution of triisopropylphenyltin (32.0g, 9.8 mmol) in tetrachloromethane (200 ml) at 0°C, was added a solution of iodine (25.2g, 19.9 mmol) in tetrachloromethane (200 ml). The solution was allowed to warm to room temperature and stirred for 22 hours. Total decolourisation of the iodine did not occur after this period and *in vacuo* removal of the solvent produced an inviscid purple oil. Distillation of the crude product at reduced pressure yielded two fractions, the first being iodobenzene (b.p. 72°C/0.2 mmHg), and the second triisopropyltin iodide (29.1g, 78.6%), b.p. 100°C/0.2 mmHg.

Analysis: Found(Calc. for $C_9H_{21}ISn$): C 28.8(28.8); H 5.58(5.63)%

^{1}H NMR [δ(ppm), $CDCl_3$ solution]: 1.35 [d,18H,$(CH_3)_2CH$]; 1.80 [3H,m,$(CH_3)_2CH$].

^{13}C NMR [δ(ppm), $CDCl_3$ solution]: 20.24 [$(CH_3)_2CH$]; 21.93 [$(CH_3)_2CH$]; $^{2}J[(^{13}CH_3)_2CH\text{-}^{117,119}Sn]$ 15.5 Hz. (unresolved).

^{119}Sn NMR [δ(ppm), $CDCl_3$ solution]: +110.0

^{119m}Sn Mössbauer (mms^{-1}): I.S.=1.61; Q.S.=2.83.

IR [(cm^{-1}), liq.film]: 2957, 2936, 2861, 2721, 1462, 1385, 1367, 1197, 1152, 1084, 995, 918, 870, 731.

2.8.5 Synthesis of tri-isopropyltin azide (4)

A solution of tri-isopropyltin iodide (15.0g, 4.0 mmol) in diethyl ether was shaken with a five to one excess of sodium azide (13.1g, 20 mmol) in distilled water (50 ml). The resulting yellow ethereal layer was separated and the aqueous layer washed with a further 50 ml of diethyl ether. The combined washings were dried over sodium sulphate. *In vacuo* removal of the solvent afforded a greasy, low melting off-white solid. which was distilled at reduced pressure. The product, a colourless crystalline solid, boiled at 65-70°C/0.3 mmHg. ^{119}Sn NMR revealed unreacted amounts of the starting iodide which proved inseparable by further distillation and attempted sublimation of the azide. Crude product collected, 26.2g.

Analysis: Found(Calc. for $C_9H_{21}N_3Sn$): C 32.5(32.5); H 6.66(6.31); N 11.1(12.6)%

^{1}H NMR [δ(ppm), $CDCl_3$ solution]: 1.38 [d,18H,$(CH_3)_2CH$]; 1.85 [m,3H,$(CH_3)_2CH$]; $^3J[(C^1H_3)_2CH\text{-}^{117,119}Sn]$ 74.8, 88.4 Hz.

^{13}C NMR [δ(ppm), $CDCl_3$ solution]: 20.7 $[(CH_3)_2CH]$; 21.5 $[(CH_3)_2CH]$; $^1J[(CH_3)_2{}^{13}CH\text{-}^{117,119}Sn]$ 304.0, 317.4 Hz.

^{119}Sn NMR [δ(ppm) $CDCl_3$ solution]: +43.8.

^{119m}Sn Mössbauer (mms^{-1}): I.S.=1.27; Q.S.=3.39.

IR [(cm^{-1}), liq. film]: 2926, 2859, 2062 [ν_{asym} N_3], 1462, 1379, 1341, 1202, 1156, 1001, 918, 874, 634.

2.8.6 Synthesis of tetraethyltin (5)

The ethyl Grignard was prepared with magnesium turnings (5.2g, 21.7 mmol) and ethyl bromide (22.6g, 20.8 mmol) in diethyl ether (50 ml). When the exothermic reaction had ceased, the resulting cloudy solution was stirred for a further hour before filtration through a glass wool plug to remove unreacted magnesium. Tin(IV) chloride (11.1g, 4.25 mmol) was added slowly via a

dropping funnel producing a dense white precipitate of magnesium halides. Excess ethyl Grignard was hydrolysed with dilute ammonium chloride solution, the organic phase separated and dried over magnesium sulphate. *In vacuo* removal of solvent yielded a pale yellow oil which was used in subsequent reactions without further purification.

Analysis: Found(Calc. for $C_8H_{20}Sn$): C 40.7(40.9); H 8.88(8.52)%

^1H NMR [δ(ppm), $CDCl_3$ solution]: 0.72 [q,8H,CH_2CH_3]; 1.10 [t,12H,CH_2CH_3]; $^2J[C^1H_2$-$^{117,119}Sn]$ 56.5 Hz. (unresolved); $^3J[C^1H_3$-$^{117,119}Sn]$ 66.2, 68.7 Hz.

^{13}C NMR 0.1 [CH_2CH_3]; 11.4 [CH_2CH_3]; $^1J[^{13}CH_2CH_3$-$^{117,119}Sn]$ 315.2, 319.8 Hz; $^2J[CH_2{}^{13}CH_3$-,$^{117,119}Sn]$ 22.1 Hz. (unresolved).

^{119}Sn NMR [δ(ppm), $CDCl_3$ solution]: +2.3; $^1J[^{119}Sn$-$^{13}CH_2]$ 318.8 Hz.

^{119m}Sn Mössbauer (mms^{-1}): I.S.= 1.37; Q.S.=1.23.

2.8.7 Synthesis of triethyltin chloride (6)

(5) (4.85g, 2.1 mmol) and tin(IV) chloride (1.80g, 0.7 mmol) were heated to 180°C under nitrogen for three hours. This resulted in an amber oil which was used in subsequent reactions without further purification.

Analysis: Found(Calc. for $C_6H_{15}ClSn$): C 28.9(29.9); H 6.09(6.22)%

^1H NMR [δ(ppm), $CDCl_3$ solution]: 0.98-1.38 [m,15H,CH_2CH_3]

^{13}C NMR [δ(ppm), $CDCl_3$ solution]: 8.8 [CH_2CH_3]; 9.8 [CH_2CH_3]; $^1J[^{13}CH_2CH_3$-$^{117,119}Sn]$ 329.4, 344.8 Hz; $^2J[CH_2{}^{13}CH_3$-$^{117,119}Sn]$ 27.6 Hz. (unresolved).

^{119}Sn NMR [δ(ppm), $CDCl_3$ solution]: +160.2.

2.8.8 Synthesis of triethyltin azide (7)

(6) (4.5g, 1.9 mmol) in diethyl ether (50 ml) and sodium azide (2.5g, 3.8 mmol) in distilled water (20 ml) were shaken together as a two phase system. The organic layer was separated and the aqueous layer extracted with further

diethyl ether (50 ml). The combined ethereal washings were combined and dried over magnesium sulphate before *in vacuo* removal of the solvent. This yielded a pale brown oil whch solidified on standing. Distillation on a Kügelruhr apparatus gave a colourless oil, (3.6g, 78%), b.p. 105°C/1.5 mmHg, which solidified on standing.

Analysis: Found(Calc. for $C_6H_{15}N_3$): C 29.4(29.2); H 6.33(6.10); N 15.8(16.8)%

^{1}H NMR [δ(ppm), $CDCl_3$ solution]: 1.07 [q,6H,CH_2CH_3]; 1.24 [t,9H,CH_2CH_3]

^{13}C NMR [δ(ppm), $CDCl_3$ solution]: 10.2 [CH_2CH_3]; 10.4 [CH_2CH_3].

^{119}Sn NMR [δ(ppm), $CDCl_3$ solution]: +79.4.

^{119m}Sn Mössbauer (mms^{-1}): I.S.=1.47; Q.S.=3.60.

IR [(cm^{-1}), liq. film]: 2949, 2872, 2066 [ν_{asym} N_3], 1456, 1421, 1379, 1348, 1265, 1234, 1192, 1016, 952, 675.

2.8.9 Synthesis of methylene-bis-5,5'-(trimethylstannyltetrazole) (8)

Malononitrile (0.58g, 0.8 mmol) and trimethyltin azide (3.5g, 1.6 mmol) were heated together under nitrogen in a small round-bottomed flask at 140°C for 30 minutes. This resulted in a slightly charred grey mass which was dissolved in boiling methanol and decolourised with activated charcoal. Hot filtration followed by *in vacuo* removal of solvent yielded an off-white gum which was extracted with methanol in a soxhlet apparatus and reprecipitated as an amorphous solid (1.8g, 44%), m.p. >240°C.

Analysis: Found(Calc. for $C_9H_{20}N_8Sn_2$): C 23.1(22.6); H 4.18(4.18); N 22.9(23.4)%

^{1}H NMR [δ(ppm), DMSO-d^6 solution]: 0.57 [s,18H,CH_3]; 4.26 [s,2H,CH_2]; ^{2}J[C^1H_3-^{117,119}Sn] 70.0 Hz.(unresolved).

^{13}C NMR [δ(ppm), DMSO-d^6 solution]: -0.4 [CH_3]; 21.6 [CH_2]; 158.77 [CN_4]; ^{1}J[$^{13}CH_3$-^{117,119}Sn] 516.6 Hz.

^{119}Sn NMR [δ(ppm), DMSO-d^6 solution]: -43.8.

^{119m}Sn Mössbauer (mms^{-1}): I.S.=1.40; Q.S.=3.57.

IR [(cm^{-1}), KBr disk]: 3002, 2921, 1483, 1414, 1375, 1221, 1096, 787, 761, 662, 554.

2.8.10 Synthesis of methylene-bis-5,5′-(tributylstannyltetrazole) ***(9)***

A mixture of malononitrile (1.14g, 17.3 mmol) and tributyltin azide (11.43g, 34.5 mmol) w*as* heated slowly in a partially evacuated Schlenk tube under nitrogen at 110°C for 30 minutes. The reactants solidified to a yellow glass which was dissolved in boiling methanol. On cooling, the resultant sparingly soluble off-white solid was filtered and recrystallised as microcrystalline needles (5.72g, 45%), m.p. 209-212°C(dec) from methanol using a soxhlet apparatus.

Analysis: Found(Calc. for $C_{27}H_{56}N_8Sn_2$): C 44.7(44.6); H 7.98(7.77); N 15.5(15.4)%

^{1}H [δ(ppm), DMSO-d^6 solution]: 0.93 [t,18H,$(CH_2)_3CH_3$]; 1.12 [t,12H,$SnCH_2$-$(CH_2)_2CH_3$]; 1.40 [m,12H,$Sn(CH_2)_2CH_2CH_3$]; 1.65 [m,12H,$CH_2CH_2CH_2CH_3$]; 3.30 [s,2H,CH_2].

^{13}C NMR [δ(ppm), DMSO-d^6 solution]: 13.6 [$(CH_2)_3CH_3$]; 18.2 [$SnCH_2(CH_2)_2$-CH_3]; 22.8 [CH_2]; 26.4 [$Sn(CH_2)_2CH_2CH_3$]; 27.7 [$SnCH_2CH_2CH_2CH_3$]; 160.0 [CN_4].

^{119}Sn NMR [δ(ppm), DMSO-d^6 solution]: -52.5.

^{119m}Sn Mössbauer (mms^{-1}): I.S.=1.47; Q.S.=3.59.

IR [(cm^{-1}), KBr disk]: 2959, 2924, 2872, 2857, 1487, 1464, 1397, 1377, 1082, 879, 698, 680, 613, 509.

Mass Spectrum [(m/z), FAB]: 43, 100, 121 $[SnH]^+$, 137, 177 $[BuSn]^+$, 235 $[Bu_2SnH]^+$, 291 $[Bu_3Sn]^+$, 400, 746, 855.

2.8.11 Synthesis of 1,2-ethylene-bis-5,5′-(tributylstannyltetrazole) ***(10)***

Succinonitrile (1.28g, 1.6 mmol) and tributyltin azide (10.5g, 3.2 mmol)

were heated in a Schlenk tube under nitrogen to 120°C for 1 hour. During this period the reactants set to a solid white mass. Extended soxhlet extraction of this sparingly soluble solid with methanol resulted in a white powder (7.7g, 65%) m.p. 218°C(dec), with insufficient solubility for the collection of solution-state spectral data.

Analysis: Found(Calc. for $C_{28}H_{58}N_8Sn_2$): C 44.7(45.1); H 7.93(7.80); N 15.2(15.1)%

^{119m}Sn Mössbauer (mms^{-1}): I.S.=1.38; Q.S.=3.78.

IR [(cm^{-1}), KBr disk]: 2955, 2924 2869, 1476, 1391, 1262, 127, 1130, 1080, 1022, 870, 803, 706, 679, 615.

2.8.12 Synthesis of 1,2-phenylene-bis-5,5'-(tributylstannyltetrazole) ***(11)***

1,2 dicyanobenzene (5.61g, 4.4 mmol) was heated under nitrogen with tributyltin azide (28.9g, 8.7 mmol). Ten minutes at 170°C resulted in a viscous dark oil which solidified to a glass on cooling. This was dissolved in boiling methanol and decolourised with activated charcoal. Hot filtration afforded a yellow solution which on cooling yielded **(11)** as colourless cubic crystals (20.4g, 60%) m.p. 175°C.

Analysis: Found(Calc. for $C_{32}H_{58}N_8Sn_2$): C 48.5(48.6); H 7.48(7.45); N 14.2(14.1)%

^{1}H NMR [δ(ppm), DMSO-d^6 solution]: 0.78 [t,18H,$(CH_2)_3CH_3$]; 1.10-1.30 [m, 24H,$SnCH_2CH_2CH_2CH_3$]; 1.40 [m,12H,$SnCH_2CH_2CH_2CH_3$]; 7.54 [m,2H,*m*-C_6H_4]; 7.62 [m,2H,*o*-C_6H_4].

^{13}C NMR [δ(ppm), DMSO-d^6 solution]: 13.8 [$(CH_2)_3CH_3$]; 18.0 [$SnCH_2(CH_2)_3CH_3$]; 26.7 [$Sn(CH_2)_2CH_2CH_3$]; 27.8 [$SnCH_2CH_2CH_2CH_3$]; 128.0 [*m*-C_6H_4]; 130.3 [*o*-C_6H_4]; 133.2 [*i*-C_6H_4]; 160.9 [CN_4]; ^{2}J[$SnCH_2{}^{13}CH_2CH_3$-^{117,119}Sn] 28.6 Hz. (unresolved); ^{3}J[$(CH_2)_2{}^{13}CH_2CH_3$-^{117,119}Sn] 83.8 Hz. (unresolved).

^{119}Sn NMR [δ(ppm), DMSO-d^6 solution]: -70.5.

^{119m}Sn Mössbauer (ppm): I.S.=1.41, Q.S.=3.60.

IR [(cm^{-1}), KBr disk]: 2959, 2922, 2870, 2856, 1464, 1444, 1423, 1354, 1080, 1012, 756, 680, 613, 441.

Mass Spectrum [(m/z), FAB]: 67, 121 $[SnH]^+$, 137, 177 $[BuSn]^+$, 235 $[Bu_2SnH]^+$, 291 $[Bu_3Sn]^+$, 400, 746, 855.

2.8.13 Synthesis of 1,3-phenylene-bis-5,5'-(tributylstannyltetrazole) ***(12)***

A suspension of 1,3 dicyanobenzene (4.3g, 33.3 mmol) and tributyltin azide (22.0g, 66.6 mmol) was heated to 190°C in an analogous fashion for a period of one hour. During this time a homogeneous brown melt formed which set to a brittle glass upon cooling. This was dissolved in boiling methanol, decolourised with activated charcoal and filtered. Cooling to -20°C produced a bis methanol solvated **(12)** (20.2g, 77%) m.p. 68°C(dec) which could be converted to an amorphous, unsolvated form by gentle warming under vacuum m.p. 177-179°C(dec).

Analysis: Found(Calc. for $C_{32}H_{58}N_8Sn_2.2CH_3OH$): C 47.3(47.6); H 7.73(7.71); N 12.9(13.0)%: Found(Calc. for $C_{32}H_{58}N_8Sn_2$): C 48.9(48.6); H 7.36(7.45); N 14.2(14.1)%

^{1}H NMR [δ(ppm), DMSO-d^6 solution]: 0.87 [t,18H,$(CH_2)_3CH_3$]; 1.22-1.42 [m, 24H,$SnCH_2CH_2CH_2CH_3$]; 1.63 [m,12H,$CH_2CH_2CH_2CH_3$]; 8.08 [t,1H,*m*-C_6H_4]; 8.11 [d,2H,*o*-C_6H_4]; 8.77 [s,1H,*o*-C_6H_4].

^{13}C NMR [δ(ppm), DMSO-d^6 solution]: 13.7 [$(CH_2)_3CH_3$]; 18.4 [$CH_2(CH_2)_2CH_3$]; 26.5 [$(CH_2)_2CH_2CH_3$]; 27.8 [$CH_2CH_2CH_2CH_3$]; 124.1 [*m*-C_6H_4]; 126.4 [*o*-C_6H_4]; 129.3 [*o*-C_6H_4]; 130.6 [*i*-C_6H_4]; 162.2 [CN_4]; $^1J[^{13}CH_2(CH_2)_2CH_3$-$^{117,119}Sn]$ 484.8 Hz. (unresolved); $^2J[CH_2{}^{13}CH_2CH_2CH_3$-$^{117,119}Sn]$ 28.6 Hz. (unresolved); $^3J[(CH_2)_2{}^{13}CH_2CH_3$-$^{117,119}Sn]$ 75.0 Hz. (unresolved).

^{119}Sn NMR [δ(ppm), DMSO-d^6 solution]: -54.0.

^{119m}Sn Mössbauer (mms^{-1}): Unsolvated compound, I.S.=1.41; Q.S.=3.65.

IR [(cm^{-1}), KBr disk]: 2957, 2924, 2872, 2855, 1464, 1427, 1377, 1080, 879, 746, 696, 679, 611.

Mass Spectrum [(m/z), FAB]: 25, 88, 121 $[SnH]^+$, 137, 177 $[BuSn]^+$, 235 $[Bu_2SnH]^+$, 291 $[Bu_3Sn]^+$, 400, 746, 855.

2.8.14 Synthesis of 1,4-phenylene-bis-5,5′-(tributylstannyltetrazole) ***(13)***

1,4 dicyanobenzene (6.02g, 4.7 mmol) and tributyltin azide (30.9g, 9.3 mmol) were heated together to 150°C under nitrogen during which time the initial suspension became a solid mass. This was dissolved in boiling methanol, decolourised with activated carbon, filtered and cooled to -20°C affording **(13)** as a colourless polycrystalline solid (24.2g, 70%) m.p. 220-222°C(dec).

Analysis: Found(Calc. for $C_{32}H_{58}N_8Sn_2$): C 48.4(48.6); H 7.36(7.45); N 13.9(14.1)%

^{1}H NMR [δ(ppm), DMSO-d^6 solution]: 0.89 [t,18H,$(CH_2)_3CH_3$]; 1.29-1.49 [m,24H,$SnCH_2CH_2CH_2CH_3$]; 1.64 [m,12H,$SnCH_2CH_2CH_2CH_3$]; 8.20 [s,4H,*o*-C_6H_4].

^{13}C NMR [δ(ppm), DMSO-d^6 solution]: 13.7 $[(CH_2)_3CH_3]$; 18.4 $[SnCH_2(CH_2)_2CH_3]$; 26.4 $[Sn(CH_2)_2CH_2CH_3]$; 27.8 $[SnCH_2CH_2CH_2CH_3]$; 126.6 [*o*-C_6H_4]; 130.2 [*i*-C_6H_4]; 162.1 [CN_4]; $^2J[CH_2{}^{13}CH_2CH_2CH_3$-$^{117,119}Sn]$ 30.8 Hz. (unresolved); $^3J[(CH_2)_2{}^{13}CH_2CH_3$-$^{117,119}Sn]$ 75.0 Hz. (unresolved).

^{119}Sn NMR [δ(ppm), DMSO-d^6 solution]: -55.0.

^{119m}Sn Mössbauer (mms^{-1}): I.S.=1.43; Q.S.=3.73.

IR [(cm^{-1}), KBr disk]: 2959, 2924, 2870, 2855, 1464, 1443, 1427, 1010, 852, 752, 690, 615, 490, 478.

Mass Spectrum [(m/z), FAB]: 100, 121 $[SnH]^+$, 137, 177 $[BuSn]^+$, 235 $[Bu_2SnH]^+$, 291 $[Bu_3Sn]^+$, 400, 746, 855.

2.8.15 Synthesis of methylene-bis-5,5'-(tri-isopropylstannyltetrazole) ***(14)***

(4) (10.43g,3.6 mmol) and malononitrile (1.28g, 2.0 mmol) were heated in a partially evacuated Schlenk tube under nitrogen. One hour at 100°C resulted in a tacky brown glass. This was dissolved in hot ethanol, decolourised with activated carbon, and filtered hot resulting in a yellow solution. *In vacuo* removal of solvent yielded a light brown gum which was recrystallised several times from methanol to yield **(14)** as an off-white solid (2.52g, 22%) m.p. 190°C(dec).

Analysis: Found(Calc. for $C_{21}H_{44}N_8Sn_2$): C 38.9(39.0); H 6.80(6.85); N 16.9(16.9)%

^1H NMR [δ(ppm), DMSO-d^6 solution]: 1.23 [s,18H,$(CH_3)_2CH$]; 1.92 [m,3H,$(CH_3)_2CH$]; 4.31 [s,2H,CH_2]; $^3J[(C^1H_3)_2CH\text{-}^{117,119}Sn]$ 79.0, 83.8 Hz.

^{13}C NMR [δ(ppm), DMSO-d^6 solution]: 21.1 $[(CH_3)_2CH]$; 24.2 $[(CH_3)_2CH]$; 24.2 $[CH_2]$; 162.6 $[CN_4]$; $^1J[(CH_3)_2{}^{13}CH\text{-}^{117,119}Sn]$ 440.8 Hz. (unresolved); $^2J[(^{13}CH_3)_2CH\text{-}^{117,119}Sn]$ 19.8 Hz. (unresolved).

^{119}Sn NMR [δ(ppm), DMSO-d^6 solution]: -84.1.

^{119m}Sn Mössbauer (mms^{-1}): I.S.=1.52; Q.S.=3.68.

IR [(cm^{-1}), KBr disk]: 2963, 2936, 2861, 1464, 1385, 1367, 1273, 1224, 1206, 1156, 1109, 1088, 1006, 619, 478.

Mass Spectrum [(m/z), FAB]: 121 $[SnH]^+$, 163 $[^iPrSnH]^+$, 207 $[^iPr_2SnH]^+$, 249 $[^iPr_3Sn]^+$, 286, 372, 416, 506, 523, 603 $[M^+\text{-}^iPr]$, 648 $[M^+]$, 663, 786.

2.8.16 Synthesis of 1,2-phenylene-bis-5,5'-(tri-isopropylstannyltetrazole) ***(15)***

(4) (4.8g, 16.4 mmol) and 1,2 dicyanobenzene (1.1g, 8.0 mmol) were heated in an analogous manner to that described above to yield an inviscid pale brown oil after one hour at 100°C. Dissolution in methanol, decolourisation with activated carbon and subsequent removal of solvent yielded a yellow oil. Trituration with hexane/diethyl ether afforded **(15)** as an amorphous white

powder (2.8g, 48.3%), m.p. 192°C(dec).

Analysis: Found(Calc. for $C_{26}H_{46}N_8Sn_2$): C 46.4(44.1); H 5.92(6.50); N 16.5(15.8)%

^1H NMR [δ(ppm), DMSO-d^6 solution]: 1.33 [d,18H,$(CH_3)_2CH$]; 2.01 [br.s,3H,$(CH_3)_2CH$]; 7.73 [m,2H,*m*-C_6H_4]; 8.08 [m,2H,*o*-C_6H_4]; $^3J[(C^1H_3)_2CH-^{117,119}Sn]$ 80.4, 84.4 Hz.

^{13}C NMR [δ(ppm), DMSO-d^6 solution]: 21.3 [$(CH_3)_2CH$]; 24.6 [$(CH_3)_2CH$]; 128.8 [*m*-C_6H_4]; 129.2 [*o*-C_6H_4]; 132.4 [*i*-C_6H_4]; 160.1 [CN_4]; $^2J[(^{13}CH_3)_2CH-^{117,119}Sn]$ 22.0 Hz. (unresolved).

^{119}Sn NMR [δ(ppm), DMSO-d^6 solution]: -81.3.

^{119m}Sn Mössbauer (mms^{-1}): I.S.=1.55; Q.S.=3.73.

IR [(cm^{-1}), KBr disk]: 2961, 2942, 2861, 1462, 1426, 1358, 1206, 1154, 1013, 779, 619, 499, 476.

Mass Spectrum [(m/z), FAB]: 121 $[SnH]^+$, 137, 163 $[^iPrSn]^+$, 207 $[^iPr_2SnH]^+$, 249 $[^iPr_3Sn]^+$, 286, 372, 420, 664 $[M^+-^iPr]$, 709 $[M^+]$, 789.

2.8.17 Synthesis of 1,4-phenylene-bis-5,5'-(tri-isopropylstannyltetrazole) ***(16)***

(4) (6.5g, 2.3 mmol) and 1,4 dicyanobenzene (1.5g, 1.2 mmol) were heated in an analogous fashion to 120°C for 30 minutes. This resulted in a brown oil which solidified on cooling to a cream-coloured solid. This was extracted into methanol using a soxhlet apparatus to yield **(16)** on cooling as a white amorphous powder (2.6g, 33%), m.p. 183°C.

Analysis: Found(Calc. for $C_{26}H_{46}N_8Sn_2$): C 42.4(44.1); H 6.51(6.50); N 15.3(15.8)%

^1H NMR [δ(ppm), DMSO-d^6 solution]: 1.33 [d,18H,$(CH_3)_2CH$]; 2.01 [br.s,3H,$(CH_3)_2CH$]; 8.17 [br.m,*ca.*4H,*o,m*-C_6H_4]; $^3J[(C^1H_3)_2CH-^{117,119}Sn]$ 81.0, 84.34 Hz.

^{13}C NMR [δ(ppm), DMSO-d^6 solution]: 21.4 [$(CH_3)_2CH$]; 24.4 [$(CH_3)_2CH$];

126.6 [*o,m*-C_6H_4]; 130.1 [*i*-C_6H_4]; 161.8 [CN_4]; $^2J[(^{13}CH_3)_2CH\text{-}^{117,119}Sn]$ 19.8 Hz. (unresolved).

^{119}Sn NMR [δ(ppm), DMSO-d^6 solution]: -82.2.

^{119m}Sn Mössbauer (mms^{-1}): I.S.=1.53; Q.S.=3.64.

IR [(cm^{-1}), KBr disk]: 2936, 2861, 1464, 1426, 1385, 1367, 1269, 1209, 1156, 1121, 1021, 1005, 874, 853, 747, 513, 484.

Mass Spectrum [(m/z), FAB]: 121 $[SnH]^+$, 137, 163 $[^iPrSn]^+$, 207 $[^iPr_2SnH]$, 249 $[^iPr_3Sn]^+$, 286, 372, 568, 581.

2.8.18 Synthesis of 1,2-phenylene-bis-5,5′-(triethylstannyltetrazole) ***(17)***

(7) (3.4g, 1.3 mmol), and 1,2-dicyanobenzene (0.88g, 0.7 mmol) were heated in an analogous manner at 160°C for 45 minutes, to yield a solid off-white mass. Recrystallisation from methanol yielded **(17)** as colourless cubic crystals (2.7g, 63%) m.p. 230°C(dec).

Analysis: Found(Calc. for $C_{20}H_{34}N_8Sn_2$): C 38.3(38.5); H 5.41(5.45); N 17.7(17.8)%

^1H NMR [δ(ppm), DMSO-d^6 solution]: 0.70-0.81 [m,30H,CH_2CH_3]; 7.20 [dd,2H,*m*-C_6H_4]; 7.34 [dd,2H,*o*-C_6H_4].

^{13}C NMR [δ(ppm), DMSO-d^6 solution]: 10.0 [CH_2CH_3]; 10.0 [CH_2CH_3]; 128.6 [*m*-C_6H_4]; 129.8 [*o*-C_6H_4]; 129.9 [*i*-C_6H_4]; 161.2 [CN_4]; $^1J[^{13}CH_2CH_3\text{-}^{117,119}Sn]$ 470.6, 490.8 Hz.

^{119}Sn NMR [δ(ppm), DMSO-d^6 solution]: -47.1.

^{119m}Sn Mössbauer (mms^{-1}): I.S.=1.48; Q.S.=3.86.

IR [(cm^{-1}), KBr disk]: 2950, 2870, 1458, 1441, 1423, 1352, 1224, 1013, 961, 756, 684, 527, 442.

2.8.19 Synthesis of 1,3-phenylene-bis-5,5'-(triethylstannyltetrazole) (18)

(7) (2.0g, 0.8 mmol) and 1,3 dicyanobenzene (0.52g, 0.4 mmol) were refluxed in mesitylene (20 ml) for two hours. The insoluble product precipitated from solution as the reaction progressed and, on cooling, was filtered and washed with diethyl ether. Attempted recrystallisation from methanol yielded **(18)** as an amorphous white powder (1.7g, 68%) m.p. 208°C(dec).

Analysis: Found(Calc. for $C_{20}H_{34}N_8Sn_2$): C 38.6(38.5); H 5.53(5.45); N 17.2(17.8)%

^{1}H NMR [δ(ppm), DMSO-d^6 solution]: 1.23 [t,18H,CH_2CH_3]; 1.34 [m,12H,CH_2CH_3]; 7.58 [t,1H,*m*-C_6H_4]; 8.07 [d,2H,*o*-C_6H_4]; 8.76 [s,1H,*o*-C_6H_4].

^{13}C NMR [δ(ppm), DMSO-d^6 solution]: 10.3 [CH_2CH_3]; 10.3 [CH_2CH_3]; 126.5 [*m*-C_6H_4]; 126.8 [*o*-C_6H_4]; 130.5 [*o*-C_6H_4]; 137.1 [*i*-C_6H_4]; 162.3 [CN_4]; ^{2}J[$CH_2{}^{13}CH_3$-^{117,119}Sn] 34.2 Hz. (unresolved).

^{119}Sn NMR [δ(ppm), DMSO-d^6 solution]: -49.8.

^{119m}Sn Mössbauer (mms^{-1}): I.S.=1.50; Q.S.=3.82.

IR [(cm^{-1}), KBr disk]: 2950, 2870, 1458, 1422, 1377, 1329, 1221, 1194, 1142, 1105, 1016, 961, 808, 761, 748, 683, 523, 488.

2.8.20 Synthesis of methylene-bis-5,5'-(hydrotetrazole) (19)

To **(9)** (7.3g,10 mmol) in methanol (100ml) was added 12M HCl (1.8ml, 20 mmol). This caused the colourless suspension to dissolve and the resulting solution was refluxed for one hour. *In vacuo* removal of the solvent yielded a white oily solid whch was washed well with hexane and filtered. Recrystallisation from methanol, yielded **(19)** in stoichiometric yield.

Analysis: Found(Calc. for $C_3H_4H_8$): C 23.5(23.7); H 2.58(2.65); N 74.0(73.7)%

^{1}H NMR [δ(ppm), DMSO-d^6 solution]: 3.2 [s,2H,CH_2]; 14.74 [s,2H,N*H*].

^{13}C NMR [δ(ppm), DMSO-d^6 solution]: 18.3 [CH_2]; 151.6 [CN_4].

2.8.21 Synthesis of 1,2-phenylene-bis-5,5′-(hydrotetrazole) ***(20)***

(11) (3.0g, 3.8 mmol) was treated in an analogous fashion with 12M HCl (1ml, 12 mmol) and the resultant white solid recrystallised as white needles from methanol in stoichiometric yield. Microanalysis revealed this to be hydrated, despite drying under vacuum.

Analysis: Found(Calc. for $C_8H_6N_8.1.5H_2O$): C 40.2(40.2); H 2.76(3.21); N 46.5(46.8)%

^{1}H NMR [δ(ppm), DMSO-d^6 solution]: 5.74 [br.s,2H,H_2O]; 7.81 [m,2H,*o*-C_6H_4]; 7.90 [m,2H,*m*-C_6H_4]; 9.97 [br.s,2H,N*H*].

^{13}C NMR [δ(ppm), DMSO-d^6 solution]: 124.7 [*i*-C_6H_4]; 130.5 [*o*-C_6H_4]; 131.5 [*m*-C_6H_4]; 155.0 [*C*N_4].

IR [(cm^{-1}), nujol mull]: 3395, 1585, 1458, 1377, 1049, 745.

2.8.22 Synthesis of 1,3-phenylene-bis-5,5′-(hydrotetrazole) ***(21)***

(12) (5.0g, 6.3 mmol) was treated in an analogous fashion with 12M HCl (2ml, 24 mmol) and the resultant white solid recrystallised, again in hydrated form, as white needles in stoichiometric yield.

Analysis: Found(Calc. for $C_8H_6N_8.H_2O$): C 41.7(41.3); H 2.77(2.61); N 47.9(48.2)%

^{1}H NMR [δ(ppm), DMSO-d^6 solution]: 7.79 [t,1H,*m*-C_6H_4]; 8.17 [dd,2H,*o*-C_6H_4]; 8.74 [t,1H,*o*-C_6H_4].

^{13}C NMR [δ(ppm), DMSO-d^6 solution]: 125.4 [*m*-c_6H_4]; 125.7 [*i*-C_6H_4]; 129.4 [2x *o*-C_6H_4]; 130.7 [1x *o*-C_6H_4]; 155.6 [*C*N_4].

IR [(cm^{-1}), nujol mull]: 3407, 1622, 1568, 1462, 1377, 1246, 1093, 1032, 999, 814, 761, 733, 682.

2.8.23 Synthesis of 1,4-phenylene-bis-5,5'(hydrotetrazole) (22)

(13) (5.0g, 6.3 mmol)was treated in an analogous fashion with 12M HCl (2ml, 24 mmol) and the resultant white solid recrystallised from methanol in stoichiometric yield.

Analysis: Found(Calc. for $C_8H_6N_8$): C 44.5(44.8); H 2.68(2.81); N 51.8(52.3)%

^{1}H NMR [δ(ppm), DMSO-d^6 solution]: 8.21 [s,4H,*o*-C_6H_4].

^{13}C NMR [δ(ppm), DMSO-d^6 solution]: 127.8 [*i*-C_6H_4]; 128.0 [*o*-C_6H_4]; 155.4 [CN_4].

IR [(cm^{-1}), nujol mull]: 3400, 1586, 1504, 1489, 1456, 1408, 1377, 1280, 1176, 1084, 1053, 1030, 987, 852, 733, 706.

2.8.24 Attempted Complexation Reactions

The coordination chemistry of the various bis-(triorganostannyltetrazole) compounds was investigated using several metal salts. All reactions were carried out in methanol using a two to one ratio of bis-tetrazole to metal salt. Representative reactions are described below.

Reaction of (9) with Nickel Acetate

To a stirred solution of (**9**) (1.2g, 1.6 mmol) in methanol (40 ml) was added $Ni(OAc)_2.4H_2O$ in methanol (40 ml) and the resulting suspension refluxed for one hour. The resulting purple solid was filtered and dried.

Analysis: Found(Calc. for $C_{33}H_{60}N_{24}Ni_2Sn_2$): C 32.0(34.4); H 5.26(5.60); N 29.2(29.2)%

^{119m}Sn Mössbauer (mms^{-1}): I.S.=1.42; Q.S.=3.63.

Reaction of (15) with Nickel Perchlorate

(15) (0.21g, 0.3 mmol) was stirred as a solution in methanol (50 ml). $Ni(ClO_4)_2.6H_2O$ (0.05g, 0.15 mmol) was added as a green solid causing immediate precipitation of a small amount of pink solid. The suspension was refluxed for one hour before hot filtration to yield a pink amorphous solid. Mössbauer analysis revealed almost complete removal of tin.

Analysis: Found(Calc. for $C_{27}H_{48}N_8Ni_2Sn_2$): C 35.9(39.9); H 2.68(4.28); N 29.5(26.8)%

Reaction of (14) with Copper Acetate

(14) (0.75g, 1 mmol) was stirred in methanol solution (20 ml). Addition of $Cu(OAc)_2.4H_2O$ (0.1g, 2 mmol) caused an immediate pale blue precipitate. The suspension was refluxed for one hour before filtration to afford a small amount of pale blue amorphous powder which proved insoluble in all available solvents.

Analysis: Found(Calc. for $C_{27}H_{48}N_{24}Cu_2Sn_2$): C 27.6(30.0); H 4.45(4.45); N 28.9(31.2)%

^{119m}Sn Mössbauer (mms^{-1}): I.S.=1.55; Q.S.=3.73.

2.8.25 Attempted reaction of (11) with Sulphur Dichloride

To a stirred suspension of **(11)** (2.8g, 3.5 mmol) in acetonitrile (250 ml) under nitrogen at room temperature was added SCl_2 (0.5g, 4.7 mmol) in acetonitrile (80 ml). This was refluxed for two hours to produce a deep orange solution. *In vacuo* removal of the solvent yielded an orange solid and an oil. This was washed with hexane and filtered to yield an orange solid (0.7g, 82%). Removal of the hexane from the filtrate afforded 1.35g of an oil identified by IR as Bu_3SnCl. Although soluble in a number of polar solvents recrystallisation was not possible without decomposition.

Analysis: Found(Calc. for $C_{16}H_8N_{16}S_2$): C 35.0(39.3); H 4.05(1.60); N 41.8(45.9)%

^{1}H NMR [δ(ppm), MeOH-d^4 solution]: 27.83 [s,2H,*m*-C_6H_4]; 8.04 [s,2H, *o*-C_6H_4].

^{13}C NMR [δ(ppm), MeOH-d^4 solution]: 125.9 [*i*-C_6H_4]; 131.9 [*m*-C_6H_4]; 132.6 [*o*-C_6H_4]; 157.1 [CN_4].

2.8.26 Attempted Reaction of ***(11)*** *with Dichlorophenylphosphine*

(11) (1.92g, 2.4 mmol) was stirred as a suspension in THF (100 ml). To this was slowly added a solution of $PhPCl_2$ in THF (50 ml) under nitrogen. This was then stirred for two days to yield a colourless solution. *In vacuo* removal of the solvent afforded a sticky yellow solid which was washed successively with hexane and diethyl ether, before filtration resulting in an amorphous yellow powder (0.42g, 54%). Mössbauer revealed the product contained no tin. Although soluble in a number of solvents recrystallisation was not possible.

^{1}H NMR [δ(ppm), MeOH-d^4 solution]: 7.41 [m,2H]; 7.80 [s,7H]; 7.94 [s,6H].

^{13}C NMR [δ(ppm), MeOH-d^4 solution]: 125.8 [*i*-C_6H_4]; 129.3 [*C*H]; 129.5 [*C*H]; 131.9 [*C*H]; 132.6 [*C*H]; 152.1 [CN_4].

^{31}P NMR [δ(ppm), MeOH-d^4 solution]: 15.9 (100%); 18.2 (10%).

2.8.27 Attemted Reaction of ***(11)*** *with Dichlorophenylborane*

(11) (2.15g, 2.7 mmol) was stirred as a suspension in toluene (100 ml). $PhBCl_2$ (0.43g, 2.7 mmol) in toluene (40 ml) was added dropwise under nitrogen and the resulting suspension refluxed for two hours. This afforded a white suspension which was filtered hot to yield an amorphous white solid (0.56g) and a colourless solution. The solid proved insoluble in all available solvents and was probably polymeric in nature. *In vacuo* removal of the solvent yielded a sticky white solid which was washed with hexane and filtered to afford a white

amorphous solid. Mössbauer revealed no tin in the insoluble solid and a residual amount in the soluble solid, an observation further confirmed by both ^{1}H and ^{13}C NMR.

Analysis: Found(Calc. for $C_{28}H_{18}N_{16}B_2$): Insoluble material: C 50.4(56.2); H 3.31(3.00); N 31.7(37.5): Soluble material: C 44.8(56.2); 3.67(3.00); 43.5(37.5).

^{11}B NMR [δ(ppm), MeOH-d^4 solution]: 26.6.

Chapter 3

The Reaction of α,ω-Dibromoalkanes and Bis-(tributylstannyltetrazoles) Applied to the Synthesis of Tetra-tetrazole Macrocycles

3.1 Introduction

Chapter 2 of this thesis described the synthesis and structural chemistry of several bis-(organostannyltetrazole) compounds and outlined the difficulties encountered in attempts to employ the reactivity of the Sn-N bond in macrocycle formation. This chapter seeks to address these problems and describes work directed towards the linkage of bis-tetrazole units with more durable alkyl chains, provided by reaction of tributyltin-substituted tetrazole compounds with α,ω-dibromoalkanes.

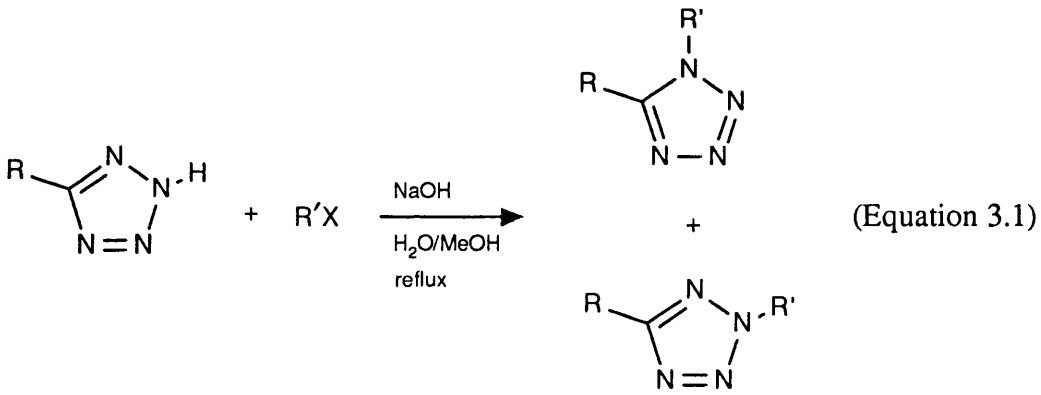

(Equation 3.1)

Alkylation of 5-substituted tetrazole derivatives generally leads to mixtures of N^1- and N^2-substituted products.[180] This is most commonly performed by the reaction of alkyl halide or dialkyl sulphate with the appropriate Na^+ or K^+ tetrazole salt (Equation 3.1), with the relative proportions of N^1- and N^2-substitution being dependent on the conditions of the alkylation and the

influence of the 5-substituent.[180] The reaction of alkyl halides with 5-R-tetrazoles N-substituted by certain transition metals such as gold[230] and cobalt[231] has been shown to yield predominantly 1,5-disubstituted tetrazoles. The regiospecificity of the alkylation in these cases is reasoned to be sterically promoted and similar reactivity and selectivity has also been noted for tri-n-butyltin-substituted tetrazoles.[232] In this case up to 90% N^1 alkylation was achieved by treating the tin-sustituted derivative with normal alkylating agents such as MeI and Me_2SO_4. This reactivity should also be applicable to the bis-(trialkylstannyltetrazole) compounds described in chapter 2 and the methodology adaptable to propose a synthetic route to novel tetra-tetrazole macrocycles.

The full proposed synthetic sequence is illustrated in Scheme 3.1, beginning with either the 1,2-phenylene-bis-5,5′-(tributylstannyltetrazole) **(11)** or its 1,3-phenylene-bridged analogue **(12)**, both of which provide a rigid link between pairs of tetrazole rings. Reaction with an excess of α,ω-dibromoalkane will provide bromoalkyl-substituted bis-tetrazole compounds although the probable mixture of isomers would require subsequent separation. The remaining functionality provided by the bromoalkyl chain can then be employed in conventional tetrazole alkylation procedures with the anions of the appropriate bis-(hydrotetrazole), **(20)** or **(21)**, to form the desired macrocycle. This procedure should be applicable to any alkyl chain length to produce tetra-tetrazole macrocycles of various cavity sizes.

Similar macrocyclic compounds with tetrazoles linked by C_6-C_8 alkyl chains have recently been reported by Butler *et al.*[233] The alternative pathway used by Butler *et al.* is depicted in Scheme 3.2 and employs a stepwise synthesis of the tetrazole rings with consecutive linkage by reaction of the free tetrazole compounds with dibromoalkane. The long-chain compounds synthesised by this method have considerable flexibility due to rotation of the bonds from the

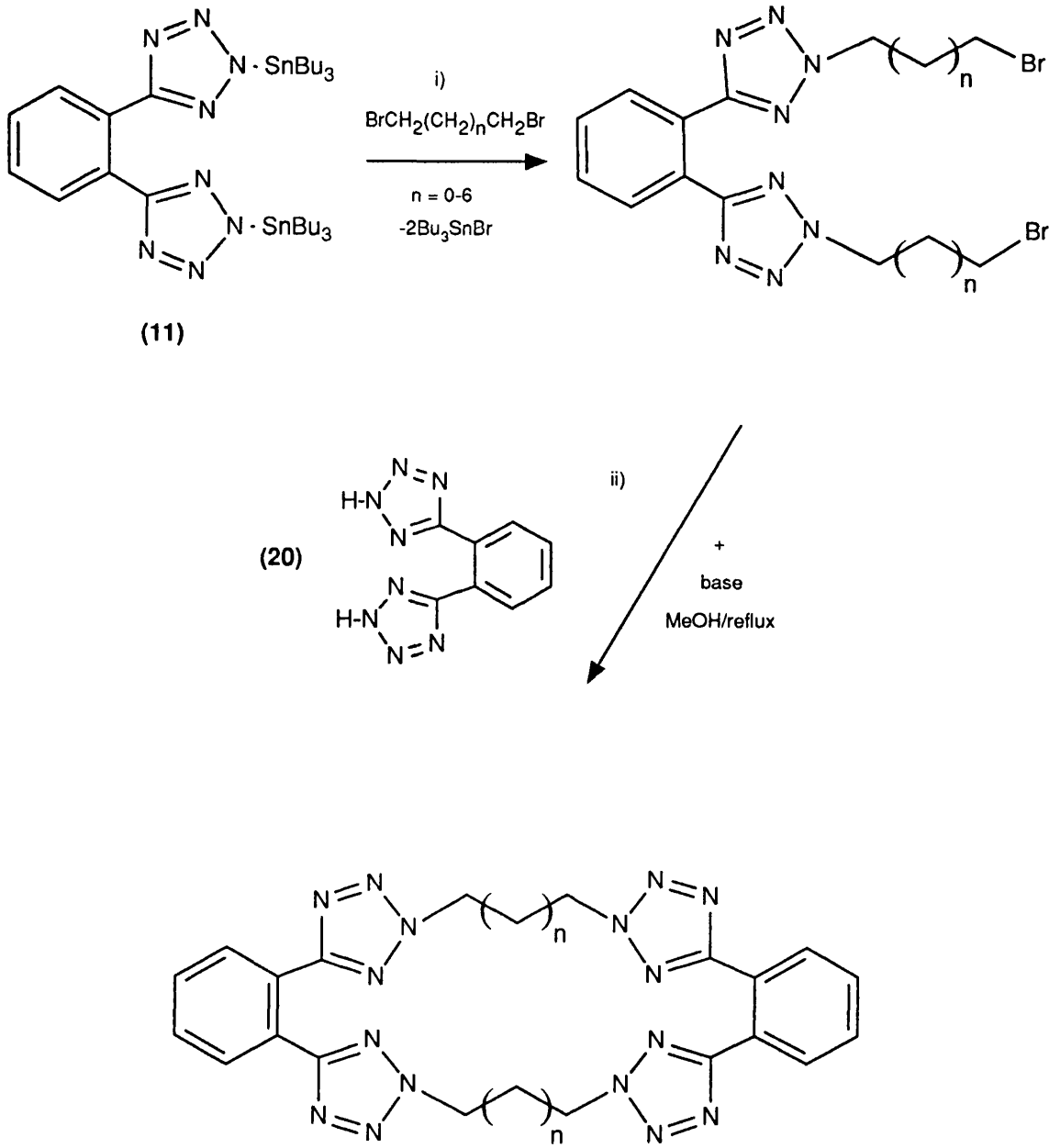
N · SnBu3
N · SnBu3
i)
BrCH2(CH2)nCH2Br
n = 0-6
-2Bu3SnBr
Br
Br
n
n
(11)
(20)
H-N
H-N
ii)
+
base
MeOH/reflux
n
n

Scheme 3.1

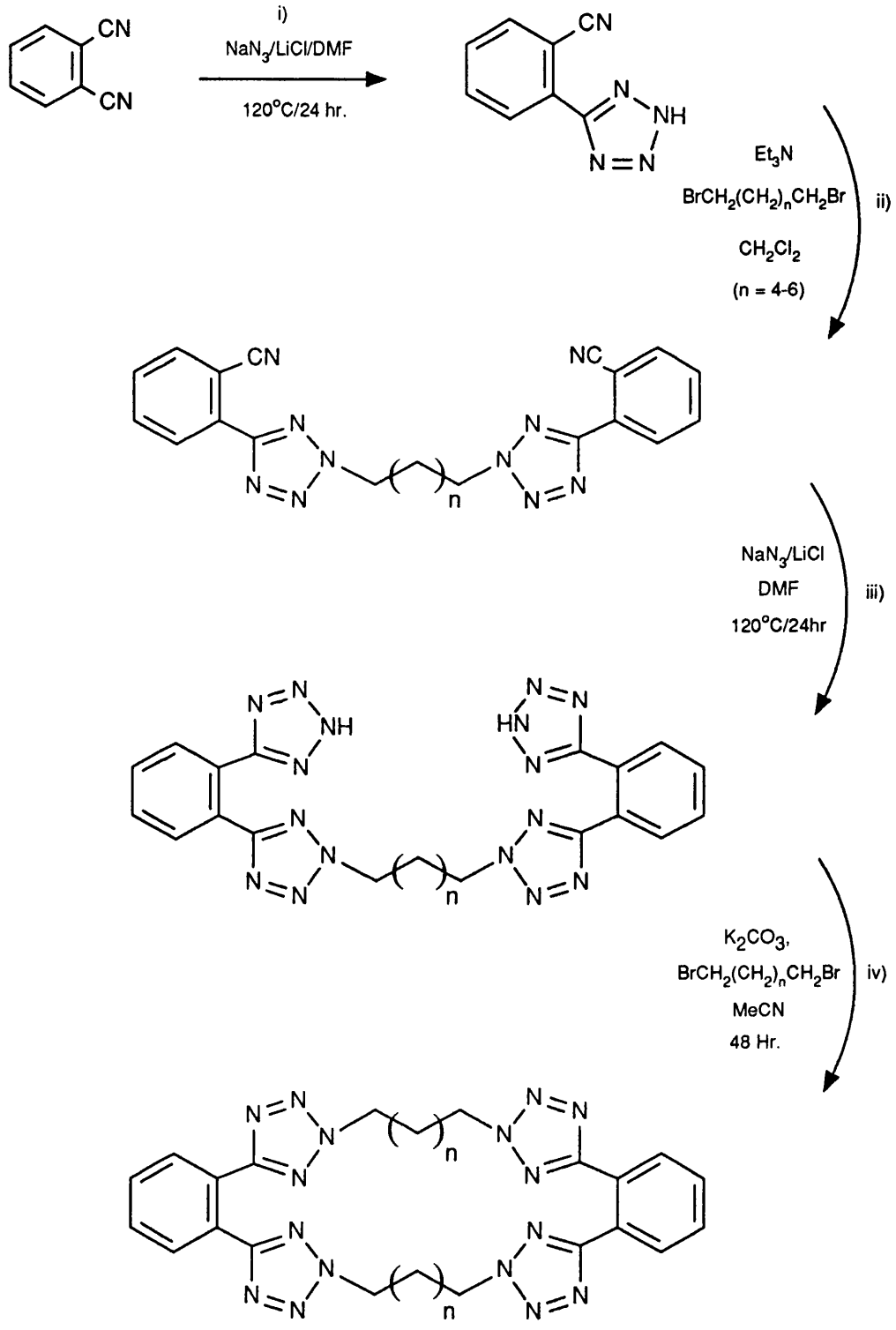
i)
NaN3/LiCl/DMF
120°C/24 hr.
Et3N
BrCH2(CH2)nCH2Br
CH2Cl2
(n = 4-6)
ii)
NaN3/LiCl
DMF
120°C/24hr
iii)
K2CO3,
BrCH2(CH2)nCH2Br
MeCN
48 Hr.
iv)

Scheme 3.2

tetrazole C^5 and N^2 atoms. This is clearly illustrated by a recent crystallographic analysis of a -$(CH_2)_8$- bridged macrocyle perfomed at the University of Bath in collaboration with the synthetic work undertaken at University College, Galway.[234] The folded conformation adopted in the solid-state by this compound is shown in Figure 3.1. Precisely this conformational flexibility and large cavity size make compounds of this type interesting in terms of metal complexation reactions. Indeed, preliminary work with the C_8-linked macrocycle has shown that up to three copper atoms can be accommodated in the resultant complex.[234] Although the sequential synthetic route illstrated in Scheme 3.2 has been unequivocably proven to be applicable to the synthesis of large cavity macrocycles, some difficulty has been encountered in realising shorter chain analogues.[235] It was hoped therefore that the organotin-based route of Scheme 3.1, requiring shorter reaction times in the cycloaddition step, would prove more generally suited to the synthesis of large, medium and small cavity macrocycles.

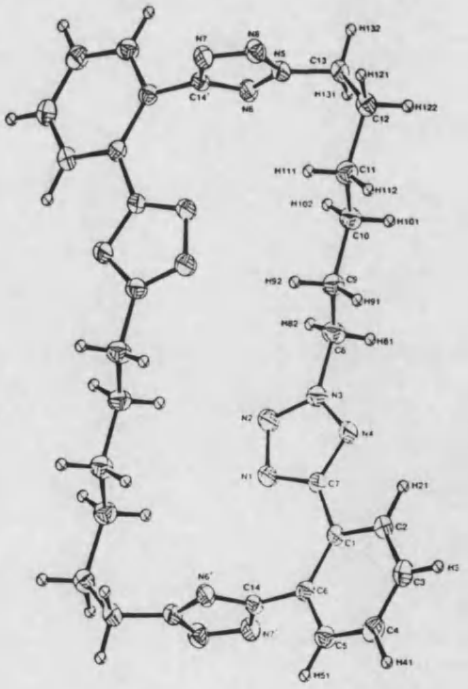

Figure 3.1: Crystal structure of a -$(CH_2)_8$- linked tetra-tetrazole macrocycle, showing the folded conformation adopted in the solid state

3.2 Synthesis

The major part of the synthetic effort detailed in this chapter concentrates on the synthesis and characterisation of the products formed from the reaction of the bis-(trialkylstannyltetrazole) compounds **(11)** and **(12)** and α,ω-dibromo-alkanes, $BrCH_2(CH_2)_nCH_2Br$ (n = 0-6), of various chain lengths.

Initial reaction of **(11)** with a ten-fold excess of 1,2-dibromoethane in refluxing methanol solution yielded a crystalline compound **(23)**. Although NMR data (see Section 3.3) and microanalysis suggested that a hydrated form of the target macrocycle had been produced directly, subsequent x-ray crystallo-graphic analysis on what proved to be an anhydrous crystal (see Section 3.4) revealed that the *ortho*-positioned tetrazole rings had in fact been linked in an inter-annular fashion between $N^1$and $N^{1'}$ by the ethyl chain (Equation 3.2). This compound is somewhat reminiscent of the cyclophane type macrocycles reported by Ried *et al.*,[236,237] the latter cases however involving N^2, $N^{2'}$ or N^1, $N^{2'}$ linkage and rather longer alkyl chains between five and ten methylene units long.

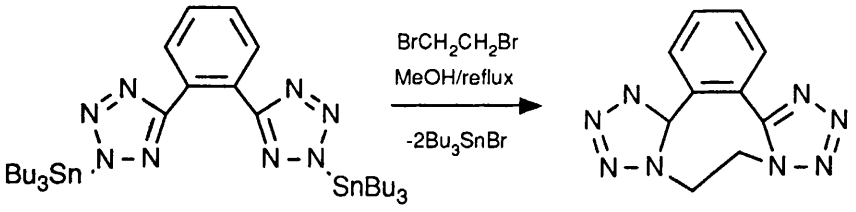

(Equation 3.2)

(11) **(23)**

A range of bis-(bromoalkyltetrazole) compounds has been prepared from **(11)** and **(12)** by employing the relevant α,ω-dibromoalkane as both reactant and solvent (i.e. in large excess, *ca.* 25:1 mole ratio) and subsequent separation of the resultant mixture of isomers by column chromatography (Equations 3.3 and 3.4). Reaction under the conditions indicated resulted, in the main, in two major products, the N^2,$N^{2'}$-substituted and N^1,$N^{2'}$-substituted isomers. In several cases the second of these, although indicated by initial thin layer chromatography, was

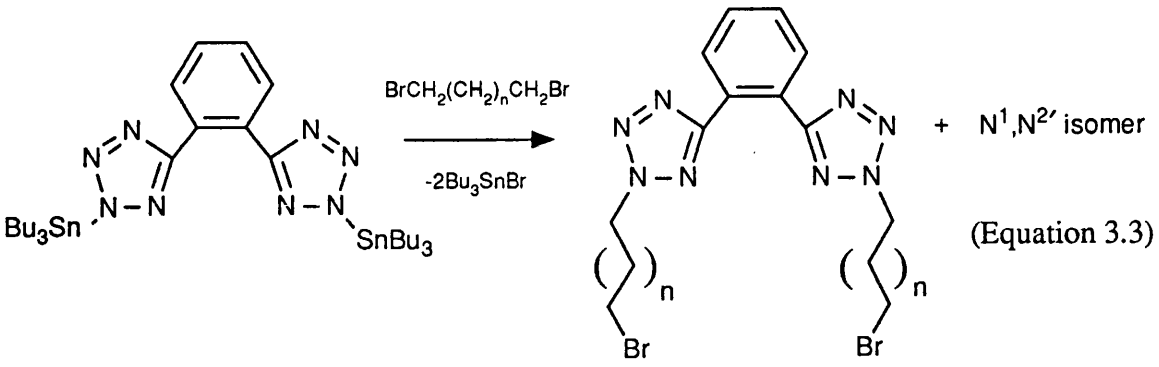

(Equation 3.3)

	$N^2,N^{2'}$	$N^1,N^{2'}$
n = 0;	**(24)**	**(25)**
n = 1;	**(26)**	-
n = 3;	**(27)**	**(28)**
n = 4;	**(29)**	**(30)**

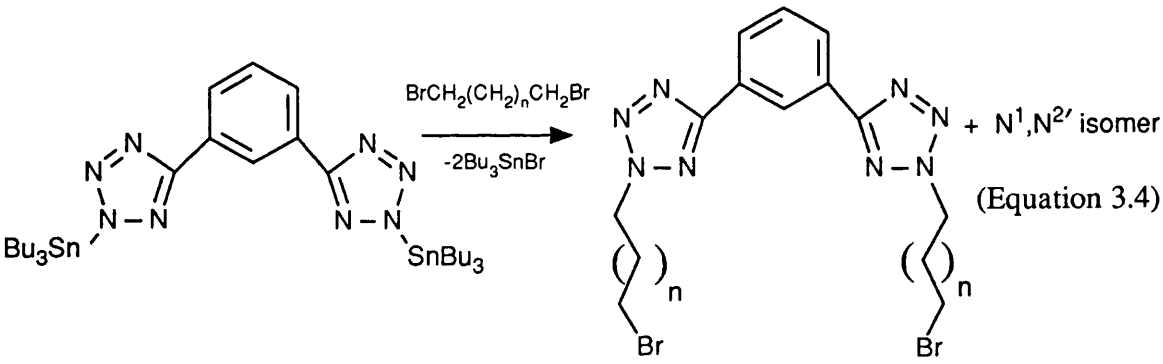

(Equation 3.4)

	$N^2,N^{2'}$	$N^1,N^{2'}$
n = 0;	**(31)**	**(32)**
n = 1;	**(33)**	**(34)**
n = 2;	**(35)**	**(36)**
n = 3;	**(37)**	**(38)**
n = 4;	**(39)**	-
n = 6;	**(40)**	-

formed in such small quantities as to be not recoverable on a preparative scale. This is reflected in the estimated relative yields of product in cases when two isomers were recovered. In such instances the $N^2,N^{2'}$-substituted isomer is observed to predominate over the $N^1,N^{2'}$-substituted isomer in an approximate three to one ratio. This observation is apparently at odds with expectation, based upon the original work of Kozima *et al.*[232] From their results at least a small amount of $N^1,N^{1'}$-substituted product would be expected and the lack of such a result would seem to suggest that isomer formation is influenced by the mutual steric requirements of the two substituted tetrazole ring systems. Molecular models indicate that an $N^2,N^{2'}$ substitution pattern presents the least hindrance to rotation of the tetrazole rings about the phenyl-attached C^5 and $C^{5'}$ atoms while $N^1,N^{1'}$-substitution brings the bromoalkyl chains into closer spatial proximity and all but prevents free rotation. Difficulty was encountered, in several instances, in obtaining microanalytically pure samples, due to some residual CH_2Cl_2 of solvation. In most cases this was readily confirmed by ^1H NMR spectra, and persisted even after the sample was dried for an extended period under vacuum. Such difficulties have previously been noted for other alkyl-substituted tetrazole compounds.[233]

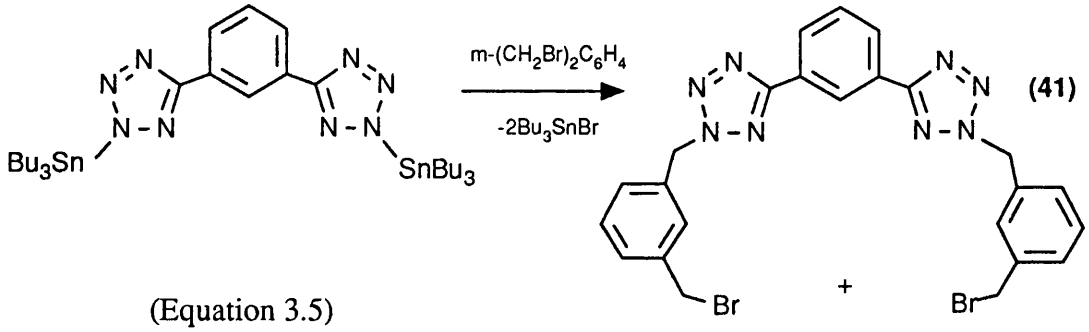

(Equation 3.5)

More rigid substituents such as the bromo-substituted *meta*-xylyl group illustrated in Equation 3.5 can also be introduced by the same general method and

work-up procedures. Again $N^2,N^{2'}$ and $N^1,N^{2'}$ isomeric derivatives can be isolated.

This general method of alkylation has also been further extended to synthesise the cyano-propyl-substituted **(43)**. The nitrile functionality has been employed in cycloaddition chemistry of the type detailed in chapter 2 to synthesise the tetra-tetrazole compound **(44)**, isolated after work up as a bis-methanol solvate (Scheme 3.3). The tetrazole functionality again gives rise to

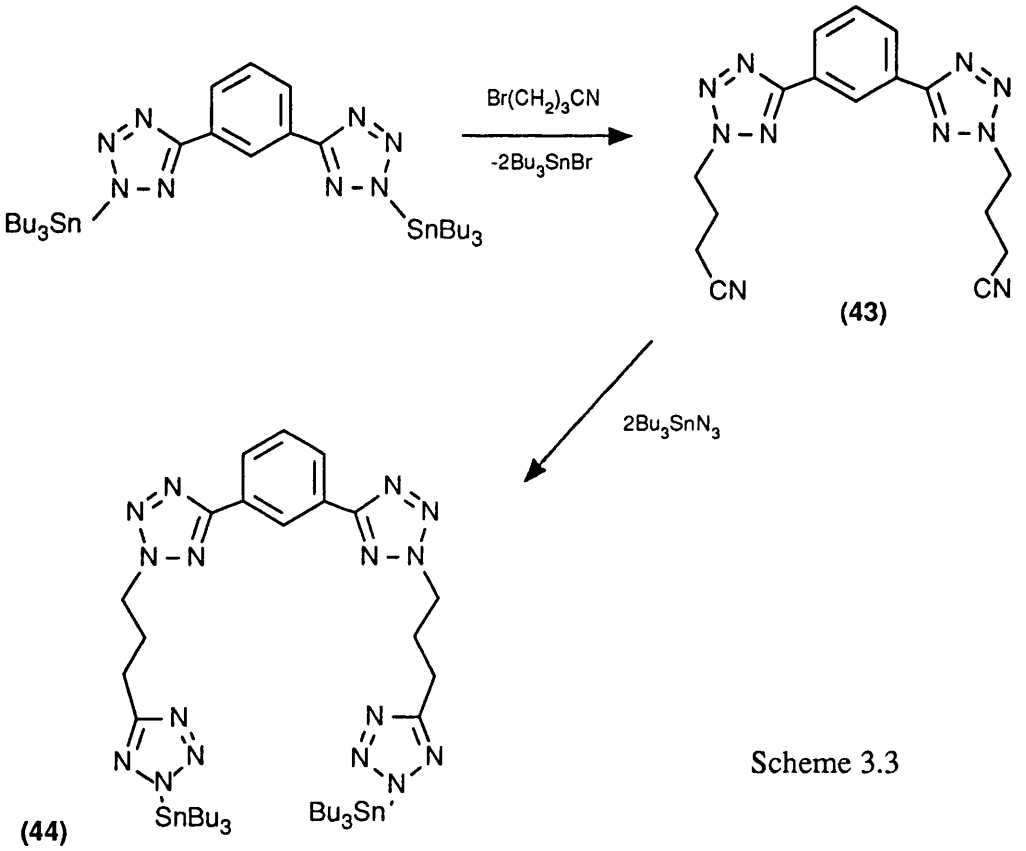

Scheme 3.3

the possiblity of continued reaction or macrocycle closure although this avenue has not been pursued further due to constraints of time.

Discussion of attempted macrocycle syntheses from the bis-(bromoalkyl-tetrazole) compounds is included in Section 3.6, while analytical and spectroscopic data for the compounds **(23)**-**(44)** are included along with experimental details in Section 3.7.

3.3 Spectroscopy of Bis-(N-alkyltetrazole) Compounds (23)-(44)

The ^{1}H and ^{13}C NMR spectra of **(23)**, formed from the reaction of **(11)** and 1,2-dibromoethane in methanol solution, show a single methylene resonance at 5.08 ppm and 45.9 ppm respectively. These values are characteristic of substitution at N^1 of the tetrazole ring,[180] as is the single resonance of the quaternary tetrazole-C^5 at 153.2 ppm. The overall simplicity of the aromatic regions of the spectra confirm this symmetrical pattern of substitution. Although this data would also be consistent with a symmetrically substituted macrocyclic compound containing two bis-tetrazole units, the x-ray crystallographic study discussed in Section 3.4 reveals that the ethyl unit in fact bridges between N^1 and $N^{1'}$ of the two tetrazole rings as illustrated in Equation 3.2.

The isomeric N^2,$N^{2'}$ and N^1,$N^{2'}$ bis-(bromoalkyl-substituted tetrazole) derivatives **(24)**-**(42)** are readily distinguishable from their respective ^{1}H and ^{13}C NMR spectra. Methylene groups attached to N^1 are more shielded by *ca.* 0.15-0.35 ppm in the ^{1}H spectra and by 4-6 ppm in the ^{13}C spectra relative to their N^2-substituted counterparts.[180] Thus the symmetrical N^2,$N^{2'}$-substituted compounds reported here show a single resonance at *ca.* 4.50 and 53.0 ppm in the ^{1}H and ^{13}C spectra respectively attributable to the equivalent $-CH_2N^2$ and $-CH_2N^{2'}$ resonances. On the other hand the unsymmetrical derivatives show additional signals at *ca.* 4.10 and 47.0 ppm arising from the $-CH_2N^1$ grouping. This difference in shielding is attributed to electron density effects arising from the differing electronegativity of the N^1 and N^2 ring nitrogen atoms which is in turn influenced by the higher electron-withdrawing power of the adjacent -N= moiety over the -C= moiety. These structural assignments are unequivocably confirmed by the x-ray crystallographic study of the N^2,$N^{2'}$-substituted **(31)** discussed in Section 3.5.

Because such differences in chemical environment are also transmitted down the length of the tetrazole-bonded chain, the alkyl region spectra of the

unsymmetrically-substituted compounds are more complex with, in most cases, a separate signal resolvable for each individual methylene group of the two bromoalkyl substituents. In contrast, the symmetrically-disposed N^2,$N^{2'}$-substs-tituted derivatives show half the number of methylene resonances because of the chemical equivalence of the chains.

The ^{13}C chemical shift of the tetrazole C^5 atom differs significantly in 1,5- and 2,5-disubstituted tetrazoles, appearing at *ca.* 155.0 and 162.0 ppm respectively.[180] The symmetrical N^2,$N^{2'}$-substituted compounds thus give rise to a single resonance corresponding to the second of these possibilities while both signals are apparent in the N^1,$N^{2'}$-substituted compounds. Variations in chemical shift of this nature for 5-aryltetrazoles have been attributed to the differing amounts of interannular conjugation between the tetrazole and aryl rings that are possible for N^1 and N^2-substituted ring systems.[238] In compounds bearing a N^1-substituent, conjugation of the type illustrated in (XXXXII) is absent or greatly diminished by the loss of ring coplanarity caused by the steric interaction of the N^1-substituent and the aryl ring system. This is especially severe when the aryl ring bears other large substituents in neighbouring positions (XXXXIII).

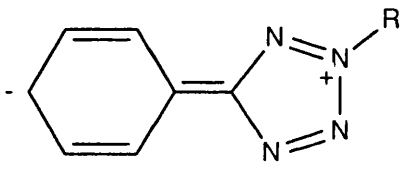

(XXXXII)

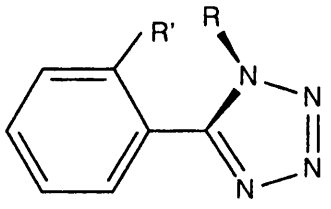

(XXXXIII)

Effects of this nature are also useful in explaining the positions of the phenyl resonances of the various 1,2- and 1,3-phenylene linked bis-(bromoalkyl-tetrazole) compounds. When enhanced interannular conjugation is present the *ortho*- signals of the proton and carbon spectra are significantly deshielded with

respect to those in the *meta-* and *para-* positions.[238] The presence of N^2-substituted tetrazole substituents therefore is the predominant effect in cases where unsymmetrical substitution of the bis-tetrazole compounds is encountered. Any additional influence of N^1-substituted ring is attributed to minor ring inductive and anisotropic effects on the *ortho-* signals.[180] Such considerations allow full assignment of the phenyl resonances observed in both the symmetrically and unsymmetrically-substituted bis-(bromoalkyltetrazole) compounds **(24)**-**(42)**. The numbering scheme adopted here and in Section 3.7 is shown in Figure 3.2 (Most shielded signals numbered first).

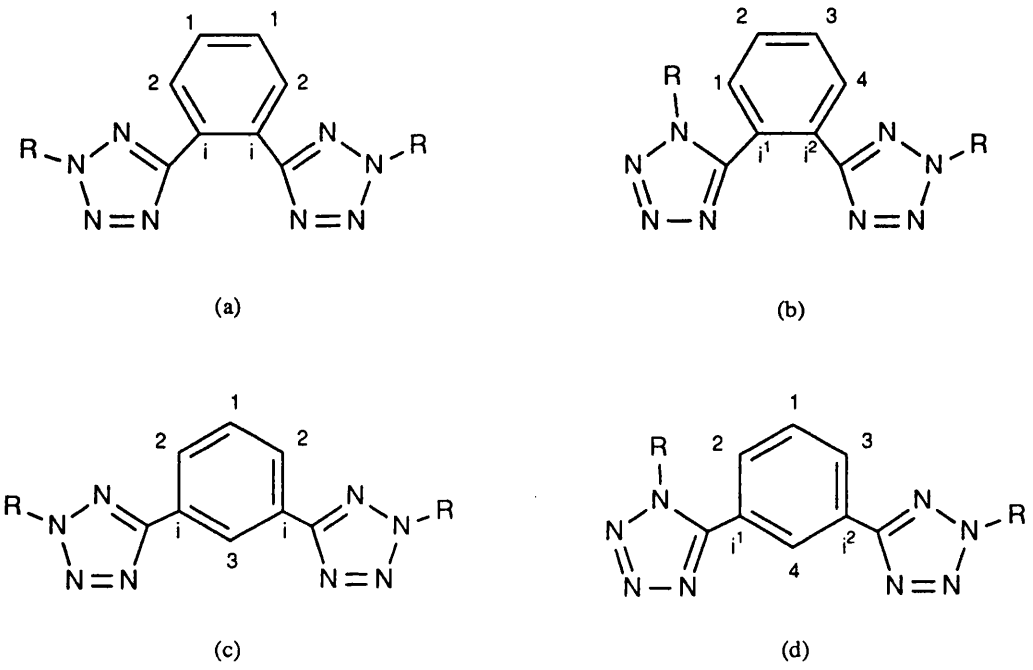

Figure 3.2: Numbering scheme of aromatic signals for (a) 1,2-phenylene-N^2,$N^{2'}$; (b) 1,2-phenylene-N^1,$N^{2'}$; (c) 1,3-phenylene-N^2,$N^{2'}$; (d) 1,3-phenylene-N^1,$N^{2'}$-substitution patterns

The aromatic region ^1H and ^{13}C spectra of the symmetrical 1,2-phenylene-linked N^2,$N^{2'}$-substituted bis-tetrazoles **(24)**, **(26)**, **(27)** and **(29)** each show separate resonances attributable to the two pairs of methine protons

and carbon atoms labelled H^1/C^1 and H^2/C^2 in Figure 3.2(a). Additionally a single *ipso*-carbon resonance is observed at *ca.* 127 ppm arising from the phenyl linkage to the two equivalent N^2-substituted tetrazole ring systems. In contrast the spectra of the the unsymmetrical compounds **(25)**, **(28)** and **(30)** are rather more complex with a signal observed for each non-equivalent proton or carbon atom, as represented by Figure 3.2(b). Use of the shielding patterns outlined above and the observed multiplicities of the ^1H spectra however again allows complete assignment. Additionally, a second *ipso*-carbon resonance is observed at *ca.* 123 ppm, attributable to the phenyl carbon atom bonded to the N^1-substituted tetrazole. The 1,3-phenylene bridged compounds show similar aromatic region differences in the ^1H and ^{13}C spectra of the symmetrical and unsymmetrical compounds. Again full correlation with the expected structures is possible as represented by Figures 3.2(c) and 3.2(d).

The formation of the cyano-alkyl derivative **(43)** is clearly evidenced by the sharp ν(CN) stretch observed in the infra-red (2249 cm^{-1}) while the $N^2,N^{2'}$-pattern of substitution depicted in Scheme 3.3 is readily deduced from the characteristic resonances observed in the ^1H and ^{13}C NMR as explained above. The course of the azide cycloaddition (Scheme 3.3) was monitored as in chapter 2 by the disappearance of the $\nu(N_3)$ and ν(CN) stretches in the infra-red. The collated ^{119}Sn NMR (δ -55.1, DMSO-d^6 solution) for **(44)** is of the same order as the values reported for the bis(trialkylstannyltetrazole) compounds of chapter 2 and is thus indicative of similar *trans*-trigonal bipyramidal coordination in the solution state. The $^1J(^{119}Sn, ^{13}C)$ value of 478.0 Hz is also consistent with such five-coordinate geometry. The solid-state Mössbauer quadrupole splitting data (ΔEq = 3.50 mms^{-1}) is also indicative of similar geometry at tin. However the bis-methanol solvated nature of **(44)** and the precedent created by the deduced structure of **(12)** leave the identity of the axial substituents ($\underline{N}_2SnBu_3$ vs.$\underline{NO}SnBu_3$) open to question.

3.4 The Crystal Structure of [1,5-d][5,1-h]-ditetrazolo-[1,2-f]-benzo-1,4-diazacine (23)

Suitable crystals for single crystal x-ray crystallography were grown by slow evaporation of a methanolic solution at ambient temperature. Full details of the crystallographic analysis, atomic coordinates and isotropic thermal parameters are included in Appendix V. The asymmetric unit of **(23)** is illustrated in Figure 3.3 and bond lengths (Å) and bond angles (°) are presented in Tables 3.1 and 3.2 respectively.

Although microanalysis of the bulk compound indicated a monohydrate, the crystal chosen for crystallographic analysis proved to be completely anhydrous. Inspection of Figure 3.3 reveals that the *o*-bis-tetrazole is symmetrically bridged by the ethyl group between the N^1 and $N^{1'}$ ring nitrogens [N(1) and N(5)]. This results in an overall tetra-cyclic molecule built around a central eight-membered C_6N_2 macrocycle.

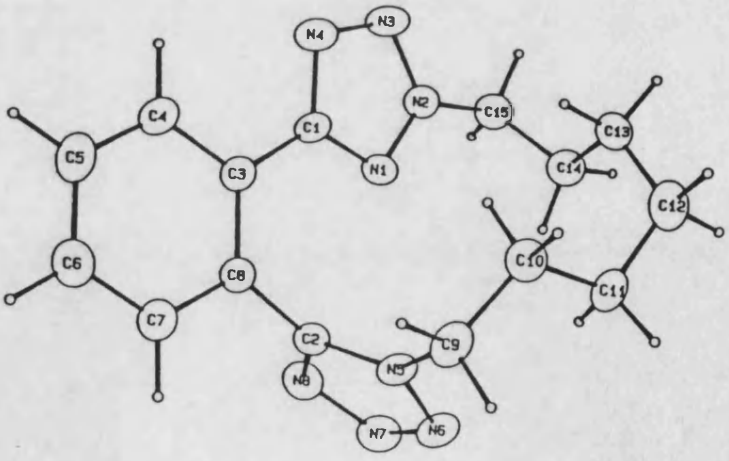

Figure 3.4: The Structure of 2-(1,2)benzeno-1,3-bis-(5,2)-tetrazolo-cyclodecaphane

The phenyl and tetrazole rings are planar [maximum deviations from least

squares planes of 0.009Å and 0.004Å for the C(1) and C(8) tetrazole rings respectively] and the two CN_4 rings subtend angles of 45.8° and 50.9° with the plane of the phenyl ring. The tetrazole rings are necessarily twisted from coplanarity in this manner to accommodate the tetrahedral nature of the methylene groups of the ethyl chain. The analogous angles in the -$(CH_2)_7$-N^2,$N^{2'}$-linked cyclophane illustrated in Figure 3.4 are 58.5° and 38.3° respectively,[236] and do not reflect the greater freedom of rotation of the tetrazole rings allowed by the octyl chain. The internal C-N-N, N-C-N and N-N-N angles of both the tetrazole ring systems vary little from the 108° expected for a regular pentagon.

The overall dimensions of the two tetrazole rings are suggestive of some π-delocalisation around the rings although the individual rings are slightly inequivalent. However the C(1)-N(4) [1.314(7)Å], C(1)-N(1) [1.324(7)Å] and C(8)-N(5) [1.348(7)Å], C(8)-N(8) [1.322(8)Å] bond lengths indicate the retention of some single bond character while the increased double bond character concentrated in the shorter N(6)-N(7) [1.227(8) Å] and N(2)-N(3) [1.308(8) Å] bonds is probably significant given their respective estimated standard deviations. Minor bond length variations of this order are typical of N^1-alkyl-substituted tetrazoles and the are comparable to those observed in, for example, the pentamethylene tetrazole iodine monochloride complex (PMT.ICl),[239] and more recently the amino acid-substituted Phe-(CN_4)-L-Ala[240] (Phe = phenylalanine; Ala = alanine) and tetrazolo-[1,5]furazano-[4,5]-pyridine-1-oxide[241] (see Table 3.3). The N(1)-C(10) [1.461(7)Å] and N(5)-C(9) [1.462(8)Å] bonds are typical of tetrazole N-alkyl substituents (e.g. for PMT.ICl, N^1-CH_2 = 1.45 Å). The inter-ring C(1)-C(2) and C(7)-C(8) distances of 1.467(8)Å and 1.486(8)Å are shorter than expected for a C-C single bond (1.54 Å) and thus indicative of interannular conjugation of the type implicated in the aromatic region pattern of chemical shifts of the NMR spectra.

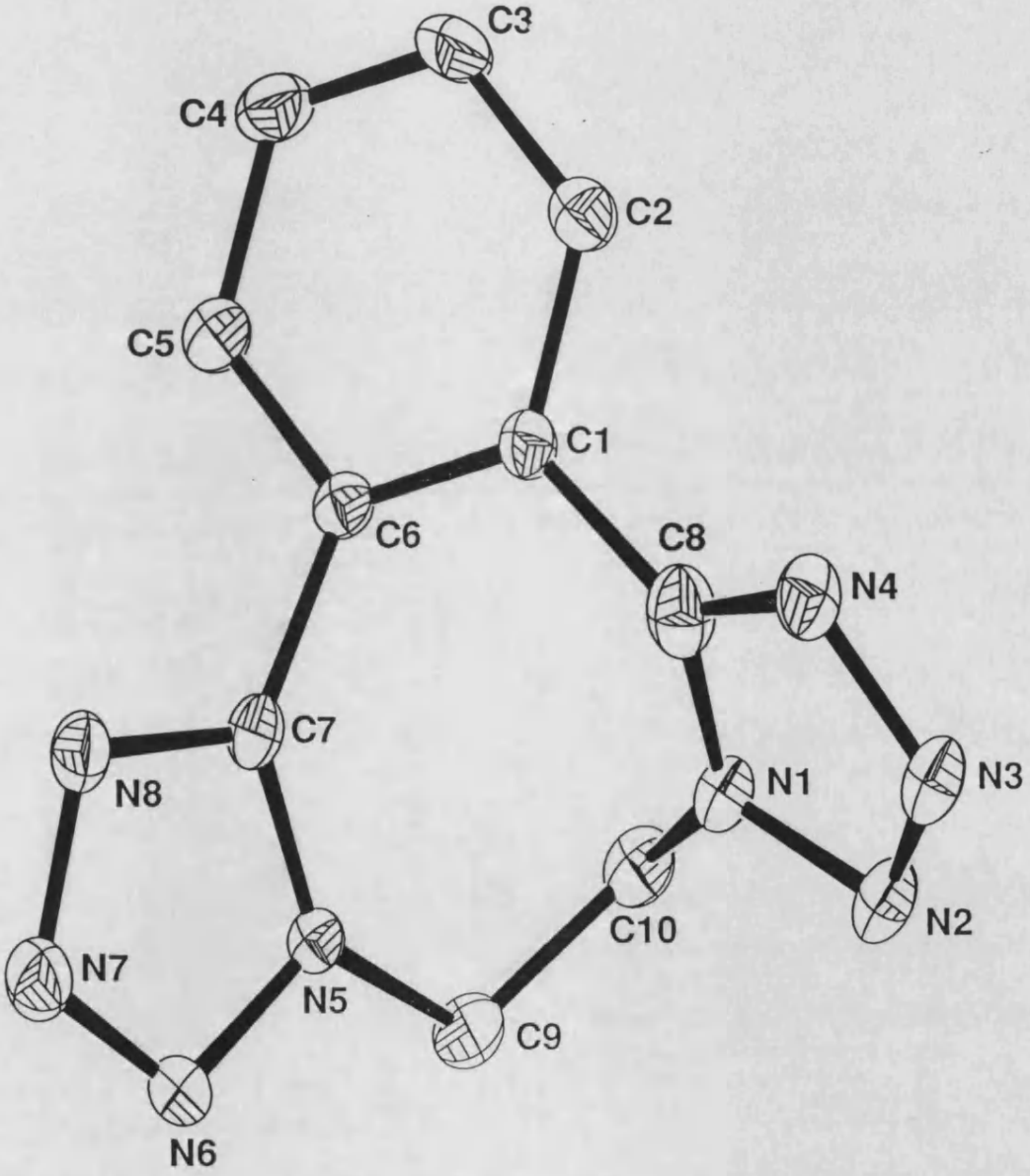

Figure 3.3: The asymmetric unit of (23). Hydrogen atoms omitted for clarity.

Table 3.1: Selected bond Lengths (Å) of **(23)** with estimated standard deviations in parentheses

N(1)-N(2)	1.344(6)	N(1)-C(1)	1.324(7)
N(1)-C(10)	1.461(7)	N(2)-N(3)	1.308(8)
N(3)-N(4)	1.367(7)	N(4)-C(1)	1.314(7)
N(5)-N(6)	1.346(7)	N(5)-C(8)	1.348(7)
N(5)-C(9)	1.462(8)	N(6)-N(7)	1.277(8)
N(7)-N(8)	1.365(7)	N(8)-C(8)	1.322(8)
C(1)-C(2)	1.467(8)	C(2)-C(3)	1.404(8)
C(2)-C(7)	1.403(8)	C(3)-C(4)	1.373(9)
C(4)-C(5)	1.379(10)	C(5)-C(6)	1.387(9)
C(6)-C(7)	1.404(8)	C(7)-C(8)	1.486(8)
C(9)-C(10)	1.526(9)		

Table 3.2: Selected bond angles (°) of **(23)** with estimated standard deviations in parentheses

C(1)-N(1)-N(2)	109.2(5)	C(10)-N(1)-N(2)	121.4(5)
C(10)-N(1)-C(1)	128.9(4)	N(3)-N(2)-N(1)	105.7(4)
N(4)-N(3)-N(2)	110.4(4)	C(1)-N(4)-N(3)	105.5(5)
C(8)-N(5)-N(6)	107.5(5)	C(9)-N(5)-N(6)	116.5(4)
C(9)-N(5)-C(8)	135.4(5)	N(7)-N(6)-N(5)	107.9(5)
N(8)-N(7)-N(6)	110.4(5)	C(8)-N(8)-N(7)	105.8(5)
N(4)-C(1)-N(1)	109.2(5)	C(2)-C(1)-N(1)	124.4(5)
C(2)-C(1)-N(4)	126.2(6)	C(3)-C(2)-C(1)	117.2(5)
C(7)-C(2)-C(1)	123.1(5)	C(7)-C(2)-C(3)	119.5(5)
C(4)-C(3)-C(2)	120.6(6)	C(5)-C(4)-C(3)	120.3(6)
C(6)-C(5)-C(4)	120.3(6)	C(7)-C(6)-C(5)	120.4(6)
C(6)-C(7)-C(2)	118.8(5)	C(8)-C(7)-C(2)	124.7(5)
C(8)-C(7)-C(6)	115.6(5)	N(8)-C(8)-N(5)	108.4(5)
C(7)-C(8)-N(5)	130.8(6)	C(7)-C(8)-N(8)	120.7(5)
C(10)-C(9)-N(5)	113.8(5)	C(9)-C(10)-N(1)	112.0(6)

Table 3.3: Comparison of CN_4 ring internal bond lengths (Å) for several N^1-alkyl sustituted tetrazole derivatives

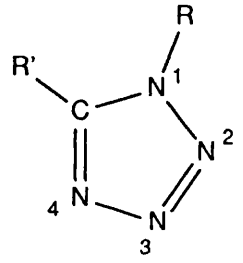

	(23): C(1) ring	(23): C(8) ring	PMT.ICl[a]	Phe-(CN_4)-L-Ala[b]	Tetrazolo-[1,5]-furazano [4,5]-pyridine-1-oxide[c]
C-N^1	1.324(7)	1.348(7)	1.34	1.317(2)	1.354
N^1-N^2	1.344(6)	1.346(7)	1.38	1.348(2)	1.356
N^2-N^3	1.308(8)	1.277(8)	1.28	1.299(2)	1.290
N^3-N^4	1.367(7)	1.365(7)	1.39	1.354(2)	1.362
N^4-C	1.314(7)	1.322(8)	1.33	1.318(2)	1.321

[a] Ref. 239; [b] Ref. 240; [c] Ref. 241; Phe = phenylalanine; Ala = alanine.

3.5 The Crystal Structure of 1,3-phenylene-bis-5,5′-[$N^2N^{2'}$-(2-bromoethyl)-tetrazole] (31)

Suitable crystals for x-ray crystallography were grown grown by the slow evaporation of a CH_2Cl_2 solution. Complete details of the crystallographic analysis, atomic coordinates and isotropic temperature factors are given in Appendix VI. The asymmetric unit is shown in Figure 3.5 and bond lengths (Å) and bond angles (°) are presented in Tables 3.4 and 3.5 respectively.

Examination of Figure 3.5 confirms the N^2 and $N^{2'}$ atoms of the tetrazole rings as the positions of substitution. The tetrazole rings are planar (maximum deviation from the least squares plane: 0.004Å) and make angles of 13.5° with the plane of the phenyl ring, while the bromoethyl substituents are directed to opposite sides of this plane.

The two tetrazole rings are identical and the C-N [1.331(11) and 1.354(11) Å] and N-N bond lengths [1.328(9), 1.328(10) and 1.318(11) Å] within the molecule are all shorter than found in single bonds, suggesting considerable electron delocalisation in common with other tetrazole systems. Comparison of the individual C-N [1.331(11) and 1.354(11)Å] and N-N [1.328(9), 1.328(10) and 1.318(11) Å] tetrazole ring bond lengths reveals only slight variation given the large estimated standard deviations and there is little evidence for alternation of double and single bonds around the rings. These values and this observation are typical of N^2-substituted tetrazoles linked via C^5 to aryl substituents[237] and are perhaps attributable to increased delocalisation through inter-ring conjugation. Further evidence of this phenomenon is provided by the shortened interannular C(3)-C(5) bond length of 1.465(12) Å.

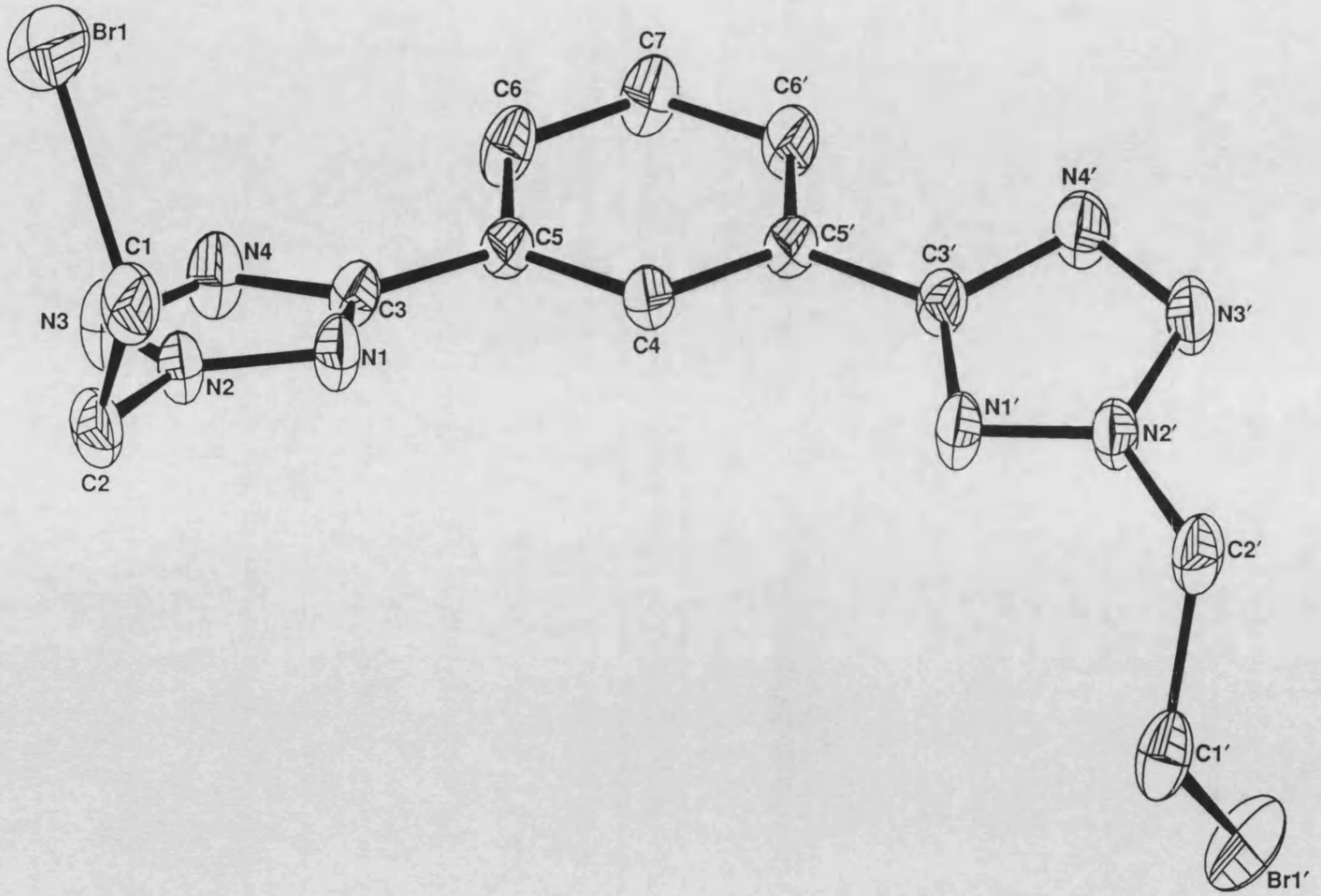

Figure 3.5: The asymmetric unit of (**31**). Hydrogen atoms omitted for clarity.

Table 3.4: Selected bond lengths of **(31)** (Å) with estimated standard deviations in parentheses

C(1)-Br(1)	1.947(10)	N(2)-N(1)	1.328(9)
C(3)-N(1)	1.331(11)	N(3)-N(2)	1.328(10)
C(2)-N(2)	1.459(11)	N(4)-N(3)	1.318(11)
C(3)-N(4)	1.354(11)	C(2)-C(1)	1.469(12)
C(5)-C(3)	1.465(12)	C(5)-C(4)	1.391(10)
C(6)-C(5)	1.413(12)	C(7)-C(6)	1.375(11)

Table 3.5: Selected bond angles of **(31)** (Å) with estimated standard deviations in parentheses

C(3)-N(1)-N(2)	101.4(7)	N(3)-N(2)-N(1)	113.8(7)
C(2)-N(2)-N(1)	124.2(7)	C(2)-N(2)-N(3)	122.0(7)
N(4)-N(3)-N(2)	106.3(7)	C(3)-N(4)-N(3)	105.7(7)
C(2)-C(1)-Br(1)	112.8(7)	C(1)-C(2)-N(2)	111.4(8)
N(4)-C(3)-N(1)	112.7(8)	C(5)-C(3)-N(1)	124.5(8)
C(5)-C(3)-N(4)	122.8(8)	C(4)-C(5)-C(3)	122.0(8)
C(6)-C(5)-C(3)	118.9(8)	C(6)-C(5)-C(4)	119.1(8)
C(5)-C(4)-C(5)	121.0(10)	C(7)-C(6)-C(5)	119.5(9)
C(6)-C(7)-C(6)	121.8(11)		

3.6 Attempted macrocyclisation reactions

Of the nineteen bis-(bromoalkyltetrazole) compounds **(24)**-**(42)** described above, several were utilised in attempted macrocyclisation reactions with the bis-(hydrotetrazole) compounds **(20)** and **(21)** (step (ii) in Scheme 3.1). Experimental details of typical reactions involving compounds of various chain length are given in Section 3.7.

A number of bases (e.g. Et_3N, NaOH, K_2CO_3) were employed to form the anion of the relevant bis-tetrazole, paralleling established tetrazole-alkylation procedures of previous workers.[180.233] Although anion formation and reaction was apparent from the dissolution of the insoluble bis-(hydrotetrazole) in the solvent used and, in the case of the triethylamine-mediated reactions, the recovery of triethylamine hydrobromide, in no case was the desired macrocyclic compond isolated. Column chromatography of the crude reaction products either yielded the unreacted bis-(bromoalkyltetrazole) as the only product or nothing at all, perhaps indicating the formation of polymeric products.

From the above comments it can be inferred that dilution plays a large part in the observed reaction. Too small volumes of solvent will give polymers and too large volumes will not allow reaction to occur. The establishment of suitable conditions during the course of this work was curtailed due to constraints of time. Further work therefore is recommended and should concentrate on ascertaining the correct conditions for the formation of oligomeric products

3.7 Experimental

^{1}H and ^{13}C NMR phenyl ring assignments are indicated using the numbering scheme adopted in Figure 3.2 for symmetrically (N^2, $N^{2'}$) and unsymmetrically-substituted (N^1, $N^{2'}$) isomers.

3.7.1 Synthesis of [1,5-d]95,1-h]-ditetrazolo-[1,2-f]-benzo-1,4-diazacine (23)

(11) (1.75g, 2.2 mmol) was refluxed with 1,2-dibromoethane (4.1g, 22.0 mmol) in methanol (50 ml) for three hours. *In vacuo* removal of solvent from the colourless solution yielded a glass which was triturated with hexane to afford a colourless powder which was collected by filtration. **(23)** was isolated as colourless needles by fractional crystallisation from methanol solution (0.20g, 37%).

Analysis: Found(Calc. for $C_{10}H_8N_8.H_2O$): C 46.7(46.5); H 3.20(3.87); N 43.3(43.4)%

^{1}H NMR [δ(ppm), MeOD-d^4 solution]: 5.08 [s,4H,2xCH_2]; 7.91 [m,4H,H^1,H^2-C_6H_4].

^{13}C NMR [δ(ppm), MeOH-d^4 solution]: 45.9 [2xCH_2]; 123.5 [*i*-C_6H_4]; 131.9 [C^1-C_6H_4]; 132.1 [C^2-C_6H_4]; 153.2 [CN_4].

3.7.2 Synthesis of 1,2-phenylene-bis-5,5'-[N^2,$N^{2'}$-(2-bromoethyl)tetrazole] (24) and 1,2-phenylene-bis-5,5'-[N^1,$N^{2'}$-(2-bromoethyl)tetrazole] (25)

(11) (2.0g, 2.5 mmol) was heated to 110°C as a neat suspension in 1,2-dibromoethane (7 ml) for three hours. This resulted in a viscous amber solution which, on cooling, was chromatographed on silica gel employing a gradient of 40/60 petroleum ether to CH_2Cl_2. **(24)** and **(25)** were isolated as crystalline solids after recrystallisation from CH_2Cl_2.

(24):

Analysis: Found(Calc. for $C_{12}H_{12}N_8Br_2$): C 34.1(33.7); H 2.84(2.81); N 25.9(26.1)%

^{1}H NMR [δ(ppm), $CDCl_3$ solution]: 3.73 [t,4H,2x-CH_2Br]; 4.89 [t,4H,-CH_2N^2,-CH_2N$^{2'}$]; 7.54 [dd,2H,H^1-C$_6H_4$]; 7.85 [dd,2H,H^2-C$_6H_4$].

^{13}C N[δ(ppm), $CDCl_3$ solution]: 27.0 [2x-CH$_2$Br]; 53.9 [-CH$_2$N^2,-CH$_2$N$^{2'}$]; 127.3 [i-C_6H_4]; 130.3 [C^1-C_6H_4]; 130.6 [C^2-C_6H_4]; 164.7 [CN$_4$].

(25):

Analysis: Found(Calc. for $C_{12}H_{12}N_8Br_2$): C 33.5(33.7); H 3.20(2.81); N 25.6(26.1)%

^{1}H NMR [δ(ppm), $CDCl_3$ solution]: 3.65 [m,4H,2x-CH_2Br]; 4.36 [t,2H,-CH_2N^1]; 4.84 [t,2H,-CH_2N$^{2'}$]; 7.50-7.75 [m,3H,H^{1}H^{2}H^3-C$_6H_4$]; 8.28 [d,1H,H^4-C$_6H_4$].

^{13}C NMR [δ(ppm), $CDCl_3$ solution]: 27.3 [-CH$_2$Br]; 27.8 [-CH$_2$Br]; 48.5 [-CH$_2$N^1]; 54.0 [-CH$_2$N$^{2'}$]; 122 2 [i^1-C_6H_4]; 126.9 [i^2-C_6H_4]; 29.3 [C^1-C_6H_4]; 130.6 [C^2-C_6H_4]; 131.8 [C^3-C_6H_4]; 131.9 [C^4-C_6H_4]; 154.3 [CN$_4$, (N^{1}CH$_2$)]; 163.0 [CN$_4$, (N$^{2'}$CH$_2$)].

3.7.3 Synthesis of 1,2-phenylene-bis-5,5'-[N^2,N$^{2'}$-(3-bromopropyl)tetrazole] (26).

This compound was prepared by the same general method from **(11)** and 1,3-dibromopropane as a waxy solid.

Analysis: Found(Calc. for $C_{14}H_{16}N_8Br_2$): C 36.7(36.8); H 3.46(3.51); N 24.1(24.5)%

^{1}H NMR [δ(ppm), $CDCl_3$ solution]: 2.51 [m,4H,CH_2]; 3.40 [t,4H,2x-CH_2Br]; 4.77 [t,4H,-CH_2N^2,-CH_2N$^{2'}$]; 7.60 [dd,2H,H^1-C$_6H_4$]; 7.89 [dd,2H,H^2-C$_6H_4$].

^{13}C NMR [δ(ppm), $CDCl_3$ solution]: 29.3 [CH$_2$]; 32.2 [2x-CH$_2$Br]; 51.3 [-CH$_2$N^2,-CH$_2$N$^{2'}$]; 127.3 [i-C_6H_4]; 130.6 [C^1-C_6H_4]; 130.8 [C^2-C_6H_4]; 164.7 [CN$_4$].

3.7.4 Synthesis of 1,2-phenylene-bis-5,5′-[N^2,$N^{2'}$-(5-bromopentyl)tetrazole] (27) and 1,2-phenylene-bis-5,5′-[N^1,$N^{2'}$-(5-bromopentyl)tetrazole] (28).

These compounds were prepared by the same general method from **(11)** and 1,5-dibromopentane as waxy solids.

(27):

Analysis: Found(Calc. for $C_{18}H_{24}N_8Br_2$): C 42.9(42.2); H 5.12(4.69); N 21.6(21.8)%

^{1}H NMR [δ(ppm), $CDCl_3$ solution]: 1.39 [m,4H,2xCH_2]; 1.76-1.82 [m,4H,2xCH_2]; 1.88-1.94 [m,4H,2xCH_2]; 3.31 [t,4H,2x-CH_2Br]; 4.50 [t,4H,-CH_2N^2,-$CH_2N^{2'}$]; 7.52 [dd,2H,H^1-C_6H_4]; 7.80 [dd,2H,H^2-C_6H_4].

^{13}C NMR [δ(ppm), $CDCl_3$ solution]: 24.6 [2xCH_2]; 28.2 [2xCH_2]; 31.6 [2xCH_2]; 33.0 [2x-CH_2Br]; 52.5 [-CH_2N^2,-$CH_2N'^2$]; 127.1 [*i*-C_6H_4]; 129.9 [C^1-C_6H_4]; 130.3 [C^2-C_6H_4]; 164.1 [CN_4].

(28):

Analysis: Found(Calc. for $C_{18}H_{24}N_8Br_2$): C 42.6(42.2); H 4.86(4.69); N 21.5(21.8)%

^{1}H NMR [δ(ppm), $CDCl_3$ solution]: 1.23-1.35 [m,4H,2xCH_2]; 1.62-1.86 [m,8H,4xCH_2]; 3.23 [t,2H,-CH_2Br]; 3.33 [t,2H,-CH_2Br]; 3.99 [t,2H,-CH_2N^1]; 4.42 [2,2H,-$CH_2N^{2'}$]; 7.42 [d,1H,H^1-C_6H_4]; 7.57-7.71 [m,2H,H^2,H^3-C_6H_4]; 8.25 [d,1H,H^4-C_6H_4].

^{13}C NMR [δ(ppm), $CDCl_3$ solution]: 24.5 [CH_2]; 24.6 [CH_2]; 27.8 [CH_2]; 27.9 [CH_2]; 31.4 [CH_2]; 31.5 [CH_2]; 32.9 [-CH_2Br]; 33.0 [-CH_2Br]; 47.0 [-CH_2N^1]; 52.7 [-$CH_2N^{2'}$]; 122.7 [i^1-C_6H_4]; 127.3 [i^2-C_6H_4]; 129.2 [C^1-C_6H_4]; 130.2 [C^2-C_6H_4]; 130.9 [C^3-C_6H_4]; 131.4 [C^3-C_6H_4]; 153.8 [CN_4, (N^1CH_2)]; 162.7 [CN_4, ($N^{2'}CH_2$)].

3.7.5 Synthesis of 1,2-phenylene-bis-5,5′-[N^2,$N^{2'}$-(6-bromohexyl)tetrazole] (29) and 1,2-phenylene-bis-5,5′-[N^1,$N^{2'}$-(6-bromohexyl)tetrazole] (30)

These compounds were prepared by the same general method from **(11)** and 1,6-dibromohexane as viscous oils.

(29):

Analysis: Found(Calc. for $C_{20}H_{28}N_8Br_2$): C 45.3(44.5); H 5.30(5.19); N 20.6(20.7)%

^{1}H NMR [δ(ppm), $CDCl_3$ solution]: 1.15-1.26 [m,4H,2xCH_2]; 1.31-1.36 [m,4H,2xCH_2]; 1.73 [m,4H,2xCH_2]; 1.88 [m,4H,2xCH_2]; 3.29 [t,4H,2x-CH_2Br]; 4.48 [t,4H,-CH_2N^2,-$CH_2N^{2'}$]; 7.51 [dd,2H,H^1-C_6H_4]; 7.79 [dd,2H,H^2-C_6H_4].

^{13}C NMR [δ(ppm), $CDCl_3$ solution]: 24.96 [2xCH_2]; 27.0 [2xCH_2]; 28.7 [2xCH_2]; 32.0 [2xCH_2]; 33.3 [2x-CH_2Br]; 52.5 [-CH_2N^2,-$CH_2N^{2'}$]; 127.0 [*i*-C_6H_4]; 129.8 [C^1-C_6H_4]; 130.1 [C^2-C_6H_4]; 163.8 [CN_4].

(30):

Analysis: Found(Calc. for $C_{20}H_{28}N_8Br_2$): C 44.7(44.5); H 5.40(5.19); N 19.3(20.7)%

^{1}H NMR [δ(ppm), $CDCl_3$ solution]: 1.18-1.45 [m,8H,4xCH_2]; 1.64-1.86 [m,8H,4xCH_2]; 3.26 [t,2H,-CH_2Br]; 3.34 [t,2H,-CH_2Br]; 3.97 [t,2H,-CH_2N^1]; 4.41 [t,2H,-$CH_2N^{2'}$]; 7.41 [d,1H,H^1-C_6H_4]; 7.59 [t,1H,H^2-C_6H_4]; 7.69 [t,1H,H^3-C_6H_4]; 8.28 [d,1H,H^4-C_6H_4].

^{13}C NMR [δ(ppm), $CDCl_3$ solution]: 25.4 [CH_2]; 25.4 [CH_2]; 27.3 [CH_2]; 27.3 [CH_2]; 28.8 [CH_2]; 29.1 [CH_2]; 32.2 [CH_2]; 32.3 [CH_2]; 33.3 [-CH_2Br]; 33.5 [-CH_2Br]; 47.3 [-CH_2N^1]; 53.0 [-$CH_2N^{2'}$]; 127.7 [i^1-C_6H_4]; 129.51[i^2-C_6H_4]; 130.7 [C^1-C_6H_4]; 130.5 [C^2-C_6H_4]; 131.1 [C^3-C_6H_4]; 131.2 [C^4-C_6H_4];154.0 [CN_4, (N^1CH_2)]; 162.9 [CN_4, ($N^{2'}CH_2$)].

3.7.6 Synthesis of 1,3-phenylene-bis-5,5′-[N^2,$N^{2'}$-(2-bromoethyl)tetrazole] (31) and 1,3-phenylene-bis-5,5′-[N^1,$N^{2'}$-(2-bromoethyl)tetrazole] (32)

These compounds were prepared by the same general method from **(12)** and 1,2-dibromoethane and isolated, after recrystallisation from CH_2Cl_2, as colourless crystalline solids.

(31):

Analysis: Found(Calc. for $C_{12}H_{12}N_8Br_2$): C 34.1(33.7); H 2.91(2.81); N 25.4(26.1)%

^{1}H NMR [δ(ppm), $CDCl_3$ solution]: 3.86 [t,4H,2x-CH_2Br]; 5.01 [t,4H,-CH_2N^2,-CH_2N$^{2'}$]; 7.57 [t,1H,H^1-C$_6H_4$]; 8.20 [dd,2H,2xH^2-C$_6H_4$]; 8.86 [s,1H,H^3-C$_6H_4$].

^{13}C NMR [δ(ppm), $CDCl_3$ solution]: 27.1 [2x-*C*H$_2$Br]; 54.0 [-*C*H$_2$N^2, -*C*H$_2$N$^{2'}$]; 125.3 [C^1-*C*$_6$H$_4$]; 127.9 [2xC^2-*C*$_6$H$_4$]; 128.7 [C^3-*C*$_6$H$_4$]; 129.6 [*i*-*C*$_6$H$_4$]; 164.8 [*C*N$_4$].

(32):

Analysis: Found(Calc. for $C_{12}H_{12}N_8Br_2$): C 33.0(33.7); H 2.89(2.81); N 25.5(26.2)%

^{1}H NMR [δ(ppm), $CDCl_3$ solution]: 3.81 [t,2H,-CH_2Br]; 3.86 [t,2H,-CH_2Br]; 4.80 [t,2H,-CH_2N^1]; 5.02 [t,2H,CH_2N$^{2'}$]; 7.66 [m,1H,H^1-C$_6H_4$]; 7.76 [m,1H,H^2-C$_6H_4$]; 8.33 [m,1H,H^3-C$_6H_4$]; 8.42 [m,1H,H^4-C$_6H_4$].

^{13}C NMR [δ(ppm), $CDCl_3$ solution]: 27.1 [-*C*H$_2$Br]; 28.0 [-*C*H$_2$Br]; 49.0 [-*C*H$_2$N^1]; 54.2 [-*C*H$_2$N$^{2'}$]; 124.5 [*i*^{1}-*C*$_6$H$_4$];

127.2 [C^1-*C*$_6$H$_4$]; 128.5 [*i*^{2}-*C*$_6$H$_4$]; 129.6 [C^2-*C*$_6$H$_4$]; 130.2 [C^3-*C*$_6$H$_4$]; 130.9 [C^4-*C*$_6$H$_4$]; 154.5 [*C*N$_4$, (N^{1}CH$_2$)]; 164.1 [*C*N$_4$, (N$^{2'}$CH$_2$)].

3.7.8 Synthesis of 1,3-phenylene-bis-5,5′-[N^2,$N^{2'}$-(3-bromopropyl)tetrazole] ***(33)*** *and 1,3-phenylene-bis-5,5′-[N^1,$N^{2'}$-(3-bromopropyl)tetrazole]* ***(34)***

These compounds were prepared by the same general method from **(12)** and 1,3-dibromopropane and isolated as waxy solids.

(33):

Analysis: Found(Calc. for $C_{14}H_{16}N_8Br_2$): C 36.5(36.8); H 3.40(3.51); N 23.7(24.5)%

^{1}H NMR [δ(ppm), $CDCl_3$ solution]: 2.56 [m,4H,2xCH_2]; 3.41 [t,4H,2x-CH_2Br]; 4.80 [t,4H,-CH_2N^2,-$CH_2N^{2'}$]; 7.54 [t,2H,H^1-C_6H_4]; 8.17 [dd,2H,2xH^2-C_6H_4]; 8.81 [dd,1H,H^3-C_6H_4].

^{13}C NMR [δ(ppm), $CDCl_3$ solution]: 28.9 [2xCH_2]; 31.9 [2x-CH_2Br]; 51.3 [-CH_2N^2,-$CH_2N^{2'}$]; 125.1 [C^1-C_6H_4]; 128.1 [2xC^2-C_6H_4]; 128.5 [*i*-C_6H_4]; 129.5 [C^3-C_6H_4]; 164.6 [CN_4].

(34):

Analysis: Found(Calc. for $C_{14}H_{16}N_8Br_2$): C 36.8(36.8); H 3.63(3.51); N 23.8(24.5)%

^{1}H NMR [δ(ppm), $CDCl_3$ solution]: 2.51 [m,4H,2xCH_2]; 3.36 [t,2H,-CH_2Br]; 3.41 [t,2H,-CH_2Br]; 4.60 [t,2H,-CH_2N^1]; 4.80 [t,2H,-$CH_2N^{2'}$]; 7.63 [t,1H,H^1-C_6H_4]; 7.74 [d,1H,H^2-C_6H_4]; 8.27 [d,1H,H^3-C_6H_4]; 8.37 [s,1H,H^4-C_6H_4].

^{13}C NMR [δ(ppm), $CDCl_3$ solution]: 28.8 [CH_2]; 28.9 [CH_2]; 31.7 [-CH_2Br]; 31.8 [-CH_2Br]; 46.3 [-CH_2N^1]; 51.3 [-$CH_2N^{2'}$]; 124.4 [i^1-C_6H_4]; 126.8 [C^1-C_6H_4]; 128.5 [i^2-C_6H_4]; 129.3 [C^2-C_6H_4]; 130.0 [C^3-C_6H_4]; 130.41 [C^4-C_6H_4]; 153.9 [CN_4, (N^1CH_2)]; 163.80 [CN_4, ($N^{2'}CH_2$)].

3.7.9 Synthesis of 1,3-phenylene-bis-5,5'-[N^2,$N^{2'}$-(4-bromobutyl)tetrazole] (35) and 1,3-phenylene-bis-5,5'-[N^1,$N^{2'}$-(4-bromobutyl)tetrazole] (36)

These compounds were prepared by the same general method from **(12)** and 1,4-dibromobutane as a crystalline solid and a viscous oil respectively.

(35):

Analysis: Found(Calc. for $C_{16}H_{20}N_8Br_2$): C 39.2(39.7); H 4.18(4.13); N 22.6(23.1)%

^{1}H NMR [δ(ppm), $CDCl_3$ solution]: 1.89-1.99 [m,4H,2xCH_2]; 3.46 [t,4H,2x-CH_2Br]; 4.72 [t,4H,-CH_2N^2,-$CH_2N'^2$]; 7.62 [t,1H,H^1-C_6H_4]; 8.24 [dd,2H,2x$H^2C_6H_4$]; 8.90 [t,1H,H^3-C_6H_4].

^{13}C NMR [δ(ppm), $CDCl_3$ solution]: 27.8 [2xCH_2]; 29.2 [2xCH_2]; 32.1 [2x-CH_2Br]; 52.2 [-CH_2N^2,-$CH_2N^{2'}$]; 125.2 [C^1-C_6H_4]; 128.2 [*i*-C_6H_4]; 128.5 [2xC^2-C_6H_4]; 129.5 [C^3-C_6H_4]; 164.6 [CN_4].

(36):

Analysis: Found(Calc. for $C_{16}H_{20}N_8Br_2$): C 40.4(39.7); H 4.26(4.13); N 22.7(23.1)%

^{1}H NMR [δ(ppm), $CDCl_3$ solution]: 1.87-1.98 [m,4H,2xCH_2]; 2.11-2.18 [m,2H,CH_2]; 2.19-2.32 [m,2H,CH_2]; 3.41 [t,2H,-CH_2Br]; 3.47 [t,2H,-CH_2Br]; 4.55 [t,2H,-CH_2N^1]; 4.74 [t,2H,-$CH_2N^{2'}$]; 7.73 [t,1H,H^1-C_6H_4]; 7.88 [d,1H,H^2-C_6H_4]; 8.37 [d,1H,H^3-C_6H_4]; 8.45 [s,1H,H^4-C_6H_4].

^{13}C NMR [δ(ppm), $CDCl_3$ solution]: 27.8 [CH_2]; 28.2 [CH_2]; 29.1 [CH_2]; 29.2 [CH_2]; 32.0 [-CH_2Br]; 32.1 [-CH_2Br]; 47.3 [-CH_2N^1]; 52.4 [-$CH_2N^{2'}$]; 124.8 [i^1-C_6H_4]; 126.7 [C^1-C_6H_4]; 128.7 [i^2-C_6H_4]; 129.4 [C^2-C_6H_4]; 130.1 [C^3-C_6H_4]; 130.5 [C^4-C_6H_4]; 153.8 [CN_4, (N^1CH_2)]; 163.9 [CN_4, ($N^{2'}CH_2$)].

3.7.10 Synthesis of 1,3-phenylene-bis-5,5′-[N^2,$N^{2'}$-(5-bromopentyl)tetrazole] (37) and 1,3-phenylene-bis-5,5′-[N^1,$N^{2'}$-(5-bromopentyl)tetrazole] (38)

These compounds were prepared by the same general method from **(12)** and 1,5-dibromopentane as viscous oils.

(37):

Analysis: Found(Calc. for $C_{18}H_{24}N_8Br_2$): C 43.3(42.2); H 4.76(4.69); N 20.9(21.8)%

^{1}H NMR [δ(ppm), $CDCl_3$ solution]: 1.51 [m,4H,2xCH_2]; 1.90 [m,4H,2xCH_2]; 2.08 [m,4H,2xCH_2]; 3.38 [t,4H,2x-CH_2Br]; 4.66 [t,4H,-CH_2N^2,-$CH_2N^{2'}$]; 7.59 [t,1H,H^1-C_6H_4]; 8.21 [dd,2H,2xH^2-C_6H_4]; 8.88 [t,1H,H^3-C_6H_4].

^{13}C NMR [δ(ppm), $CDCl_3$ solution]: 24.9 [2xCH_2]; 28.4 [2xCH_2]; 31.8 [2xCH_2]; 33.0 [2x-CH_2Br]; 52.9 [-CH_2N^2,-$CH_2N^{2'}$]; 125.1 [C^1-C_6H_4]; 128.2 [*i*-C_6H_4]; 128.4 [2xC^2-C_6H_4]; 129.5 [C^3-C_6H_4]; 164.5 [CN_4].

(38):

Analysis: Found(Calc. for $C_{18}H_{24}N_8Br_2$): C 42.0(42.2); H 4.80(4.69); N 20.8(21.8)%

^{1}H NMR [δ(ppm), $CDCl_3$ solution]: 1.37-1.53 [m,4H,2xCH_2]; 1.74-2.07 [m,8H,4xCH_2]; 3.27-3.56 [m,4H,2x-CH_2Br]; 4.43 [t,2H,-CH_2N^1]; 4.63 [t,2H,-$CH_2N^{2'}$]; 7.62-7.76 [m,2H,H^1H^2-C_6H_4]; 8.29-8.36 [m,2H,H^3H^4-C_6H_4]..

^{13}C NMR [δ(ppm), $CDCl_3$ solution]: 24.9 [2xCH_2]; 28.4 [CH_2]; 28.8 [CH_2]: 31.7 [CH_2]; 31.8 [CH_2]; 32.9 [-CH_2Br]; 33.0 [-CH_2Br]; 47.9 [-CH_2N^1]; 53.0 [-$CH_2N^{2'}$]; 124.8 [i^1-C_6H_4]; 126.7 [C^1-C_6H_4]; 128.8 [i^2-C_6H_4]; 129.4 [C^2-C_6H_4]; 130.1 [C^3-C_6H_4]; 130.4 [C^4-C_6H_4]; 153.7 [CN_4, (N^1CH_2)]; 163.8 [CN_4, ($N^{2'}CH_2$)].

3.7.11 Synthesis of 1,3-phenylene-bis-5,5'-[N^2,$N^{2'}$-(6-bromohexyl)tetrazole] (39)

This compound was prepared by the same general method from **(12)** and 1,6-dibromohexane as a waxy solid.

Analysis: Found(Calc. for $C_{20}H_{28}N_8Br_2$): C 44.6(44.5); H 5.29(5.19); N 20.5(20.7)%

^{1}H NMR [δ(ppm), $CDCl_3$ solution]: 1.21-1.32 [m,4H,2xCH_2]; 1.35-1.45 [m,4H,2xCH_2]; 1.63-1.82 [m,4H,2xCH_2]; 1.85-1.96 [m,4H,2xCH_2]; 3.31 [t,4H,2x-CH_2Br]; 4.50 [t,4H,-CH_2N^2,-$CH_2N^{2'}$]; 7.53 [t,1H,$H^1C_6H_4$]; 7.81 [dd,2H,2xH^2-C_6H_4]; 8.41 [t,1H,H^3-C_6H_4].

^{13}C NMR [δ(ppm), $CDCl_3$ solution]: 25.2 [2xCH_2]; 27.2 [2xCH_2]; 28.9 [2xCH_2]; 32.2 [2xCH_2]; 33.4 [2x-CH_2Br]; 52.7 [-CH_2N^2,-$CH_2N^{2'}$]; 127.2 [*i*-C_6H_4]; 129.3 [C^1-C_6H_4]; 129.9 [2xC^2-C_6H_4]; 130.3 [C^3-C_6H_4]; 164.1 [CN_4].

3.7.12 Synthesis of 1,3-phenylene-bis-5,5'-[N^2,$N^{2'}$-(8-bromooctyl)tetrazole] (40)

This compound was prepared by the same general method from **(12)** and 1,8-dibromooctane as a colourless oil whch solidified to a waxy solid on standing.

Analysis: Found(Calc. for $C_{24}H_{36}N_8Br_2$): C 48.8(48.4); H 6.23(6.04); N 18.9(18.8)%

^{1}H NMR [δ(ppm), $CDCl_3$ solution]: 1.21-1.32 [m,4H,2xCH_2]; 1.35-1.45 [m,4H,2xCH_2]; 1.63-1.82 [m,4H,2xCH_2]; 1.85-1.96 [m,4H,2xCH_2]; 3.31 [t,4H,2x-CH_2Br]; 4.50 [t,4H,-CH_2N^1,-$CH_2N^{2'}$]; 7.53 [t,1H,H^1-C_6H_4]; 7.81 [dd,2H,2xH^2-C_6H_4]; 8.29 [s,1H,H^3-C_6H_4].

^{13}C NMR [δ(ppm), $CDCl_3$ solution]: 25.2 [2xCH_2]; 27.2 [2xCH_2]; 28.9 [2xCH_2]; 32.2 [2xCH_2]; 33.4 [2x-CH_2Br]; 52.7 [-CH_2N^1,-$CH_2N^{2'}$]; 127.2 [*i*-C_6H_4]; 129.3 [C^1-C_6H_4]; 129.9 [2xC^2-C_6H_4]; 130.3 [C^3-C_6H_4]; 164.1 [CN_4].

3.7.13 Synthesis of 1,3-phenylene-bis-5,5′-[N^2,$N^{2'}$-(4-bromomethyl)benzyl-tetrazole] (41) and 1,3-phenylene-bis-5,5′-[N^1,$N^{2'}$-(4-bromomethyl)benzyl-tetrazole] (42)

These compounds were prepared by heating **(11)** (1g, 1.26 mmol) and α,α′-dibromo-*m*-xylene (3.3g, 12.6 mmol) as a melt at 120°C for two hours. The opaque mass which formed on cooling was then chromatographed as previously described to yield **(41)** and **(42)** as a crystalline solid and a viscous oil respectively.

(41):

Analysis: Found(Calc. for $C_{24}H_{20}N_8Br_2$): C 49.2(49.6); H 3.53(3.45); N 18.3(19.3)%

^{1}H NMR [δ(ppm), $CDCl_3$ solution]: 4.39 [s,4H,2x-C*H*$_2$Br]; 5.74 [s,4H,-C*H*$_2$N^2,-C*H*$_2$N$^{2'}$]; 7.29 [m,6H,2x*o*,*m*-C$_6$*H*$_4$(CH$_2$-)$_2$]; 7.38 [s,2H,2x*o*-C$_6$*H*$_4$(CH$_2$-)$_2$]; 7.52 [t,1H,H^1-C$_6$*H*$_4$]; 8.16 [dd,2H,2xH^2-C$_6$*H*$_4$]; 8.82 [s,1H,H^3-C$_6$*H*$_4$].

^{13}C NMR [δ(ppm), $CDCl_3$ solution]: 32.6 [2x-*C*H$_2$Br]; 56.5 [-*C*H$_2$N^2,-*C*H$_2$N$^{2'}$]; 125.4, 128.4, 128.6, 129.0 [3x*o*,1x*m*-C$_6$H$_4$(CH$_2$-)$_2$]; 128.1 [*i*-C$_6$H$_4$]; 129.5 [C^1-C$_6$H$_4$]; 129.6 [2xC^2-C$_6$H$_4$]; 129.7 [C^3-C$_6$H$_4$]; 133.8, 138.77 [2x*i*-C$_6$H$_4$(CH$_2$-)$_2$]; 165.0 [*C*N$_4$].

(42):

Analysis: Found(Calc. for $C_{24}H_{20}N_8Br_2$): C 50.4(49.6); H 3.66(3.45); 19.3(19.3)%

^{1}H NMR [δ(ppm), $CDCl_3$ solution]: 4.32 [s,2H,-C*H*$_2$Br]; 4.38 [s,2H,-C*H*$_2$Br]; 5.56 [s,2H,-C*H*$_2$N^1]; 5.73 [s,2H,-C*H*$_2$N$^{2'}$]; 7.16-8.78 [m,8H,*o*,*m*-C$_6$*H*$_4$,*o*,*m*-C$_6$*H*$_4$(CH$_2$-)$_2$].

^{13}C NMR [δ(ppm), $CDCl_3$ solution]: 32.5 [2x-*C*H$_2$Br]; 51.3 [-*C*H$_2$N^1]; 56.6 [-*C*H$_2$N$^{2'}$]; 124.4 [*i*^{1}-C$_6$H$_4$]; 127.9 [*i*^{2}-C$_6$H$_4$]; 126.9, 127.5, 128.2, 128.3, 128.6, 128.9, 129.5, 129.5, 129.6, 129.7, 129.9, 130.6

[2x*o,m*-C_6H_4,2x*o,m*-$C_6H_4(CH_2\text{-})_2$]; 133.6, 134.0, 138.8, 138.9 [4x*i*-$C_6H_4(CH_2\text{-})_2$]; 153.9 [CN_4,(N^1CH_2)]; 164.8 [CN_4,($N^{2'}CH_2$)].

3.7.14 Synthesis of 1,3-phenylene-bis-5,5'-[N^2,$N^{2'}$-(3-cyanopropyl)tetrazole] (43)

(12) (6.0g, 7.6 mmol) and 4-bromobutyronitrile (*ca.*20g, 133 mmol) were heated at 120°C for two hours giving an amber oil. Elution with a gradient of 40/60 petrol to acetone on silica gel yielded a single fraction, **(43)**, as a viscous oil which solidified on standing to a amorphous solid.

Analysis: Found(Calc. for $C_{16}H_{16}N_{10}$): C 55.2(55.2); H 4.82(4.60); N 39.6(40.2)%

^{1}H NMR [δ(ppm), $CDCl_3$ solution]: 2.32-2.56 [m,8H,2x-CH_2CH_2CN]; 4.84 [t,4H,-CH_2N^2,-C$H_2N^{2'}$]; 7.64 [t,1H,H^1-C_6H_4]; 8.22 [dd,2H,2xH^2-C_6H_4]; 8.85 [s,1H,H^3-C_6H_4].

^{13}C NMR [δ(ppm), $CDCl_3$ solution]: 14.8 [2x-CH_2CH_2CN]; 25.2 [2x-CH_2CN]; 51.23 [-CH_3N^2,-$CH_2N^{2'}$]; 117.9 [2x-CH_2*C*N]; 127.9 [2x*i*-C_6H_4]; 128.7 [C^1-C_6H_4]; 129.6 [2xC^2-C_6H_4]; 130.3 [C^3-C_6H_4]; 164 8 [CN_4].

IR [(cm^{-1}), nujol mull]: 2249 [ν(CN)].

3.7.15 Synthesis of 1,3-phenylene-bis-5,5'-{N^2,$N^{2'}$-[3-(tributylstannyltetrazolyl)-propyl]tetrazole} (44)

(43) (0.5g, 1.44 mmol) was heated as a neat suspension under nitrogen with tributyltin azide (0.93g, 2.81 mmol) at 180°C for 1 hour. This yielded a viscous amber oil which solidified to a brittle glass on cooling. Dissolution in methanol and filtration through activated carbon afforded a colourless solution which was evaporated and dried under vacuum to give a bis-methanol solvated **(44)** as a colourless glass.

Analysis: Found(Calc. for $C_{40}H_{58}N_{16}Sn_2$.2MeOH): C 46.9(47.3); H 7.43(7.25); 20.8(21.0)%

^{1}H NMR [δ(ppm), DMSO-d^6 solution]: 0.78 [t,18H,6xCH_3]; 1.15-1.31 [m,24H,6x-$CH_2CH_2CH_2CH_3$]; 1.44-1.52 [m,12H,6x-$CH_2CH_2CH_2CH_3$]; 2.37-2.48 [m,4H,2x-$CH_2CH_2CH_2CN_4$]; 2.84 [t,4H,-CH_2CN_4]; 4.88 [t,4H,-CH_2N^2,-$CH_2N^{2'}$]; 7.76 [t,1H,H^1-C_6H_4]; 8.20 [dd,2H,2xH^2-C_6H_4]; 8.74 [s,1H,H^3-C_6H_4].

^{13}C NMR [δ(ppm), DMSO-d^6]: 13.3 [CH_3]; 18.1 [Sn$CH_2(CH_2)_2CH_3$]; 21.6 [-CH_2CN_4]; 26.2 [Sn$(CH_2)_2CH_2CH_3$]; 27.5 [Sn$CH_2CH_2CH_2CH_3$]; 27.7 [-$CH_2CH_2CN_4$]; 52.3 [-CH_2N^2]; 127.9 [C^1-C_6H_4]; 128.0 [2x*i*-C_6H_4]; 128.6 [2xC^2-C_6H_4]; 130.2 [C^3-C_6H_4]; 161.0 [CN_4SnBu_3]; 163.4 [CN_4];

$^{1}J[Sn^{13}CH_2(CH_2)_2CH_3$-$^{117,119}Sn]$ 478.0 Hz. (unresolved);

$^{3}J[Sn(CH_2)_2{}^{13}CH_2CH_3$-$^{117,119}Sn]$ 75.4 Hz. (unresolved).

^{119}Sn NMR [δ(ppm), DMSO-d^6 solution]: -55.1.

^{119m}Sn Mössbauer (mms^{-1}): I.S.=1.40; Q.S.=3.50.

3.7.16 Attempted Reaction of (26) and (20)

(20) (0.76g, 3.55 mmol) was stirred as a suspension in dichloromethane (20 ml). Triethylamine (0.75g/1.1ml, 7.2 mmol) was added and stirred for one hour giving a colourless solution. **(26)** (1.62g, 3.55 mmol) was then added dropwise in dichloromethane (90 ml). The resulting colourless solution was then stirred at ambient temperature for twenty four hours. *In vacuo* removal of the solvent yielded a sticky colourless solid which was chromatographed on silica. Initial fractions obtained by continuous elution with dichloromethane contained a a small amount of **(26)**. Subsequent fractions, obtained by acetone elution contained 1.45g of a colourless crystalline solid which was shown to be triethylamine hydrobromide by microanalysis.

Analysis: Found(Calc. for $C_6H_{16}NBr$): C 39.7(39.6); H 9.31(8.82); N 7.7(7.7)%

3.7.17 Attempted reaction of ***(37)*** and ***(21)***

(21) (0.14g, 0.65 mmol) was stirred with NaOH (0.22g, 5.5 mmol) in methanol (150 ml) until complete dissolution had occurred. At this point, **(37)** (0.31g, 0.65 mmol) in methanol (50 ml) was added slowly and the resulting colourless solution stirred at room temperature for twenty four hours before reflux for a further two hours. The solvent was removed under vacuum giving a colourless solid. This was stirred with dichloromethane and filtered, subsequent evaporation of the filtrate yielding an oil which solidified of standing. TLC analysis indicated a single major component which was purified by column chromatography to give 0.20g of a colourless solid whch was shown to be unreacted **(37)** by microanalysis.

Analysis: Found(Calc. for $C_{18}H_{24}N_8Br_2$): C 43.1(42.2); H 4.70(4.76); N 21.2(21.8)%

3.7.18 Attempted reaction of ***(40)*** and ***(21)***

(21) (0.26g, 1.21 mmol) was heated under reflux with K_2CO_3 (2.9g, 24.2 mmol) in acetonitrile (130 ml) under nitrogen for 3 hours. **(40)** (0.62g, 1.21 mmol) in acetonitrile (20 ml) was added to the resultant suspension and reflux continued for a further 18 hours. Filtration gave a colourless solution and a colourless solid after removal of the solvent. This was shown to be to be unreacted **(40)** by microanalysis.

Analysis: Found(Calc. for $C_{24}H_{36}N_8Br_2$): C 50.7(48.4); H 6.37(6.04); N 17.4(18.8)

Chapter 4

The Synthesis and Structural Chemistry of Organotin-substituted Tris-tetrazoles

4.1 Introduction

Chapter 2 showed that the scope of the organotin azide/organic nitrile reaction can be readily extended to the synthesis of bis-(triorganostannyl-tetrazole) compounds. Due to the multiplicity of Lewis basic/acidic centres, compounds of this type were found to crystallise as coordination polymers with the formation of extended supramolecular architecture. The type of structure adopted appears, at least in part, to be controlled by the space-filling requirements of the triorganotin group as is emphatically illustrated by the transition from 2-D to 3-D polymer observed for the homologous triethyltin- and tributyltin-substituted compounds (**17**) and (**11**) respectively.

Extended inorganic materials with inner cavities are currently attracting interest as host lattices for intercalative reactions where the identity of the guest molecule is determined by the shape, size and chemical nature of the cavity.[242,243] Compounds of this type may be useful as catalysts, molecular sieves, optical materials *etc.* and therefore reactions providing facile tailored routes to extended solid-state structures are highly desirable.

A recent study has shown that isomorphous 2-D structures are adopted by cobalt, zinc and cadmium bis-(tetrazolyl)borate complexes of cobalt, zinc and cadmium,[215] in each case stabilised by guest solvate (H_2O) molecules (Figure 4.1). Only the N-atom adjacent to the tetrazole ring C-H functions as a donor atom to the metal, the other two available nitrogens forming hydrogen-bonds to

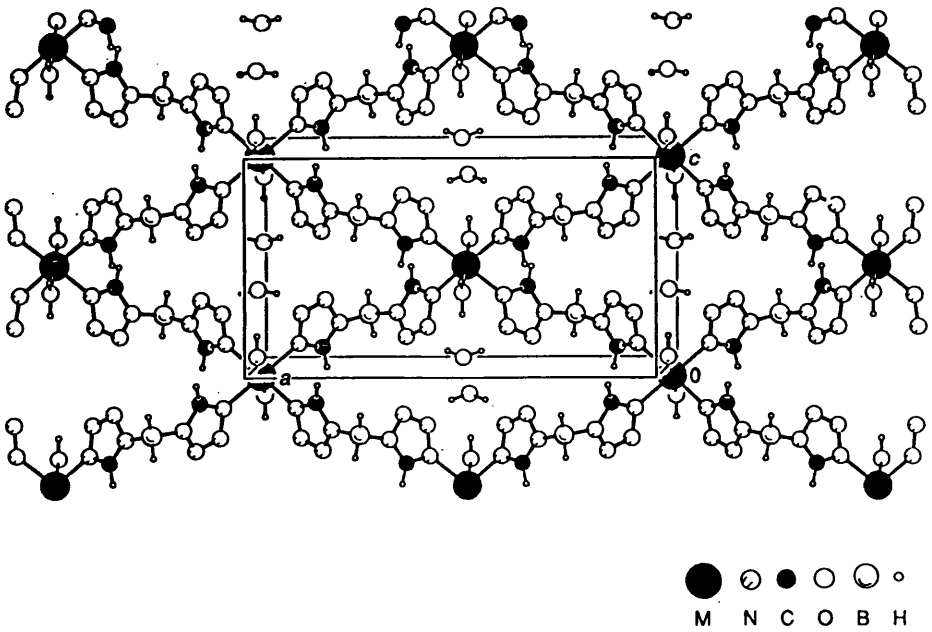

Figure 4.1: The Isomorphous Structures of $[M\{H_2B(CHN_4)_2\}_2(H_2O)_2].(H_2O)_2$, (M = Co,Zn, Cd).

the embedded water of crystallisation. The rhombohedral openings do not, however, extend through the lattice as open channels, the adjacent layers being offset by half a unit cell so that the layers interlock with the formation of solvent-containing caves.

In contrast to this 'water-filled' lattice, the cavities provided by organotin-based poly-tetrazole systems will necessarily be wholly or partially occupied by the attached alkyl groups while the structure adopted is determined by their space-filling requirements and the invariant *trans*-N_2SnR_3 geometry at tin. Observations of this nature have previously been applied to organotin hexacyanometallates[100] (Section 1.4.6) where the cavities provided by Me_3Sn-linked systems have been shown to be suitable intercalation sites for solvent inclusions.[101]

This chapter therefore seeks to extend the theme of Chapter 2 to the use of tris-nitrile cycloaddition precursors and, where possible, to examine the structures adopted the potentially heavily crosslinked tetrazole products.

4.2 Synthesis

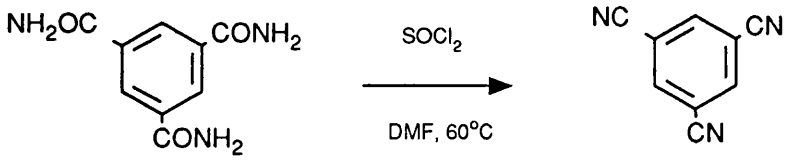

(45) (46) (Equation 4.1)

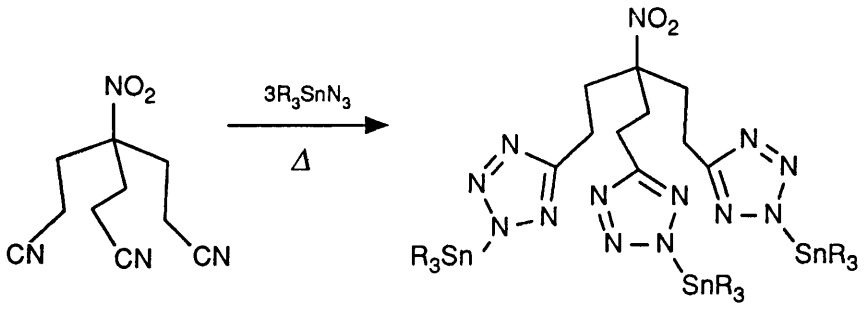

(Equation 4.2)

(47): R = Me

(48): R = Et

(49): R = Bu

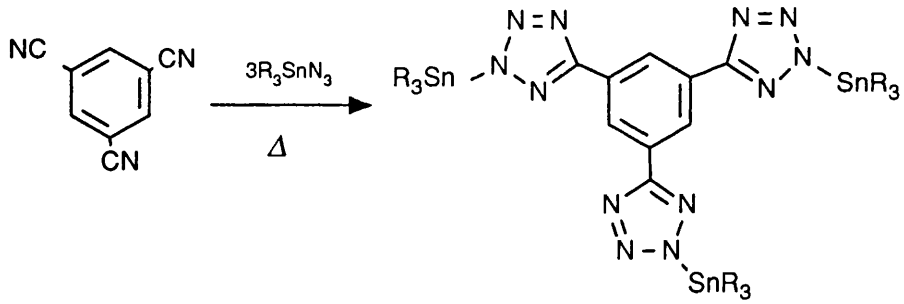

(Equation 4.3)

(50): R = Me

(51): R = Et

(52): R = Bu

Six triorganotin-substituted tris-tetrazoles have been synthesised employing either tris-(2-cyanoethyl)nitromethane (Equation 4.2) or 1,3,5-tri-cyanobenzene (**46**) (Equation 4.3) as tris-nitrile starting materials. The substituted nitromethane is commercially available (Aldrich) while (**46**) was synthesised from the corresponding amide (**45**) using thionyl chloride/dimethyl

formamide (Equation 4.1).[244,245]

The course of reaction was followed by the disappearance of the IR bands due to CN at 2250 and N_3 at 2060 cm^{-1}. **(47)**-**(50)** were synthesised by the direct reaction of the relevant nitrile and azide under nitrogen while **(51)** and **(52)** were prepared under reflux in the high boiling inert solvents *p*-xylene and mesitylene respectively. In these latter two cases the course of reaction is evident from the formation of a white precipitate in the initially clear solution. The crude products were purified where possible by recrystallisation from methanol or ethanol. **(47)** was obtained as a sticky glass while **(48)**-**(52)** were crystalline solids. The trimethyltin derivative **(50)** was isolated as a hexa-hydrate, as deduced from microanalysis and infra-red spectroscopic data (where broad bands at 3638 and 1638 cm^{-1} clearly indicate the presence of water). Analytical and physical data of **(47)**-**(52)** are presented in Table 4.1 while full details of synthetic and work-up procedures are included in Section 4.6.

Table 4.1: Analytical data for Triorganotin-substituted Tris-tetrazole Compounds

Compound	m.p (°C)	C(%)[a]	H(%)	N(%)
(47)	-	27.7(27.2)	4.78(4.60)	20.5(21.7)
(48)	235(dec)	34.8(34.9)	5.87(5.92)	18.8(18.9)
(49)	216(dec)	45.3(45.4)	7.86(7.65)	15.0(15.0)
(50)	>240[b]	24.7(24.6)[c]	4.44(4.72)[c]	19.1(19.1)[c]
(51)	>240[b]	35.9(36.1)	5.28(5.36)	18.1(18.7)
(52)	>240[b]	47.1(47.0)	7.49(7.32)	14.7(14.6)

[a] Found(Calc.)

[b] Limit of melting point apparatus

[c] Found(Calc. for hexa-hydrate)

4.3 Spectroscopy

4.3.1 NMR Spectroscopy

As was the case for the trialkyltin-substituted bis-tetrazoles of Chapter 2, the highly coordinating DMSO-d^6 was required for the collection of NMR data for **(47)**-**(52)**. ^1H, ^{13}C and ^{119}Sn NMR spectra were collected for each of the trialkyltin-substituted tris-(tetrazoles) and the relevant ^{119}Sn chemical shifts are displayed in Table 4.2.

The ^1H and ^{13}C spectra of **(47)**-**(52)** were all consistent with the proposed structures of Equations 4.1 and 4.2. In each case a single tertiary tetrazole ring carbon is discernible at *ca.* 161 ppm. in the ^{13}C spectra, demonstrating the equivalence of all three CN_4 rings on the NMR time scale.

The collated ^{119}Sn NMR chemical shift data of Table 4.2 lie within the range -36.0 to -50.1 ppm, similar to those reported for the analogous bis-tetrazole compounds of Chapter 2. Again however, the use DMSO-d^6 as solvent creates some ambiguity as to the nature of the solvated species [see (XXXVIII) and (XXXIX) in Section 2.3.1]. The data are, however, again wholly consistent with *trans*-trigonal bipyramidal geometry around tin as are the observed J^1 coupling constant data. The $^2J(^{119}Sn,^1H)$ values of 69.4 Hz and 69.1 Hz for the trimethyltin derivatives **(47)** and **(50)** respectively are consistent with such a five-coordinate arrangement, as is the $^1J(^{119}Sn,^{13}C)$ coupling of 529.4 Hz in the case of **(47)**. Use of the empirical relationship (Formula 4.1) relating the former two values with the Me-Sn-Me bond angle gives angles of 119.3° and 119.1° for **(47)** and **(50)** respectively, consistent with equatorial methyl groups in a trigonal bipyramidal coordination sphere. These data for the hexa-hydrated **(50)** do not however assist in revealing the nature of any tin/water interaction, although the hydrated nature of the compound is readily apparent from the broad singlet observed at 3.60 ppm in the ^1H spectrum.

The $^1J(^{119}Sn,^{13}C)$ value of 496.4Hz observed for the triethyltin derivative

(48) is again within the range expected for *trans*-trigonal bipyramidal coordination at tin, as is the value of 461.5 Hz resolvable for the tributyltin-substituted **(52)**. This latter value can be used to estimate the mean C-Sn-C bond angle in solution using the relationship of Holecek *et al.* (Formula 1.6)[133] and tenders an angle of 121.9°, also indicative of slightly distorted *trans*-tbp geometry at tin. Although no $^{1}J(^{119}Sn,^{13}C)$ coupling was observable for the tributyltin-substituted nitromethane derivative **(49)**, the $^{2}J(^{119}Sn,^{13}C)$ and $^{3}J(^{119}Sn,^{13}C)$ values of 27.7 Hz and 77.5 Hz respectively are internally consistent with the analogous data derived from both **(52)** (29.4 and 75.3 Hz respectively) and the tributyltin-substituted bis-tetrazoles of Chapter 2.

4.3.2 Mössbauer Spectroscopy

The Mössbauer data for the triorganotin-substituted tris-(tetrazoles) **(47)-(50)** are presented in Table 4.2. The isomer shift values and observed quadrupole splittings are comparable to those presented for the bis-(tetrazolyl) compounds of Chapter 2 and are thus exclusively indicative of *trans*-trigonal bipyramidal coordination around tin in the solid state. This geometry must occur

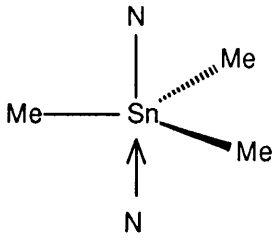

(XXXXIV)

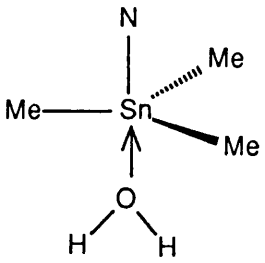

(XXXXV)

through tetrazole N-Sn-N bridging interactions of a type similar to those observed in the structures of **(17)** and **(11)**. The only possible exception to this general picture of the local bonding around tin is the hexa-hydrated **(50)**. In this case two types of tin site, bridging (XXXXIV) and hydrated (XXXXV) are possible. The

Table 4.2: ^{119}Sn NMR[a] and Mössbauer[b] Studies of Organotin-substituted Tris-(tetrazoles)

Compound	$\delta(^{119}Sn)^c$	δ	ΔEq	Γ_1	$\Gamma_2{}^d$
(47)	-49.0	1.27	3.42	1.01	1.04
(48)	-50.1	1.50	3.80	0.94	0.92
(49)	-36.0	1.42	3.60	0.90	0.98
(50)	-37.3	1.34	3.70	1.07	1.14
(51)	-45.3	1.52	3.93	1.15	1.29
(52)	-49.9	1.52	3.83	1.24	1.21

[a] All spectra run as DMSO-d^6 solutions at 25°C

[b] Mössbauer data recorded at 78K and data given in mms^{-1}

[c] Values given in ppm.

[d] Refers to full width at half height of the high and low velocity components in mms^{-1}.

quadrupole splittings of these two possibilities (N_2SnMe_3 versus $NOSnMe_3$) are expected to be of the same order (e.g. for Me_3SnNCO, ΔEq = 3.31 mms^{-1})[246] and thus it is not possible to say which gives rise to the observed spectrum. Both environments may be present, and indeed a precedent exists for the observation of both these tin sites in a trimethyltin-substituted tetrazole compound. The structure of bis-(trimethyltin)-5,5′-azobis(tetrazole).H_2O[247] is illustated in Figure 4.2 and shows that each ligand molecule is bridged by a trimethyltin group [via N(4) and N(8)] to form a polymeric chain. In addition, a hydrated trimethyltin unit is bonded to N(2). Both types of tin have a planar arrangement of methyl groups leading to similar Mössbauer data as reported here for **(50)** (I.S.=1.41; Q.S.=3.90 mms^{-1}).[247] A mixture of tin sites such as this would also explain the observed line broadening in the spectrum of **(50)**, although the equally broad lines lines of the other phenylene-linked tris-tetrazoles **(51)** and **(52)** suggest that this may be an inherent feature of these compounds due to a multiplicity of slightly differing tin sites.

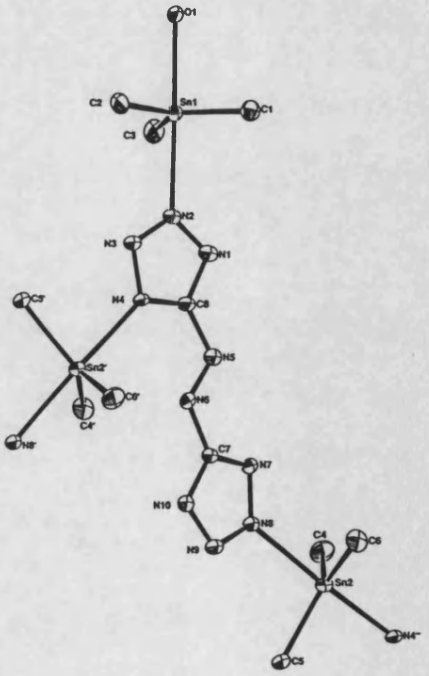

Figure 4.2: The Structure of Bis-(trimethyltin)-5,5′-azobis(tetrazole).H_2O

4.4 The Crystal Structure of Tris-[2-(5-tributylstannyltetrazolyl)ethyl]nitro-methane (49)

Suitable crystals for x-ray study were grown by very slow evaporation of a methanol solution. Full details of the crystallographic analysis are included in Appendix VIII along with atomic coordinates and isotropic temperature factors. The asymmetric unit consisting of three molecular units is shown in Figure 4.3 while selected bond lengths and bond angles are presented in Tables 4.3 and 4.4 respectively.

Examination of the molecular packing diagram, Figure 4.4, reveals a highly polymeric lattice propagated in two dimensions via *trans*-trigonal bipyramidal N_2SnBu_3 bridging interactions. The resultant sheet-like array is dominated by a 24 atom hexagonal motif constructed from six molecules of pairs of symmetry-related asymmetric units. N^1-Sn-$N^{3'}$ stannyl-tetrazole linkages prevail through out (Figure 4.3). The hexagonal constructions are inter-linked into the overall honeycomb-like appearance of Figure 4.4 via the ethyl chains of the substituted nitromethane units. In this manner the hexagonal rings are bounded by six approximately rhombohedral openings each incorporting four tin centres. These latter openings are constructed from the adjacent sides of two hexagonal rings, linked at each end by the five carbon chain provided by two ethyl groups and the nitro-bonded methane carbon. Each substituted nitromethane thus provides the bridgehead for three six-sided rings, with facile hexamer packing assisted by the inherent 3-fold symmetry of the tris-tetrazole ligand. The cavities provided by the hexagonal rings are of the order of 12Å across and are completely filled by the tin-bonded butyl groups which protrude to the interior of each.

Only the α-methylene carbon of each butyl group is shown in Figure 4.4 for clarity and these occupy the equatorial sites of what are three unique slightly distorted *trans*-trigonal bipyramidal tin sites. The axial positions are provided by

tetrazole N^1 and N^3 atoms and in each case the N-Sn-N bond angle is close to 180° [N(1)-Sn(1)-N(11) = 175.6(5)°; N(3)-Sn(2)-N(5) = 175.9(5)°; N(7)-Sn(3)-N(9) = 176.0(5)°] while the six individual N-Sn bond lengths are equivalent within experimental error [N(1)-Sn(1) = 2.43(1)Å; N(11)-Sn(1) = 2.38(2)Å; N(3)-Sn(2) = 2.37(1)Å; N(5)-Sn(2) = 2.41(2)Å; N(7)-Sn(3) = 2.37(2)Å; N(9)-Sn(3) = 2.37(2)Å] and typical of similar bonding environments (see Table 2.5). This bond length equivalence precludes identification of the nominally covalent and coordinative Sn-N bonds and is possibly attributable to the flexibility imparted to the molecular packing by the tetrazole-bonded ethyl chains. The nitrogen atoms each form part of what are three aromatic, delocalised CN_4 rings [maximum deviations from least squares planes of 0.005Å, 0.009Å and 0.030Å for the C(1), C(2) and C(3)-containing rings respectively.

As can be seen from Figure 4.5 (tributyltin units omitted), the individual polymeric sheets lie approximately parallel to one another. The interlamellar region is populated by the tin-bonded butyl groups and the tripodal nitromethane units which alternately project above and below the plane of polymer propagation. This latter feature ensures that the individual sheets are not planar but are puckered and stacked rather like the layers of an egg box carton. This provides for a mean interlayer separation of 10.07Å, measured orthogonally between the approximately linear N-Sn-N vectors of the individual sheets. Although the individual cavities of each sheet are not positioned perpendicular to each other, Figure 4.6 reveals that when the array of stacked layers is viewed obliquely the structure is observed to consist of linear microchannels. Two types of channels can be discerned, constructed respectively from the arrayed large hexagonal and rhombohedral cavities described above. Again the channels are entirely filled by the butyl carbon chains, precluding in this case the formation of any clathrate compound.

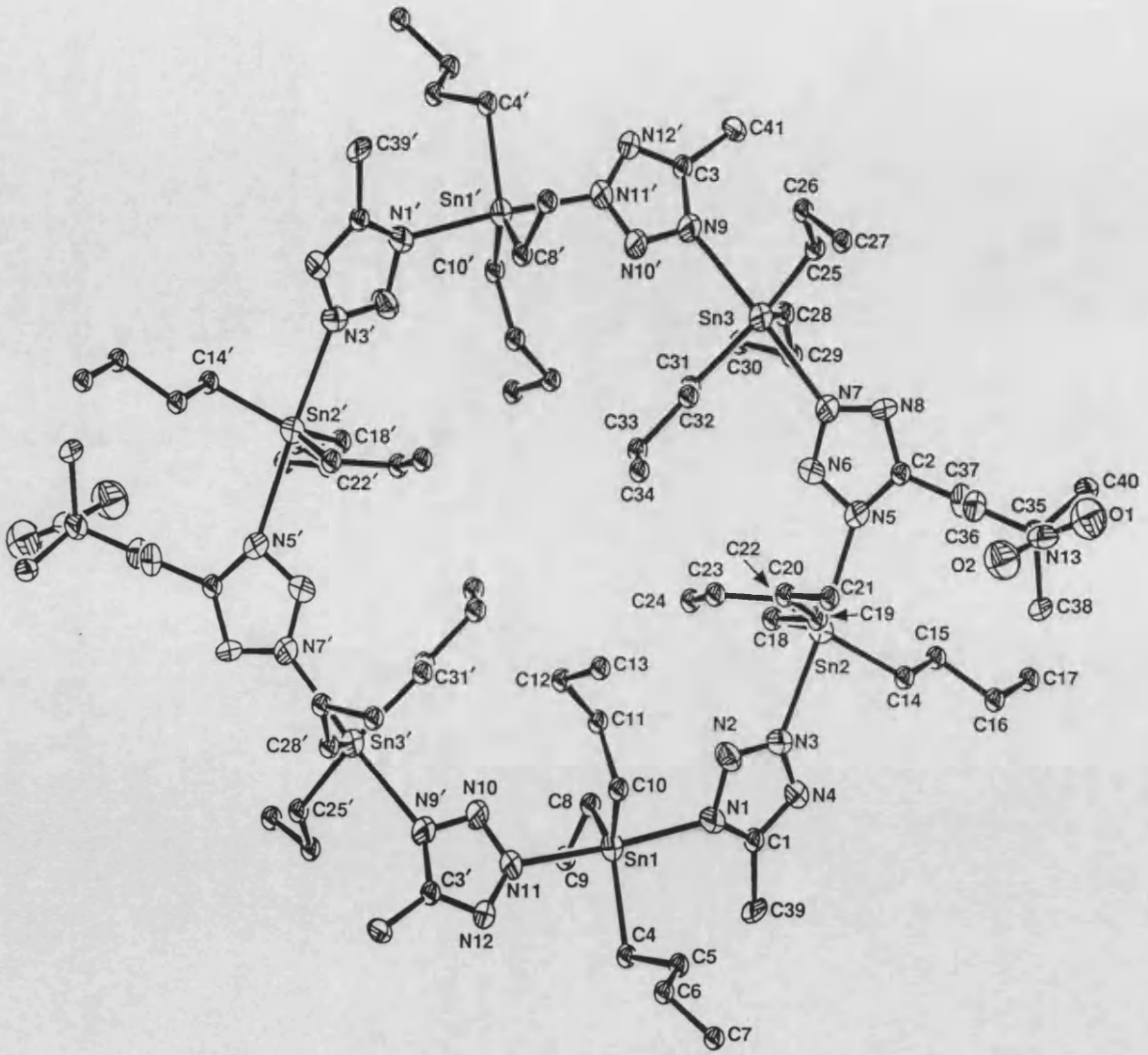

Figure 4.3: The asymmetric unit of (49). Hydrogen atoms omitted for clarity

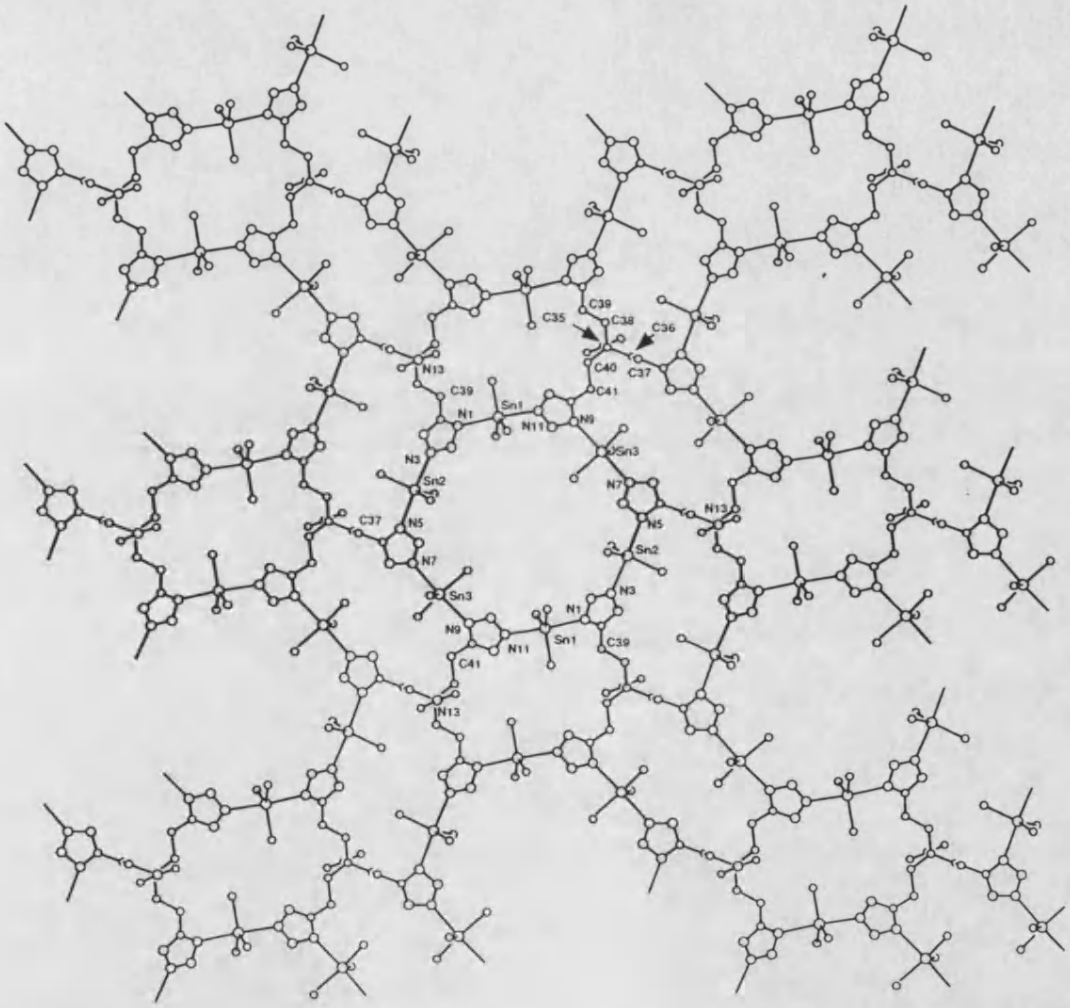

Figure 4.4: The sheet-like array of **(49)** showing N-Sn-N polymer propagation.

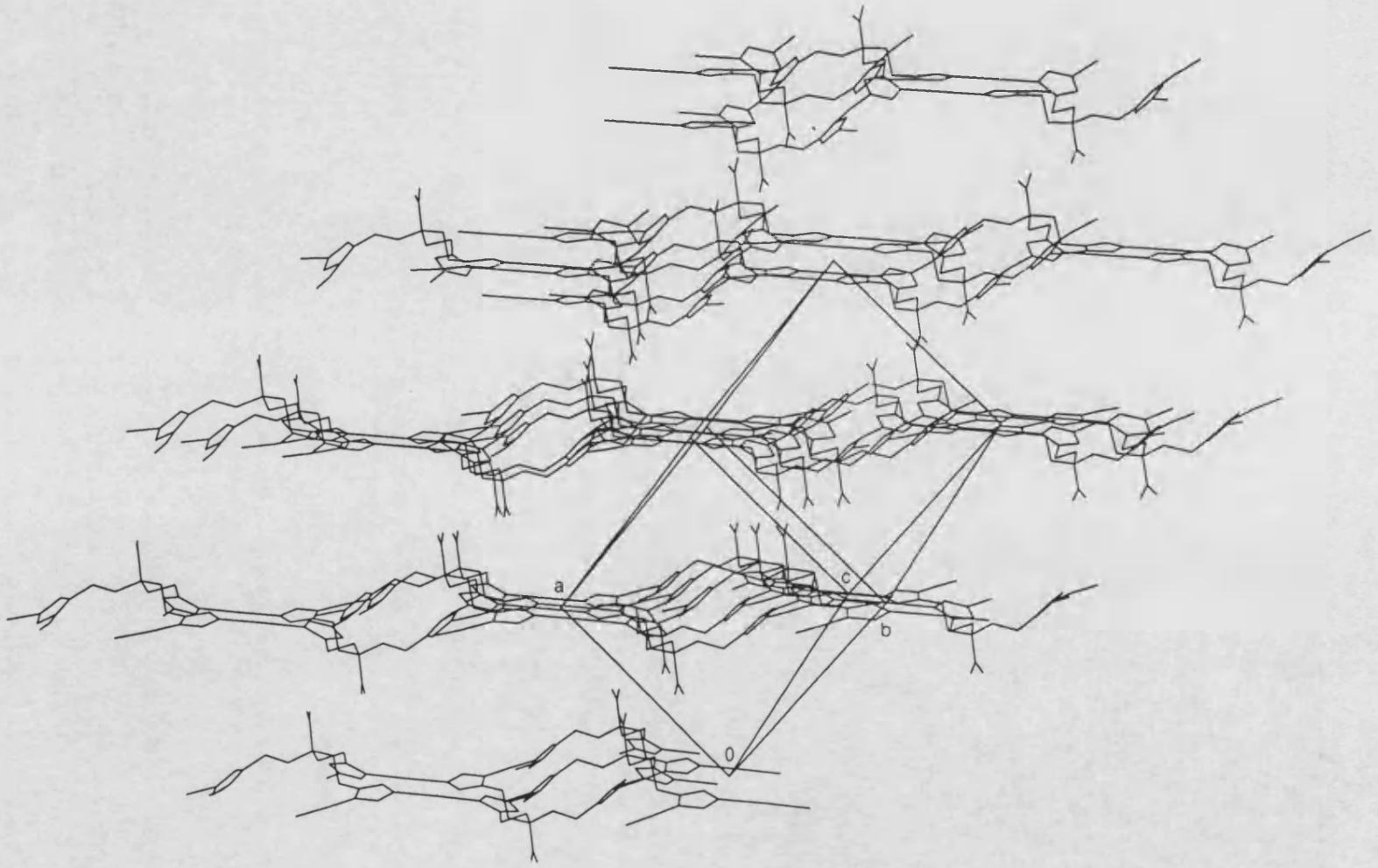

Figure 4.5: Side view of the sheet structure of **(49)**. Tributyltin groups omitted for clarity.

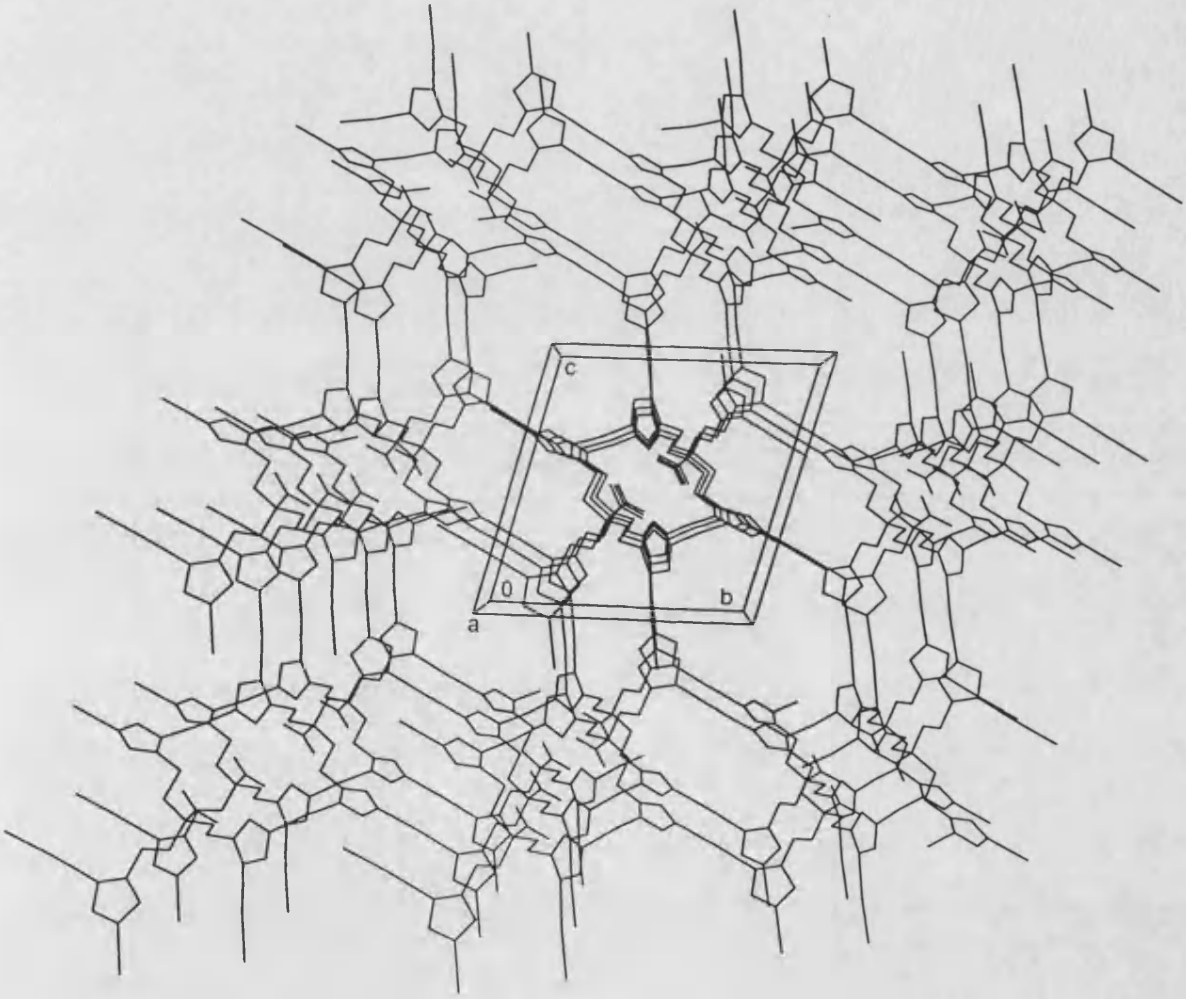

Figure 4.6: Perspective view of (**49**), showing the channels formed by the arrayed cavities.

Table 4.3: Selected Bond Lengths (Å) of Compound **(49)** and their estimated standard deviations in parentheses.

N(1)-Sn(1)	2.43(1)	N(11)-Sn(1)	2.38(2)
C(4)-Sn(1)	2.15(2)	C(8)-Sn(1)	2.11(2)
C(10)-Sn(1)	2.13(2)	N(3)-Sn(2)	2.37(1)
N(5)-Sn(2)	2.41(2)	C(14)-Sn(2)	2.14(2)
C(18)-Sn(2)	2.08(2)	C(22)-Sn(2)	2.14(2)
N(7)-Sn(3)	2.37(2)	N(9)-Sn(3)	2.37(2)
C(25)-Sn(3)	2.12(2)	C(28)-Sn(3)	2.14(2)
C(31)-Sn(3)	2.12(2)		

Table 4.4: Selected bond angles (°) of Compound **(49)** and their estimated standard deviations in parentheses.

N(11)-Sn(1)-N(1)	175.6(5)	C(4)-Sn(1)-N(1)	94.8(9)
C(4)-Sn(1)-N(11)	89.3(10)	C(8)-Sn(1)-N(1)	87.8(15)
C(8)-Sn(1)-N(11)	88.5(15)	C(8)-Sn(1)-C(4)	126.5(17)
C(10)-Sn(1)-N(1)	90.2(15)	C(10)-Sn(1)-N(11)	89.8(16)
C(10)-Sn(1)-C(4)	109.2(17)	C(10)-Sn(1)-C(8)	124.3(21)
N(5)-Sn(2)-N(3)	175.9(5)	C(14)-Sn(2)-N(3)	87.7(8)
C(14)-Sn(2)-N(5)	95.9(8)	C(18)-Sn(2)-N(3)	87.6(10)
C(18)-Sn(2)-N(5)	88.8(10)	C(18)-Sn(2)-C(14)	125.3(11)
C(22)-Sn(2)-N(3)	90.1(15)	C(22)-Sn(2)-N(5)	90.0(15)
C(22)-Sn(2)-C(14)	116.5(16)	C(22)-Sn(2)-C(18)	117.9(16)
N(9)-Sn(3)-N(7)	176.0(5)	C(25)-Sn(3)-N(7)	91.1(10)
C(25)-Sn(3)-N(9)	92.5(11)	C(28)-Sn(3)-N(7)	88.3(14)
C(28)-Sn(3)-N(9)	91.9(14)	C(28)-Sn(3)-C(25)	111.0(16)
C(31)-Sn(3)-N(7)	90.8(18)	C(31)-Sn(3)-N(9)	85.3(18)
C(31)-Sn(3)-C(25)	150.9(11)	C(31)-Sn(3)-C(28)	98.1(14)
N(2)-N(1)-Sn(1)	112.0(10)	C(1)-N(1)-Sn(1)	139.4(10)
C(1)-N(1)-N(2)	106.6(13)	N(3)-N(2)-N(1)	106.6(13)

Table 4.4 continued.

N(2)-N(3)-Sn(2)	120.8(11)	N(4)-N(3)-Sn(2)	127.7(11)
N(4)-N(3)-N(2)	110.6(13)	C(1)-N(4)-N(3)	104.1(14)
N(6)-N(5)-Sn(2)	107.5(10)	C(2)-N(5)-Sn(2)	147.4(12)
C(2)-N(5)-N(6)	104.3(13)	N(7)-N(6)-N(5)	109.3(13)
N(6)-N(7)-Sn(3)	118.9(12)	N(8)-N(7)-Sn(3)	131.0(10)
N(8)-N(7)-N(6)	109.7(13)	C(2)-N(8)-N(7)	105.0(14)
N(10)-N(9)-Sn(3)	116.9(11)	C(3)-N(9)-Sn(3))	138.8(11)
C(3)-N(9)-N(10)	102.7(14)	N(12)-N(11)-Sn(1)	131.4(11)
N(4)-C(1)-N(1)	112.1(15)		

4.5 The Crystal Structure of 1,3,5-phenylene-tris-5-(tributylstannyl)tetrazole (52)

Suitable crystals for x-ray study were grown by very slow evaporation of a methanol solution. Full details of the crystallographic analysis are included in Appendix IX, along with atomic coordinates and isotropic temperature factors. The asymmetric unit is illustrated in Figure 4.7 and selected bond lengths and bond angles are presented in Tables 4.5 and 4.6 respectively.

Examination of Figure 4.7 and the molecular packing diagram Figure 4.8 reveals that **(52)** adopts a an equivalent two-dimensional structural motif to that of the substituted nitromethane derivative **(49)**. The asymmetric unit, as presented by unprimed labels in Figure 4.7, consists of one $C_6H_3(CN_4)_3$ moiety and three Bu_3Sn fragments. This molecule is linked with its lattice neighbours to form a two-dimensional infinitely polymeric network of tetrazole hexamers effectively cemented by N^1-Sn-$N^{3'}$ interactions (Figures 4.8 and 4.9). Facile hexamer packing is again assisted by the inherent three-fold character of the tris-(tetrazole) ligand (Figure 4.9) which serves an identical role in lattice construction as the ethyl-substituted nitromethane unit of **(49)**.

The geometry of all three unique tin sites is slightly distorted *trans*-trigonal bipyramidal with axial N-Sn-N bond angles varying little from the ideal 180°. It is also noteworthy that in contrast to **(49)** a definite pattern of long and short Sn-N bonds is apparent, the N(2)-Sn(1), N(10)-Sn(2), N(6)-Sn(3) bonds averaging 2.36Å and the N(8)-Sn(1), N(4)-Sn(2), N(12)-Sn(3) lengths 2.46Å. This long-short/covalent-dative pattern probably reflects the more rigid nature of the phenylene-based tris-(tetrazole) ligand in comparison to the more flexible ethyl-bonded nitromethane bridgehead. As was the case in the structure of **(49)** the equatorial butyl groups protrude to the interior of the hexameric cavities (*ca.* 12Å across), filling the available space.

Polymer planarity is proportional to the planarity of the ligand participating in polymer propagation. In the case of **(49)** the tripodal 'piano

stool'-shaped ligands were necessarily directed alternately above and below the plane of polymer propagation to maintain planarity. In the case of **(52)**, however, the inherent planarity of the tetrazole-bridging phenylene unit allows no such structural compromise and the overall planarity of the individual sheets is controlled by the angle of twist between this C_6 plane and those of the respective tetrazoles in the 1, 3 and 5 ring positions. Figure 4.10 illustrates that the C(2)-containing tetrazole is virtually coplanar with the phenyl ring [N(8)-C(2)-C(8)-C(7) = 1.6°] whereas the remaining tetrazoles are somewhat skewed [C(5)-C(4)-C(1)-N(1) = 21.8°; C(5)-C(6)-C(3)-N(12) = 21.1°]. The resulting array of parallel sheets is illustrated in Figure 4.11. Although only the α-carbon of each tin-bonded butyl group is shown for clarity, as was the case for **(49)**, the interlamellar region is entirely occupied by their bulk resulting in a mean inter-planar distance of 11.29Å.

The individual cavities, as was the case for **(49)**, are offset so that the arrayed sheets must be viewed obliquely to observe the open channels running through the structure as illustrated in Figure 4.12. Again it should be emphasized that the apparently open structure illustrated is in fact entirely filled or 'packed' by the pendant butyl chains.

The introductory comments to this chapter indicated a possible analogy between the role played by the space-filling ability of the trialkyltin moiety of the current poly-(tetrazole) compounds and the guest molecules of clathrate compounds in determining the type of structure adopted. The structural contrast between the homologous bis-(tetrazole) compounds **(17)** and **(11)** described in Chapter 2 raises similar questions about the structures of the tris-(tetrazole) compounds described above. The apparently large openings created throughout the lattice by the tin-tetrazole framework of **(49)** and **(52)** are completely filled and possibly a direct result of the space-filling ability of the butyl chains.

Similar two-dimensional lattice networks have been reported for trimesic

acid (benzene-1,3,5-tricarboxylic acid, TMA) (Figure 4.13) and TMA inclusion compounds have been noted to exhibit many unusual structural variations depending on the size and identity of the clathrated molecule.[248]

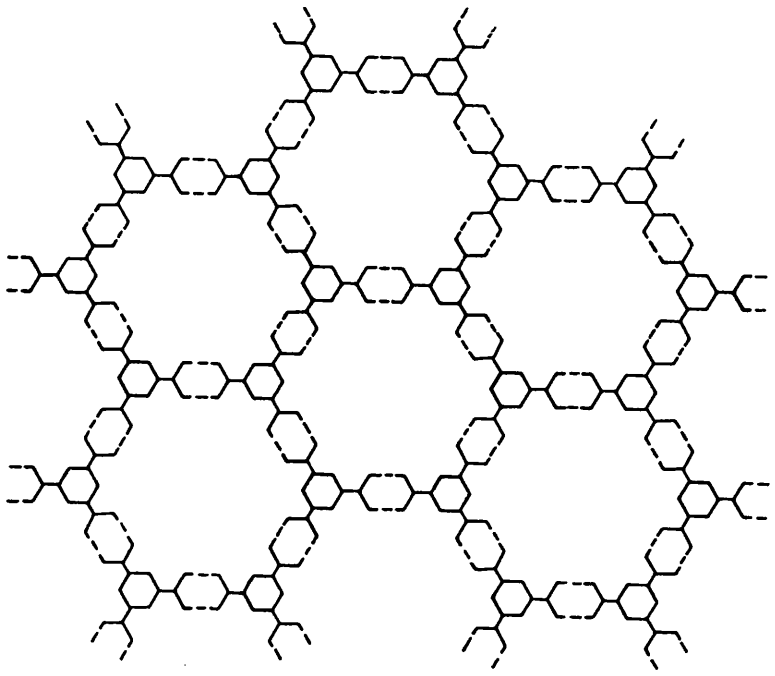

Figure 4.13: A representation of the hexagonal network formed by six TMA molecules H-bonded through their carboxylic acid groups. The holes have diameters of 12-13Å.

With this in mind, the compounds **(47)**, **(48)**, **(50)** and **(51)**, based around the smaller trimethyl and triethyltin substituents may adopt more 'closed' or even completly different lattice types to **(49)** and **(52)** in order that the trigonal bipyramidal tin geometry is not compromised. Alternatively it may be possible to induce a similar assembly to those of **(49)** and **(52)** by co-crystallisation with suitably sized organic molecules with the aim of augmenting the space-filling capacity of the smaller methyl and ethyl units. Indeed the hexa-hydrated nature of **(50)** may be a direct consequence of just such a requirement, although complete structural characterisation of this compound requires further study.

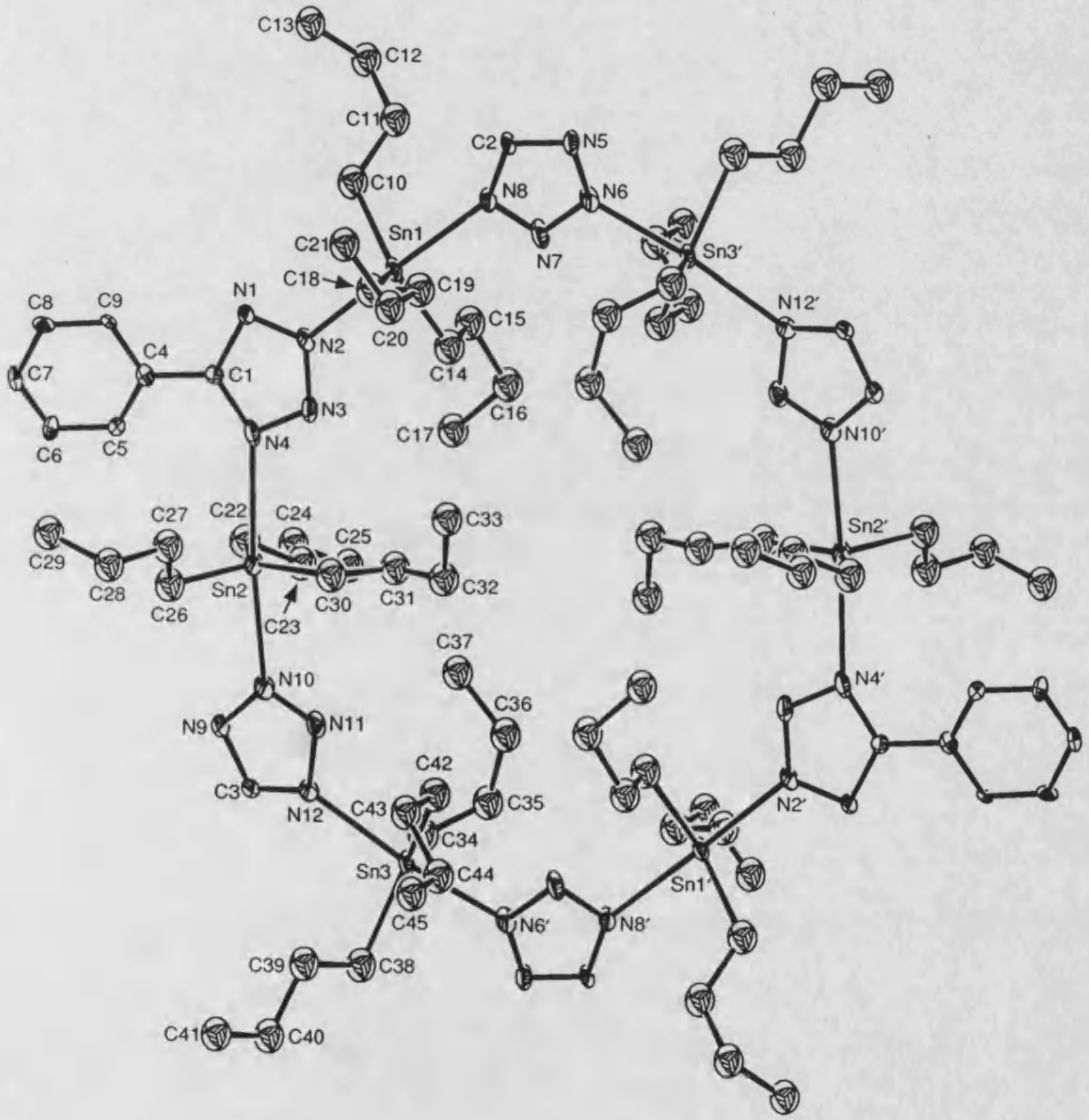

Figure 4.7: The asymmetric unit of (52) and the numbering scheme used. Hydrogen atoms omitted for clarity.

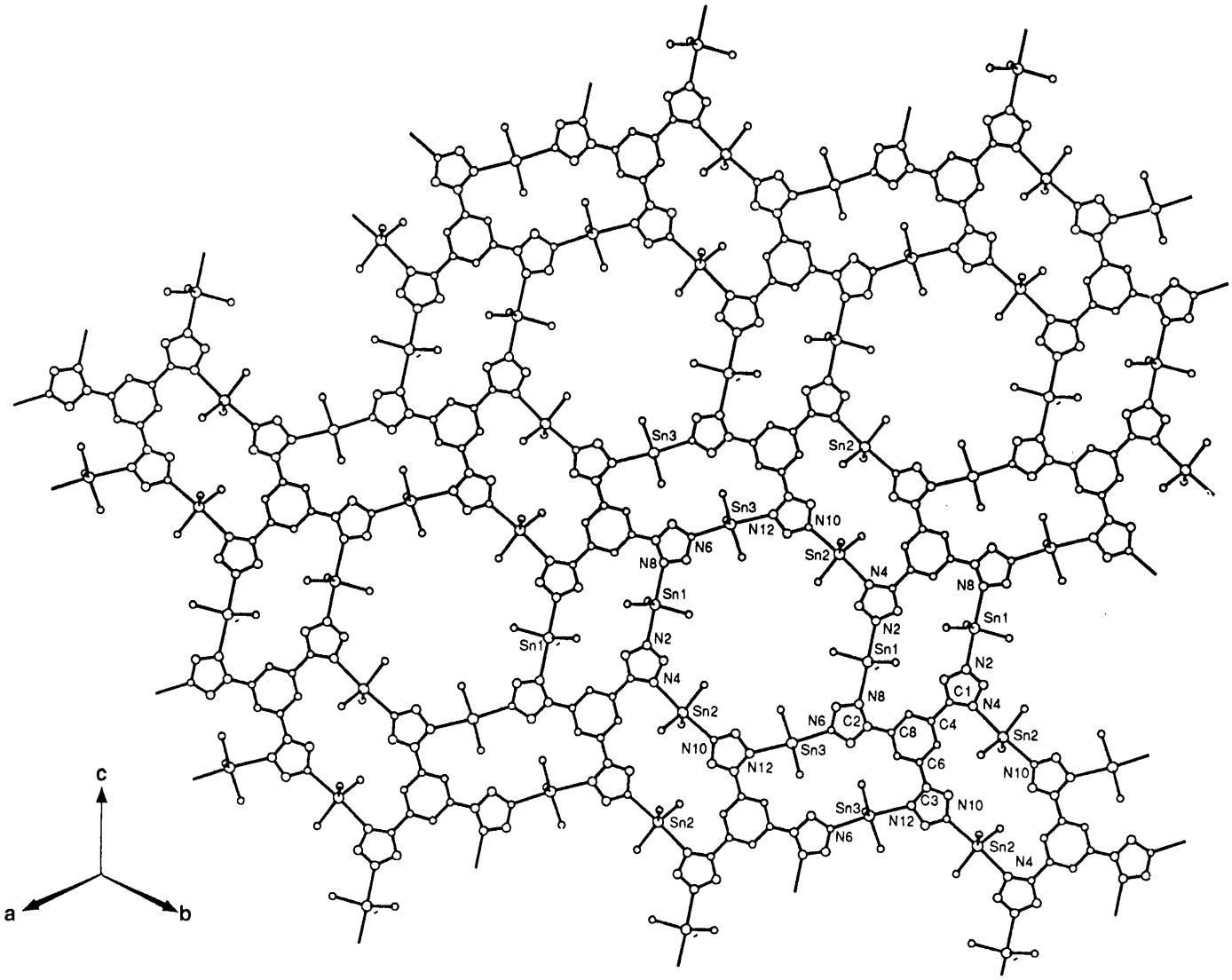

Figure 4.8: The 2-dimensional polymeric lattice of (52), α-butyl carbons only illustrated for clarity.

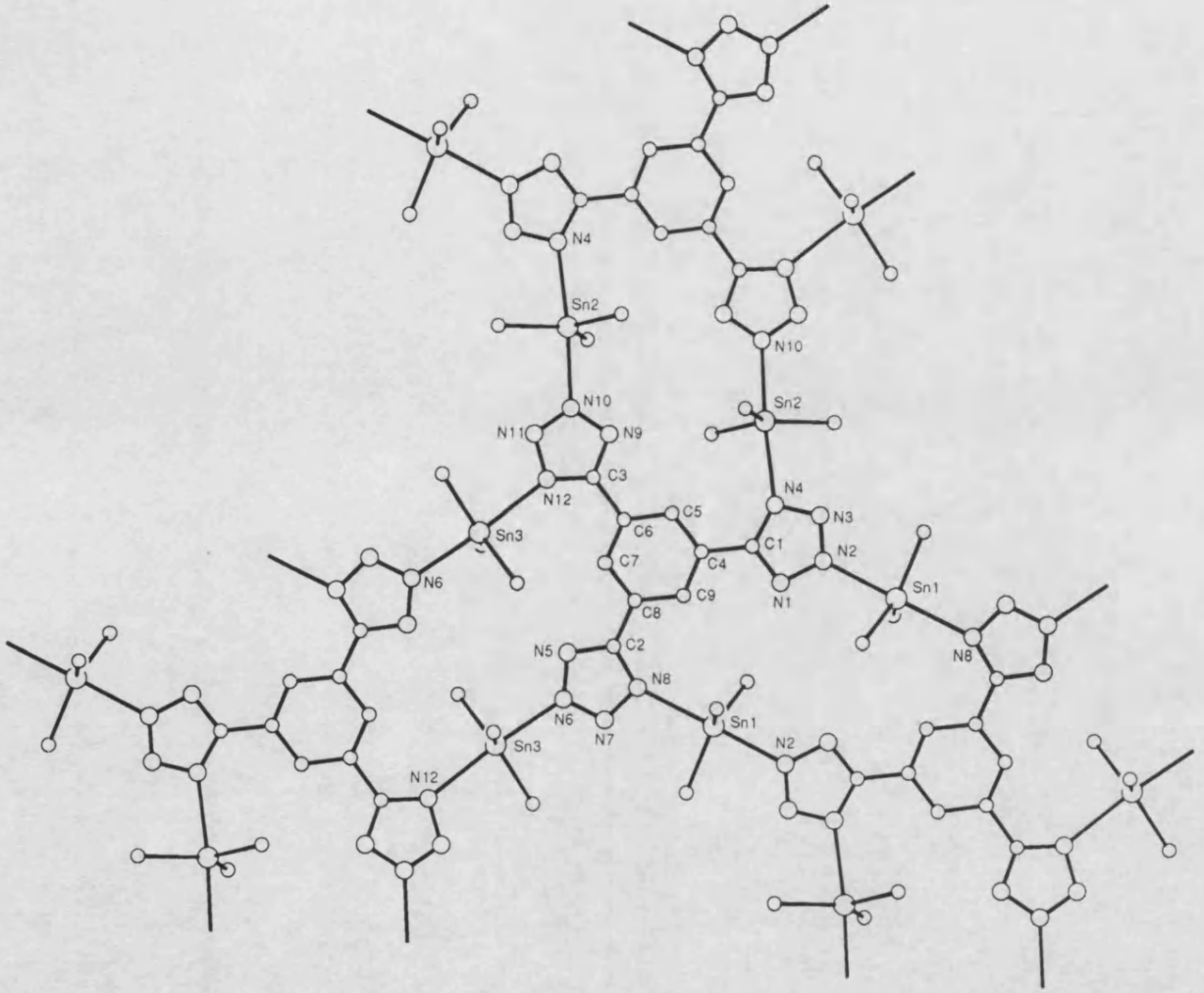

Figure 4.9: The 3-fold symettric tris-tetrazole ligand of **(52)**.

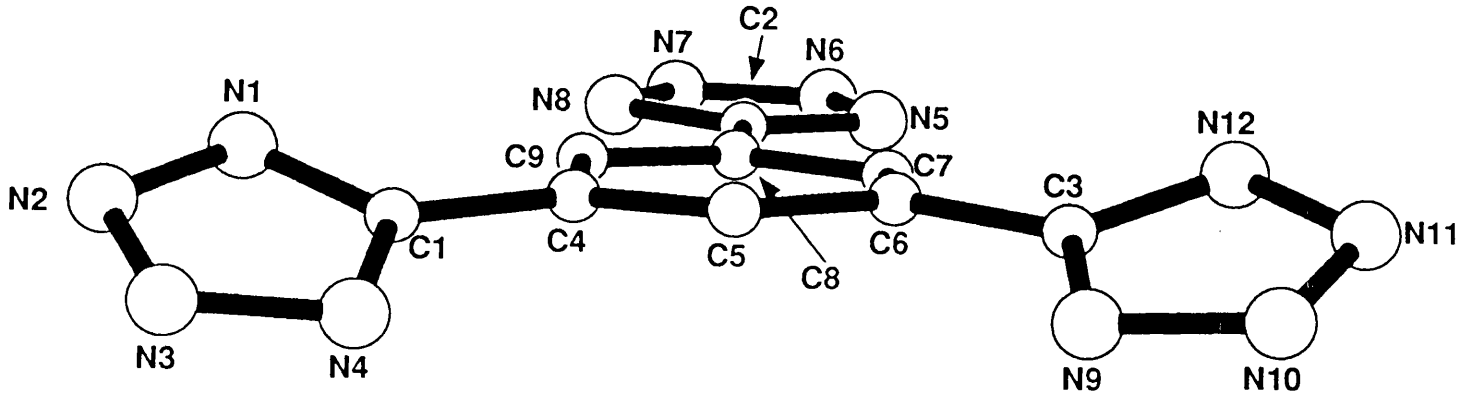

Figure 4.10: The tris-tetrazole ligand of **(52)** illustrating the coplanarity of the phenyl and C(2) tetrazole rings.

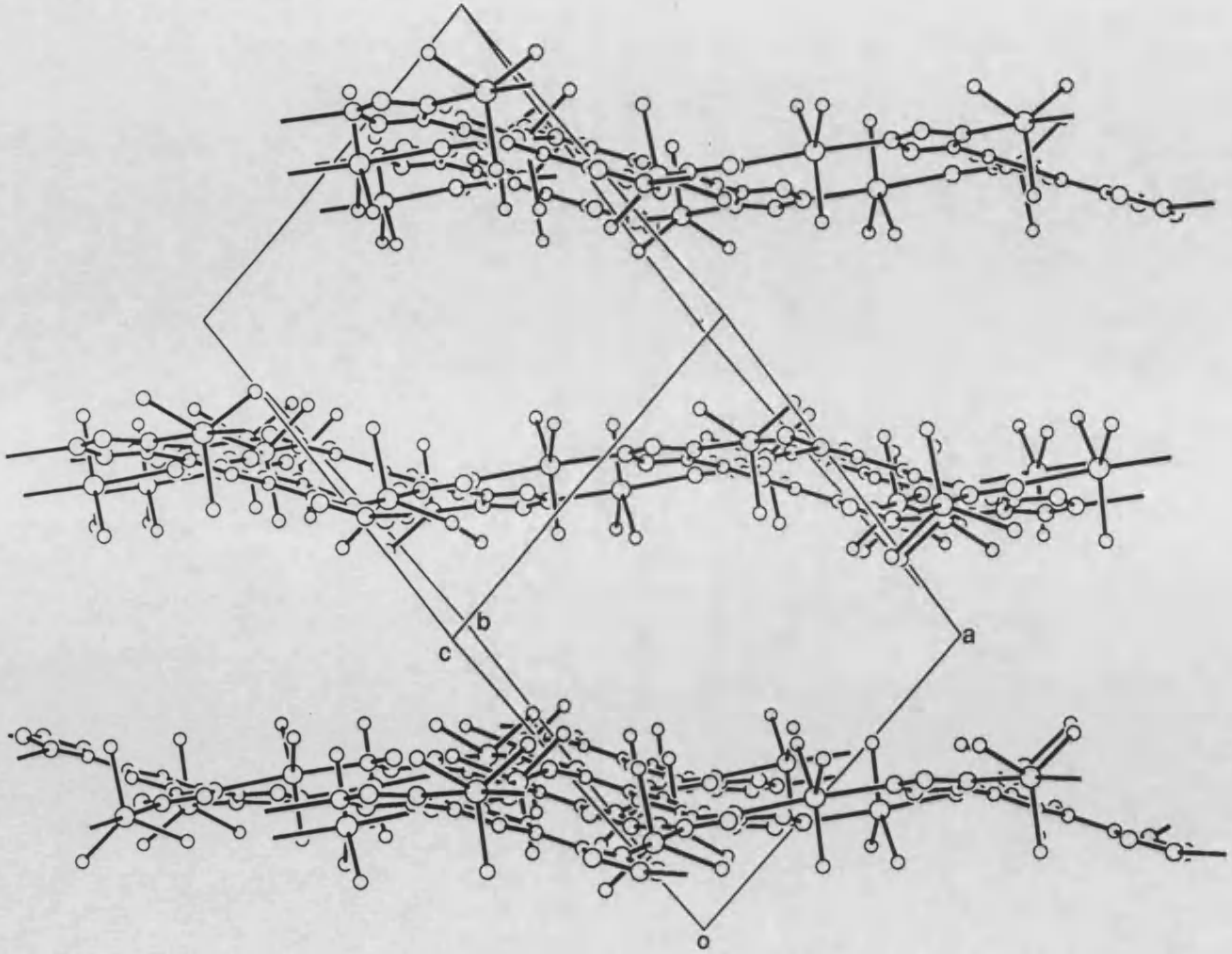

Figure 4.11: Side on view of the layer structure of **(52)**. α-butyl carbons only shown for clarity.

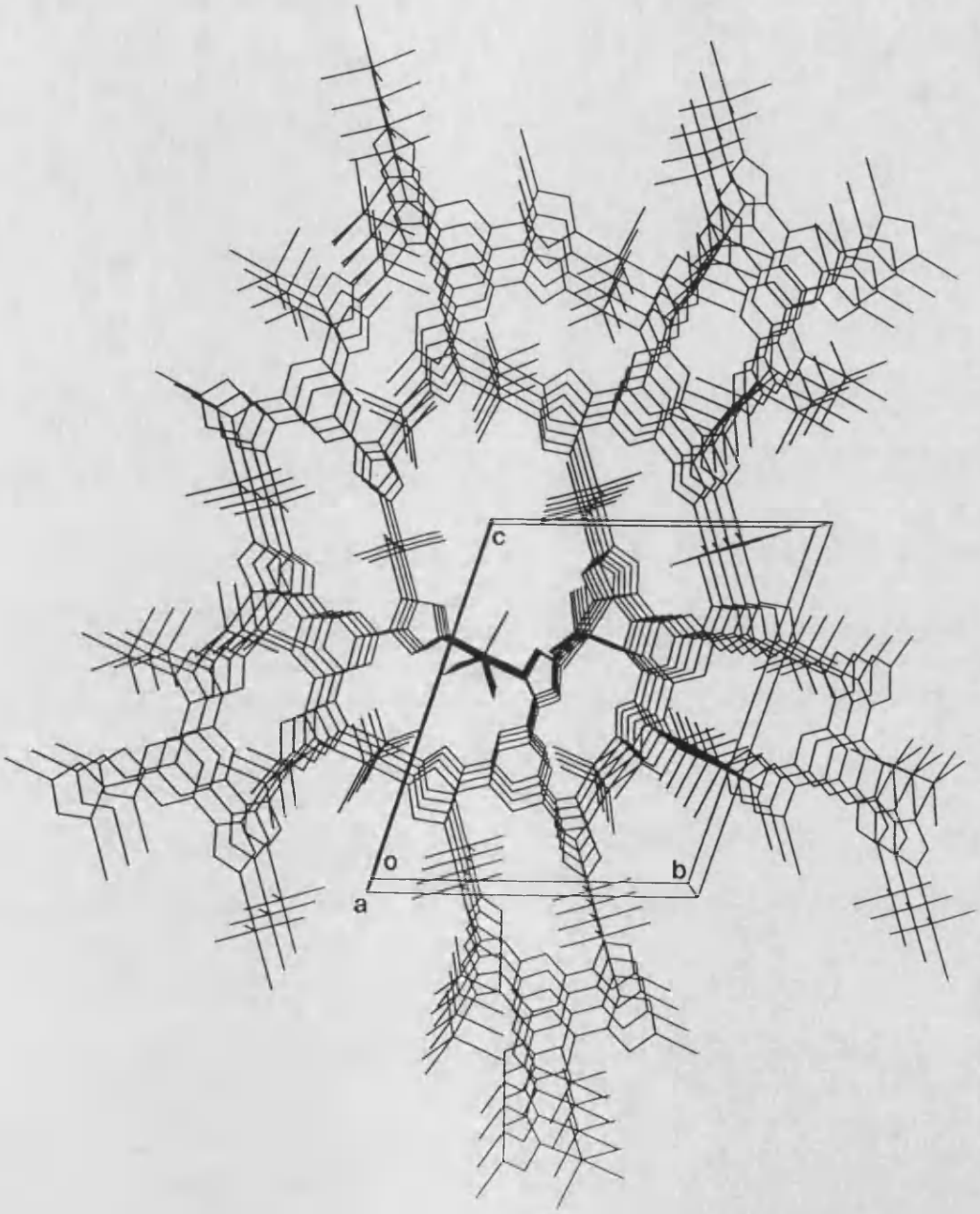

Figure 4.12: Perspective view of the arrayed layer structure of (**52**) looking down a hexagonal microchannel.

α-butyl carbon atoms only illustrated for clarity.

Table 4.5: Selected bond lengths (Å) of **(52)** and their estimated standard deviations in parentheses.

N(2)-Sn(1)	2.362(11)	N(8)-Sn(1)	2.452(11)
C(10)-Sn(1)	2.094(15)	C(14)-Sn(1)	2.144(16)
C(18)-Sn(1)	2.113(19)	N(4)-Sn(2)	2.469(12)
N(10)-Sn(2)	2.348(12)	C(22)-Sn(2)	2.130(15)
C(26)-Sn(2)	2.135(14)	C(30)-Sn(2)	2.150(3)
N(12)-Sn(3)	2.476(11)	C(34)-Sn(3)	2.145(15)
C(38)-Sn(3)	2.134(14)	C(42)-Sn(3)	2.146(16)
N(2)-N(1)	1.357(14)	C(1)-N(1)	1.323(15)
N(3)-N(2)	1.303(15)	N(4)-N(3)	1.338(14)
C(1)-N(4)	1.352(16)	N(6)-N(5)	1.346(14)
C(2)-N(5)	1.332(15)	N(7)-N(6)	1.332(14)
N(8)-N(7)	1.335(14)	C(2)-N(8)	1.373(15)
N(10)-N(9)	1.363(13)	C(3)-N(9)	1.323(15)
N(11)-N(10)	1.308(14)	N(12)-N(11)	1.355(14)
C(3)-N(12)	1.365(15)	C(4)-C(1)	1.483(16)

Table 4.6: Selected bond angles (°) for **(52)** and their estimated standard deviations in parentheses.

N(8)-Sn(1)-N(2)	178.3(4)	C(10)-Sn(1)-N(2)	87.5(5)
C(10)-Sn(1)-N(8)	94.2(5)	C(14)-Sn(1)-N(2)	87.4(6)
C(14)-Sn(1)-N(8)	91.8(5)	C(14)-Sn(1)-C(10)	118.7(7)
C(18)-Sn(1)-N(2)	87.1(6)	C(18)-Sn(1)-N(8)	92.1(6)
C(18)-Sn(1)-C(10)	120.2(7)	C(18)-Sn(1)-C(14)	120.4(7)
N(10)-Sn(2)-N(4)	174.8(3)	C(22)-Sn(2)-N(4)	89.6(5)
C(22)-Sn(2)-N(10)	89.1(5)	C(26)-Sn(2)-N(4)	94.0(5)
C(26)-Sn(2)-N(10)	91.0(5)	C(26)-Sn(2)-C(22)	118.8(6)
C(30)-Sn(2)-N(4)	89.2(8)	C(30)-Sn(2)-N(10)	88.0(8)
C(30)-Sn(2)-C(22)	134.1(6)	C(30)-Sn(2)-C(26)	107.1(7)
C(34)-Sn(3)-N(12)	89.2(5)	C(38)-Sn(3)-N(12)	94.4(5)
C(38)-Sn(3)-C(34)	115.6(6)	C(42)-Sn(3)-N(12)	87.4(6)
C(42)-Sn(3)-C(34)	123.8(6)	C(42)-Sn(3)-C(38)	120.6(6)
C(1)-N(1)-N(2)	101.8(10)	N(1)-N(2)-Sn(1)	125.5(8)
N(3)-N(2)-Sn(1)	121.9(8)	N(3)-N(2)-N(1)	112.6(10)
N(4)-N(3)-N(2)	107.8(10)	N(3)-N(4)-Sn(2)	110.8(8)
C(1)-N(4)-Sn(2)	144.5(7)	C(1)-N(4)-N(3)	104.7(10)

Table 4.6: continued.

C(2)-N(5)-N(6)	104.5(6)	N(7)-N(6)-N(5)	111.6(10)
N(8)-N(7)-N(6)	107.1(10)	N(7)-N(8)-Sn(1)	110.0(7)
C(2)-N(8)-Sn(1)	142.8(7)	C(2)-N(8)-N(7)	106.5(10)
C(3)-N(9)-N(10)	103.2(10)	N(9)-N(10)-Sn(2)	123.2(8)
N(11)-N(10)-Sn(2)	123.6(8)	N(11)-N(10)-N(9)	112.1(10)
C(3)-N(12)-Sn(3)	143.5(7)	C(3)-N(12)-N(11)	105.0(10)
N(4)-C(1)-N(1)	113.1(11)	C(4)-C(1)-N(1)	122.8(11)
C(4)-C(1)-N(4)	124.0(11)	N(12)-C(3)-N(9)	112.1(10)
C(5)-C(4)-C(1)	120.8(11)	C(9)-C(4)-C(1)	119.5(11)

4.6 Experimental

4.6.1 Synthesis of 1,3,5-triamidobenzene (45)

1,3,5 Benzenetricarbonyl trichloride (8.0g, 30 mmol) was stirred cautiously with aqueous concentrated ammonia solution (75 ml). Once the vigourous exothermic reaction had subsided, the resulting dense white precipitate was stirred at room temperature for a further two hours. The solid was then filtered, washed successively with ethanol and diethyl ether before drying for sixteen hours at 110°C. This yielded **(45)** (5.46g, 88%) as an amorphous white solid, insoluble in all available solvents.

Analysis: Found(Calc. for $C_9H_9N_3O_3$): C 50.2(52.2); H 4.20(4.34); N 18.6(20.2)%

IR [(cm^{-1}), nujol mull]: 3391, 3198, 1698, 1655, 1632, 1590, 1111, 633.

4.6.2 Synthesis of 1,3,5-tricyanobenzene (46)

(45) (4.6g, 22.2 mmol) was stirred in dimethylformamide (35 ml) and thionyl chloride (6 ml) added to the suspension over one hour, with the temperature maintained at 60°C. Stirring at this temperature was maintained for a further six hours, during which time complete dissolution occurred. The resulting solution was poured into dilute HCl (100 ml) to decompose unreacted $SOCl_2$ giving a dense white precipitate. This solid was collected by filtration,washed with water until neutral to litmus and dried at 120°C for fourteen hours. Crystallisation from ethanol and acetone yielded **(46)** as colourless needles (1.50g, 45%).

Analysis: Found(Calc. for $C_9H_3N_3$): C 70.4(70.6); H 1.90(1.96); N 27.4(27.5)%

^1H NMR [δ(ppm), DMSO-d^6 solution]: 8.80 [s,3H,*o*-C_6H_3].

^{13}C NMR [δ(ppm), DMSO-d^6 solution]: 114.1 [*C*N]; 115.9 [*i*-C_6H_3]; 140.4 [*o*-C_6H_3].

IR [(cm^{-1}), nujol mull]: 3083 υ_{asym}(CH), 2249 υ(CN), 1377, 911, 675.

4.6.3 Synthesis of Tris-[2-(5-trimethylstannyltetrazolyl)ethyl]nitromethane (47)

Trimethyltin azide (1.65g, 8.0 mmol) was heated neat under nitrogen with tris-(2-cyanoethyl)nitromethane (0.60g, 2.7 mmol) to 190°C for one hour resulting in a viscous brown oil which solidified on cooling. This was dissolved in methanol and filtered through activated charcoal to give a colourless solution. *In vacuo* removal of the solvent yielded **(47)** as a sticky colourless glass which was dried under vacuum (1.42g, 63%).

Analysis: Found(Calc. for $C_{19}H_{39}N_{13}O_2Sn_3$): C 27.7(27.2); H 4.78(4.60); N 20.5(21.7)%

^1H NMR [δ(ppm), DMSO-d^6 solution]: -0.17 [s,27H,CH_3]; 1.64-1.77 [m,6H,-CH_2CN$_4$]; 2.01-2.08 [m,6H,NO_2C(CH_2-)$_3$]; ^2J[C$^1H_3$-^{117}Sn] 66.5, 69.4 Hz.

^{13}C NMR [δ(ppm), DMSO-d^6 solution]: -0.3 [CH_3]; 19.6 [-CH_2CN$_4$]; 33.7 [NO_2C(CH_2-)$_3$]; 93.8 [NO_2C]; 160.6 [CN_4]; ^1J[$^{13}CH_3$-^{117}Sn] 507.4, 529.4 Hz.

^{119}Sn NMR [δ(ppm), DMSO-d^6 solution]: -49.0.

^{119m}Sn Mössbauer (mms^{-1}): I.S.=1.27; Q.S.=3.42.

4.6.4 Synthesis of Tris-[2-(5-triethylstannyltetrazolyl)ethyl]nitromethane (48)

(7) (6.0g, 24.2 mmol) and tris-(2-cyanoethyl)nitromethane (1.78g, 8.08 mmol) were heated neat under nitrogen to 170°C for one hour. The reactants set to a solid mass during this period and this was extracted with methanol in a soxhlet apparatus. Decolourisation with activated charcoal, followed by crystallisation at -20°C yielded **(48)** as colourless needles (3.2g, 42%) m.p. 235°C (dec).

Analysis: Found(Calc. for $C_{28}H_{57}N_{13}O_2Sn_3$): C 34.8(34.9); H 5.87(5.92); N 18.8(18.9)%

^1H NMR [δ(ppm), DMSO-d^6 solution]: 1.16 [t,27H,CH_3]; 1.25 [m,18H,CH_2-CH_3]; 2.50 [m,6H,CH_2CN$_4$]; 2.74 [,6H,NO_2C(CH_2-)$_3$].

^{13}C NMR [δ(ppm), DMSO-d^6 solution]: 10.1 [CH_2CH_3]; 10.2 [CH_2CH_3]; 19.6 [CH_2CN_4]; 33.6 [$NO_2C(CH_2\text{-})_3$]; 93.7 [NO_2C]; 161.1 [CN_4]; $^1J[^{13}CH_2CH_3\text{-}^{117,119}Sn]$ 474.3, 496.4 Hz.

^{119}Sn NMR [δ(ppm), DMSO-d^6 solution]: -50.1.

^{119m}Sn Mössbauer (mms^{-1}): I.S.=1.50; Q.S.=3.80.

IR [(cm^{-1}), KBr disk]: 2969, 2946, 2870, 1541, 1482, 1451, 1383, 684.

4.6.5 Synthesis of Tris-[2-(5-tributylstannyltetrazolyl)ethyl]nitromethane ***(49)***

A suspension of tris-(2-cyanoethyl)nitromethane (4.35g, 19.8 mmol) im tributyltin azide (20.14g, 60.9 mmol) was heated to 200°C under nitrogen for a period of two hours. This resulted in a solid off-white mass. Extended extraction with methanol in a soxhlet apparatus gave **(49)** as a microcrystalline solid (11.04g, 46%) m.p. 216°C (dec).

Analysis: Found(Calc. for $C_{46}H_{93}N_{13}O_2Sn_3$): C 45.3(45.4); H 7.86(7.65); N 15.0(15.0)%

^1H NMR [δ(ppm), DMSO-d^6 solution]: 0.80 [t,27H,-CH_3]; 1.19-1.32 [m,36H,-$CH_2CH_2CH_2CH_3$]; 1.50 [m,18H,$CH_2CH_2CH_2CH_3$]; 2.50 [m,6H,CH_2CN_4]; 2.75 [s,6H,$NO_2C(CH_2\text{-})_3$].

^{13}C NMR [δ(ppm), DMSO-d^6 solution]: 13.6 [-CH_3]; 18.2 [-$CH_2(CH_2)_2CH_3$]; 19.8 [-CH_2CN_4]; 26.4 [-$(CH_2)_2CH_2CH_3$]; 27.7 [-$CH_2CH_2CH_2CH_3$]; 33.7 [$NO_2C(CH_2\text{-})_3$]; 92.7 [NO_2C]; 160.6 [CN_4]; $^2J[\text{-}CH_2{}^{13}CH_2CH_2CH_3\text{-}^{117,119}Sn]$ 31.0 Hz (unresolved); $^3J[\text{-}(CH_2){}^{13}CH_2CH_3\text{-}^{117,119}Sn]$ 77.5 Hz (unresolved).

^{119}Sn NMR [δ(ppm), DMSO-d^6 solution]: -36.0.

^{119m}Sn Mössbauer (mms^{-1}): I.S.=1.42; Q.S.=3.61.

IR [(cm^{-1}), KBr disk]: 2959, 2924, 2872, 2855, 1549, 1477, 1464, 1402, 1377, 1358, 1225, 1140, 1080, 879, 700, 680.

*4.6.6 Synthesis of 1,3,5-phenylene-tris-5-(trimethylstannyl)tetrazole (**50**)*

(46) (0.58g, 3.8 mmol) and trimethyltin azide (2.34g, 11.4 mmol) were refluxed under nitrogen in *p*-xylene for one hour. The initial colourless solution became a suspensison as the reaction progressed. This was then cooled, filtered and washed with diethyl ether. Crystallisation from methanol gave **(50)** (2.21g, 70%) as a hexa-hydrate m.p. >240°C.

Analysis: Found(Calc. for $C_{18}H_{30}N_{12}Sn_3.6H_2O$): C 24.7(24.6); H 4.44(4.72); N 19.1(19.1)%

^{1}H NMR [δ(ppm), DMSO-d^6 solution]: 0.70 [s,27H,CH_3]; 3.60 [br.s,12H,H_2O]; 8.73 [s,3H,*o*-C$_6H_3$]; ^{2}J[C$^1H_3$-^{117,119}Sn] 69.1 Hz (unresolved).

^{13}C NMR [δ(ppm), DMSO-d^6 solution]: -0.2 [CH_3]; 124.3 [*o*-C_6H_3]; 131.0 [*i*-C_6H_3]; 162.0 [CN_4].

^{119}Sn NMR [δ(ppm), DMSO-d^6 solution]: -37.3.

^{119m}Sn Mössbauer (mms^{-1}): I.S.=1.34; Q.S.=3.70.

IR [(cm^{-1}),KBr disk]: 3638, 2999, 2918, 2791, 1638, 1418, 1217, 1163, 1010, 785, 750, 551, 461.

*4.6.7 Synthesis of 1,3,5-phenylene-tris-5-(triethylstannyl)tetrazole (**51**)*

(7) (2.0g, 8.07 mmol) and **(46)** (0.41g, 2.68 mmol) were refluxed in mesitylene under nitrogen for two hours. The resulting colourless suspension was filtered and washed with diethyl ether. Successive crystallisation from methanol and ethanol yielded **(51)** (1.24g, 52%) as colourless needles m.p. >240°C.

Analysis: Found(Calc. for $C_{27}H_{48}N_{12}Sn_3$): C 35.9(36.1); H 5.28(5.36); N 18.1(18.7)%

^{1}H NMR [δ(ppm), DMSO-d^6 solution]: 1.26 [t,27H,CH_2CH_3]; 1.37 [m,18H,CH_2CH_3]; 8.76 [s,3H,*o*-C$_6H_3$].

^{13}C NMR [δ(ppm), DMSO solution]: 7.8 [CH_2CH_3]; 10.3 [CH_2CH_3]; 124.1

[*o*-C_6H_3]; 131.0 [*i*-C_6H_3]; 162.0 [CN_4].

^{119}Sn NMR [δ(ppm), DMSO-d^6 solution]: -45.3.

^{119m}Sn Mössbauer (mms^{-1}): I.S.=1.52; Q.S.=3.93.

IR [(cm^{-1}), KBr disk]: 2975, 2950, 2923, 2870, 1456, 1412, 1325, 1217, 1024, 791, 749, 683, 526, 454.

4.6.8 Synthesis of 1,3,5-phenylene-tris-5-(tributylstannyl)tetrazole (52)

(46) (1.0g, 6.54 mmol) was heated under nitrogen as a suspension in tributyltin azide (6.50g, 19.6 mmol). Although the reaction mixture set to a white solid at 110°C heating was continued to 160°C at which point it was allowed to cool. The resulting white solid was crystallised by methanol extraction in a soxhlet to yield **(52)** as a colourless microcrystalline solid (4.8g, 65%) m.p. >240°C.

Analysis: Found(Calc. for $C_{45}H_{84}N_{12}Sn_3$): C 47.1(47.0); H 7.49(7.32); N 14.7(14.6)%

^{1}H NMR [δ(ppm), DMSO-d^6 solution]: 0.83 [t,27H,-CH_3]; 1.26-1.47 [m,36H,-CH_2CH$_2$CH_2CH$_3$]; 1.54-1.62 [m,18H,CH$_2$CH_2CH$_2$CH$_3$]; 8.73 [s,3H,*o*C$_6H_3$].

^{13}C NMR [δ(ppm), DMSO-d^6 solution]: 13.5 [-CH_3]; 18.3 [CH_2(CH$_2$)$_2$CH$_3$]; 26.3 [(CH$_2$)$_2$$CH_2CH_3$]; 27.7 [CH$_2$$CH_2CH_2CH_3$]; 124.0 [*o*-$C_6H_3$]; 131 0 [*i*-$C_6H_3$]; 162.0 [$CN_4$]; ^{1}J[^{13}$CH_2$(CH$_2$)$_2CH_3$-^{117,119}Sn] 461.1 Hz (unresolved); ^{2}J[CH$_2^{13}CH_2$CH$_2$CH$_3$-^{117,119}Sn] 29.4 Hz (unresolved); ^{3}J[(CH$_2$)$_2^{13}CH_2$CH$_3$-^{117,119}Sn] 75.3 Hz (unresolved).

^{119}Sn NMR [δ(ppm), DMSO-d^6 solution]: -49.9.

^{119m}Sn Mössbauer (mms^{-1}): I.S.=1.50; Q.S.=3.83.

IR [(cm^{-1}), KBr disk]: 2957, 2925, 2870, 2856, 1464, 1412, 1377, 1321, 1219, 1080, 880, 789, 748, 679, 455.

Chapter 5

The Synthesis and Characterisation of some C-triorganometallated (Metal = Sn, Si) Bis-heterocycles (Het. = thiophene, pyrazole)

5.1 Introduction

Chapter 2 reported the successful synthesis of several triorganotin-substituted bis-tetrazoles. Problems were encountered however when attempting coordination or linkage reactions in efforts to produce macrocyclic compounds. This was reasoned to be largely due to the ease with which cleavage of the N-bonded tin moiety occurred, either from the coordinating metal cation or the reacting electrophile. In view of these difficulties it was speculated that bis-heterocylic compounds bonded through carbon to tin (and also silicon) would provide a more controllable reaction centre, while still providing a directing site for macrocyclisation. Compounds substituted at carbon by tin have previously been employed in heteroatom-carbon bond-forming reactions, for example in the synthesis of phenyl-substituted borepins (Equation 5.1).[249,250] Carbon-carbon bonds have also been successfully

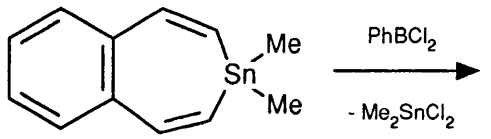

(Equation 5.1)

generated via palladium-catalysed coupling reactions with suitable organic halides.[251] Macrocycle formation, as described in Chapter 1, from C-substituted bis-heterocyles should thus be realisable by reaction with appropriate heterotom

electrophiles or organic di-halides. The synthetic strategy involved (with or without a templating metal) would subsequently be determined by the properties of the substituted bis-heterocycles. This chapter therefore sets out to describe the synthesis and characterisation of various triorganotin- and triorganosilicon C-substituted bis-thiophene and bis-pyrazole compounds which may be applied to this end.

The thiophene ring system is readily lithiated at the 2-position by reaction with n-butyl lithium in ether or tetrahydrofuran[252] and this generality applies for both substituted and unsubstituted derivatives. The resulting species can subsequently be quenched with a trialkylstannyl or trialkylsilyl halide to yield the corresponding 2-substituted tetralkyltin or tetralkylsilicon compound (e.g. Equation 5.2).[253] This reactivity extends to ring-substituted thiophenes,

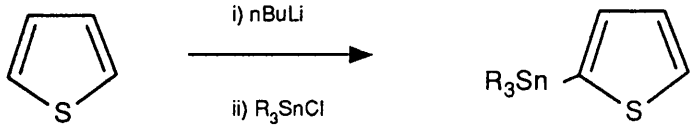

(Equation 5.2)

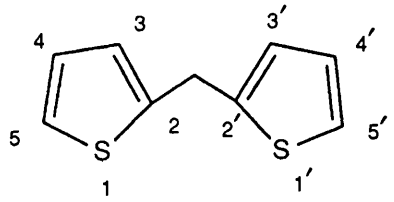

(53)

including the readily prepared dithienylmethane **(53)** shown below, (together with the numbering scheme used in subsequent discussion and spectral analysis). The room temperature lithiation of this compound with two equivalents of n-butyl lithium has been reported to result in the 5 and 5′ dimetallated species[161] can then be employed in reaction with the relevant triorganotin- or triorgano-silicon chloride to form the desired triorganometallated compound. Thiophene

compounds do not readily form coordination complexes[254] and it is reasonable that any macrocyclisation reaction would have to be in direct reaction with the bridging electrophile at high dilution. Macrocycles incorporating dithienylmethane units have previously been constructed along these lines via Schiff base condensation of aldehyde-substituted thiophene and aliphatic diamines.[255]

In contrast, pyrazole derivatives have a well established and wide-ranging coordination chemistry.[256] The C_3N_2 pyrazole ring is particularly difficult to cleave and derivatives have found wide-ranging use as pharmaceuticals and dyestuffs.[257] Studies of geminal bis-(pyrazol-1-yl)alkanes such as **(54)** and **(55)** indicate that lithiation with a single equivalent of n-butyl lithium at -78°C followed by reaction with an electrophile such as CH_3I or PhCOCl gives the ring-substituted product.[258] This is directed to the 5-position of the ring (using

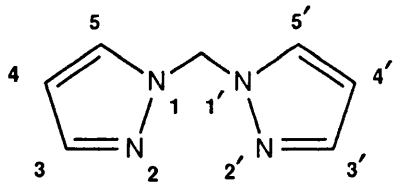

(54)

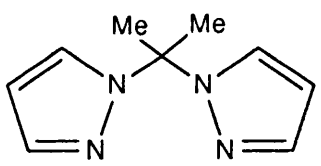

(55)

the numbering scheme shown) and contrasts with the analogous reaction at room temperature where substitution occurs at the bridgehead carbon.[258] The work reported here therefore seeks to assess and fully characterise the products of the low temperature bi-lithiation of **(54)** and **(55)** and their subsequent reaction with a variety of triorganotin and triorganosilicon chlorides.

5.2 Synthesis

Dithienylmethane (**53**) was synthesised via the condensation of thiophene and 1,3,5-trioxane employing 37% hydrochloric acid as catalyst (Equation 5.3).[259,260] This was isolated from the higher condensation products also produced by vacuum distillation as a colourless oil which crystallised on standing. The bis-pyrazolyl-substituted methane (**54**) was synthesised by the

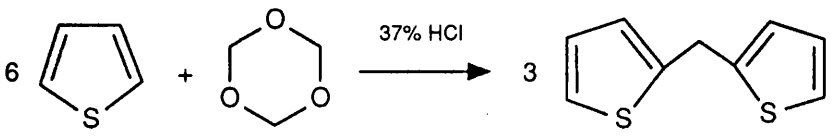

(Equation 5.3)

(53)

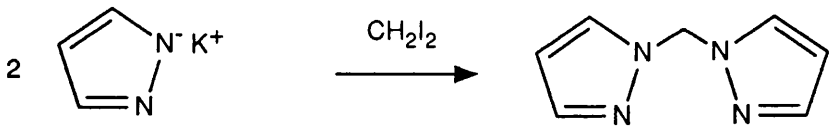

(Equation 5.4)

(54)

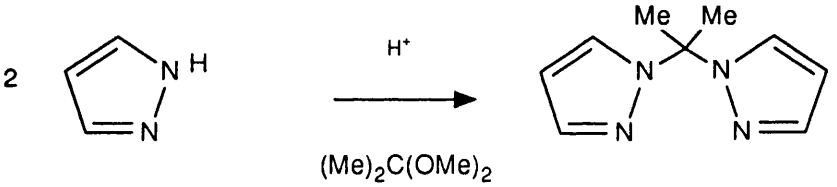

(Equation 5.5)

(55)

reaction of potassium pyrazolide and methylene iodide in THF solution (Equation 5.4).[261] The bis-pyrazole-substituted propane (**55**) meanwhile was synthesised by the acid-catalysed reaction of pyrazole and the acetal, 2,2-dimethoxy-propane, and purified by recrystallisation from heptane (Equation 5.5).[261]

Using standard dry, anaerobic conditions, (**53**) was lithiated at room temperature with 1.6M BuLi in diethyl ether. Under these conditions lithiation occurred at the 5 and 5′-positions, anion formation being apparent from the

formation of a dark brown solution. The appropriate triorganotin or triorgano-silicon chloride was then added dropwise to quench the di-lithio-bis-thiophene with a resulting precipitate of lithium chloride (Equation 5.6). After filtration the

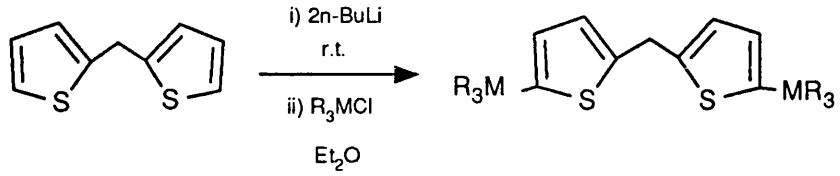

(Equation 5.6)

M = Sn; R = Bu **(56)**, Ph **(57)**

M = Si; R = Me **(58)**, Ph **(59)**

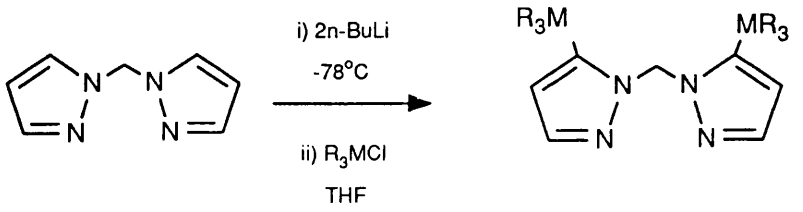

(Equation 5.7)

M = Sn; R = Me **(60)**, Bu **(61)**, Ph **(62)**

M = Si; R = Me **(63)**

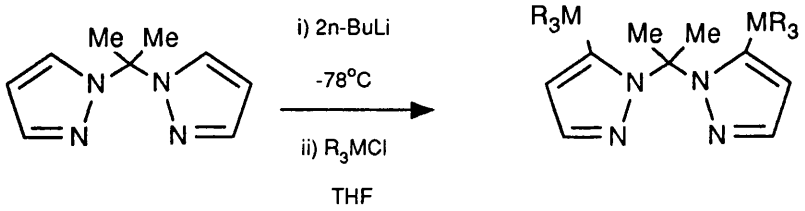

(Equation 5.8)

M = Sn; R = Me **(64)**

M = Si; R = Me **(65)**

crude products were purified either by vacuum distillation [**(56)** and **(58)**] to produce yellow moderately air stable oils, or by column chromatography [**(57)** and **(59)**] as amorphous pale yellow solids in moderate yield (30-40%). It was found that the analogous lithiation reactions performed in THF solution produced excessive charring and non-specific ring substitution, as evidenced by ^{119}Sn and ^{29}Si NMR spectra of the quenched products. Analytical and physical data for all

four compounds are presented in Table 5.1.

The bis-pyrazole compounds **(54)** and **(55)** were lithiated with 2 equivalents of 1.6M n-butyl-lithium in THF solution at -78°C, the appearance of a yellow solution and a yellow suspension, respectively, indicating that anion formation was complete. This was then quenched with a variety of triorganotin and triorganosilicon chlorides at 0°C to give in each case the 5,5′ ring substituted products **(60)**-**(65)** [as deduced from NMR data and the crystal structure of **(62)**, Section 5.4] (Equations 5.7 and 5.8). **(61)** and **(64)** were isolated by column chromatograpy on silica gel as moisture-sensitive, colourless oils while **(60)**, **(62)**, **(63)** and **(65)** were recrystallised in air to yield colourless, moderately air-stable crystalline materials in poor to fair yield (12-60%). Analytical and physical data are presented in Table 5.1. and full experimental and work-up details are included in Section 5.6.

Table 5.1: Physical and Analytical Data of C-triorganometallated Bis-thiophene and Bis-pyrazole Compounds

Compound	m.p/b.p. (°C)	C(%)[a]	H(%)	N(%)
(56)	190/1mm	52.3(52.3)	8.28(7.92)	-
(57)	-[c]	61.4(61.5)	4.35(4.33)	-
(58)[b]	180/0.5mm	56.6(55.6)	7.88(7.41)	-
(59)	-[c]	77.1(77.5)	5.37(5.17)	-
(60)	88	33.1(33.0)	5.21(5.11)	11.9(11.8)
(61)[b]	oil	50.2(51.3)	8.54(8.33)	7.7(7.7)
(62)	154	60.7(60.9)	4.26(4.26)	6.7(6.6)
(63)	82	53.0(53.4)	8.22(8.22)	19.1(19.2)
(64)[b]	oil	36.2(35.9)	5.94(5.58)	9.9(11.2)
(65)	58	56.6(56.3)	9.03(8.80)	17.6(17.5)

[a] Found(calc)

[b] Although care was taken to present the sample for analysis under anaerobic conditions, no special precautions were used during analysis to protect the sample from atmospheric moisture.

[c] Amorphous solid.

5.3 Spectroscopy

5.3.1 NMR Spectroscopy

The ^{1}H and ^{13}C NMR data of all the compounds **(53)**-**(65)** are consistent with the proposed structures. Thienyl compounds are known to undergo lithiation exclusively at the 2-position [5 and 5′-positions in the case of **(53)**] of the ring and this is confirmed by the disappearance of the C^5 and $C^{5'}$ proton resonance of the metallated bis-thiophenes. In common with other stannylated thiophene compounds, attachment of the triorganotin moiety in the cases of **(56)** and **(57)** is accompanied by a pronounced downfield shift of *ca.* 10 ppm. of the *ipso*-C^5 and *ortho*-C^4 ^{13}C signals while the *meta*-positioned methine C^3 and quaternary C^2 signals are left largely unaffected.[262,263] This phenomenon has been attributed to both resonance inductive effects[262] and more recently to pπ-dπ polarisation between the tin atom and the π-excessive thiophene ring.[263] Similar trends are noted for the silicon-substituted **(58)** and **(59)**. It is speculated that the larger downfield shifts of the triphenylsilyl-substituted **(59)** over the trimethylsilyl derivative **(58)** (10 ppm. vs. 7 ppm) are due to the enhanced possibility for resonance interaction with the thiophene ring provided by the phenyl substituents.

The $^{1}J(^{13}C,^{119}Sn)$ value obtained for the tributyltin-substituted bis-thiophene **(56)** of 356.9 Hz is typical of tetrahedral 4-coordinate geometry at tin. The semi-empirical equation of Holecek and Lycka[133] for the estimation of C-Sn-C bond angles in n-tributyltin compounds (Formula 1.6) gives a calculated value of 108.3° consistent with this structural assignment. The $^{2}J(o\text{-}^{13}C_6H_5\text{-}^{119}Sn)$ and $^{3}J(m\text{-}^{13}C_6H_5\text{-}^{119}Sn)$ values of 36.3 Hz and 56.2 Hz are consistent with other 4-coordinate tetra-aryltin compounds[263] confirming the tetrahedral nature of all these compounds. Similarly the ^{119}Sn chemical shifts in $CDCl_3$ solution [presented in Table 5.2(a)] are consistent with a 4-coordinate, near tetrahedral geometry at the metal. The resonances at -39.4 ppm for the

tributyltin derivative (**56**) and -137.4 ppm for the triphenyltin derivative (**57**) compare with the values reported for the similar tin environments in $(2\text{-}C_4H_3S)SnMe_3$ [$\delta(^{119}Sn)$ = -27.5 ppm][263] and $(2\text{-}C_4H_3S)SnPh_3$ [δ(ppm) = -135.5 ppm][125] and are both to considerably lower field than tetraorganotins which show enhanced coordination at tin e.g. the pseudo-octahedral bis-[3-(2-pyridyl)-2-thienylC-N]diphenyltin [$\delta(^{119}Sn)$ = -245.5 ppm].[65]

The ^1H and ^{13}C NMR spectra of the bis-pyrazolyl alkanes (**54**) and (**55**) are assigned following the work of Julia *et al.*[264] Lithiation and subsequent organometallation in the cases of (**60**)-(**65**) is observed to occur at the 5 and 5′ positions as would be expected from the work of Karitsky *et al.*[257] This is confirmed by the disappearance of the signals at 7.61 ppm and 7.37 ppm in the proton spectra of (**54**) and (**55**) respectively and the collapse of the doublet of doublets splitting pattern attributed to the 4 and 4′ protons at *ca.* 6.2 ppm to a simple doublet. This is confirmed by the crystallographic analysis of (**62**) reported in Section 5.4. As was noted in the case of the bis-thiophene compounds (**56**) and (**57**) the presence of the ring-bonded tin causes some interesting variations in chemical shift of the pyrazole ring carbons. The *ipso*- and *ortho*-carbon atom signals (C^5 and C^4 respectively) are deshielded by *ca.* 10 ppm compared to the parent bis-pyrazole, while the signal due to the *meta*-positioned C^3 is affected much less, experiencing a minor shielding of 0.5-1.0 ppm. The ^1H chemical shifts of the H^4 and H^3 protons are left largely unaffected.

Four-coordinate tetrahedral trimethyltin compounds generally have $^2J(^1H,^{119}Sn)$ values of less than 59 Hz. Accordingly the $^2J(^1H,^{119}Sn)$ values recorded for the bis-pyrazolyl trimethyltin derivatives (**60**) and (**64**) are 55.7 Hz and 57.3 Hz yielding calculated bond angles of 109.8° and 110.6° respectively (Formula 1.4). The free N^2 and $N^{2'}$ pyrazole atoms therefore take part in no inter- or intramolecular coordinative interactions in $CDCl_3$ solution. The $^1J(^{13}C,^{119}Sn)$ values for (**60**) and (**64**) of 382.3 Hz and 366.8 Hz respectively are

also typical of 4-coordinate trimethyltin C-substituted heterocyclic compounds, as is the corresponding constant for the triphenyltin derivative (**62**) of 587.6 Hz.[128] This latter assignment is unequivocably confirmed by the crystallographic study reported in Section 5.4.

The ^{119}Sn NMR data of (**60**)-(**62**) and (**64**) are presented in Table 5.2(a) where the recorded chemical shifts are seen to be similar to those of the corresponding substituted bis-thiophenes. The tributyltin and triphenyltin-substituted bis-pyrazoles (**61**) and (**62**) are observed to have slightly higher field shifts than the analogous bis-thiophene compounds (**56**) and (**57**) (-162.5 ppm vs. -137.4 ppm and -47.1 ppm vs. -39.4 ppm). This can be attributed to differences in the electronic effect of the respective ring heteroatom(s) on the overall electron density at tin and the data therefore again indicate tetrahedraral coordination with no additional interactions through the free pyrazole N^2 and $N^{2'}$ atoms.

5.3.2 ^{119m}Sn Mössbauer Spectroscopy

The ^{119}Sn Mössbauer data for the tetraorganotin compounds are presented in Table 5.2(a). All the compounds except for (**57**) yielded partially resolved spectra with quadrupole splitting values ranging from 0.62 mms^{-1} to 1.00 mms^{-1}. Such splittings are unusual for R_4Sn compounds for which differences in Sn-C bond polarities are often too small to generate an electric field gradient at the tin nucleus. That no resolvable splitting was apparent for the triphenyltin-substituted (**57**) however, is to be expected given that similar spectra have previously been noted in numerous comparable cases such as (2-C_4H_3S)$SnPh_3$[125] and (3-$C_4H_3S)_2$-Sn(*p*-tolyl)$_2$.[57] Small diffferences in bond polarities have been proposed to account for the similar small splittings (Q.S. = 0.80-1.20 mms^{-1}) observed for Ph_3SnBox, Ph_3SnBtz and Bu_3SnBtz (Box = 2-benzoxazole; Btz = 2-benzothiazole). The tetrahedral geometry at tin in these cases was confirmed by an x-ray crystallographic study of Ph_3SnBtz.[33] 3-Pyridyl-substitiuted thienyl

Table 5.2(a): ^{119}Sn NMR[a] andMössbauer[b] Studies of C-organotin-substituted Bis-heterocycles

Compound	$\delta(^{119}Sn)$[c]	(δ)	ΔEq	Γ_1	Γ_2[d]
(56)	-39.4	1.21	0.61	1.17[e]	1.17[e]
(57)	-137.4	1.16	0.00	1.05	-
(60)	-47.1	1.20	0.81	0.99[e]	1.05[e]
(61)	-58.9	1.31	1.00	0.86	0.89
(62)	-162.5	1.23	0.62	0.91	0.90
(64)	-35.7	1.22	0.93	1.18[e]	1.17[e]

[a] All spectra run as $CDCl_3$ solutions at 25°C.

[b] Mössbauer data recorded at 78K and data given in mms^{-1}.

[c] Values given in ppm.

[d] Refers to full width at half height of the high and low velocity components in mms^{-1}.

[e] Some decompoosition of sample prior to analysis.

Table 5.2(b): ^{29}Si NMR[a] Studies of C-triorganosilyl-substituted Bis-heterocycles

Compound	**(58)**	**(59)**	**(63)**	**(65)**
$\delta(^{29}Si)$	-6.8	-19.2	-9.0	-9.9

[a] All spectra run as $CDCl_3$ solutions at 25°C. Chemical shifts in ppm.

tetraorganotin compounds also produce similar partially resolved Mössbauer spectra[65] (Q.S. = 0.57-0.96 mms^{-1}). In these cases it has been unambiguously demonstrated by x-ray analysis that the pyridyl nitrogen acts as a donor atom resulting in an increase in coordination number to five- and six-coordinate species. In the light of these results the Mössbauer data of Table 5.2(a), taken in isolation, are somewhat ambiguous given the availability of the ring heteroatoms for some form of coordinative linkage. This problem is conclusively resolved by the crystallographic study of **(62)** described in Section 5.4 which reveals purely 4-coordinate tin and that the former of the two possibilities prevails.

Following the work of Molloy *et al.*[33] therefore, the magnitudes of the observed quadrupole splittings can be taken to reflect the polarity imbalance in the Sn-C bonds. This allows the relative polarities of the Sn-R bonds to be estimated as: R = Me, Bu < Ph, thiophene < pyrazole < Box, Btz.

The observed isomer shifts can also be accounted for by employing a similar rationale since the observed value δ reflects the *s*-electron density at tin. This in turn depends on the electronegativity of the attached ligands. From the above ordering it might be expected that for common R_3Sn groups (i.e. Ph or Bu) the compounds containing pyrazole-substituted tin would have lower isomer shifts than the corresponding thiophene-bonded compounds. That the reverse is true however has previously been rationalised[33] by suggesting that the sp^3 hybrid orbital bonded to the heterocyclic ligand is richer in *p*-character than those involved in bonding to the other three R groups. In rehybridising in this manner the *s*-density is concentrated in the less polar Sn-C bonds affording tin a greater share of the electron density.

5.4 The Crystal Structure of methylene-bis-[1,1'-(5,5'-triphenylstannyl)pyrazole] (62)

Suitable crystals for x-ray study were obtained by recrystallisation from a chloroform/ether solution. Full details of the crystallographic analysis are presented in Appendix X along with tables of atomic coordinates and isotropic thermal parameters. The asymmetric unit is displayed in Figure 5.1 along with the atomic numbering scheme and selected bond lengths and bond angles are presented in Tables 5.3 and 5.4 respectively.

Examination of Figure 5.2 confirms the C^5 and $C^{5'}$ [C(3) and C(5)] positions as the points of lithiation and subsequent substitution. The tin-substituted C(3) and C(5) atoms of the pyrazole rings are positioned in an essentially *trans*- configuration with respect to the bridging methylene carbon C(4) so as to minimise steric interactions between the large triphenyltin groups. The two unique tin sites show the expected tetrahedral geometry, although in both cases the bond angles are somewhat distorted from a perfectly regular 109° varying between 103.4(2)° and 120.6(2)° for Sn(1) and 101.5(2)° and 115.9(2)° for Sn(2). Similar distortions in the structure of triphenyltin benzothiazole have been employed to rationalise the the observed reactivity and Mössbauer quadrupole splittings based upon the observation that the angles involving the heterocycle carbon were in each case smaller [*ca.* 104-108°] than those involving only the phenyl groups.[33] Examination of Table 5.4 however reveals that this is not the case for **(62)**. Rather the distortions are induced by the presence of the non-bonded pyrazole ring adjacent to each tin site and its steric interaction with the tin-bonded phenyl groups. Although it is also apparent from Figure 5.2 that the free pyrazole ring atoms N(3) and N(1) are oriented towards the Sn(1) and Sn(2) sites respectively, the non-bonded Sn(1)-N(3) and Sn(2)-N(1) distances of 4.13Å and 3.46Å are rather long and make it unlikely that any residual Sn-N interaction affects the overall disposition of the molecule.

In contrast to the bond angle data, the eight Sn-C bond lengths are identical within experimental error and closely compare to the bond lengths determined for the similar tin environments presented by Ph_3SnBtz (2.16Å),[33] and tetrakis-(2-thienyl)tin (2.15Å).[30]

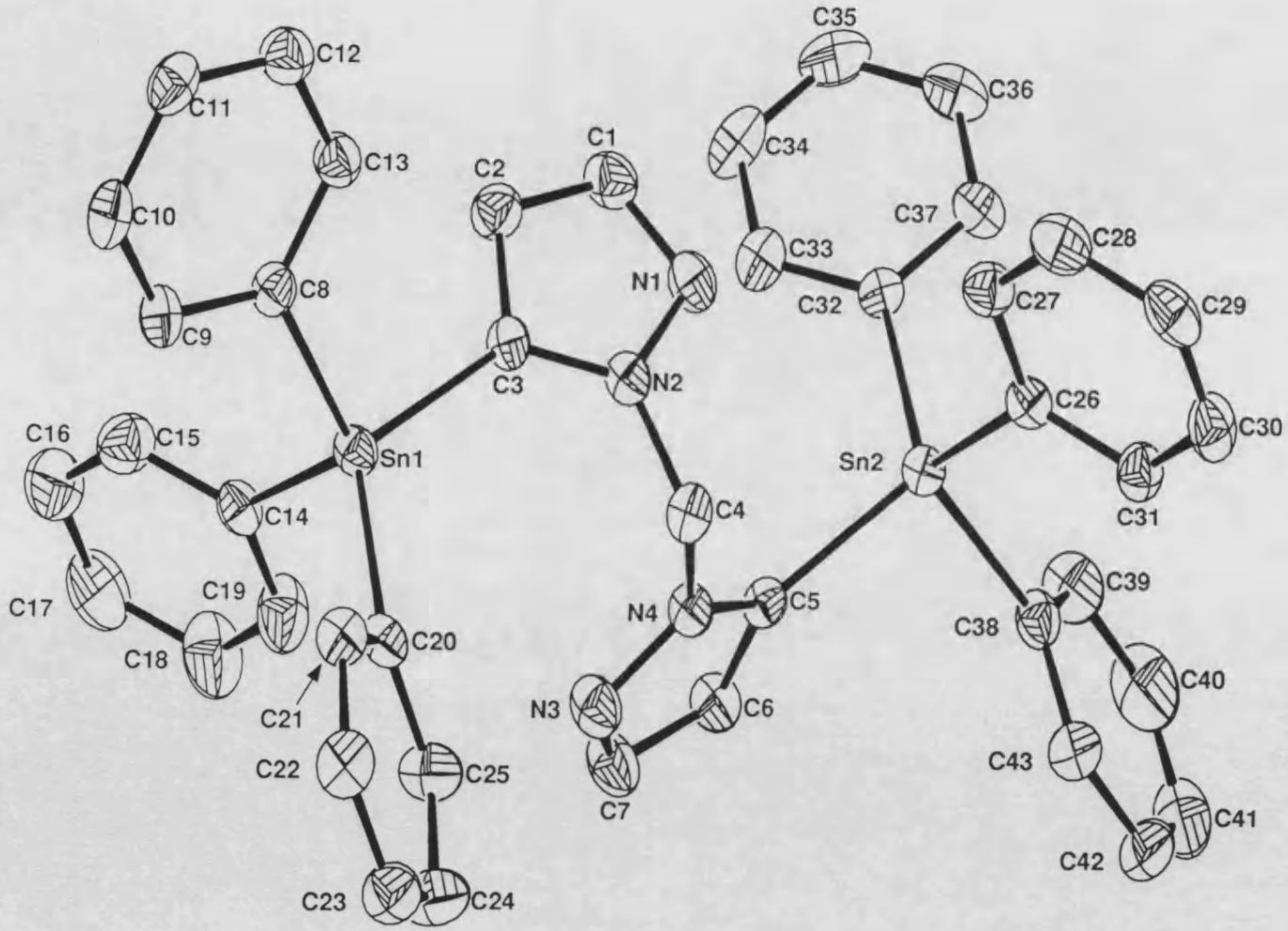

Figure 5.1: The asymmetric unit of methylene-bis-[1,1-(5,5′-triphenylstannyl)pyrazole] **(62)**.

Table 5.3: Selected bond lengths for compound **(62)** with their estimated standard deviations in parentheses.

C(3)-Sn(1)	2.136(5)	C(8)-Sn(1)	2.152(4)
C(14)-Sn(1)	2.142(5)	C(20)-Sn(1)	2.151(4)
C(5)-Sn(2)	2.140(5)	C(26)-Sn(2)	2.155(4)
C(32)-Sn(2)	2.136(4)	C(38)-Sn(2)	2.152(5)

Table 5.4: Selected bond angles for compound **(62)** with their estimated standard deviations in parentheses.

C(8)-Sn(1)-C(3)	104.5(2)	C(14)-Sn(1)-C(3)	103.4(2)
C(14)-Sn(1)-C(8)	112.3(2)	C(20)-Sn(1)-C(3)	120.6(2)
C(20)-Sn(1)-C(8)	107.0(2)	C(20)-Sn(1)-C(14)	109.0(2)
C(26)-Sn(2)-C(5)	115.9(2)	C(32)-Sn(2)-C(5)	111.7(2)
C(32)-Sn(2)-C(26)	111.6(2)	C(38)-Sn(2)-C(5)	101.5(2)
C(38)-Sn(2)-C(26)	107.4(2)	C(38)-Sn(2)-C(32)	107.8(2)
N(2)-C(3)-Sn(1)	132.9(3)	C(3)-C(3)-Sn(1)	122.3(4)
N(4)-C(5)-Sn(2)	130.8(3)	C(6)-C(5)-Sn(2)	124.6(4)

5.5 Reaction Chemistry

Of the ten C-triorganometallated bis-heterocycles synthesised it was noted that in general those compounds isolated as oils at ambient temperatures [**(56)**, **(58)**, **(61)** and **(64)**] exhibited a lower degree of air/moisture stability than the remaining crystalline or amorphous solids. In common with other C-organometallated heterocycles[33] however, all the compounds are attacked by atmospheric H_2O and do not exhibit indefinite stability if exposed to the open atmosphere. This degradation eventually leads to the free bis-heterocyle and the corresponding organotin or organosilicon oxide (Equations 5.9-5.11).

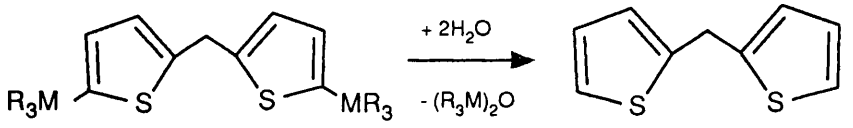

(Equation 5.9)

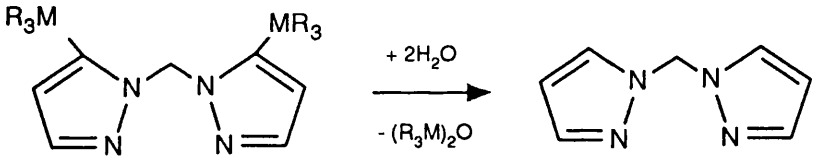

(Equation 5.10)

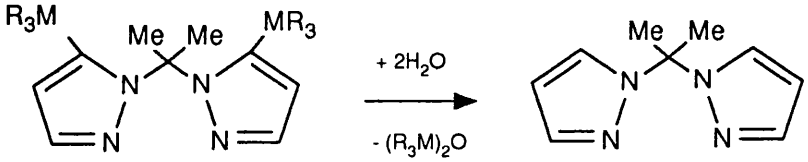

(Equation 5.11)

(M = Sn, Si; R = Me, Bu, Ph)

Following the B-C bond-forming methodology of Equation 5.1, the direct synthesis of a boron-linked tetra-thiophene macrocycle was attempted by the reaction of both the tributyltin- and triphenyltin-substituted **(56)** and **(57)** with

$PhBCl_2$ in THF solution (Equation 5.12). Both reactions yielded an identical product, a fluffy crystalline solid readily soluble in hydrocarbon solvents, and a stoichiometric amount of the expected triorganotin chloride. Although micro-

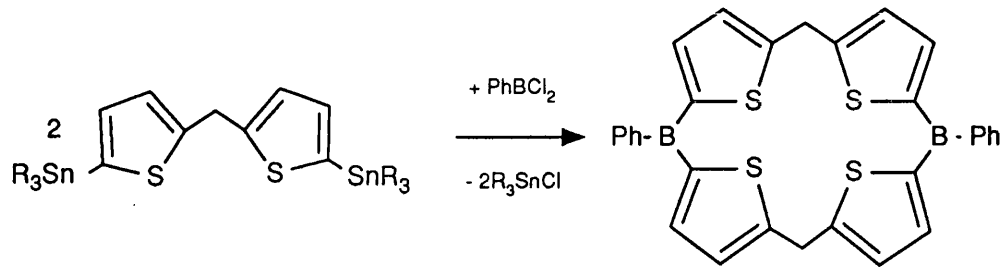

(R = Bu, Ph)

(Equation 5.12)

analysis in both cases was consistent with the expected product, the collected NMR data was somewhat confusing. In both the ^{1}H and ^{13}C spectra the resonances associated with the bis-thiophene units were somewhat obscured by the more intense phenyl absorbtions or indeed entirely absent. The reasons for this are unclear and although both products give internally consistent ^{11}B NMR spectra (*ca.* +27 ppm), complete structural elucidation requires further study.

5.6 Experimental

5.6.1 Synthesis of dithienylmethane (53)

Thiophene (20.2g, 24.0 mmol) was stirred at room temperature with 1,3,5-trioxane (3.6g, 4.0 mmol). 37% HCl (20 ml) was added to this and stirring continued for a further twenty four hours resulting in a dark brown oil which was extracted and separated from the aqueous layer with diethyl ether (80 ml) to produce a brown ethereal solution. This was washed consecutively with dilute sodium carbonate solution and distilled water before being dried over magnesium sulphate. *In vacuo* removal of the ether yielded a brown oil which was distilled at reduced pressure to give a single fraction **(53)** as a colourless oil which crystallised on exposure to the atmosphere (10.6g, 48%) b.p. 120°C/0.05mmHg.

Analysis: Found(Calc. for $C_9H_8S_2$): C 59.9(60.0); H 4.44(4.45)%

^{1}H NMR [δ(ppm), $CDCl_3$ solution]: 4.32 [s,2H,-CH_2-]; 6.85 [m,2H,5+5′-C_4H_3S]; 6.91 [t,2H,4+4′-C_4H_3S]; 7.13 [dd,2H,3+3′-C_4H_3S].

^{13}C NMR [δ(ppm), $CDCl_3$ solution]: 30.1 [-CH_2-]; 124.1 [5+5′-C_4H_3S]; 125.2 [4+4′-C_4H_3S]; 126.8 [3+3′-C_4H_3S]; 143.1 [*i*-C_4H_3S].

5.6.2 Synthesis of methylene-bis-(1,1′-pyrazole) (54)

A solution of pyrazole (7.5g, 110.0 mmol) in THF (100 ml) was added dropwise to potassium metal (3.9g, 100.0 mmol) stirred under nitrogen in THF (200 ml). The reaction mixture was stirred and refluxed for four hours resulting in a fine white suspension. Methylene iodide (13.4g, 50.0 mmol) in THF (20 ml) was then added and the reaction refluxed and stirred for a further three hours and twenty four hours respectively. This white suspension was then filtered and the colourless filtrate evaporated to produce a yellow oil. Trituration with heptane gave a cream-coloured solid which after several recrystallisations from heptane yielded **(54)** as white needles (4.12g, 51%) m.p. 108°C.

Analysis: Found(Calc. for $C_7H_8N_4$): C 56.7(56.5); H 5.44(5.26); N 37.7(37.8)%

^{1}H NMR [δ(ppm), $CDCl_3$ solution]: 6.23 [dd,2H,4+4′-$C_3H_3N_2$]; 6.25 [s,2H,-CH_2-]; 7.50 [d,2H,3+3′-$C_3H_3N_2$]; 7.60 [d,2H,5+5′-$C_3H_3N_2$].

^{13}C NMR [δ(ppm), $CDCl_3$ solution]: 65.0 [-CH_2-]; 106.9 [4+4′-$C_3H_3N_2$]; 129.5 [5+5′-$C_3H_3N_2$]; 140.6 [3+3′-$C_3H_3N_2$].

IR [(cm^{-1}), KBr disk]: 3129, 3107, 1514, 1435, 1375, 1291, 1271, 1205, 1093, 1051, 951, 783, 763, 720, 653, 613.

5.6.3 Synthesis of 2,2′-isopropylidene-bis-(1,1′-pyrazole) (55)

A mixture of pyrazole (13.6g, 200.0 mmol) and 2,2-dimethoxy-propane (10.4g, 100 mmol) was heated with *p*-toluenesulphonic acid (0.1g, 0.6 mmol) so that methanol distilled out slowly. After *ca.* 8 ml (200 mmol) had been collected, the melt was poured into cold heptane (40 ml) and cooled. Recrysallisation of the resulting solid three times from heptane yielded **(55)** as a crystalline solid (8.2g, 47%) m.p. 82°C.

Analysis: Found(Calc. for $C_9H_{12}N_4$) C 60.8(61.3); H 6.03(6.86); N 31.4(31.7)%

^{1}H NMR [δ(ppm), $CDCl_3$ solution]: 2.24 [s,6H,-CH_3]; 6.21 [dd,2H,4+4′$C_3H_3N_2$]; 7.37 [d,2H,5+5′-$C_3H_3N_2$]; 7.54 [d,2H,3+3′-$C_3H_3N_2$].

^{13}C NMR [δ(ppm), $CDCl_3$ solution]: 27.8 [-CH_3-]; 106.0 [4+4′-$C_3H_3N_2$]; 126.8 [5+5′-$C_3H_3N_2$]; 133.4 [$C(CH_3)_2$]; 139.4 [3+3′-$C_3H_3N_2$].

IR [(cm^{-1}), KBr disk]: 3112, 2998, 1510, 1422, 1387, 1313, 1259, 1210, 1169, 1148, 1097, 1082, 1045, 955, 770, 706, 686, 653, 632.

5.6.4 Synthesis of methylene-bis-[5,5′-(2,2′-tributylstannyl)thiophene] (56)

(53) (2.2g 12 mmol) was stirred in diethyl ether (80 ml) under nitrogen. 1.6M BuLi in hexane (17ml, 27 mmol) was added over a period of 30 minutes at room temperature causing the formation of a dark brown solution. After stirring for a further one hour, tributyltin chloride (8.0g, 24.5 mmol) in diethyl ether (20 ml) was added dropwise resulting in a light brown suspension. This was stirred

for a further two hours before filtration under nitrogen to yield a dark brown oil. Distillation on a Kühgelrohr apparatus gave two fractions, unreacted tributyltin chloride (0.74g) and **(56)** as a colourless oil (accompanied by a large amount of thermal depomposition) (3.1g, 33%) b.p. 190-200°C/1mmHg.

Analysis: Found(Calc. for $C_{33}H_{60}S_2Sn_2$) C 52.3(52.3); H 8.21(7.92)%

^{1}H NMR [δ(ppm), $CDCl_3$ solution]: 0.91 [m,18H,-C*H*$_3$]; 1.12 [m,12H,-C*H*$_2$-$CH_2)_2CH_3$]; 1.34 [m,12H,-$(CH_2)_2$C*H*$_2$$CH_3$]; 1.62 [m,12H,-$CH_2$C*H*$_2$$CH_2CH_3$]; 5.30 [s,2H,-C*H*$_2$-]; 7.21-7.30 [m,2H,4+4′-C_4*H*$_2$S]; 7.66 [d,2H,3+3′-C_4*H*$_2$S]; ^{3}J[3+3′-C_4^{1}*H*$_2$S-^{117,119}Sn] 14.8 Hz (unresolved).

^{13}C NMR [δ(ppm), $CDCl_3$ solution]: 10.8 [-*C*$H_2(CH_2)_2CH_3$]; 13.6 [-*C*H_3]; 27.2 [-$(CH_2)_2$*C*H_2CH_3]; 28.9 [-CH_2*C*$H_2CH_2CH_3$]; 30.1 [-*C*H_2-]; 127.8 [3+3′-*C*$_4H_2$S]; 135.1 [4+4′-*C*$_4H_2$S]; 135.2 [Sn-5+5′-*C*$_4H_2$S]; 148.9 [*i*-*C*$_4H_2$S]; ^{1}J[-^{13}*C*$H_2(CH_2)_2CH_3$-^{117,119}Sn]; 344.5, 356.9 Hz; ^{2}J[-CH_2^{13}*C*$H_2CH_2CH_3$-^{117,119}Sn] 20.9 Hz (unresolved); ^{3}J[-(CH_2)^{13}*C*H_2CH_3-^{117,119}Sn] 47.4 Hz (unresolved).

^{119}Sn NMR [δ(ppm), $CDCl_3$ solution]: -39.4.

^{119m}Mössbauer (mms^{-1}): I.S.=1.21; Q.S.=0.61.

IR [(cm^{-1}), liq. film]: 2959, 2926, 2872, 1464,1418, 1377, 1340, 1211, 1074, 961, 939, 875, 769, 698, 594.

5.6.5 Synthesis of methylene-bis-[5,5′-(2,2′-triphenylstannyl)thiophene] (57)

(53) (2.0g, 11.1 mmol) was stirred in diethyl ether (80 ml) under nitrogen. 1.6M BuLi in hexanes (15ml, 24 mmol) was added at room temperature over a period of one hour resulting in a dark brown solution. To this was then added triphenyltin chloride (8.5g, 22.0 mmol) in diethyl ether (80 ml) giving a brown suspension which was stirred for a further two hours. This was then filtered and the solvent evaporated giving a sticky dark brown mass. Flash chromatagraphy on silica gel using a gradient of hexane to CH_2Cl_2 yielded **(57)** as a pale yellow

amorphous solid (3.8g, 40%).

Analysis: Found(Calc. for $C_{45}H_{36}S_2Sn_2$) C 61.4(61.5); H 4.35(4.15)%

^{1}H NMR [d(ppm), $CDCl_3$ solution]: 4.35 [-CH_2-]; 7.23-7.60 [m,34H,*o,m,p*-C$_6H_5$,4+4′,3+3′-C$_4H_2$S].

^{13}C NMR [δ(ppm), $CDCl_3$ solution]:: 30.2 [-CH_2-]; 128.6 [3+3′-C_4H_2S]; 128.7 [*m*-C_6H_5]; 129.3 [*p*-C_6H_5]; 131.5 [Sn-5+5′-C_4H_3S]; 137.0 [*o*-C_6H_5]; 137.5 [*i*-C_6H_5]; 137.6 [4+4′-C_4H_2S]; 150.0 [*i*-C_4C_2S]; ^{2}J[*o*-$^{13}C_6H_5$-^{117,119}Sn] 36.3 Hz (unresolved); ^{3}J[*m*-$^{13}C_6H_5$-^{117,119}Sn] 56.2 Hz (unresolved); ^{2}J[3+3′-$^{13}C_4H_2$S-^{117,119}Sn] 39.6 Hz (unresolved).

^{119}Sn NMR [δ(ppm), $CDCl_3$ solution]: -137.4.

^{119m}Sn Mössbauer (mms^{-1}): I.S.=1.16; Q.S.=0.0.

IR [(cm^{-1}), KBr disk]: 3061, 1480, 1428, 1383, 1332, 1302, 1259, 1074, 1022, 997, 731, 698, 657, 455, 446.

5.6.6 Synthesis of methylene-bis-[5,5′-(2,2′-trimethylsilyl)thiophene] (58)

(53) (2.0g, 11.1 moml) in diethyl ether (100 ml) under nitrogen was treated with 1.6M BuLi (15ml, 24 mmol) at room temperature giving a dark brown solution which was stirred for a further one hour. Trimethylsilyl chloride (2.4g, 22.1 mmol) was then added via a syringe and the resulting cream-coloured precipitate stirred for two hours. Filtration under nitrogen and *in vacuo* removal of solvent gave a brown oil which was vacuum distilled on a Kügelrohr apparatus to give **(58)** as a colourless oil (1.4g, 39%) b.p. 180°C/0.5mmHg.

Analysis: Found(Calc. for $C_{15}H_{24}S_2Si_2$) C 56.6(55.6); H 7.88(7.41)%

^{1}H NMR [δ(ppm), $CDCl_3$ solution]: 0.48 [s,18H,-CH_3]; 4.58 [s,2H,-CH_2-]; 7.09-7.13 [m,2H,4+4′C$_4H_2$S]; 7.26 [m,2H,3+3′C$_4H_2$S].

^{13}C NMR [δ(ppm), $CDCl_3$ solution]: -0.03 [-CH_3]; 30.2 [-CH_2-]; 126.7 [Si-5+5′-C_4H_2S]; 126.8 [3+3′-C_4H_2S]; 134.0 [4+4′-C_4H_2S]; 148.5 [*i*-C_4H_2S].

^{29}Si NMR [δ(ppm), $CDCl_3$ solution]: -6.8.

IR [(cm^{-1}), liq. film]: 2953, 2897, 1464, 1262, 1250, 1214, 1157, 1097, 1042, 1033, 993, 839, 805, 757, 705.

5.6.7 Synthesis of methylene-bis-[5,5′-(2,2′-triphenylsilyl)thiophene] (59)

(53) (2g, 11.1 mmol), stirred in diethyl ether (150 ml) under nitrogen was treated with 1.6M BuLi (15ml, 24 mmol) at room temprerature giving a dark brown solution. After stirring for one hour, triphenylsilyl chloride (6.55g, 22.1 mmol) in diethyl ether (75 ml) was added dropwise giving a dark brown suspension. This was stirred for a further one hour before filtration and evaporation of the solvent. The resulting brown tar was chromatographed on silica gel using 40-60° petroleum ether as eluant to give **(59)** as an off-white amorphous solid (2.2g, 30%).

Analysis: Found(Calc. for $C_{45}H_{36}S_2Si_2$) C 77.1(77.5); H 5.37(5.17)%

^{1}H NMR [δ(ppm), $CDCl_3$ solution]: 4.31 [s,2H,-CH_2-]; 7.23-7.50 [m,34H,*o,m,p*-C_6H_5,3+3′,4+4′-C_4H_2S].

^{13}C NMR [δ(ppm), $CDCl_3$ solution]: 34.0 [-CH_2-]; 127.1 [3+3′-C_4H_2S]; 127.9 [*m*-C_6H_5]; 129.8 [4+4′-C_4H_2S]; 134.1 [*i*-C_6H_5]; 135.0 [Si-5+5′-C_4H_2S]; 136.1 [*o*-C_6H_5]; 138.6 [3+3′-C_4H_2S]; 150.3 [*i*-C_4H_2S].

^{29}Si NMR [δ(ppm), $CDCl_3$ solution]: -19.2.

5.6.8 Synthesis of methylene-bis-[1,1′-(5,5′-trimethylstannyl)pyrazole] (60)

To **(54)** (1.0g, 6.75 mmol) in THF (50 ml) under nitrogen at -78°C was added 1.6M BuLi in hexanes (9 ml, 14.4 mmol) and the resulting yellow solution stirred for two hours. Trimethyltin chloride (2.7g, 13.5 mmol) in THF (20 ml) was then added at 0°C and the resulting solution stirred for two hours. *In vacuo* removal of the solvent gave a sticky white solid. This was extracted with 40-60 petrol/diethyl ether (50/50) and filtered to remove LiCl. Evaporation of the filtrate gave a white solid and two successive recrystallisations from 40-60

petrol/diethyl ether (50/50) yielded (**60**) as a colourless crystalline solid (1.58g, 49%) m.p. 88°C.

Analysis: Found(Calc. for $C_{13}H_{24}N_4Sn$) C 33.1(33.0); H 5.21(5.11); N 11.9(11.8)%

^1H NMR [δ(ppm), $CDCl_3$ solution]: 0.44 [s,18H,-CH_3]; 6.34 [m,4H,-CH_2-coincident with 4+4′-$C_3H_2N_2$]; 7.54 [d,2H,3+3′-$C_3H_2N_2$]; $^2J[C^1H_3\text{-}^{117,119}Sn]$ 55.7, 58.4 Hz.

^{13}C NMR [δ(ppm), $CDCl_3$ solution]: -7.69 [-CH_3]; 67.3 [-CH_2-]; 115.9 [4+4′-$C_3H_2N_2$]; 139.7 [3+3′-$C_3H_2N_2$]; 142.9 [*i*-$C_3H_2N_2$]; $^1J[^{13}CH_3\text{-}^{117,119}Sn]$ 364.7, 382.3 Hz; $^2J[4+4'\text{-}^{13}C_3H_2N_2\text{-}^{117,119}Sn]$ 50.6 Hz (unresolved); $^3J[3+3'\text{-}^{13}C_3H_2N_2\text{-}^{117,119}Sn]$ 44.0 Hz (unresolved).

^{119}Sn NMR [δ(ppm), $CDCl_3$ solution]: -47.1.

^{119m}Sn Mössbauer (mms^{-1}): I.S.=1.20; Q.S.=0.81.

IR [(cm^{-1}), KBr disk]: 2980, 2915, 1435, 1379, 1348, 1321, 1257, 1190, 1177, 944, 925, 777, 745, 650.

5.6.9 Synthesis of methylene-bis-[1,1′-(5,5′-tributylstannyl)pyrazole] ***(61)***

To (**54**) (0.33g, 2.25 mmol) under nitrogen in THF (30 ml) was added 1.6M BuLi in hexanes (3ml,4.8 mmol) at -78°C. The resulting yellow solution was stirred for one hour before addition of tributyltin chloride (1.45g, 4.6 mmol) at 0°C. This gave a yellow solution which was stirred for 2 hours before being heated to reflux for a further hour. *In vacuo* removal of solvent gave a brown oil containing some suspended solids. This was extracted with diethyl ether and filtered to remove LiCl. Evaporation of the filtrate gave a yellow oil which was chromatographed on silica gel using a gradient of 40-60° petrol/diethyl ether to yield (**61**) (0.95g, 58%) as a yellow oil which turns brown on standing.

Analysis: Found(Calc. for $C_{31}H_{60}N_4Sn_2$) C 50.2(51.3); H 8.54(8.33); N 7.7(7.7)%

^{1}H NMR [δ(ppm), $CDCl_3$ solution]: 0.79 [t,18H,-CH_3]; 1.18-1.30 [m,24H,CH_2-CH_2C$H_2$$CH_2$$CH_3$]; 1.40-1.59 [m,12H,$CH_2CH_2$$CH_2$$CH_3$]; 6.20 [d,2H,4+4′-$C_3H_2N_2$]; 6.31 [2,2H,-C$H_2$-]; 7.50 [d,2H,3+3′-$C_3H_2N_2$].

^{13}C NMR [δ(ppm), $CDCl_3$ solution]: 13.42 [-CH_3]; 26.7 [-$CH_2$$(CH_2)_2$$CH_3$]; 27.7 [-$(CH_2)_2$$CH_2$$CH_3$]; 28.8 [-$CH_2$$CH_2$$CH_2$$CH_3$]; 67.6 [-$CH_2$-]; 116.1 [4+4′$C_3H_2N_2$]; 139.5 [3+3′-$C_3H_2N_2$]; 142.3 [*i*-$C_3H_2N_2$]; ^{3}J[-$(CH_2)_2$$CH_2$$CH_3$-^{117,119}Sn] 22.1 Hz (unresolved).

^{119}Sn NMR [δ(ppm), $CDCl_3$ solution]: -58.9.

^{119m}Sn Mössbauer (mms^{-1}): I.S.=1.31; Q.S.=1.00.

IR [(cm^{-1}), liq. film]: 2959, 2926, 2872, 2855, 1464, 1377, 1358, 1342, 1260, 1078, 1047, 875, 789, 752, 695, 673, 599.

5.6.10 Synthesis of methylene-bis-[1,1′-(5,5′-triphenylstannyl)pyrazole] (62)

To **(54)** (0.5g, 3.4 mmol), stirred under nitrogen in THF (50 ml) at -78°C was added 1.6M BuLi in hexanes (4.5ml, 7.2 mmol) giving a yellow solution. This was stirred for one hour before being allowed to warm to 0°C when triphenyltin chloride (2.62g, 6.8 mmol) was added in THF (25 ml) resulting in a yellow solution. *In vacuo* removal of solvent yielded a pale brown tar which was dissolved in toluene and reprecipitated by the addition of pentane. The resulting off-white solid was filtered and recrystallised from chloroform to yield **(62)** as a colourless crystalline solid (0.32g, 12%) m.p. 154°C.

Analysis: Found(Calc. for $C_{43}H_{36}N_4Sn_2$) C 60.7(60.9); H 4.26(4.26); N 6.7(6.6)%

^{1}H NMR [δ(ppm), $CDCl_3$ solution]: 5.97 [s,2H,-CH_2-]; 6.25 [d,2H,4+4′$C_3H_2N_2$]; 7.08 [d,2H,3+3′-$C_3H_2N_2$]; 7.22-7.25 [m,18H,*m,p*-C_6H_5]; 7.54 [dd,12H,*o*-C_6H_5].

^{13}C NMR [δ(ppm), $CDCl_3$ solution]: 66.3 [-CH_2-]; 117.5 [4+4′-$C_3H_2N_2$]; 128.6 [*m*-C_6H_5]; 129.2 [*p*-C_6H_5]; 137.3 [*o*-C_6H_5]; 137.8 [*i*-C_6H_5]; 139.7 [*i*-$C_3H_2N_2$]; 140.2 [3+3′-$C_3H_2N_2$]; ^{2}J[*o*-$^{13}C_6H_5$-^{117,119}Sn] 39.4 Hz (unresolved); ^{3}J[*m*-$^{13}C_6H_5$-

$^{117,119}Sn$] 56.2 Hz (unresolved); $^{4}J[p\text{-}^{13}C_6H_5\text{-}^{117,119}Sn]$ 12.1 Hz (unresolved).

^{119}Sn NMR [δ(ppm), $CDCl_3$ solution]: -162.5; $^{1}J[i\text{-}^{13}C_6H_5\text{-}^{119}Sn]$ 587.6 Hz; $^{2}J[o\text{-}^{13}C_6H_5\text{-}^{119}Sn]$ 36.4 Hz; $^{3}J[m\text{-}^{13}C_6H_5\text{-}^{119}Sn]$ 59.2 Hz.

^{119m}Sn Mössbauer (mms^{-1}): I.S.=1.23; Q.S.=0.62.

IR [(cm^{-1}), KBr disk]: 3092, 3065, 2990, 1429, 1352,1257, 1074 727, 698, 447.

5.6.11 Synthesis of methylene-bis-[1,1′-(5,5′-trimethylsilyl)pyrazole] ***(63)***

To a solution of **(54)** (1.0g, 6.75 mmol) stirred under nitrogen in THF was added 1.6M BuLi in hexanes (9ml, 14.4 mmol) at -78°C. The resulting yellow solution was stirred at this temperature for a further one hour before the temperature was allowed to rise to 0°C and the addition of trimethylsilyl chloride (1.46g, 13.5 mmol). This resulted in an orange solution which was stirred at room temperature for a further two hours. *In vacuo* removal of the solvent gave an orange oil. Extraction with diethyl ether followed by filtration and evaporation of the filtrate gave an off-white solid. This was twice recrystallised fom 40-60° petroleum ether to yield **(63)** as colourless needles (0.81g, 41%) m.p. 82°C.

Analysis: Found(Calc. for $C_{13}H_{24}N_4Si_2$): H 53.0(53.4); H 8.22(8.22); N 19.1(19.2)%

^{1}H NMR [δ(ppm), $CDCl_3$ solution]: 0.00 [s,18H,-CH_3]; 6.03 [s,2H,-CH_2-]; 6.04 [d,2H,4+4′-$C_3H_2N_4$]; 7.14 [d,2H,3+3′-$C_3H_2N_4$]; $^{1}J[C^{1}H_3\text{-}^{29}Si]$ 6.84 Hz.

^{13}C NMR [δ(ppm), $CDCl_3$ solution]: 0.0 [-CH_3]; 66.6 [-CH_2]; 116.5 [4+4′-$C_3H_2N_4$]; 140.0 [3+3′-$C_3H_2N_4$]; 144.2 [*i*-$C_3H_2N_4$]; $^{1}J[^{13}CH_3\text{-}^{29}Si]$ 55.2 Hz.

^{29}Si NMR [δ(ppm), $CDCl_3$ solution]: -9.0.

IR [(cm^{-1}), KBr disk]: 2957, 1518, 1483, 1346, 1280, 1184, 1097, 1933, 943, 927, 843, 792, 758, 632, 443.

5.6.12 Synthesis of 2,2-bis-[1,1'-(5,5'-trimethylstannyl)pyrazole]propane (64)

To a solution of (**55**) (1.0g, 5.7 mmol) in THF (20 ml) under nitrogen at -78°C was added 1.6M BuLi in hexanes (8ml, 12.8 mmol) and the resulting yellow suspension stirred for one hour. The temperature was then allowed to rise to 0°C and trimethyltin chloride (2.26g, 11.4 mmol) in THF (20 ml) added to give a yellow solution whch was stirred at room temperature overnight. *In vacuo* removal of the solvent gave a yellow oil containing some suspended solid and Mössbauer analysis of this revealed some unreacted trimethyltin chloride. Chromatography on silica gel employing CH_2Cl_2 yielded (**64**) as a moisture-sensitive colourless oil (0.92g, 32%).

Analysis: Found(Calc. for $C_{15}H_{28}N_4Sn_2$: C 36.2(35.9); H 5.94(5.98); N 9.90(11.2)%

^{1}H NMR [δ(ppm), $CDCl_3$ solution]: 0.05 [s,18H,Sn-CH_3]; 2.09 [s,6H,C(CH_3)$_2$]; 6.45 [d,2H,4+4'-C$_3H_2N_2$]; 7.55 [d,2H,3+3'-C$_3H_2N_2$]; ^{2}J[-C$^1H_3$-^{117,119}Sn] 50.2, 57.3 Hz.

^{13}C NMR [δ(ppm), $CDCl_3$ solution]: -7.23 [Sn-*C*H_3]; 31.5 [C(*C*H_3)$_2$]; 80.4 [*C*(CH$_3$)$_2$]; 118.6 [4+4'-*C*$_3H_2N_2$]; 137.7 [3+3'-C$_3H_2N_2$]; 141.0 [*i*-*C*$_3H_2N_2$]; ^{1}J[-C$^1H_3$-^{117,119}Sn] 366.8 (unresolved).

^{119}Sn NMR [δ(ppm), $CDCl_3$ solution]: -35.7.

^{119m}Sn Mössbauer (mms^{-1}): I.S.=1.22; Q.S.=0.93.

IR [(cm^{-1}), liq.film]: 2980, 2919, 1415, 1388, 1369, 1305, 1259, 1199, 1170, 989, 924, 787, 736, 588.

5.6.13 Synthesis of 2,2'-bis-[1,1'-(5,5'-trimethylsilyl)pyrazole]propane (65)

To a solution of (**55**) (1.0g, 5.7 mmol) in THF (20 ml) under nitrogen at 0°C was added 1.6M BuLi in hexanes (9ml, 14.4 mmol). This produced a yellow suspension which was stirred for one hour before addition of trimethylsilyl chloride (1.24g, 11.4 mmol) at 0°C. The resulting yellow solution was stirred for

two hours and the solvent evaporated. This gave a yellow oil containing some suspended solid. Extraction with diethyl ether followed by filtration and evaporation of the filtrate yielded a yellow oil which crystallised on standing. This was recrystallised from hexane to give **(65)** as colourless crystals (1.15g, 63%) m.p. 58°C.

Analysis: Found(Calc. for $C_{15}H_{28}N_4Si_2$): C 56.6(56.3); H 9.03(8.80); 17.6(17.5)%

^{1}H NMR [δ(ppm), $CDCl_3$ solution]: 0.05 [s,18H,Si-CH_3]; 2.10 [s,6H,C(CH_3)$_2$]; 6.54 [d,2H,4+4′-C$_3H_2N_2$]; 7.48 [d,2H,3+3′-C$_3H_2N_2$].

^{13}C NMR [δ(ppm), $CDCl_3$ solution]: 0.08 [Si-CH_3]; 32.0 [C(CH_3)$_2$]; 81.1 [C(CH$_3$)]; 119.8 [4+4′-$C_3H_2N_2$]; 137.0 [3+3′-$C_3H_2N_2$]; 143.3 [i-$C_3H_2N_2$].

^{29}Si NMR [δ(ppm), $CDCl_3$ solution]: -9.9.

IR [(cm^{-1}), KBr disk]: 2953, 2901, 1307, 1296, 1263, 1182, 1103, 1014, 924, 843, 788, 765, 636, 526.

5.6.14 Reaction of (56) and $PhBCl_2$

(56) (1.1g, 1.45 mmol) was stirred as a pale yellow solution in diethyl ether (80ml) under nitrogen. $PhBCl_2$ (0.23g/0.19ml, 1.45 mmol) in diethyl ether (30ml) was added dropwise at room temperature with no change in appearance before heating to reflux for two hours. *In vacuo* removal of the solvent gave an off-white solid and an oil which were separated by washing with ice-cold pentane and filtration. Evaporation of the filtrate yielded an oil and a small amount of solid. Continued pentane washing in this manner yielded an oil identified as tributyltin chloride by infra-red (0.81g, 86%). The combined solids were recrystallised from hexane as fine fluffy colourless needles and dried under vacuum (0.21g, 55%).

Analysis: Found(Calc. for $C_{30}H_{22}B_2S_4$): C 67.6(67.9); H 4.66(4.15).

^{1}H NMR [δ(ppm), $CDCl_3$ solution]: 2.14 [s,1H,CH_2?]; 7.48 [t,4H,m-C$_6H_5$]; 7.57

[t,2H,*p*-C_6H_5]; 8.21 [dd,4H,*o*-C_6H_5].

^{13}C NMR [δ(ppm), $CDCl_3$ solution]: 127.9 [*m*-C_60H_5]; 132.6 [*p*-C_6H_5]; 135.6 [*o*-C_6H_5].

^{11}B NMR [δ(ppm), $CDCl_3$ solution]: +27.7.

5.6.15 Reaction of (57) and $PhBCl_2$

(57) (0.5g, 0.6 mmol) in dry diethyl ether (100 ml) was stirred as a pale yellow solution under nitrogen. To this was added $PhBCl_2$ (0.1g, 0.6 mmol) in diethyl ether (50 ml) over a period of thirty minutes with no change in appearance. After stirring for 24 hours, *in vacuo* removal of the solvent gave a sticky brown solid. This was washed with hexane and filtered. Evaporation of the filtrate gave a pale yellow solid which was recrystallised from hexane as fluffy colourless needles.

Analysis: Found(Calc. for $C_{30}H_{22}B_2S_4$): C 66.6(67.9); H 4.80(4.15)%

^1H NMR [δ(ppm), $CDCl_3$ solution]: 7.04-7.99 [m,aromatics].

^{13}C NMR [δ(ppm), $CDCl_3$ solution]: 33.0 [-CH_2-]; 128.0 [*m*-C_6H_5]; 129.1 [4+4′-C_4H_2S]; 130.5 [3+3′-C_4H_2S]; 132.7 [*p*-C_6H_5]; 133.4 [*i*-C_6H_5]; 135.1 [*o*-C_6H_5]; 136.1 [*i*-C_4H_2S].

^{11}B NMR [δ(ppm), $CDCl_3$ solution]: +26.6.

Appendix I

Instrument Details

(a) Infra-red Spectroscopy

Infra-red spectra were recorded either as KBr disks or nujol mulls on NaCl using a Nicolet 510P FT-IR spectrometer in the region 4000-400 cm^{-1}.

(b) NMR Spectroscopy

^{1}H and ^{13}C spectra were recorded either on a Jeol GX 270 MHz spectrometer or a Jeol EX 400 MHz spectrometer using TMS as an internal standard. ^{119}Sn, ^{29}Si, ^{11}B and ^{31}P (^{1}H decoupled) spectra were recorded on a Jeol GX 400 MHz spectrometer. Chemical sifts [$\delta(^{119}Sn)$] for the tin spectra are relative to Me_4Sn.

(c) Mass Spectrometry

Mass spectra were collected on a V.G. 70-70E instrument under fast atom bombardment conditions as a suspension in nitrobenzyl alcohol.

(e) Microanalysis

Carbon, hydrogen and nitrogen were analysed for using a Carlo Erba Strumentazione E.A. mod 1106 analyser at the University of Bath.

(f) Mössbauer Spectroscopy

Mössbauer spectra were recorded on a constant acceleration Mössbauer spectrometer (Cryophysics) fitted with a 10 mCi calcium metastannate-119m

source (Amersham Int.) and operated in sawtooth mode. The sample temperature was controlled using a continuous flow liquid nitrogen cryostat linked to a DTC-2 digital variable temperature controller (Oxford Instruments). Temperature stability was +/- 0.1K of the set temperature (78K). The source was at room temperature. Samples were prepared either as finely ground powders or frozen solutions. Calibration was based on the spectrum of natural iron with ^{119}Sn isomer shifts relative to SnO_2 (zero velocity). Spectra were fitted to Standard Lorentzian line shapes, with a correction for parabolic background curvature using a conventional least squares fit technique.

Appendix II

Crystallographic Analysis and Structural Refinement of 1,3-phenylene-bis-5,5′-(tributylstannyltetrazole) (12)

A crystal of approximate dimensions 0.3 x 0.2 x 0.2 mm was used for data collection.

Crystal data: $C_{34}H_{66}O_2N_8Sn_2$, M = 856.3, monoclinic, a = 16.414(3), b = 13.321(4), c = 19.114(5)Å, β = 91.18(2)°, U = 4178.4Å^3, space group $P2_1/n$, Z = 4, D_c = 1.36 gcm^{-3}, μ(Mo-K_α) = 12.4 cm^{-1}, F(000) = 608. Data were measured at 170 K on a CAD4 automatic four-circle diffractometerin the range $2\leq\theta\leq24°$. 5607 reflections were collected of which 3131 were unique with $I\geq2\sigma\geq(I)$. Data were corrected for Lorentz and polarisation and also for absorbtion.[265] (Max. and Min. absorbtion corrections; 1.168, 0.875 respectively). The structure was solved by Patterson methods and refined using the SHELX[266,267] suite of programs. In the final least squares cycles all atoms were allowed to vibrate anisotropically except for the triply disordered C(32) positions. Hydrogen atoms were included at calculated positions except for the methoxy protons attached to C(33) and C(34). These hydrogens were located in an advanced Difference Fourier and refined at a distance of 0.98 Å from the relevant parent atoms.

Final residuals after ten cycles were R = 0.0500, R_w = 0.0442 for a weighting scheme of $w = 2.6333/[\sigma^2(F) + 0.000224(F)^2]$. Max. final shift/esd was 0.113. The max. and min. residual densities were 0.25 and -0.28 eÅ^{-3} respectively. The ORTEP[268] program was used to obtain the drawings. Fractional atomic coordinates (x10^4) and equivalent isotropic temperature factors (Å^{2}x10^3) are given in Table A.1 and tables of anisotropic temperature factors and full bond lengths and bond angles are available as supplementary data.

Table A.1: Fractional Atomic Coordinates ($x10^4$) and Equivalent Isotropic Temperature Factors ($Å^2x10^3$) for **(12)**.

	x	y	z	U
Sn(1)	2718	2286(1)	1700	45
Sn(2)	-2856(1)	9825(1)	1725	52
O(1)	3735(4)	998(6)	1639(4)	59(3)
O(2)	-3883(4)	11098(5)	1645(3)	48(3)
N(1)	1467(5)	4079(6)	1268(4)	48(3)
N(2)	1800(5)	3562(6)	1801(5)	53(3)
N(3)	1614(6)	3955(7)	2405(5)	63(4)
N(4)	1127(5)	4741(6)	2272(4)	52(3)
N(5)	-1441(5)	8277(7)	1326(5)	60(4)
N(6)	-1914(6)	8581(7)	1836(5)	70(4)
N(7)	-1785(6)	8052(8)	2417(5)	78(4)
N(8)	-1206(6)	7383(7)	2280(4)	62(4)
C(1)	1053(6)	4802(8)	1580(6)	43(4)
C(2)	579(6)	5581(7)	1214(5)	40(4)
C(3)	637(6)	5707(7)	489(5)	44(4)
C(4)	185(6)	6449(8)	140(5)	47(4)
C(5)	-351(6)	7040(7)	519(5)	43(4)
C(6)	-418(6)	6914(8)	1235(5)	41(4)
C(7)	46(6)	6192(7)	1577(5)	41(4)
C(8)	-1009(7)	7541(8)	1607(5)	51(4)

	x	y	z	U
C(9)	2185(7)	1741(8)	742(6)	76(5)
C(10)	1563(11)	947(14)	797(13)	190(13)
C(11)	1394(17)	220(14)	792(17)	344(25)
C(12)	777(9)	-590(10)	837(8)	115(8)
C(13)	2338(6)	1629(9)	2649(6)	63(4)
C(14)	2650(7)	2156(8)	3309(5)	60(5)
C(15)	2322(7)	1687(10)	3971(6)	75(5)
C(16)	2517(8)	2300(10)	4639(6)	86(6)
C(17)	3741(9)	3289(12)	1600(10)	129(9)
C(18)	3982(15)	3818(20)	2006(13)	311(21)
C(19)	4678(17)	4554(21)	1904(17)	263(22)
C(20)	5064(18)	4755(24)	1487(21)	557(58)
C(21)	-3162(6)	9690(8)	2794(5)	46(4)
C(22)	-2611(6)	10263(9)	3307(4)	58(4)
C(23)	-2872(7)	10129(9)	4062(5)	67(5)
C(24)	-2349(9)	10678(12)	4585(6)	121(8)
C(25)	-2007(8)	10830(12)	1302(8)	112(7)
C(26)	-1404(8)	11281(9)	1787(8)	86(6)
C(27)	-791(8)	11958(11)	1429(8)	107(7)
C(28)	-189(9)	12420(12)	1891(9)	136(9)
C(29)	-3581(10)	9010(10)	990(6)	101(7)
C(30)	-4073(16)	8277(14)	1231(10)	256(16)
C(31)	-4574(23)	7766(24)	610(13)	282(22)
C(33)	4008(8)	453(11)	1068(6)	102(7)
C(34)	-3998(8)	11737(8)	1054(5)	73(5)

Appendix III

Crystallographic analysis and Structural Refinement of 1,2-phenylene-bis-5,5′-(triethylstannyltetrazole) (17)

A crystal of approximate dimensions 0.25 x 0.25 x 0.2 mm was used for data collection.

Crystal data: $C_{20}H_{34}N_8Sn_2$, M = 623.9, monoclinic, a = 8.549(2), b = 20.952(4), c = 14.046(3)Å, β = 96.41(2)°, U = 2500.2Å^3, space group $P2_1/c$, Z = 4, D_c = 1.66 gcm^{-3}, μ(Mo-K_α) = 20.3 cm^{-1}, F(000) = 1240. Data were measured at 170 K on a CAD4 automatic four-circle diffractometer in the range $2 \leq \theta \leq 24°$. 4318 reflections were collected of which 3014 were unique with $I \geq 2\sigma(I)$. Data were collected for Lorentz and polarisation but not for absorbtion. The structure was solved by Patterson methods and refined using the SHELX[266,267] suite of programs. In the final least squares cycles all atoms were allowed to vibrate anisotropically. Hydrogen atoms were included at calculated positions.

Final residuals after ten cycles of least squares were R = 0.0321, R_w = 0.0313, for a weighting scheme of $w = 2.1396/[\sigma^2(F) + 0.000544(F)^2]$. Max. final shift/esd was 0.001. The max. and min. residual densities were 0.51 and -0.53 eÅ^{-3} respectively. Final fractional atomic coordinates and isotropic thermal parameters are presented in Table A.2 and tables of anisotropic thermal parameters and full bond lengths and bond angles are available as supplementary data.

Table A.2: Fractional Atomic Coordinates ($x10^4$) and Equivalent Temperature Factors ($Å^2x10^3$) for **(17)**

	x	y	z	U
Sn(1)	2378.7(4)	4251.6(2)	-2407.2(2)	17.3(2)
Sn(2)	-2732.6(4)	2439.7(2)	-16.8(2)	17.7(2)
N(1)	-2653(5)	3908(2)	-3663(3)	21(1)
N(2)	-1779(5)	3473(2)	-4073(3)	22(1)
N(3)	-266(5)	3570(2)	-3852(3)	22(1)
N(4)	-106(5)	4089(2)	-3278(3)	21(1)
N(5)	-3555(5)	3388(2)	-836(3)	22(1)
N(6)	-4996(5)	3623(2)	-880(3)	24(1)
N(7)	-5009(5)	4187(2)	-1338(3)	22(1)
N(8)	-2586(5)	3790(2)	-1248(3)	20(1)
C(1)	-1587(6)	4283(2)	-3180(3)	18(1)
C(2)	-3525(6)	4276(2)	-1550(3)	18(2)
C(3)	-2962(5)	4873(2)	-1948(3)	16(2)
C(4)	-1961(5)	4872(2)	-2685(3)	15(1)
C(5)	-1366(6)	5452(3)	-2967(4)	22(2)
C(6)	-1771(6)	6021(3)	-2568(4)	25(2)
C(7)	-2797(6)	6019(3)	-1858(4)	24(2)
C(8)	-3375(6)	5450(2)	-1558(4)	22(2)
C(9)	3077(6)	3337(2)	-2862(4)	21(2)
C(10)	2416(6)	2791(3)	-2309(4)	30(2)
C(11)	1437(6)	4445(3)	-1089(4)	25(2)

	x	y	z	U
C(12)	1655(7)	5143(3)	-801(4)	32(2)
C(13)	3019(7)	5059(3)	-3226(4)	30(2)
C(14)	2727(12)	4964(4)	-4295(5)	74(4)
C(15)	-3442(7)	2840(3)	1264(4)	30(2)
C(16)	-2175(9)	3027(5)	2008(5)	84(4)
C(17)	-434(6)	2566(2)	-449(4)	23(2)
C(18)	682(6)	2948(3)	240(4)	31(2)
C(19)	-4402(6)	1853(3)	-849(4)	25(2)
C(20)	-5798(7)	1675(3)	-317(4)	39(2)

Appendix IV

Crystallographic Analysis and Structural Refinement of 1,2-phenylene-bis-5,5′-(tributylstannyltetrazole) (11)

A crystal of approximate dimensions 0.3 x 0.3 x 0.2 mm was used for data collection.

Crystal data: $C_{32}H_{58}N_8Sn_2$, M = 790.2, orthorhombic, a = 13.819(2), b = 23.075(3), c = 24.043(6)Å, U = 7666.4 Å^3, space group $P22_12_1$, Z = 4, D_c = 1.37 gcm^{-3}, μ(Mo-K_α) = 12.21 cm^{-1}, F(000) = 3248. Data were measured at room temperature on a CAD4 automatic four-circle diffractometer in the range $2 \leq \theta \leq 24°$. 6645 reflections were collected of which 3948 were unique with $I \geq 2\sigma(I)$. Data were corrected for Lorentz and polarisation but not for absorbtion. The structure was solved by Patterson methods and refined using the SHELX[266,267] suite of programs.

The tin atoms only were anisotropically refined, the remainder of the atoms being treated isotropically. Hydrogen atoms were not included and the phenyl groups were refined as rigid hexagons.

Final residuals after eight cycles of least squares were $R = R_w = 0.1503$, Max. final shift/esd was 0.011. The max. and min. residual densities were 0.96 and -0.73 eÅ^{-3} respectively. Final fractional atomic coordinates and isotropic thermal parameters are given in Table A.3 and tables of anisotropic temperature factors and full bond lengths and bond angles are available as supplementary data.

Table A.3: Fractional Atomic Coordinates ($x10^4$) and Equivalent Isotropic Temperature Factors ($Å^2x10^3$) for **(11)**

	x	y	z	U
N(1)	7637(30)	3871(18)	2216(17)	46(11)
N(2)	6708(33)	3818(19)	2114(21)	58(12)
N(3)	6298(46)	4291(26)	2318(24)	95(19)
N(4)	7048(42)	4664(23)	2524(24)	81(17)
N(5)	8391(35)	7616(19)	3722(19)	57(12)
N(6)	8808(38)	7407(21)	4155(21)	70(15)
N(7)	8114(28)	7399(16)	4565(17)	38(10)
N(8)	7486(32)	7715(18)	3747(18)	50(12)
N(9)	6099(33)	6609(19)	3844(19)	58(13)
N(10)	5847(38)	6423(20)	3327(20)	69(14)
N(11)	5172(31)	6766(18)	3127(19)	51(11)
N(12)	5000(30)	2172(18)	1516(17)	46(11)
N(13)	10254(30)	8327(18)	2144(19)	50(11)
N(14)	10509(28)	7922(18)	1763(17)	50(11)
N(15)	8972(49)	6755(30)	6411(28)	111(22)
N(16)	8996(52)	6263(31)	6529(30)	116(23)
C(1)	7841(46)	4398(27)	2400(25)	64(17)
C(2)	5548(31)	7063(20)	3871(18)	34(11)
C(3)	7380(48)	7587(28)	4320(27)	71(19)
C(4)	10574(48)	8761(28)	2027(30)	78(19)

C(5)	5540(31)	7442(16)	4441(14)	51(15)
C(6)	4684(31)	7530(16)	4737(14)	86(22)
C(7)	4687(31)	7870(16)	5216(14)	70(18)

	x	y	z	U
Sn(1)	5881(2)	3029(1)	1848(2)	54(1)
Sn(2)	9320(3)	7931(2)	2906(2)	55(1)
Sn(3)	6416(4)	5566(2)	2938(2)	76(2)
Sn(4)	8625(4)	7073(2)	5466(2)	89(2)

Appendix V

The Crystal Structure, Solution and Refinement of 1,2-phenylene-bis-(hydrotetrazole).4H_2O (20)

A crystal of approximate dimensions 0.2 x 0.2 x 0.2 mm was used for data collection.

Crystal data: $C_8H_{14}O_4N_8$, M = 286.2, a = 7.2650(6), b = 12.408(2), c = 14.529(2)Å, β = 96.35(1)°, U = 1301.7 Å^3, space group $P2_1/a$, Z = 4, D_c = 1.46 gcm^{-3}, μ(Mo-K_α) = 0.79 cm^{-1}, $F(000)$ = 600. Data were measured at room temperature on a Hilger and Watts Y290 four-circle diffractometer in the range $2 \leq \theta \leq 24°$. 2250 reflections were collected of which 1279 were unique with $I \geq 3\sigma(I)$. Data were corrected for Lorentz and polarisation effects but not for absorbtion. The structure was solved by Direct methods and refined using the SHELX[266,267] suite of programs.

In the final least squares cycles all atoms were allowed to vibrate anisotropically. Hydrogen atoms were included at calculated positions on the bridging phenyl group of the ligand. However the hydrogen atoms bonded to both N(1) and N(8) and to the water oxygens were located in the penultimate difference map and refined at a fixed distance from the parent atoms (1.08Å and 0.88Å respectively). Final residuals after ten cycles of least squares were R = 0.0367, R_w = 0.0431, for a weighting scheme of $w = 1.0000/[\sigma^2(F) + 0.005575(F)^2]$. Max.final shift/esd was 0.048. The max. and min. residual densities were 0.09 and -0.10 eÅ^{-3} respectively. Final fractional atomic coordinates and isotropic thermal parameters, bond lengths and bond angles are given in Tables A.4, A.5 and A.6 respectively. Tables of anisotropic temperature factors and intermolecular distances are available as supplementary data. The asymmetric unit is shown in Figure A.1, along with the labelling scheme used

while the extensively hydrogen-bonded molecular network is illustrated in Figure A.2.

Molecules related by one full unit-cell translation in the *c* direction are bridged by a chain of four waters between N(4) and N(8) [N(4)-O(2)-O(3)-O(4)-O(1)-N(8)]. This linear array is coupled with additional linkage in the *b* direction where each molecule is bonded to its two nearest neighbours related by a screw axis affording a two-dimensional network in the *bc* plane [N(6)-O(1)-N(8) and N(2)-O(2)-N(4)]. These planes are linked by inter-layer hydrogen bonds to give a rigid three-dimensional packing arrangement where ligand molecules are aqua-cemented [N(6)-O(1) and N(5)-O(3) links].

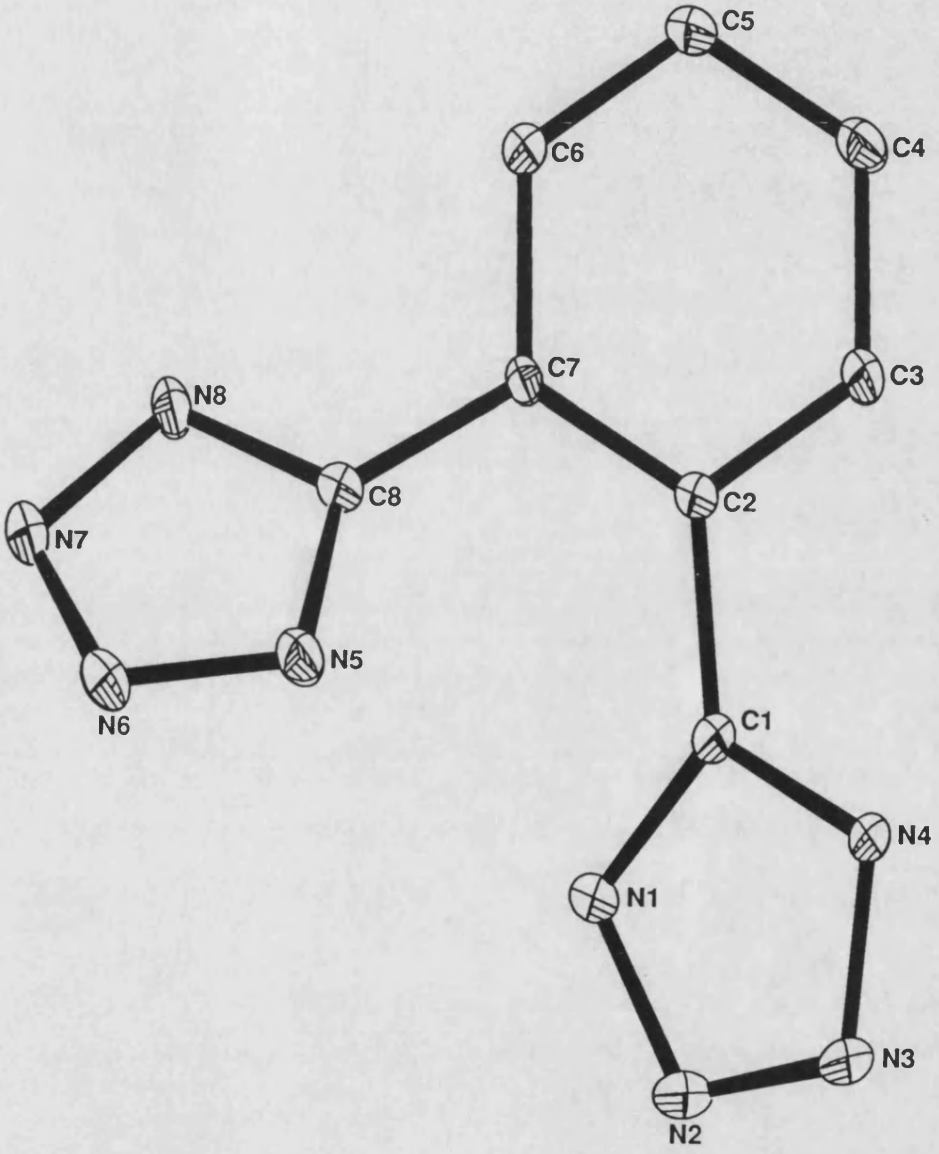

Figure A.1: The asymmetric unit of **(20)** showing the numbering scheme adopted.

Hydrogen atoms omitted for clarity.

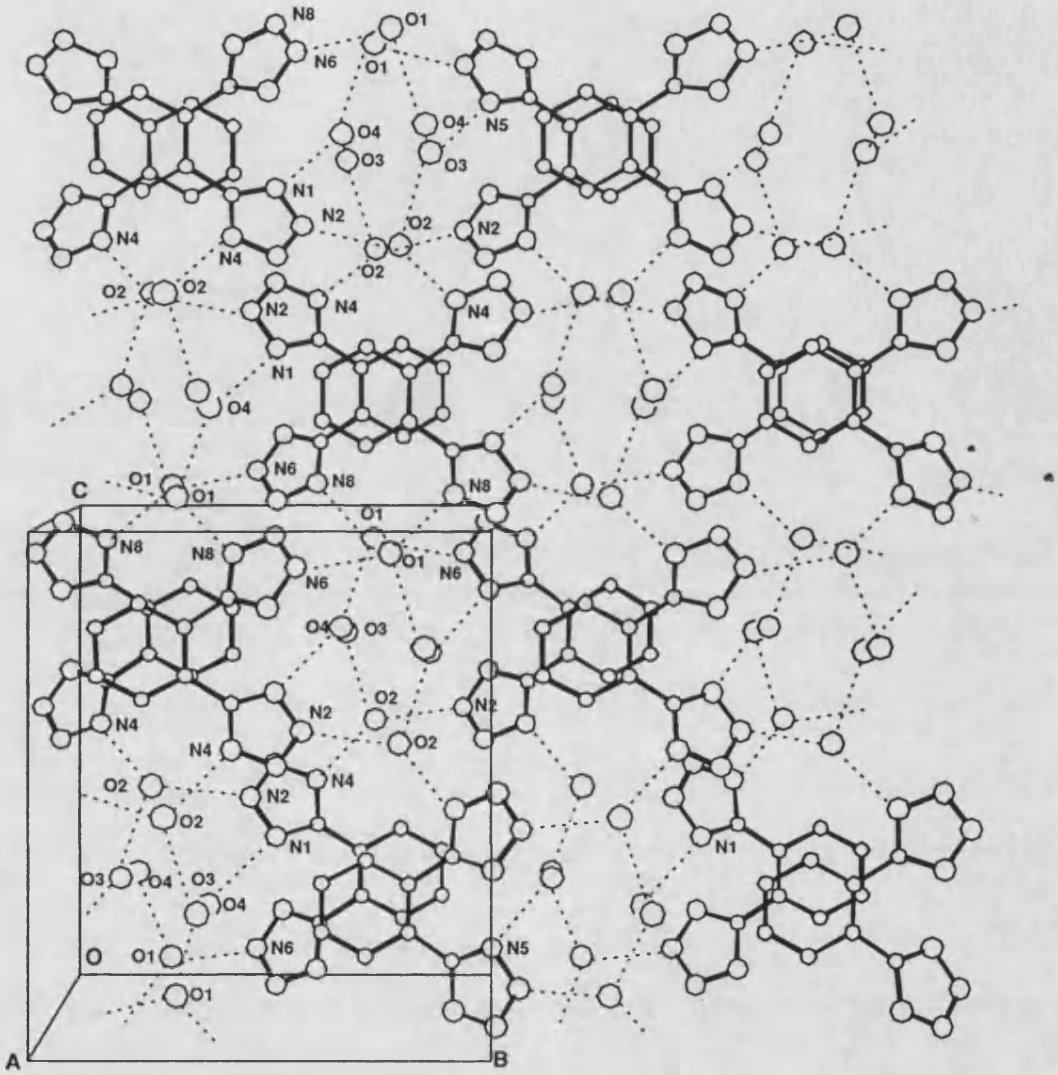

Figure A.2: The molecular packing of **(20)** perpendicular to the *bc* plane.

Table A.4: Fractional Atomic Coordinates ($x10^4$) and Thermal Parameters ($Å^2x10^3$) for **(20)**

Atom	x	y	z	Uiso or Ueq	(***)
N1	0.13754(20)	-0.00521(11)	0.65894(10)	0.0338(9)	***
N2	0.1578(2)	-0.0673(1)	0.5839(1)	0.041(1)	***
N3	0.2464(2)	-0.0163(1)	0.5250(1)	0.043(1)	***
N4	0.2851(2)	0.0807(1)	0.5615(1)	0.037(1)	***
N5	0.35233(20)	-0.00236(11)	0.84336(10)	0.0339(9)	***
N6	0.3339(2)	-0.0633(1)	0.9194(1)	0.040(1)	***
N7	0.2427(2)	-0.0120(1)	0.9772(1)	0.042(1)	***
N8	0.2005(2)	0.0838(1)	0.9389(1)	0.035(1)	***
C1	0.2184(2)	0.0876(1)	0.6439(1)	0.029(1)	***
C2	0.2330(2)	0.1863(1)	0.7007(1)	0.028(1)	***
C3	0.2239(2)	0.2839(1)	0.6539(1)	0.031(1)	***
C4	0.2325(2)	0.3816(1)	0.7003(1)	0.033(1)	***
C5	0.2498(2)	0.3823(1)	0.7960(1)	0.033(1)	***
C6	0.2593(2)	0.2858(1)	0.8440(1)	0.031(1)	***
C7	0.2515(2)	0.1872(1)	0.7984(1)	0.026(1)	***
C8	0.2675(2)	0.0893(1)	0.8565(1)	0.028(1)	***
O1	0.02808(20)	0.22274(11)	1.04302(9)	0.0442(9)	***
O2	0.45412(21)	0.21461(11)	0.45330(9)	0.0486(9)	***
O3	0.44140(20)	0.14225(12)	0.26777(10)	0.0478(9)	***
O4	0.0532(2)	0.1480(1)	0.2259(1)	0.048(1)	***

H7	0.4979(29)	0.0922(14)	0.2402(15)	0.060(7)
H8	0.4721(31)	0.2056(13)	0.2532(15)	0.083(9)
H9	0.1739(24)	0.1488(22)	0.2421(17)	0.108(11)
H10	0.0037(27)	0.0968(15)	0.2547(14)	0.049(6)
H1	0.3513(25)	0.1259(15)	0.5298(13)	0.046(3)
H2	0.1374(25)	0.1316(15)	0.9707(13)	0.046(3)
H3	0.0165(39)	0.1863(18)	1.0959(14)	0.081(9)
H4	0.0818(32)	0.2883(13)	1.0520(16)	0.061(7)
H5	0.4164(35)	0.2837(13)	0.4438(18)	0.072(8)
H6	0.4662(42)	0.1809(19)	0.4001(14)	0.088(10)

Table A.5: Bond Lengths (Å) for **(20)**

N1	-N2	1.356(2)	N1	-C1	1.321(2)
N2	-N3	1.291(2)	N3	-N4	1.333(2)
N4	-C1	1.343(2)	N4	-H1	0.898(14)
N5	-N6	1.357(2)	N5	-C8	1.318(2)
N6	-N7	1.293(2)	N7	-N8	1.333(2)
N8	-C8	1.344(2)	N8	-H2	0.907(14)
C1	-C2	1.475(2)	C2	-C3	1.387(2)
C2	-C7	1.410(3)	C3	-C4	1.385(2)
C4	-C5	1.382(3)	C5	-C6	1.383(2)
C6	-C7	1.390(2)	C7	-C8	1.475(2)
O1	-H3	0.904(16)	O1	-H4	0.906(14)
O2	-H5	0.906(15)	O2	-H6	0.892(16)
O3	-H7	0.867(14)	O3	-H8	0.850(16)
O4	-H9	0.882(17)	O4	-H10	0.861(14)

Table A.6: Bond Angles (°) for **(20)**

C1	-N1	-N2	105.8(1)	N3	-N2	-N1	111.1(1)
N4	-N3	-N2	106.1(1)	C1	-N4	-N3	109.3(1)
H1	-N4	-N3	117(1)	H1	-N4	-C1	133(1)
C8	-N5	-N6	105.9(1)	N7	-N6	-N5	110.9(1)
N8	-N7	-N6	106.2(1)	C8	-N8	-N7	109.1(1)
H2	-N8	-N7	118(1)	H2	-N8	-C8	132(1)
N4	-C1	-N1	107.6(1)	C2	-C1	-N1	129.6(1)
C2	-C1	-N4	122.8(1)	C3	-C2	-C1	117.0(1)
C7	-C2	-C1	124.2(1)	C7	-C2	-C3	118.7(1)
C4	-C3	-C2	121.9(2)	C5	-C4	-C3	119.3(1)
C6	-C5	-C4	119.7(1)	C7	-C6	-C5	121.7(2)
C6	-C7	-C2	118.7(1)	C8	-C7	-C2	124.2(1)
C8	-C7	-C6	117.1(1)	N8	-C8	-N5	107.8(1)
C7	-C8	-N5	129.5(2)	C7	-C8	-N8	122.6(1)
H4	-O1	-H3	114(2)	H6	-O2	-H5	112(2)
H8	-O3	-H7	113(2)	H10	-O4	-H9	110(2)

Appendix VI

Crystallographic Analysis and Refinement of (23)

A crystal of approximate dimensions 0.2 x 0.2 x 0.3 mm was used for data collection.

Crystal data: $C_{10}H_8N_8$, M = 240.2, tetragonal, a = 24.522(2), b = 24.513(2), c = 7.035(1)Å, U = 4227.2 Å^3, space group $I4_1cd$, Z = 16, D_c = 1.51 gcm^{-3}, μ(Mo-K_α) = 1.00 cm^{-1}, F(000) = 1984. Data were measured at room temperature on a CAD4 automatic four-circle diffractometer in the range $2 \leq \theta \leq 24°$. 1897 reflections were collected of which 597 were unique with $I \geq 3\sigma(I)$. Data were corrected for Lorentz and polarisation effects but not absorbtion. The structure was solved by Patterson methods and refined using the SHELX[266,267] suite of programs. In the final least squares cycles all atoms were allowed to vibrate anisotropically. Hydrogen atoms were included at calculated positions. Final residuals after ten cycles of least squares were R = 0.0389, R_w = 0.0404, for a weighting scheme of $w = 1.0000/[\sigma^2(F) + 0.004824(F)^2]$. Max. final shift/esd was 0.020. The max. and min. residual densities were 0.08 and -0.12 eÅ^{-3} respectively. Final fractional atomic coordinates and isotropic thermal parameters are given in Table A.7 while tables of anisotropic thermal parameters and full intra- and intermolecular bond lengths and angles are available as supplementary data.

Table A.7: Fractional Atomic Coordinates ($x10^4$) and Thermal Parameters ($Å^2x10^3$) for **(23)**

Atom	x	y	z	Uiso or Ueq (***)
N1	0.18890(19)	0.44783(18)	0.12162	0.0334(27) ***
N2	0.2196(2)	0.4928(2)	0.0983(11)	0.044(3) ***
N3	0.1902(2)	0.5333(2)	0.1634(11)	0.045(3) ***
N4	0.1406(2)	0.5148(2)	0.2251(11)	0.041(3) ***
N5	0.2038(2)	0.3526(2)	0.3709(11)	0.032(3) ***
N6	0.2309(2)	0.3324(2)	0.5216(12)	0.043(3) ***
N7	0.1960(2)	0.3216(2)	0.6510(11)	0.047(3) ***
N8	0.1446(2)	0.3343(2)	0.5906(11)	0.040(3) ***
C1	0.1413(2)	0.4618(2)	0.1964(12)	0.049(3) ***
C2	0.0957(2)	0.4240(2)	0.2264(12)	0.033(3) ***
C3	0.0443(2)	0.4403(2)	0.1592(13)	0.046(4) ***
C4	0.0004(3)	0.4057(3)	0.1705(15)	0.053(4) ***
C5	0.0068(3)	0.3536(3)	0.2412(13)	0.049(4) ***
C6	0.0571(2)	0.3365(2)	0.3093(13)	0.043(4) ***
C7	0.1021(2)	0.3719(2)	0.3051(12)	0.032(3) ***
C8	0.1504(2)	0.3538(2)	0.4165(12)	0.032(3) ***
C9	0.2355(2)	0.3608(3)	0.1972(13)	0.046(4) ***
C10	0.2063(3)	0.3950(2)	0.0471(12)	0.041(3) ***

Appendix VII

Crystallographic Analysis and Refinement of (31)

A crystal of approximate dimensions 0.4 x 0.4 x 0.3 mm was used for data collection.

Crystal data: $C_{12}H_{12}N_8$, M = 428.1, monoclinic, a = 15.959(3), b = 11.370(2), c = 8.974(1)Å, β = 102.82(1)°, U = 1587.8 Å^3, space group $C2/c$, Z = 4, D_c = 1.79 gcm^{-3}, μ(Mo-K_α) = 50.6 cm^{-1}, $F(000)$ = 840. Data were measured at room temperature on a CAD4 automatic four-circle diffractometer in the range $2 \leq \theta \leq 24°$. 1369 reflections were collected of which 815 were unique with $I \geq 3\sigma(I)$. Data were corrected for Lorentz and polarisation effects but not absorbtion. The structure was solved by Patterson methods and refined using the SHELX[266,267] suite of programs. In the final least squares cycles all atoms were allowed to vibrate anisotropically. Hydrogen atoms were included at calculated positions except in the instance of the H(41), H(61) and H(71) atoms [attached to C(4), C(6) and C(7) respectively] where the protons were located in an advanced Difference Fourier and refined at a distance of 0.96 Å from the parent carbon atom. Final residuals after twelve cycles of least squares were R = 0.0653, R_w = 0.0660, for a weighting scheme of $w = 2.6231/[\sigma^2(F) + 0.002460(F)^2]$. Max. final shift/esd was 0.000. The max and min. residual densities were 0.72 and -0.34 eÅ^{-3} respectively. Final fractional atomic coordinates and isotropic thermal parameters are given in Table A.8 while tables of anisotropic thermal parameters and full intra- and intermolecular bond lengths and angles are available as supplementary data.

Table A.8: Fractional Atomic Coordinates ($x10^4$) and Equivalent Isotropic Temperature Factors ($Å^2x10^3$) for **(31)**

	x	y	z	U
Br(1)	3922(1)	3520(1)	598(1)	81(1)
N(1)	3854(4)	2853(6)	4842(7)	46(2)
N(2)	3194(4)	2968(6)	3654(7)	43(2)
N(3)	2750(4)	1983(7)	3277(8)	55(2)
N(4)	3136(5)	1169(6)	4234(8)	53(2)
C(1)	3660(6)	4527(7)	2190(10)	60(3)
C(2)	2955(5)	4069(8)	2833(10)	53(3)
C(3)	3803(5)	1717(6)	5173(9)	41(3)
C(4)	5000	1705(8)	7500	37(4)
C(5)	4410(5)	1102(6)	6388(8)	36(3)
C(6)	4410(5)	-140(7)	6405(9)	49(3)
C(7)	5000	-728(9)	7500	51(4)

Appendix VIII

Crystallograpic Analysis and Refinement of Tris-[2-(5-tributylstannyltetrazole)ethyl]nitromethane (49)

A crystal of approximate dimensions 0.3 x 0.3 x 0.2 mm was used for data collection.

Crystal data: $C_{46}H_{91}N_{13}O_2Sn_3$, M = 1214.3, triclinic, a = 13.241(4), b = 15.568(5), c = 15.621(12)Å, $\underline{\alpha}$ = 75.01(3), $\underline{\beta}$ = 85.27(5), $\underline{\gamma}$ = 85.36(3)°, U = 3093.7 Å^3, space group $P\bar{1}$, Z = 2, D_c = 1.30 gcm^{-3}, μ(Mo-K_α) = 11.37 cm^{-1}, F(000) = 1984. Data were measured at room temperature on a CAD4 automatic four-circle diffractometer in the range $2 \leq \theta \leq 24°$. 10118 reflections were collected of which 3379 were unique with $I \geq 3\sigma(I)$. Data were corrected for Lorentz and polarisation effects and also for linear crystal decay of approximately 37% in the x-ray beam. No absorbtion correction was applied. The structure was solved by Direct methods and refined using the SHELX[266,267] suite of programs. In the final least squares cycles all atoms were allowed to vibrate anisotropically except for the butyl carbons [C(4)-C(34)]. Unfortunately not all of the butyl carbon atoms could be located, primarily as a consequence of crystal decay but also as a result of thermal vibration in the solid state. This is clearly evidenced by the relatively large isotropic thermal parameters associated with those butyl carbons which were not 'positionally challenged'. To assist convergence in the latter stages of refinement the C-C bond lengths therein were refined at a fixed distance of 1.54 Å. In addition, the distance between alternating pairs of carbons was restricted to a value of 2.52 Å. Hydrogen atoms were not included.

Final residuals after ten cycles of least squares were R = 0.0629, R_w = 0.0710, for a weighting scheme of $w = 0.3137/[\sigma^2(F) + 0.020194(F)^2]$. Max. final

shift/esd was 0.022. The max and min. residual densities were 0.33 and -0.18 $eÅ^{-3}$ respectively. Final fractional atomic coordinates and isotropic thermal parameters are given in Table A.9 while tables of anisotropic thermal parameters and full intra- and intermolecular bond lengths and angles are available as supplementary data.

Table A.9: Fractional Atomic Coordinates ($x10^4$) and Equivalent Isotropic Temperature Factors ($Å^2x10^3$) for **(49)**

	x	y	z	U
Sn(1)	3426(1)	9407(1)	7180(1)	96(1)
Sn(2)	2623(1)	6267(1)	10649(1)	94(1)
Sn(3)	-690(1)	6985(1)	13495(1)	109(1)
N(1)	3623(12)	7846(9)	7976(8)	94(6)
N(2)	3360(14)	7718(8)	8852(9)	111(8)
N(3)	3306(12)	6851(9)	9181(9)	100(7)
N(4)	3520(13)	6413(8)	8530(9)	101(7)
N(5)	1905(13)	5780(10)	12153(9)	104(7)
N(6)	1105(13)	6347(10)	12250(9)	111(8)
N(7)	793(11)	6189(10)	13083(10)	102(7)
N(8)	1358(12)	5495(10)	13560(9)	109(6)
N(9)	-2167(12)	7850(9)	13809(10)	111(7)
N(10)	-2216(14)	8705(9)	13389(12)	142(9)
N(11)	3098(13)	10933(9)	6442(10)	112(7)
N(12)	3689(12)	11521(9)	5948(10)	102(6)
N(13)	5350(15)	4267(14)	14303(11)	92(8)
O(1)	5742(13)	3782(12)	14938(12)	133(8)
O(2)	5603(13)	5031(10)	13976(11)	133(8)
C(35)	4531(17)	3949(10)	13848(10)	78(7)
C(36)	3718(15)	4726(10)	13655(12)	78(7)
C(37)	2814(18)	4490(10)	13186(12)	94(7)
C(38)	5022(13)	3781(9)	12960(9)	74(6)
C(39)	4025(14)	6890(10)	6913(9)	82(7)
C(40)	4126(13)	3051(9)	14448(9)	74(6)
C(41)	-3475(15)	6801(9)	14695(10)	91(7)

Appendix IX

Crystallographic Analysis and Refinement of 1,3,5-phenylene-tris-5-(tributylstannyltetrazole) (52)

A crystal of approximate dimensions 0.3 x 0.2 x 0.15 mm was used for data collection.

Crystal data: $C_{45}H_{84}N_{12}Sn_3$, M = 1149.3, triclinic, a = 12.544(4), b = 13.846(5), c = 17.035(7), $\underline{\alpha}$ = 71.54(3), $\underline{\beta}$ = 74.28(4), $\underline{\gamma}$ = 86.97(5)°, U = 2699.7 Å^3, space group $P\bar{1}$, Z = 2, D_c = 1.41 gcm^{-3}, μ(Mo-K_α) = 14.2 cm^{-1}, F(000) = 1176. Data were measured at 170 K on a CAD4 automatic four-circle diffractometer in the range $2 \leq \theta \leq 24°$. 9248 reflections were collected of which 3379 were unique with $I \geq 3\sigma(I)$. Data were corrected for Lorentz and polarisation effects but not absorbtion. The structure was solved by Patterson methods and refined using the SHELX[266,267] suite of programs. In the final least squares cycles all atoms except for the butyl carbons [C(10)-C(45)] were allowed to vibrate anisotropically. Anisotropic treatment of these atoms would have impaired convergence and resulted in unsatisfactory thermal parameters in many cases. In addition, three butyl groups [C(10)-C(13), C(18)-C(21) and C(30)-C(33)] were restricted to maintain C-C bond lengths of 1.54 Å during the latter stages of refinement, which helped to reduce the final shift/esd maxima and afforded a small reduction in the residual values. Hydrogen atoms were included at calculated positions.

Final residuals after twelve cycles of least squares were R = 0.0700, R_w = 0.0721, for a weighting scheme of $w = 2.4176/[\sigma^2(F) + 0.001679(F)^2]$. Max. final shift/esd was 0.001. The max. and min. residual densities were 1.18 and -0.56 eÅ^{-3} respectively. An empirical absorbtion did not significantly reduce this

maximum [which is primarily a result of some disorder in the C(33) region]. Final fractional atomic coordinates and isotropic thermal parameters are given in Table A.10 while tables of anisotropic thermal parameters and full intra- and intermolecular bond lengths and angles are available as supplementary data.

Table A.10: Fractional Atomic Coordinates ($x10^4$) and Equivalent Isotropic Temperature Factors ($Å^2 x10^3$) for **(52)**

	x	y	z	U
Sn(1)	9121(1)	-2720(1)	-659(1)	19
Sn(2)	5518(1)	-3909(1)	3002(1)	25
Sn(3)	1280(1)	-1166(1)	3697(1)	18
N(1)	8855(9)	-4564(8)	1212(6)	28(4)
N(2)	8397(9)	-3716(8)	790(6)	29(4)
N(3)	7475(9)	-3502(7)	1269(6)	25(4)
N(4)	7285(9)	-4202(7)	2047(6)	25(4)
N(5)	10295(8)	-859(7)	-3568(6)	22(4)
N(6)	9670(9)	-277(7)	-3132(6)	25(4)
N(7)	9382(9)	-756(7)	-2289(6)	24(4)
N(8)	9816(9)	-1676(7)	-2166(6)	24(4)
N(9)	3573(8)	-3792(7)	4713(6)	21(4)
N(10)	3862(9)	-3473(8)	3837(6)	25(4)
N(11)	3225(8)	-2760(7)	3525(6)	21(4)
N(12)	2460(8)	-2593(7)	4197(6)	19(4)
C(1)	8144(10)	-4831(9)	1983(7)	19(4)
C(2)	10386(10)	-1723(9)	-2964(7)	19(4)
C(3)	2719(10)	-3229(8)	4911(7)	19(4)
C(4)	8274(10)	-5743(9)	2692(7)	20(4)
C(5)	7795(10)	-5803(9)	3547(7)	21(4)
C(6)	7887(10)	-6690(9)	4201(7)	19(4)
C(7)	8464(10)	-7485(9)	3987(7)	21(4)
C(8)	8982(9)	-7411(9)	3142(7)	17(4)
C(9)	8918(9)	-6523(9)	2503(7)	18(4)

Appendix X

Crystallographic Analysis and Refinement of Methylene-bis-[1,1′-(5,5′-triphenylstannyl)pyrazole] (62)

A crystal of approximate dimensions 0.3 x 0.3 x 0.3 mm was used for data collection.

Crystal data: $C_{43}H_{36}N_4Sn_2$, M = 846.2, triclinic, a = 10.486(2), b = 13.446(2), c = 13.998(2)Å, $\underline{\alpha}$ = 99.28(1), $\underline{\beta}$ = 97.26, $\underline{\gamma}$ = 101.90(1), U = 1879.7 Å^3, space group $P\bar{1}$, Z = 2, D_c = 1.50 gcm^{-3}, μ(Mo-K_α) = 13.7 cm^{-1}, F(000) = 844. Data were measured at room temperature on a CAD4 automatic four-circle diffractometer in the range $2 \leq \theta \leq 24°$. 6232 reflections were collected of which 4622 were unique with $I \geq 3\sigma(I)$. Data were corrected for Lorentz and polarisation effects but not absorbtion. The structure was solved by Patterson methods and refined using the SHELX[266,267] suite of programs. In the final least squares cycles all atoms were allowed to vibrate anisotropically. Hydrogen atoms were included at calculated positions.

Final residuals after ten cycles of least squares were R = 0.0275, R_w = 0.0300, for a weighting scheme of $w = 1.6111/[\sigma^2(F) + 0.000722(F)^2]$. Max. final shift/esd was 0.001. The max. and min. residual densities were 0.27 and -0.23 eÅ^{-3} respectively. Final fractional atomic coordinates and isotropic thermal parameters are given in Table A.11 while tables of anisotropic thermal parameters and full intra- and intermolecular bond lengths and angles are available as supplementary data.

Table A.11: Fractional Atomic Coordinates ($x10^4$) and Equivalent Isotropic Temperature Factors ($Å^2x10^3$) for **(62)**

	x	y	z	U
Sn(1)	1541.5(2)	375.2(2)	3469.4(2)	44.6(2)
Sn(2)	-1331.9(2)	-4979.4(2)	1977.3(2)	41.6(2)
N(1)	974(4)	-2933(2)	3492(3)	55(1)
N(2)	531(3)	-2062(2)	3423(2)	44(1)
N(3)	-1089(4)	-1853(3)	1413(3)	61(1)
N(4)	-1141(3)	-2570(2)	1992(2)	45(1)
C(1)	2265(4)	-2604(3)	3706(3)	61(2)
C(2)	2665(4)	-1535(3)	3771(3)	60(2)
C(3)	1519(4)	-1198(3)	3564(3)	45(1)
C(4)	-860(4)	-2207(3)	3047(3)	48(1)
C(5)	-1253(3)	-3546(3)	1483(3)	42(1)
C(6)	-1298(4)	-3438(3)	524(3)	54(2)
C(7)	-1199(5)	-2394(3)	518(3)	66(2)
C(9)	3161(3)	2339(2)	4924(2)	55(1)
C(10)	3899(3)	2927(2)	5808(2)	63(2)
C(11)	4235(3)	2441(2)	6580(2)	63(2)
C(12)	3834(3)	1367(2)	6468(2)	63(2)
C(13)	3097(3)	779(2)	5583(2)	53(1)
C(8)	2760(3)	1265(2)	4811(2)	47(1)
C(15)	3709(3)	1219(2)	2274(2)	70(2)
C(16)	4257(3)	1316(2)	1426(2)	86(2)
C(17)	3552(3)	778(2)	514(2)	92(3)

C(18)	2299(3)	143(2)	448(2)	97(3)
C(19)	1750(3)	46(2)	1295(2)	81(2)
C(14)	2455(3)	584(2)	2208(2)	51(1)
C(21)	-367(2)	1725(2)	4041(2)	52(2)
C(22)	-1455(2)	2167(2)	3928(2)	65(2)
C(23)	-2443(2)	1783(2)	3108(2)	69(2)
C(24)	-2343(2)	957(2)	2400(2)	80(2)
C(25)	-1255(2)	515(2)	2513(2)	67(2)
C(20)	-266(2)	899(2)	3333(2)	48(1)
C(27)	-1353(2)	-4622(2)	4230(2)	55(2)
C(28)	-1874(2)	-4735(2)	5086(2)	69(2)
C(29)	-3157(2)	-5315(2)	5028(2)	67(2)
C(30)	-3920(2)	-5783(2)	4115(2)	67(2)
C(31)	-3400(2)	-5670(2)	3259(2)	55(2)
C(26)	-2116(2)	-5089(2)	3317(2)	44(1)
C(33)	1656(2)	-4748(2)	1878(2)	54(1)
C(34)	2840(2)	-5071(2)	1896(2)	71(2)
C(35)	2887(2)	-6059(2)	2063(2)	77(2)
C(36)	1751(2)	-6724(2)	2211(2)	72(2)
C(37)	567(2)	-6402(2)	2193(2)	57(2)
C(32)	520(2)	-5414(2)	2026(2)	42(1)
C(39)	-2335(3)	-6865(2)	250(2)	78(2)
C(40)	-3239(3)	-7541(2)	-515(2)	113(3)
C(41)	-4520(3)	-7403(2)	-724(2)	116(3)
C(42)	-4897(3)	-6588(2)	-167(2)	97(2)
C(43)	-3994(3)	-5911(2)	598(2)	70(2)
C(38)	-2712(3)	-6050(2)	807(2)	52(1)

References

(1) W.P. Neumann, '*The Organic Chemistry of Tin*', Wiley, New York (1970).

(2) R.C. Poller, '*The Chemistry of Organotin Compounds*', Logos, London (1970).

(3) A.K. Sawyer, ed., '*Organotin Compounds*', vols 1, 2, 3, Dekker, New York (1971).

(4) P.G. Harrison, ed., '*Chemistry of Tin*', Blackie, London (1989).

(5) A.G. Davies and P.J. Smith, *Adv. Inorg. Chem. Radiochem.* **23**, 1 (1980).

(6) A.G. Davies and P.J. Smith, in '*Comprehensive Organometallic Chemistry*' p.519, eds. G. Wilkinson, F.G.A. Stone and E.W. Abel, Pergamon Press, Oxford (1982).

(7) J.J. Zuckerman, '*Organotin Compounds*', Wiley, New York (1970).

(8) I. Omae, '*Organotin Chemistry*', (JOMC Chemistry Library vol. 21), Elsevier, Amsterdam (1989).

(9) B.J. Aylett, '*Organometallic Compounds*', 4th ed., vol.1, part 2, Groups IV and V, Chapman and Hall, London (1989).

(10) P.G. Harrison, *Coord. Chem. Revs.*, **75**, 200 (1986).

(11) K.C. Molloy, *Adv. Organometal. Chem.*, **33**, 171 (1991).

(12) J.T.B.H. Jastrzebski, *Adv. Organometal. Chem.*, **35**, 242 (1993).

(13) M. Peryere, J-P. Quintard and A. Rahm, '*Tin in Organic Synthesis*', Butterworth, London (1987).

(14) Y. Yamamoto, '*Organotin Compounds in Organic Synthesis*', Tetrahedron Symposia in print 36, **45**(4), 909 (1989).

(15) A. Medici, M. Fogognolo, P. Pedrini, and A. Dondoni, *J. Org. Chem.*, **47**, 3844 (1982).

(16) Y. Xu, F. Gin and W. Huang, *J. Org. Chem.*, **59**, 2638 (1994).

(17) K.A. Kocheshkov, *Chem. Ber.*, **62**, 996 (1926).

(18) A.C. Smith and E.G. Rochow, *J. Am. Chem. Soc.*, **75**, 4103 (1953).

(19) R.J. Hulme, *J. Chem. Soc.*, 1524 (1963).

(20) J.A. Zubieta and J.J. Zuckerman, *Prog. Inorg. Chem.*, **24**, 252 (1978).

(21) P.A. Cusack, P.J. Smith, J.D. Donaldson and S.M. Grimes, '*A Bibliography of X-ray Crystal Structures of Tin Compounds*', I.T.R.I. pulication no. 588, London (1981).

(22) D.E. Goldberg, D.H. Harris, M.F. Lappert and K.M. Thomas, *J. Chem. Soc.; Chem. Commun.*, 2268 (1976).

(23) D.E. Goldberg, P.B. Hitchcock, M.F. Lappert, K.M. Thomas, A.J. Thorne, T. Fjeldberg, A. Haarland and B.E.R. Schilling, *J. Chem. Soc. Dalton Trans.*, 2387 (1986).

(24) H. Meyer, G. Baum, W. Massa, S. Berger and A. Berndt, *Angew. Chem. Int. Ed. Engl.*, **26**, 546, (1987).

(25) H. Grützmacher, S. Freitag, R. Herbst-Irmer and G.S. Sheldrick, *Angew. Chem. Int. Ed. Engl.*, **31**, 437 (1992).

(26) G. Trinquier and J-P. Malrieu, *J. Am. Chem. Soc.*, **109**, 5303 (1987).

(27) H. Grützmacher, W. Deck, H. Pritzkow and M. Sander, *Angew. Chem. Int. Ed. Engl.*, **33**, 456 (1994).

(28) P.C. Chieh and J. Trotter, *J. Chem. Soc. A*, 911 (1970).

(29) A. Karipides and K. Wolfe, *Acta. Cryst.*, **B31**, 605 (1975).

(30) A. Karipides, A.T. Reed, D.A. Haller and F. Hayes, *Acta. Cryst.*, **B33**, 950 (1977).

(31) C.J. Cardin, J.M. Kelley, R.J. Norton, Abhijit Roy, B.J. Hathaway and T.J. King, *J. Chem. Soc. Dalton Trans.*, 671 (1983).

(32) P.G. Harrison and K.C. Molloy, *J. Organometal. Chem.*, **152**, 53 (1978).

(33) K.C. Molloy, P.C. Waterfield and M.F. Mahon, *J. Organometal. Chem.*, **365**, 61 (1989).

(34) S. Selvaratnam, Kong Mun Lo and V.G. Kumar Das, *J. Organometal. Chem.*, **464**, 143 (1994).

(35) S.S. Al-Juaid, M. Al-Rawi, C. Eaborn, P.B. Hitchcock and J.D. Smith, *J. Organometal. Chem.*, **446**, 161 (1993).

(36) M.J.S. Gyanne, M.F. Lappert, S.J. Miles, A.J. Carty and N.J. Naylor, *J. Chem. Soc. Dalton Trans.*, 2009 (1977).

(37) R. Alan-Howie, J.N. Ross and J.L. Wardell, *Acta. Cryst.*, **C50**, 229 (1994).

(38) P. Brown, M.F. Mahon and K.C. Molloy, *J. Chem. Soc.; Chem. Commun.*, 1621 (1989).

(39) H. Von Schuman, *Z. Anorg. Allg. Chem.*, **354**, 192 (1967).

(40) P.A. Bates, M.B. Hursthouse, A.G. Davies and S.D. Slater, *J. Organometal. Chem.*, **363**, 45 (1989).

(41) D. Kobelt, E.F. Paulus and H. Scherer, *Acta. Cryst.*, **B28**, 2323 (1972).

(42) J.S. Tse, M.J. Collins, F.L. Lee and E.J. Gabe, *J. Organometal. Chem.*, **310**, 169 (1986).

(43) A. Rank, L.C. Allen and K. Mislow, *J. Am. Chem. Soc.*, **94**, 3035 (1972).

(44) R. Hoffman, J.M. Howell and E.L. Muetterties, *J. Am. Chem. Soc.*, **94**, 3047 (1972).

(45) R.S. Berry, *J. Chem. Phys.*, **32**, 933 (1960).

(46) S.W. Ng, Chem Wei, V.G. Kumar Das and T.C.W. Mak, *J. Organometal. Chem.*, **334**, 283 (1987).

(47) R.R. Holmes, S. Shafieezad, J.M. Holmes and R.O. Day, *Inorg. Chem.*, **27**, 1232 (1988).

(48) V.G. Kumar Das, L.K. Mun, Chen Wei, S.J. Blunden and T.C.W. Mak, *J. Organometal. Chem.*, **322**, 163 (1987).

(49) K. Jurkschat and A. Tzsach, *J. Organometal. Chem.*, **272**, C13 (1984).

(50) A. Tzsach and K. Jurkschat, *Pure Appl. Chem.*, **58**, 639 (1986).

(51) B. Wrackmeyer, S. Kundler, W. Milius and B. Boese, *Chem. Ber.*, **127**, 333 (1994).

(52) H.J. Reich and N.H. Philips, *J. Am. Chem. Soc.*, **108**, 2102 (1986).

(53) W.A. Gustavson, L.M. Principe, W-Z. Min Rhee and J.J. Zuckerman, *J. Am. Chem. Soc.*, **103**, 4126 (1981).

(54) P.G. Harrison, K. Lambert, T.J. King and B. Magee, *J. Chem. Soc. Dalton Trans.*, 363 (1983).

(55) D.W. Allen, D.J. Derbyshire, I.W. Nowell and J.S. Brooks, *J. Organometal. Chem.*, **260**, 263 (1984).

(56) S-G. Teoh, S-B. Teo, G-Y. Yeap, H-K. Fun and P.J. Smith, *J. Organometal. Chem.*, **454**, 73 (1993).

(57) S.W. Ng, V.G. Kumar Das, S-L. Li and T.C.W. Mak, *J. Organometal. Chem.*, **467**, 47 (1994).

(58) G.M. Bancroft, B.W. Davies, N.C. Payne and T.K. Sham, *J. Chem. Soc. Dalton Trans.*, 973 (1975).

(59) B.D. James, R.J. Magee, W.C. Patalinghug, B.W. Skelton and A.H. White, *J. Organometal. Chem.*, **467**, 51 (1994).

(60) E.G. Martinez, A.S. Gonzalez, A. Castineiras, J.S. Casas and J. Sordo, *J. Organometal. Chem.*, **469**, 41, (1994).

(61) A.C. Sau, R.O. Day and R.R Holmes, *Inorg. Chem.*, **20**, 3076 (1981).

(62) B. Salgado, E. Freijanes, A.S. Gonzalez, J.S. Casas, J. Sordo, U. Casellato and R. Graziani, *Inorg. Chim. Acta,* **185**, 137 (1991).

(63) M. Webster, K.R. Mudd and D.J. Taylor, *Inorg. Chim. Acta*, **20**, 231 (1976).

(64) D. Dakternieks, G. Dyson, K. Jurkschat, R. Tozar and E.R.T Tiekienk, *J. Organometal. Chem.*, **458**, 29 (1993).

(65) V.G. Kumar Das, L.K. Mun, C. Wei and T.C.W. Mak, *Organometallics*, **6**, 10 (1987).

(66) B.K. Nicholson, *J. Organometal. Chem.*, **265**, 153 (1984).

(67) J.T.B.H. Jastrzebski, P.A. van der Schaaf, J. Boersma, G. van Koten, D.J.A. de Ridder and D. Heijdenrijk, *Organometallics*, **11**, 1521 (1992).

(68) W.A. Schenk, A. Khadra and C. Burschka, *J. Organometal. Chem.*, **468**, 75 (1994).

(69) A.S. Gonzalez, B. Alberte, J.S. Casas, J. Sordo, A. Casteneiras, W. Hiller and J. Strahle, *J. Organometal. Chem.*, **353**, 169 (1988).

(70) E.G. Martinez, A.S. Gonzalez, A. Macias, M.V. Castano, J.S. Casas and J. Sordo, *J. Organometal. Chem.*, **385**, 329 (1990).

(71) M. Calligaris, G. Nardin and L. Randaccio, *J. Chem. Soc. Dalton Trans.*, 2003, (1972).

(72) F. Caruso, M. Giomini, A.M. Giuliani and E. Rivarola, *J. Organometal. Chem.*, **466**, 69 (1994).

(73) N. Seth, V.D. Gupta, H. Nöth and M. Thomann, *Chem. Ber.*, **125**, 1523 (1994).

(74) V.G. Kumar Das, Y.C. Keong, C. Wei, P.J. Smith and I.W. Nowell, *J. Chem. Soc. Dalton Trans.*, 129, (1987).

(75) P.F. Lindley and P. Carr, *J. Cryst. Molec. Struct.*, **4**, 173, (1974).

(76) E.O. Schlemper, *Inorg. Chem.*, **6**, 2012, (1967).

(77) C. Le Comte, J. Protas and M. Devaud, *Acta Cryst.*, **B32**, 923, (1976).

(78) P.G. Harrison and A. Mangia, *J. Organometal. Chem.*, **120**, 211, (1976).

(79) G.G. Lobbia, S. Callogero, B. Bovio and P. Cecchi, *J. Organometal. Chem.*, **440**, 27, (1992).

(80) D.V. Naik and W. Scheidt, *Inorg. Chem.*, **12**, 272 (1973).

(81) S.W Ng, C. Wei, V.G. Kumar Das, G.B. Jameson and R.J. Butcher, *J. Organometal. Chem.*, **365**, 75 (1989).

(82) M.Schürmann and F. Huber, *Acta Cryst.*, **C50**, 206 (1994).

(83) R. Schmiedgen, F. Huber and M. Schürmann, *Acta Cryst.*, **C50**, 391 (1994).

(84) M.B. Hossain, J.L. Lefferts, K.C. Molloy, D. van der Helm and J.J. Zuckerman, *Inorg. Chim. Acta*, **36**, 409 (1979).

(85) R. Allman, R. Hohlfeld, A. Waskowska and J. Lörbeth, *J. Organometal. Chem.*, **192**, 353 (1980).

(86) A. Blaschute, I. Lange, J. Krahl, D. Koch and P.G. Jones, *J. Organometal. Chem.*, **467**, 169, (1994).

(87) A.G. Davies, J. Milledge, D.C. Puxley and P.J. Smith, *J. Chem. Soc. (A)*, 2862 (1970).

(88) N.W. Allcock and J.F. Sawyer, *J. Chem. Soc. Dalton Trans.*, 1090 (1977).

(89) Y.M. Chow, *Inorg. Chem.*, **9**, 794, (1970).
R.A. Forder and G.M. Sheldrick, *J. Organometal. Chem.*, **22**, 611 (1970).

(90) K.C. Molloy, S.J. Blunden and R. Hill, *J. Chem. Soc. Dalton Trans.*, 1259 (1988).

(91) M. Gielen, A. El Khloufi, M. Biesemans, F. Kayser, R. Willem, B. Mahieu, D. Mais, J.N. Lisgarten, L Wyns, A. Moreira, T.K. Chattopadhay and R.A. Palmer, *Organometallics*, **13**, 2849 (1994).

(92) M.G. Newton, I. Haiduc, R.B. King and C. Silvestru, *J. Chem. Soc,; Chem. Commun.*, 1229 (1993).

(93) K.C. Molloy, F.A.K. Nasser, C.L. Barnes, D. van der Helm and J.J. Zuckerman, *Inorg. Chem.*, **21**, 960 (1982).

(94) J.G. Masters, F.A.K. Nasser, M.B. Hossain, A.P. Hagen, D. van der Helm and J.J. Zuckerman, *J. Organometal. Chem.*, **385**, 39 (1990).

(95) J.P. Ashmore, T. Chivers, K.A. Kerr and J.H.G. van Roode, *Inorg. Chem.*, **16**, 191 (1977).

(96) J. Konnert, D. Britton and Y.M. Chow, *Acta Cryst.*, **B28**, 180 (1972).

(97) F. Mistry, S.J. Rettig, J. Trotter and F. Aubke, *Acta Cryst.*, **C46**, 2091 (1990).

(98) R.R. Holmes, *Acc. Chem. Res.*, **22**, 190 (1989).

(99) H. Puff and H. Reuter, *J. Organometal. Chem.*, **373**, 173 (1989).

(100) K. Yünlü, N. Höck and R.D. Fischer, *Angew. Chem. Int. ed. Engl.*, **24**, 879 (1985).

(101) M. Adam, A.K. Brimah, R.D. Fischer and L. Xing-Fu, *Inorg. Chem.*, **29**, 1595 (1990).

(102) T. Tanaka, *Organometal. Chem. Rev. (A)*, **5**, 1 (1970).

(103) N.N. Greenwood and T.C. Gibb, '*Mössbauer Spectroscopy*', Chapman and Hall, London, (1971).

(104) A. Vertes, L. Korecz and K. Burger, 'Mössbauer Spectroscopy', Elsevier, Amsterdam (1979).

(105) G.M. Bancroft, '*Mössbauer Spectroscopy - An Introduction for Chemists and Geochemists*', M^{c}Graw-Hill, London (1973).

(106) R.V. Parish, '*NMR, NQR, EPR and Mössbauer Specroscopy in Inorganic Chemistry*', Ellis Horwood, London (1990).

(107) J.J. Zuckerman, *Adv. Organometal. Chem.*, **9**, 21 (1970).

(108) J.R. Ruddick, *Rev. Silicon, Germanium, Tin and Lead Compounds,* **2**, 115 (1976).

(109) G.M. Bancroft and R.H. Platt, *Adv. Inorg. Radiochem.*, **15**, 59 (1976).

(110) J.J. Zuckerman in '*Chemical Mössbauer Spectroscopy*' ed. R.H. Herber, Plenum, New York (1984).

(111) R.V. Parish and R.H. Platt, *J. Chem. Soc. (A)*, 2145 (1969).

(112) R.V. Parish and R.H. Platt, *Inorg. Chim. Acta,* **4**, 65 (1970).

(113) T.K. Sham and G.M Bancroft, *Inorg. Chem.*, **14**, 2281 (1975).

(114) R.K. Harris and B.E. Mann, '*NMR and the Periodic Table*', Academic Press, London (1979).

(115) J. Mason ed., '*Multinuclear NMR*', Plenum Press, New York and London (1987).

(116) P.J. Smith and A.P. Tupciauskas, *Ann. Rev. NMR Spec.*, **8**, 291 (1978).

(117) V.S. Petrosyan, *Prog. NMR Spec.*, **11**, 115 (1977).

(118) B. Wrackmeyer, *Ann. Rep. NMR Spec.*, **16**, 73 (1985).

(119) J.D. Kennedy and W. M^{c}Farlane, *Rev. Si, Ge, Sn and Pb,* **1**, 235 (1974).

(120) J.D. Kennedy, *J. Chem. Soc. Perkin II*, 242 (1977).

(121) E. van den Berghe and G.P. van der Kelen, *J. Mol. Struct.*, **20**, 147 (1974).

(122) M. Barnard, P.J. Smith and R.F.M. White, *J. Organometal. Chem.*, **77**, 189 (1974).

(123) J.D. Kennedy, W. M^{c}Farlane and G.S. Pyne, *Bull. Soc. Chim. Belge.*, **84**, 289 (1975).

(124) D.W. Allen, D.J. Derbyshire, J.S. Brookes, S.J. Blunden and P.J. Smith, *J. Chem. Soc. Dalton Trans.*, 1889 (1984).

(125) V.G. Kumar Das, K.M. Lo and S.J. Blunden, *J. Organometal. Chem.*, **334**, 307 (1987).

(126) K. Handlir, J. Holecek, M. Navornick, S.M. Teleb, and A. Lycka, *Inorg. Chim. Acta*, **150**, 287 (1988).

(127) W. M^{c}Farlane and R.J. Wood, *J. Organometal. Chem.*, **40**, C17 (1972).

(128) J. Holecek, M. Nadvornik, K. Handlir and A. Lycka, *J. Organometal. Chem.*, **241**, 177 (1983).

(129) M. Nadvornik, J. Holecek, K. Handlir and A. Lycka, *J. Organometal. Chem.*, **275**, 43 (1984).

(130) A. Lycka, J. Jirman, A. Kolonicny and J. Holecek, *J. Organometal. Chem.*, **333**, 305 (1987).

(131) W.F. Howard, R.W. Crecely and W.H. Nelson, *Inorg. Chem.*, **24**, 2204 (1985).

(132) T.P. Lockhart and W.F. Manders, *Inorg. Chem.*, **25**, 892 (1986).

(133) J. Holecek and A. Lycka, *Inorg. Chim. Acta*, **118**, L15 (1986).

(134) R.A. Cummins and P. Dunn, *'The Infra-red Spectra of Organotin Compounds'*, Australian Defence Scientific Service (1963).

(135) R. Okawara and M Wada, *Adv. Organometal. Chem.*, **5**, 137 (1967).

(136) T. Tanaka, *Organometal. Chem. Rev. A*, **5**, 1 (1970)

(137) G.K. Sandhu, G. Kaur, J. Holecek and A. Lycka, *J. Organometal. Chem.*, **345**, 51 (1988).

(138) G.K. Sandhu, G. Kaur, J. Holecek and A. Lycka, *J. Organometal. Chem.*, **365**, 215 (1989).

(139) G.K Sandhu and G. Kaur, *J. Organometal. Chem.*, **388**, 63 (1990).

(140) D.C. M^{c}Kean, A.R. Morrison and P.W. Clark, *Spectrochim. Acta,* **41A**, 1467 (1985).

(141) W.F. Edgell and C.H. Ward, *J. Am. Chem. Soc.*, **77**, 6486 (1955).

(142) R.C. Poller, *J. Inorg. Nucl. Chem.*, **4**, 593 (1962).

(143) A. Marchand, C. Lemerle, M.T. Forel and M.H. Soulard, *J. Organometal. Chem.*, **42**, 353 (1972).

(144) P.G. Harrison and S.R. Stobart, *J. Organometal. Chem.*, **47**, 89 (1973).

(145) R.G.H. Clark, A.G. Davis and R.J. Puddephatt, *J. Chem. Soc. (A)*, 1828 (1968).

(146) D.B. Chambers, F. Glockling and M. Watson, *J. Chem. Soc. (A)*, 1759 (1967).

(147) K.C. Molloy and P.C. Waterfield, *J. Organometal. Chem.*, **424**, 281 (1992).

(148) S.J. Blunden, M.F. Mahon, K.C. Molloy and P.C. Waterfield, *J. Chem. Soc. Dalton Trans.*, 2135 (1994).

(149) M.F. Mahon, K.C. Molloy and P.C. Waterfield, *J. Organometal. Chem.*, **361**, C5 (1989).

(150) B.D. Berezin, '*Coordination Compounds of Porphyrins and Phthalocyanines*', Wiley, London (1981).

(151) B.M. Hoffman and J.A. Ibers, *Acc. Chem. Res.*, **16**, 15 (1983).

(152) T.J. Marks, *Angew. Chem. Int. ed. Engl.*, **29**, 857 (1990).

(153) K.J. Wynne, *Inorg. Chem.*, **24**, 1339 (1985) and references therein.

(154) T. Inabe, J.G. Gaudiello, M.K. Maguel, J.W. Lyding, R.L. Burton, W.J. M^{c}Carthy, C.R. Kannewurf and T.J. Marks, *J. Am. Chem. Soc.*, **108**, 7595 (1986) and references therein.

(155) J. Metz and M. Hanack, *J. Am. Chem. Soc.*, **105**, 828 (1983).

(156) M. Hanack, A. Hirsch, A. Lange, M. Rein, G. Renz and P. Vermeheren, *J. Mater. Res.*, **6**, 385 (1991).

(157) N. Jagerovic, J-M. Barbe, M. Farnier and R. Guilard, *J. Chem. Soc. Dalton Trans.*, 2569 (1988).

(158) W. Kobel and M. Hanack, *Inorg. Chem.*, **25**, 103 (1986).

(159) W.H. Brown and W.N. French, *Can. J. Chem.*, **36**, 537 (1958) and references therein.

(160) W. Haas, B. Knipp, M. Sicken, J. Leux, and E. Vogel, *Angew. Chem. Int. ed. Engl.*, **27**, 409 (1988).

(161) M. Ahmed and O. Meth-Cohn, *J. Chem. Soc. (C)*, 2104 (1971).

(162) G. Tarrago, C. Marzin, O. Najimi and V. Pellegrin, *J. Org. Chem.*, **55**, 420(1990) and references therein.

(163) E. Vogel, W. Haas, B. Knipp, J. Leux and H. Schmickler, *Angew. Chem. Int. ed. Engl.*, **27**, 406 (1988).

(164) J. Lisowski, J. Latos-Grazynski and L. Szterenberg, *Inorg. Chem.*, **31**, 1933 (1992) and references therein.

(165) A. Ulmann and J. Manassen, *J. Am. Chem. Soc.*, **97**, 6540 (1952).

(166) A. Ulmann, J. Manassen, F. Frolow and D. Rabinovich, *Tetrahedron Lett.*, 167 (1978).

(167) A. Ulmann, J. Manassen, F. Frolow and D. Rabinovich, *Tetrahedron Lett.*, 1885 (1978).

(168) E. Vogel, W. Haas, B. Knipp, J. Leux and H. Schmickler, *Angew. Chem. Int. ed. Engl.*, **27**, 406 (1988).

(169) E. Vogel, P. Röhrig, M. Sicken, B. Knipp, A. Herrmann, M. Pohl, H. Schmickler and J. Leux, *Angew. Chem. Int. ed. Engl.*, **28**, 1651 (1989).

(170) P.J. Chmielewski, L. Latos-Grazynski, K. Rachlewicz and T. Glowiak, *Angew. Chem. Int. ed. Engl.*, **33**, 779 (1994).

(171) S. Beckmann, T. Wessel, B. Franck, W. Hönle, H. Borrmann and H.G. von Schering, *Angew. Chem. Int. ed. Engl.*, **29**, 1395 (1990).

(172) T. Wessel, B. Franck, M. Möller, U. Rodewald and M. Löge, *Angew. Chem. Int. ed. Engl.*, **32**, 1148 (1993).

(173) H. König, C. Eickmeir, M. Möller, U. Rodewald and B. Franck, *Angew. Chem. Int. ed. Engl.*, **29**, 1393 (1990).

(174) A.K. Burrell, G. Hemmi, V. Lynch and J.L. Sessler, *J. Am. Chem. Soc.*, **113**, 4690 (1991).

(175) J.L. Sessler, S.J. Weghorn, T. Morishima, M. Rosingana, V. Lynch and V. Lee, *J. Am. Chem. Soc.*, **114**, 8306, (1992).

(176) J.L. Sessler, M. Cyr and A.K. Burrell, *Tetrahedron*, **48**, 1661 (1992).

(177) D.C. Miller, M.R. Johnson and J.A. Ibers, *J. Org. Chem.*, **59**, 2877 (1994).

(178) J.L. Sessler, S.J. Weghorn, V. Lynch and M.R. Johnson, *Angew. Chem. Int. ed. Engl.*, **33**, 1509 (1994).

(179) C.P. Brock, A.L. Companion, L.D. Kock and K. Niedenzu, *Inorg. Chem.*, **30**, 784 (1991).

(180) R.N. Butler, '*Comprehensive Heterocyclic Chemistry*', **5**, 791 (1984).

(181) L. Birkofer and P. Wegner, *Chem. Ber.*, **99**, 2512 (1966).

(182) S.S. Washburne and W.R. Peterson Jr., *J. Organometal. Chem.*, **21**, 427 (1970).

(183) A. Alvanipour, N.H. Buttrus, C. Eaborn, P.B. Hitchcock, A.I. Mansour and A.K. Saxena, *J. Organometal. Chem.*, **349**, 29 (1988).

(184) K. Sisido, K. Nabika, T. Isida and S. Kozima, *J. Organometal. Chem.*, **33**, 337 (1971).

(185) P. Dunn and D. Oldfield, *Aust. J. Chem.*, **24**, 645 (1971).

(186) R. Guilard, S.S. Gerges, A. Tabard, P. Richard, M.A. El Borui and C. Lecomte, *J. Am. Chem. Soc.*, **109**, 7228 (1987).

(187) L. Busetto, A. Pallazi and R. Ros, *Inorg. Chim. Acta*, **13**, 233 (1975).

(188) P. Paul and K. Nag, *Inorg. Chem.*, **26**, 2969 (1987).

(189) B. T. Hsieh, A.E. Takach, E.B. Milosaljevic, J.H. Nelson, T. Kemerich, W. Beck, N. Bresciani-pahor, L. Randoccio and K.R. Brower, *Inorg. Chim. Acta*, **134**, 31 (1987).

(190) E.O. John, R.D. Willet, B. Scott, R.L. Kirchmeir and J.M. Shreeve, *Inorg. Chem.*, **28**, 893 (1989).

(191) P. Paul, S. Chakladar and K. Nag, *Inorg. Chim. Acta*, **170**, 27 (1990).

(192) R. Das, P. Paul, K. Nag and K. Venkatslibramanian, *Inorg. Chim. Acta*, **185**, 221 (1991).

(193) I. Fleming, '*Frontier Orbitals and Organic Chemical Reactions*', Wiley-Interscience, London (1976).

(194) S.J. Wittenberger and B.G. Donner, *J. Org. Chem.*, **58**, 4139 (1993).

(195) R.J. Deeth, K.C. Molloy, M.F. Mahon and S. Whittaker, *J. Organometal. Chem.*, **430**, 25 (1992).

(196) J.S. Thayer and R. West, *Inorg. Chem.*, **3**, 889 (1964).

(197) W.T. Reichle, *Inorg. Chem.*, **3**, 402 (1964).

(198) S. Kozima, T. Hitomi, T. Akiyama and T. Isida, *J. Organometal. Chem.*, **32**, 303 (1975).

(199) W. Beck and K. Schorpp, *Chem. Ber.*, **108**, 3317 (1975).

(200) W.G. Jackson and S. Cortez, *Inorg. Chem.*, **23**, 1921 (1994).

(201) J.H. Nelson, D.L. Schmitt, R.A. Henry, D.W. Moore and H.B. Jonassen, *Inorg. Chem.*, **9**, 2678 (1970).

(202) R. Barbieri, F. Di Bianca, E. Rivarola and F. Huber, *Inorg. Chim. Acta*, **108**, 141 (1985).

(203) J. Charambous, G.C. Georgiou, K. Henrick, L.R. Bates and M. Healy, *Acta Cryst.*, **C43**, 659 (1987).

(204) E.S. Greaber and B. Morosin, *Acta Cryst.*, **C39**, 567 (1983).

(205) N.E. Takach, E.M. Holt. N.W. Allcock, R.A. Henry and J.H. Nelson, *J. Am. Chem. Soc.*, **102**, 2968 (1980).

(206) A.P. Gaughan, K.S. Bowman and Z. Dori, *Inorg. Chem.*, **11**, 601 (1972).

(207) D.S. Moore and S.D. Robinson, *Adv. Inorg. Chem.*, **32**, 171 (1988).

(208) S.W. Ng, V.G. Kumar Das, M.B. Hossain, F. Goerlitz and D. van der Helm, *J. Organometal. Chem.*, **390**, 19 (1990).

(209) R. Allman, R. Hohlfeld, S. Olejnik and J. Lörbeth, *J. Organometal. Chem.*, **210**, 51 (1981).

(210) R.A. Forder and G.M. Sheldrick, *J. Chem. Soc. (A)*, 1107 (1971).

(211) I. Hammann, K.H. Buchel, K. Bungarz and L. Born, *Planzen-Nachrichten Bayer*, **31**, 61 (1978).

(212) V. Perruzo, G. Plazzogna and G. Valle, *J. Organometal. Chem.*, **395**, 167 (1989).

(213) M.J. Hampden-Smith, D. Lei and E.N. Duesler, *J. Chem. Soc. Dalton Trans.*, 2953 (1990).

(214) E.O. John, R.D. Willet, B. Scott, R.L. Kirchmeir and J.M. Shreeve, *Inorg. Chem.*, **28**, 893 (1989).

(215) C. Janiak, *J. Chem. Soc.; Chem. Commun.*, 545 (1994).

(216) R. Huisgen, C. Axen and H. Seil, *Chem. Ber.*, **98**, 2966 (1965).

(217) This work and J. M^{c}Ginley and K.C. Molloy, unpublished results.

(218) D.M. Bowers and I. Popov, *Inorg. Chem.*, **7**, 1594 (1968).

(219) M.M. Degtyark, P.N. Gaponik, A.I. Lesnikovich and A.I. Vrublevskii, *Chem. Abstr.*, **103**, 47180u (1985).

(220) P.N. Gaponik, M.M. Degtyark and V.V. Svididov, *Chem. Abstr.*, **97**, 119541v (1982).

(221) G.L. Gilbert and C.H. Brubaker, *Inorg. Chem.*, **2**, 1216 (1963).

(222) H. Keller and M. Regitz, *Tetrahedron Lett.*, **29**, 925 (1988).

(223) R. Lang, H. Nöth, P. Otto and W. Storch, *Chem. Ber.*, **118**, 186 (1985).

(224) M. Bürklin, E. Haneker, H. Nöth and W. Storch, *Angew. Chem. Int. ed. Engl.*, **24**, 999 (1985).

(225) M.I. Kahn, Y-S. Lee, C.J. O'Connor, R.C. Haushalter and J. Zubieta, *Chem. Mater.*, **6**, 721 (1994).

(226) M. Fujita, Y.J. Kwon, S. Washizu and K. Ogara, *J. Am. Chem. Soc.*, **116**, 1151 (1994).

(227) R.F. Carina, G. Bernardinelli and A.F. Williams, *Angew. Chem. Int. ed. Engl.*, **32**, 1463, (1993).

(228) J. Kim, D. Whang, Y-S. Koh and K. Kim, *J. Chem. Soc.; Chem. Commun.*, 673 (1994).

(229) B.F. Abrahams, M.J. Hardie, B.F. Hoskins, R. Robson and E.E. Sutherland, *J. Chem. Soc.; Chem. Commun.*, 1049, (1994).

(230) R.L. Kieft, W.M. Peterson, G.L. Blundell, S. Horton, R.A. Henry and H.B. Jonassen, *Inorg. Chem.*, **15**, 1721 (1976).

(231) N.E. Takach, E.M. Holt, N.W. Alcock, R.A. Henry and J.H. Nelson, *J. Am. Chem. Soc.*, **102**, 2968 (1980).

(232) T. Isida, T. Akiyama, K. Nabika, K. Sisido and S. Kozima, *Bull. Chem. Soc. Jpn.*, **46**, 2176 (1973).

(233) R.N. Butler, K.F. Quinn and B. Welke, *J. Chem. Soc.; Chem. Commun.*, 1481 (1992).

(234) R.N. Butler, M.F. Mahon, J. M^{c}Ginley and K.C. Molloy, unpublished results.

(235) R.N. Butler to K.C. Molloy, private communication.

(236) W. Ried and S. Aboul-Fetouh, *Tetrahedron*, **44**, 3399 (1988).

(237) W. Ried, C-H. Lei and J.W. Bats, *Liebigs Ann. Chemie*, 497 (1989).

(238) R.N. Butler and T.M. M^{c}Evoy, *J. Chem. Soc. Perkin II*, 1087, (1978).

(239) N.C. Baeziger, A.D. Nelson, A. Tulinsky, J.H. Bloor and A.I. Popov, *J. Am. Chem. Soc.*, **89**, 6463, (1967).

(240) J. Zabrocki, G.D. Smith, J.B. Dunbar Jr., H. Ijima and G.R. Marshall, *J. Am. Chem. Soc.*, **110**, 5875 (1988).

(241) C.K. Lowe-Ma, R.A. Nisson and W.S. Wilson, *J. Org. Chem.*, **55**, 3755, (1990).

(242) S.L. Suib, *Chem. Rev.*, **93**, 803, (1993).

(243) P. Behrens and G.D. Stucky, *Angew. Chem. Int. ed. Engl.*, **32**, 696 (1993).

(244) G.M. Bennett and R.L. Wain, *J. Chem. Soc.*, 1108 (1936).

(245) A.S. Baily, B.R. Henn and J.M. Langdon, *Tetrahedron*, **19**, 161 (1963).

(246) K.L. Leung and R.H. Herber, *Inorg. Chem.*, **10**, 1020 (1971).

(247) K.C. Molloy and S.F. Sayers, University of Bath, unpublished results.

(248) J.L Atwood in '*Inclusion Compounds*', vol. 2, J.E.D. Davies and D.D. MacNicol eds., Academic Press (1984).

(249) A.J. Leusink, W. Drenth, J.G. Noltes and G.J.M. van der Kerk, *Tetrahedron Lett.*, 1263 (1967).

(250) A.J. Ashe, W. Klein and R. Rouseau, *Organometallics*, **12**, 3225 (1993).

(251) J.K. Stille, *Angew. Chem.. Int. ed. Engl.*, **25**, 508 (1986).

(252) H. Gilman and D.A. Shirley, *J. Am. Chem. Soc.*, **71**, 1870, (1949).

(253) V.G. Kumar Das, K.M. Lo and S.J. Blunden, *J. Organometal. Chem.*, **334**, 307, (1987).

(254) M. Draganjac, C.J. Ruffing and T.B. Rauchfuss, *Organometallics*, **4**, 1909, (1985).

(255) T. Sone, Y. Ohba and R. Watanabe, *Bull. Chem. Soc. Jpn.*, **62**, 1346 (1989).

(256) S. Trofimenko, *Chem. Revs.*, **72**, 497 (1972).

(257) A.R. Karitsky, '*Comprehensive Heterocyclic Chemistry*', **5**, 105 (1984).

(258) A.R. Karitsky, A.E. Abdel-Rahman, D.E. Leary and O.A. Schwarz, *Tetrahedron*, **39**, 4133 (1983).

(259) T.L. Cairns, B.C. M^{c}Kusick and V. Weinmayr, *J. Am. Chem. Soc.*, **73**, 1270 (1951).

(260) J.W. Schwick and D.J. Crowley, *J. Am. Chem. Soc.*, **73**, 1377 (1951).

(261) S. Trofimenko, *J. Am. Chem. Soc.*, **92**, 5118 (1970).

(262) D. Doddrell, K.G. Lewis, C.E. Mulquiney, W. Adcock, W. Kitching and M. Bullpitt, *Aust. J. Chem.*, **27**, 417 (1974).

(263) E. Lukevits, O.A. Pudova, Y. Popelis and N. Erchak, *J. Gen. Chem. U.S.S.R., (Engl. Trans.)*, **51**, 102 (1981).

(264) S. Julia, P. Sala, J. del Mazo, M. Sancho, C. Ochoa, J. Elguero, J-P. Fayet and M-C. Vertut, *J. Heterocyclic Chem.*, **19**, 1141 (1982).

(265) N. Walker and D. Stewart, *Acta Cryst.*, **A39**, 158 (1983).

(266) G.M. Sheldrick, SHELX86, a computer program for crystal structure determination, University of Göttingen (1986).

(267) G.M. Sheldrick, SHELX76, a computer program for crystal structure determination, University of Cambridge (1976).

(268) C.K. Johnson, ORTEP, Oak Ridge Ntl. Lab. (Rep.) ORNL. (US) 1965-3794 revised (1971).

Numerical Index of Compounds Included in this Thesis

$PhSnCl_3$	$^{i}Pr_3SnPh$	$^{i}Pr_3SnI$
(1)	**(2)**	**(3)**
$^{i}Pr_3SnN_3$	Et_4Sn	Et_3SnCl
(4)	**(5)**	**(6)**
Et_3SnN_3		
(7)		

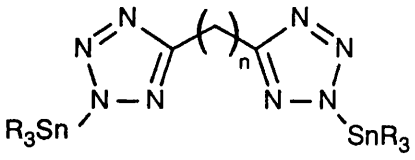

(8) n = 1; R = Me

(9) n = 1; R = Bu

(10) n = 2; R = Bu

(14) n = 1; R = ^{i}Pr

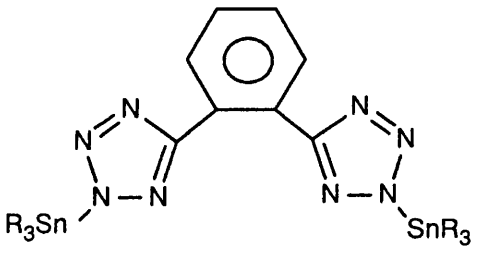

(11) R = Bu

(15) R = ^{i}Pr

(17) R = Et

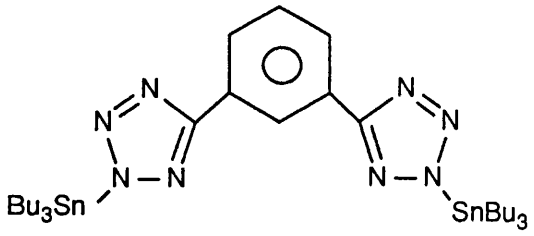

(12) R = Bu

(18) R = Et

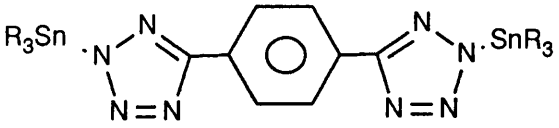

(13) R = Bu

(16) R = ^{i}Pr

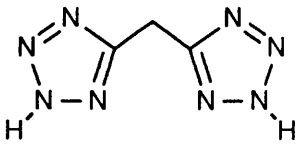

(19)

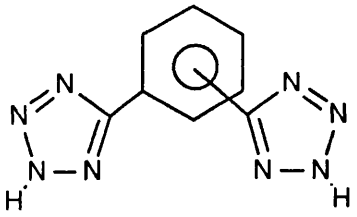

(20) 1,2-C_6H_4 isomer

(21) 1,3-C_6H_4 isomer

(22) 1,4-C_6H_4 isomer

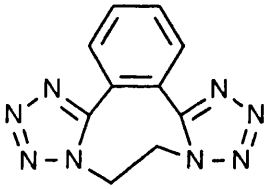

(23)

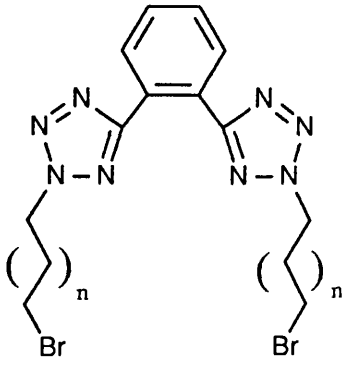

(24) n = 0

(26) n = 1

(27) n = 3

(29) n = 4

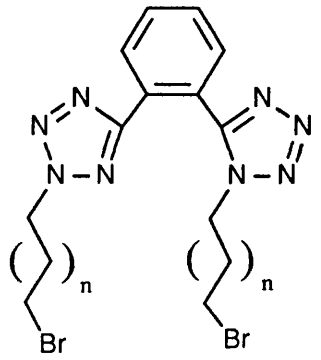

(25) n = 0

(28) n = 3

(30) n = 4

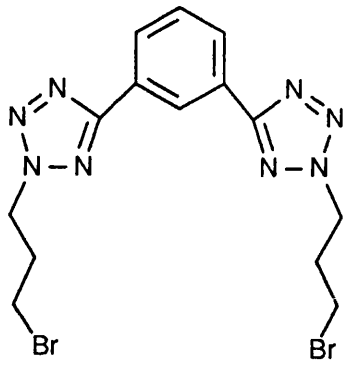

(31) n = 0

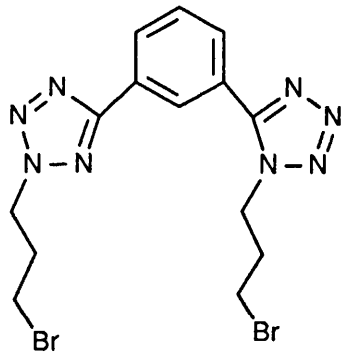

(32) n = 0

(33) n = 1

(34) n = 1

(35) n = 2

(36) n = 2

(37) n = 3

(38) n = 3

(39) n = 4

(40) n = 6

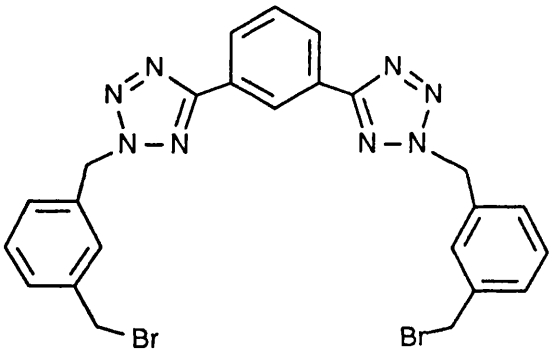

(41)

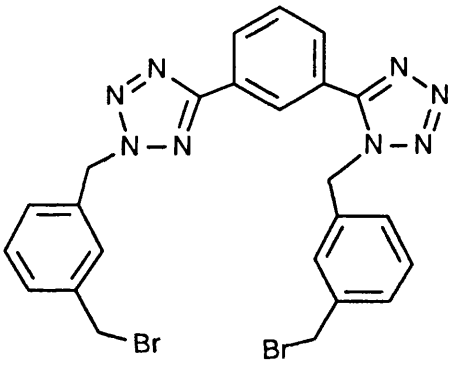

(42)

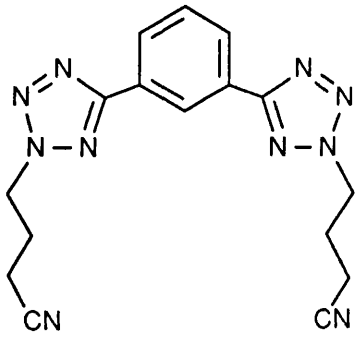

(43)

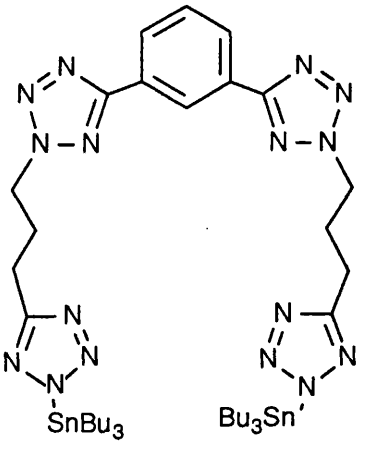

(44)

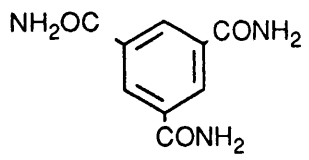

(45)

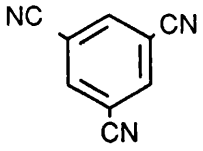

(46)

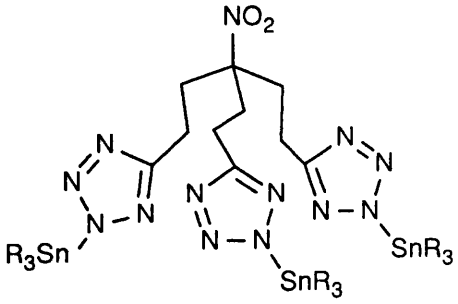

(47) R = Me

(48) R = Et

(49) R = Bu

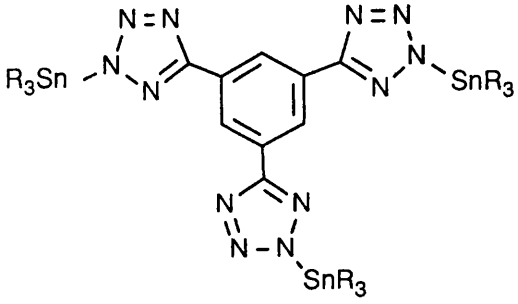

(50) R = Me

(51) R = Et

(52) R = Bu

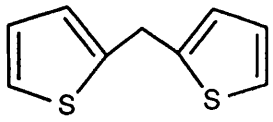

(53)

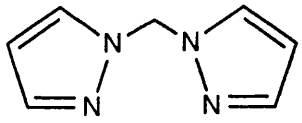

(54)

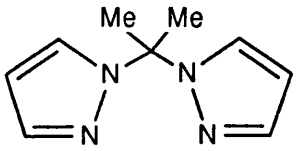

(55)

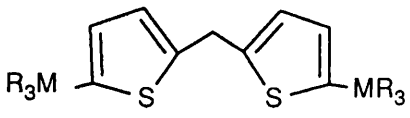

M = Sn; R = Bu (**56**), Ph (**57**)

M = Si; R = Me (**58**), Ph (**59**)

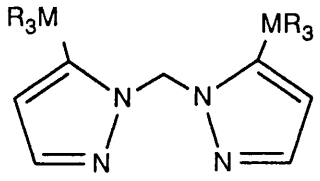

M = Sn; R = Me (**60**), Bu (**61**), Ph (**62**)

M = Si; R = Me (**63**)

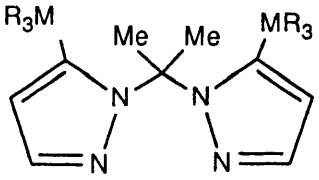

M = Sn; R = Me (**64**)

M = Si; R = Me (**65**)